The Mind's Interaction with the Laws of Physics and Cosmology

Jeffrey S Keen

The Mind's Interaction with the Laws of Physics and Cosmology

The Mind's Interaction with the Laws of Physics and Cosmology

By

Jeffrey S Keen

Cambridge
Scholars
Publishing

The Mind's Interaction with the Laws of Physics and Cosmology

By Jeffrey S Keen

**To
Marilyn, Alexandra, Olivia,
David, and Sophia**

CONTENTS

ABOUT THE AUTHOR

Jeffrey Keen has become one of the world's leading experts in the Physics of Consciousness. He has an Honours degree in Physics and Maths from Imperial College, London University.

Jeffrey has been involved in scientific research for over 50 years, maintaining a passionate interest in physics whilst developing a career in industry and business. He has written various books including Managing Systems Development (2 editions published by John Wiley) which became standard curricula at universities worldwide. Jeffrey has also published his well-acclaimed ground-breaking book *Consciousness, Intent and the Structure of the Universe*. He has now retired as Chairman and Managing Director of a national company, allowing him to concentrate on his scientific research.

Jeffrey is from a traditional scientific background, where the belief is that science is always correct. Accordingly, he was initially dismissive of anything considered "alternative".

However, as a result of experimental findings, through the wisdom of age, and after many years of being detached from academia, he now accepts that orthodox science is neither comprehensive nor infallible, and that there is enormous scope in investigating non-mainstream science. This view has become strongly reinforced following the recent announcements that conventional science can only explain and understand about **4%** of the universe.

For over 30 years, Jeffrey Keen has successfully published in well-respected peer reviewed technical journals and on scientific websites, over 56 relevant scientific papers, detailing his significant and original research. He regularly receives about 400 downloads a month for his published papers and website articles.

Numerous queries are received by him, as well as requests for advice by relevant universities and top Mind Science researchers around the world. He has been a member of the UK Dowsing Research Group (DRG). The British Society of Dowsers awarded him the prestigious Bell Essay Award in recognition of his prolific unique research and numerous published papers.

ACKNOWLEDGEMENTS

PREFACE

My initial motivation for researching subtle energies was threefold:-

1. I have always been intrigued why the act of consciously observing quantum experiments could affect their results.
2. I wished to discover why quantum effects were not observed in the macro world.
3. After nearly 100 years of unsuccessful theoretical research, there were so many untestable theories of quantum gravity.

Hence, I believed a new approach was required.

Although comprehension of the structure of the universe probably requires a theory of quantum gravity, one current approach is attempting to link quantum physics with general relativity – a "top-down approach" such as string theory. My mainly contrarian approach is bottom-up, experimental research, involving subtle energies and conscious acts of observation. Together with many other researchers, I believe that the solution lies not just in physics, but also in the incorporation of consciousness and cognitive neuroscience, together with understanding the nature and perception of information. Traditional techniques such as Mind Science, Noetics, and Dowsing etc. are involved in many of these factors and I wished to prove scientifically (in addition to mathematics and geometry) if they could be a powerful and relevant research tool. As we shall see, they are!

The reason for writing this ground-breaking book results from the culmination of over 30 years of my research. Accepted beliefs are challenged by proving with scientific and mathematical precision that consciousness and the mind involves more than just the brain, but actually depends on the very fabric of the universe. The findings are so thought provoking and exciting that they required sharing with a wider audience, so that eventually the theoretical explanations may be developed to explain the intriguing results. I also hope that this book may significantly assist a future researcher(s) to discover the scientific Theory of Consciousness and the unification of General Relativity and Quantum Physics.

This book presents my unique experiments and findings, using this non-orthodox approach of noetics and dowsing for scientific research. The numerous measurements and data that I have collected over many years

has resulted in pioneering discoveries leading to equations, graphs, universal constants, formulae, and laws of nature that eventually connect to cosmology, and the structure of the universe.

With the benefit of hindsight, I have taken this opportunity to update my papers, that were published chronologically as discoveries were made, into a much more logical order. It should, therefore, be easier for the reader to comprehend how each topic evolved coherently, and to correct my earlier mistakes and eliminate blind alleys.

Although many people dislike the thought of mathematics, and are "switched off" at the sight of equations, it is only possible to understand the structure of the universe in its own language and this involves mathematics and geometry! To include a general readership, this book, therefore, only uses basic mathematics. Similarly, to keep to the main arguments, where appropriate, references have been made to the relevant details in the original papers. (The first number refers to the paper number on my website http://www.jeffrey keen.co.uk/Papers.htm, followed by the page number).

This book unquestionably demonstrates that the cosmos possesses a universal consciousness. Just one example is that results of experiments prove, with a high degree of mathematical accuracy, that the mind can communicate information across the solar system, not only faster than light but instantaneously.

This is not a beginner's book, as the market is currently flooded with such books, courses, and online material relating to noetics and dowsing. Instead, this book attempts to pre-empt and satisfy the emerging worldwide interest in this subject of subtle energies and the mind. It is hoped that this text will be of great interest to a broad range of readers- from interested non-professionals, relevant societies, to universities and colleges wishing to teach and research this upcoming subject.

CHAPTER ONE

INTRODUCTION

Background

Our level of understanding of both subtle energies and consciousness is probably comparable to the knowledge of astronomy about 600 years ago. This was before scientific research produced a paradigm change from the common "obvious" perception of the sun going round the earth each day, and the night sky being a mystery of lights moving in strange patterns around a sphere above the earth.

From that time, scientific progress was made starting with Copernicus having the vague notion that the earth revolves around the sun. This was followed by Tycho Brahe's meticulous but relatively primitive astronomical measurements, which led to Johannes Kepler's laws of planetary motion, which eventually resulted in Newton's laws of gravity 300 years ago. It took a further 200 years for Einstein's general theory of relativity to give an improved theory of gravity. But this did not explain how matter obtained its mass, and hence gravitational attraction. Only recently was the Higgs' boson discovered to explain mass.

I have opened this book with the above well-known sequence of events to explain the level of our current understanding of subtle energies and consciousness. Using the above astronomical analogy, it seems we are equivalent to about 400 years ago. Though I feel we have a long way to go, I hope we do not have to wait another 400 years to understand subtle energies. This book is, therefore, my attempt to reduce this timespan, and introduce science and mathematics in the traditional manner of understanding our universe.

Introduction to Scientific Dowsing

After several years of training and practice, I have learned to detect and measure universal subtle energy fields that are not detected either by the usual five senses, or by existing scientific instruments. However, unlike other people who have developed these skills for numerous well-promoted

purposes, I have used this ability as a tool for pure academic fundamental physics research, with no monetary gain or agenda. Using the mind's intent has allowed my sub-conscious to interact with nature and the cosmos.

What is scientific noetics that includes dowsing? In essence, it is like any other science, with the following interesting enhancements. This means starting with curiosity, designing protocols, followed by meticulous measurements. Not only should each reading be repeated consecutively, but also, unlike conventional science experiments, the measurements must be repeated over different periods of time. As will be developed in this book, these additional requirements on measurements result from the nature of some subtle energy fields, which have a dependence on time.

These "fields" are not only influenced by the local environment and its topological or subterranean features, but are also affected by the moon, the earth orbiting the sun, the earth spinning on its axis, as well as being influenced by electromagnetism, gravity, spin, fundamental geometry, and cosmic sources. Hence, the relevance of introducing noetics to detect and measure subtle energies when researching the structure of the universe, and the nature of information.

This explains the need for the additional protocols mentioned above, which should lead to meaningful averages and percentage variances. Hopefully, such findings will, for newcomers to subtle energy research, create interest in the phenomenon being studied, and discovering the amazing powers of the mind.

For any institution considering setting up a department to research or teach consciousness and subtle energies, it may be attractive to know that one of the advantages and pleasures of this type of research is that an expensive well equipped laboratory with large teams is initially not necessary, as many of the experiments discussed in this book can be performed at home, in a simple laboratory, office, parks, gardens, or the countryside in general. It can also be pleasurable going round the country studying such topics as subtle energies, ancient sites, measuring the directions of flow, or the complexity of lines stretching across the country.

All that is needed for getting started is a tape measure, possibly some dowsing rods, markers, a compass, and a Mager Rosette - useful if one is determining the perceived colours of different subtle energies. Not only is one measuring width, height, and breadth of subtle energy patterns, but also exploring their geometrical shapes, structure, and angles. The geometrical pattern may extend over a few centimetres, or over many acres. It is important to understand why and how the same measurements change daily, monthly, and annually, as well as during astronomical events

such as a new moon or eclipse. I have found that achieving these findings for the first time is exciting.

A Brief Explanation for the non-Dowser

Non-dowsers have difficulty in comprehending what dowsers feel, sense, or visualise. Although atoms or electricity cannot be seen, touched, smelt, tasted, or heard by the normal human senses, they are physical and can be detected by **physical** equipment and meters. Even after millions of years of evolution, only a relatively few people have developed the sixth sense, and can "see" subtle energies. Hence, noetics and dowsing that involve the mind and **consciousness** – not matter and the physical - are required by the majority of people to feel subtle energies. At present, there are no meters to measure consciousness, so it is necessary to use the mind's perception and its interaction with the body's senses. For serious research, this process needs to be made quantitative and as scientific as possible.

Sight is probably a good analogy to the dowser's perception. It is not just the physical image on the retina. Sight includes black, white, and colour information communicated from both eyes along the optic nerve that eventually forms a 3-dimensional stereo model in the brain. During early childhood, learning is by connecting sight with other senses such as touch, and the observing child believes that he or she is "seeing directly" what is being looked at. Similarly, with seeing colours. For example, the colour red is universally accepted, because reference can be made to a physical red colour. However, it is impossible to know if individuals may have different perceptions of this red colour in their brain.

Noetics and dowsing also involves building a model in the brain, but this model is based on intuition and unlike sight, it is not built on the 5 normal senses, but on an additional sense. It is unreasonable to expect that the sight and dowsing models have identical cells in the brain. When dowsing, the brain attempts to superimpose these 2 models. However, as there are no physical connections in the dowsing model, people perceive different measurements and colours. This causes many people to dismiss these techniques. In practice, it is easily possible to overcome this challenge. For example, relative, not absolute dimensions are measured, leading to ratios determining results.

In practice, the world probably contains an infinite number of different subtle energy fields. From a very early age, the mind learns to block out all subtle energies to avoid a significant information overload. A good analogy to comprehend this information challenge is that it would be like

continually watching television with every possible station simultaneously superimposed. Consequently, it is essential to tune into only one television channel and one programme at a time, and have the ability to block out all the others.

Exactly the same principle applies to all noetics and dowsing. It is, therefore, necessary to learn how to tune into a specific "channel". Dowsing involves the mind interacting with its environment in the widest sense via consciously specifying intent, and visualising what information is being sought.

Dowsing has many applications, but in this book it is purely academic, and relates to mind created and naturally occurring "subtle energy" fields. These subtle energies have a strong connection to geometry and often comprise ovals, lines, beams, cones, helices, spirals, patterns, and "flows" which can be detected by dowsing. In turn, these geometries seem to have a strong connection to the structure of the universe. At present, the nature of these subtle energies is not yet understood.

The simplest form of dowsing involves information requests of a binary nature; a "yes" or "no" answer to a question. Examples of this basic academic dowsing intent could be "give me a yes" when entering the boundary of the aura of an object, or when measuring the width of a subtle energy beam produced by the interaction of two or more bodies. With much practice, this protocol enables accurate measurements to be made to within ±2 mm.

Dowsing and associated intuitive techniques fall into several different categories. Some gifted people are able to "see" or visualize subtle energies in colour without the use of devices. Other device-less dowsers feel a positive sensation in their mind's eye, throat, solar plexus, or fingers. Most dowsers need rods, a pendulum, or other devices to amplify the dowsing sensation, which they feel. The majority of the research detailed in this book was undertaken by device-less dowsing, supplemented with angle rods, because I feel they react quickly, respond accurately to boundaries, indicate the direction of flow of the subtle energies or spirals being dowsed, and are easy to use on-site, even in the wind or rain.

Introduction to Learning the Techniques

The initial challenge is that most people cannot detect subtle energies, although many children naturally can, but after the age of about 11, they tend to lose these instinctive skills. Only after training and practice is it possible for the mind to overcome its natural inclination to block the

profusion of subtle energies, and be able to detect the subtle energies from, say, one leaf on a large tree, or even one grain of sand on a beach.

How does the reader acquire the necessary skills to understand, and repeat the numerous experiments in this book? As an example, I was initially motivated after being given a book on dowsing for detecting water and archaeological objects underground. As a conservative physicist, and never having felt or seen these subtle energies, I initially dismissed this as unscientific and unbelievable nonsense. However, being naturally inquisitive, I made my own dowsing rods out of two bent metal coat hangers, which I initially tried out over a hosepipe in the garden.

Being encouraged by a positive reaction, I then progressed to the drains and sewers buried in the road, and eventually became fully convinced after correctly measuring the depth and direction of flow of the water in the underground pipes. This led to me attend meetings of a local dowsing society, then after a short period of time, joining the British Society of Dowsers for further training, and was eventually admitted to the Dowsing Research Group to acquire more advanced skills in research. Practice will enable the reader to acquire the necessary skills to confirm and repeat the experiments in this book.

CHAPTER TWO

THE IMPORTANCE OF GEOMETRY

Introduction

Although the importance of geometry has been known since the ancient Babylonians and Greeks, its significance to understanding the structure of the universe was highlighted over 100 years ago with the advent of general relativity. Since then, we have had published papers on a Flat Universe, 10 or 11 dimensional String Theory, and dodecahedral space topology. Modern physics, cosmology, and other research topics are leading to the conclusion that the structure of the universe is linked to multi-dimensional geometry. As will become apparent, the evidence detailed in this book relating to subtle energies and the mind, leads to a similar conclusion. Hence, the title of this chapter, which sets out some interesting findings.

The Effects of Shape-1

The effects on subtle energies by the shape of a source object is an important factor. I have made extensive measurements as to how far subtle energies can be detected from their source. Shapes that have been investigated include a sphere, an ellipsoid, a point, a flat surface, a hemisphere, a cylinder, a rectangular trapezoid, as well as irregular shapes such as pebbles on a beach as well as ancient megaliths.

In general, the effects are identical in all cases of inanimate objects, irrespective of their composition. The subtle energies perceived as emanating from an object having a point, has a greater range, than from a spherical or flat surface.
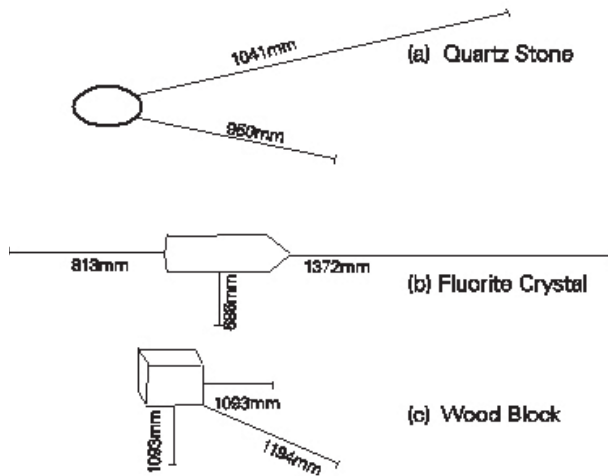
Figure 2-1 The Effects of Subtle Energies by the Source Object

Figure 2-1 illustrates this effect for 3 different source objects presenting at least 8 different surfaces. Figure 2-1(a) is an ellipsoidal quartz stone, where the furthest distance that subtle energies can be detected is when the mind's intent is on the surface with the highest curvature. Focusing on the lower flat part of the stone results in the dowser having to approach closer to the stone to detect its subtle energy.

Figure 2-1(b) is a shaped fluorite crystal, with a hexagonal cross-section, where the pointed end has about double the range of subtle energies compared to the flat sides, whilst the distance for the hemispherical end is between the other two.

Figure 2-1(c) is an old, well-seasoned block of wood, where the flat surfaces have the same range whilst the pointed corners produce a longer range.

However, the above facts are not the most interesting part of the story. The most important finding, and the reason why this section has been introduced, is that if dowsing only the **shapes** in Figure 2-1, and not the actual object, exactly the same effects are found, but with slightly different measurement scales as expected.

If the reader believes that the measurements shown in Figure 2-1 affect the findings, then they can trace out the same shapes on a separate sheet of paper, without printed dimensions, and using a sharp pointer, dowse the distances subtle energies reach and come to the similar conclusions. The important point, therefore, is that it is geometry, not the solid that produces

these results. The material in question has a secondary effect, as it can be affected by local factors such as light and heat etc.

The Effects of Shape-2

The second example of the unexpected results involving geometry, started with my study of Banks & Ditches, a common feature of Neolithic sites. Although worldwide there are probably thousands of ancient sites, the example used here has been selected for the following reasons. The substantial double dykes at Hengistbury Head in Bournemouth UK, have the advantage of no associated megalith architecture, which could influence results. Unlike most Neolithic sites, which are circular, and enclose stone circles, Hengistbury Head's banks are linear, extend for hundreds of metres, and conveniently run approximately north-south. Figure 2-2 is a photograph of part of the double dykes at Hengistbury Head, which gives a feel of its significant size.

Figure 2-2 A Photograph of Part of the Double Dykes at Hengistbury Head

My original research into banks and ditches was driven by the fact that they produce a plethora of subtle energy patterns that are easily detectable. These patterns are some of the most comprehensive, complex, and interesting in the study of subtle energies.
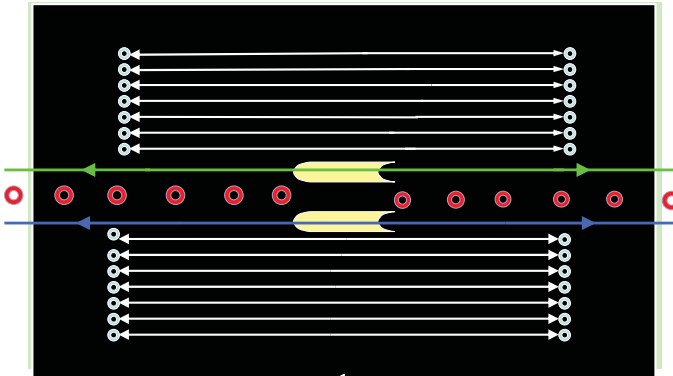
Figure 2-3 The Subtle Energy Pattern Produced by Banks and Ditches

Figure 2-3 illustrates this pattern, where the 2 source banks are depicted in white at the centre of the pattern. As is apparent, there are two groups of seven lines, making 14 in total. These 14 lines are parallel to the two banks. One group of these seven lines is to the right of one bank, whilst the other group is to the left of the other bank. Typically, these lines are longer than their source banks and have an outward flow of subtle energies. As often with subtle energies, each line ends in a clock-wise spiral.

The two groups of seven lines, as measured on the ground, are, in fact, seven concentric cylinders. The dowser, walking along the ground, initially only detects dowsable points where the cylinders meet the ground. This is then perceived, after following these dowsable points around the site, as two sets of seven lines. Subsequent realization of the three-dimensional geometry follows from further research, and leads to Figure 2-4, which illustrates this effect.
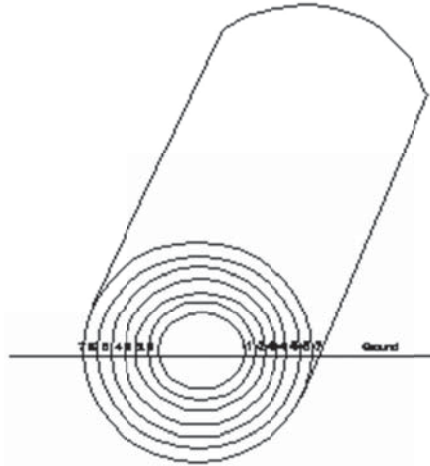
Figure 2-4 Seven Concentric Cylinders

The 2 lines running along the top of the 2 banks have very different properties to the 14 lines. Their length is perceived to extend indefinitely, but it is obviously impossible to prove this statement as the lengths are so great, measurement becomes impossible. They also have an outward perceived flow in both directions.

Finally, running through the central ditch, between the above 2 lines, is a row of equally spaced sets of spirals that also are perceived to continue indefinitely without any diminution.

However, I subsequently discovered that wind-blown sand dunes on a beach in the south of France as well as another on the north coast of Venezuela, also produced 2 banks and a ditch: they too created an identical effect of subtle energy patterns.

This encouraged me to research this phenomenon further and simulate the banks and ditches by first using 2 large plastic drain pipes. I then reduced the scale to 2 bamboo canes. Subsequently, I drew 2 short waves on a wall. All of these sources produced an identical pattern to Figure 2-3, except the measurement scales were different, as expected.

Taking these findings to a logical conclusion, I drew 2 short parallel lines, of about 5cms, on a sheet of paper, as depicted in Figure 2-5. Unbelievably this basic geometry, drawn on a sheet of paper, produced the identical effect as Figure 2-3, which was produced by mammoth earthworks several hundred metres long!

Figure 2-5 The Subtle Energy Produced by 2 Lines

Summary and Conclusions

Once again, these findings demonstrate the importance of geometry, which has a greater effect on subtle energies than the equivalent large physical source objects. It is irrelevant if the source is metal, non-metal, paper, or wire; these only have a secondary effect because of local environmental factors. Published articles have suggested that the subtle energies are produced by such causes as the composition of the source object, the angle of the slopes, chalk soil, or silica, etc. The 2-line experiments prove scientifically, that separation distance of the banks is the major factor. (see my website papers 21, 41 p27 for more details). It would be impossible to demonstrate this conclusion by moving large physical banks!

The above demonstration is also a simple introduction to the concept of the mind's perceived equivalence between 3-dimensional physical bodies, and 2-dimensional abstract geometry on paper. As a final note, the difference between these 2 extremes of the same source geometry can create a Chirality effect, whereby mirror images of the subtle energies created change right and left hand sides.

Over 100 years' ago, Einstein demonstrated that the solution to gravity involved geometry. The findings summarised in this chapter encourage future research into how and why there is a connection between consciousness, the mind, and subtle energies, to geometry.

The Way Forward and Suggested Future Research

The interaction of 2 parallel lines drawn on paper as they are separated, not only produces very interesting subtle energy patterns, but the dynamics of the separation process and the associated mathematics, should produce insights into the correlation between geometry and subtle energies.

CHAPTER THREE

SUBTLE ENERGY PATTERNS
FROM BASIC GEOMETRIC SHAPES

Introduction

The previous chapter was an introduction to the interaction between the mind, geometry, and subtle energies. One of the purposes of this chapter is to show that different geometric shapes produce their own unique subtle energy patterns. A long-term objective of this line of research is to discover mathematical equations for transforming a source geometry into its own generated subtle energy pattern.

Developing an analogy to X-ray crystallography and diffraction gratings may prove useful, similar to Crick and Watson discovering the structure of DNA by using Rosalind Franklin's diffraction images. However, in this case, we are not using electro-magnetic waves, but consciousness. Confidence in this approach is justified for several reasons. Some of the patterns observed seem similar to those produced by diffraction gratings, interference fringes, or x-ray crystallography. In particular, as a result of numerous experimental observations, resonance, interference, null points, and 2:1 ratios have been observed. These examples suggest waves are involved in subtle energies, and hence possible creation of diffraction patterns.

In the following database of different geometries, researchers are invited to find if mathematical transformations exist that would explain the relationship between mind generated geometric patterns observed noetically, and the physical source geometry that creates those patterns. Achieving this should help demonstrate how observing subtle energies, the structure of the universe, and consciousness are connected. It also could lead to clues as to how nature's information is stored and accessed: in other words, an insight into "the structure of the universe".

Confidence in the Technique

Initial experimental results are very promising, and suggest that a plethora of factors are involved in producing subtle energy patterns. These include:

1. photons, magnetism and gravity
2. the earth's spin and several astronomical factors;
3. the act of observing two objects, such as 2 lines, causes them to interact; and
4. dowsing a "n-dimensional" geometrical source produces, in some cases, the same dowsable pattern as a "n+1 dimensional" geometric source.

In other words, there are strong elements of comprehensiveness and universality in this adopted technique.

This approach also has the benefit of adding support, or otherwise, to the existence of a postulated information field, which is accessed when dowsing. A further possible result of this study is an understanding of how geometry is mirrored, stored, and accessed, and if our universe is a 5-dimensional hologram.

Protocol and Methodology

The technique adopted is dowsing simple 0, 1, 2, and 3-dimensional geometric shapes (e.g. dots, lines, circles, cubes, etc.) and measuring in 3-dimensions the different subtle energy patterns detected. Using pure geometry includes the benefit of eliminating any effects or perturbations due to mass or matter. This enables us to focus only on researching individual consciousness, astronomical factors, and the information field.

Definitions

Before progressing experiments, it is necessary to define axes. This enables a more precise mathematical representation of the 3-dimensional patterns being dowsed, and enables meaningful communication between researchers. If we define that

a) Both the x-axis, and the y-axis are in the horizontal plane
b) The z-axis is vertical i.e. the x-y plane is horizontal and the x-z plane is vertical

c) For 0, 1, and 2-dimensions the source geometry is drawn on a sheet of paper in the x-z plane where y=0. However, for practical experimental reasons, there are a few instances where the source geometry needs to be placed on the ground, i.e. on the x-y plane.

d) The centre of the source geometry is at the origin of the axes.

In general, different people perceive similar patterns, although their dimensions may vary. We know from preliminary work that this is not relevant to our objective to create a database of patterns, as key angles remain constant, and the perceived patterns only differ in scale, with possible minor perturbations that do not affect the overall observed geometry. Only the multiplying coefficients change in the mathematical description; the overall relationships are similar.

Out of an infinite number of geometric shapes, I have selected the following geometries that I have found the most interesting, and could assist in achieving the objectives of this chapter. I have also not included source geometries that produce auras, as this subject is covered in subsequent chapters. A far greater number of source geometries and their subtle energies can be found in paper 41 on my website (http://www.jeffreykeen.co.uk/Papers.htm).

An Example of 0 - Dimension Geometry

A Dot

The simplest geometry is a dot drawn on a vertical sheet of paper, which produces a dowsable horizontal beam, with an outward flow, ending in a clockwise spiral. The 3-dimensional profile of the beam can be visualised by rotating the graph shown in Figure 3-1 around its horizontal x-axis. However, this profile can vary from a sharply pointed cone to the bulbous shape shown in Figure 3-1. The typical length of this beam is in the range 0-8 metres.

The properties of dowsing a dot make it suitable for a standard yardstick that, as will be shown, has proved very effective in detailed quantitative research into subtle energies.

Taking a vertical cross section (x-z plane) as this moves along the horizontal beam in Figure 3-1, by dowsing its extremities, produces a rectangle, as depicted in Figure 3-2. This is surprising, as instinct would have suggested a circle or oval cross-section.
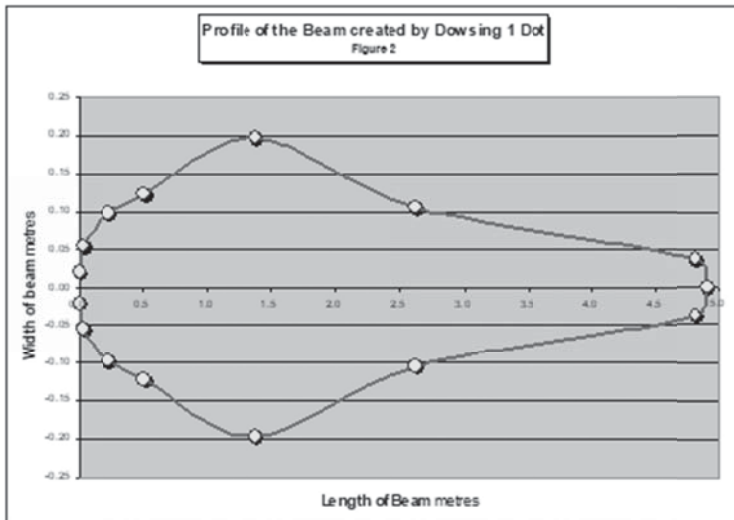
Figure 3-1 The Horizontal Beam Created By a Dot

Figure 3-2 A Single Dot x-z Plane (Vertical Cross Section)

An Example of 1–Dimension Geometry

A Straight Line

A straight line drawn on a horizontal sheet of paper dowses as 9 "reflections" on both sides of the source line, in the horizontal plane of the source line. This is illustrated in Figure 3-3. However, a **physical** line, such as a rod, only has 7 similar "reflections". These findings of 9 reflections of subtle energies for abstract geometry, but only 7 reflections for physical source geometry, can be generalised for numerous source geometries and is very common
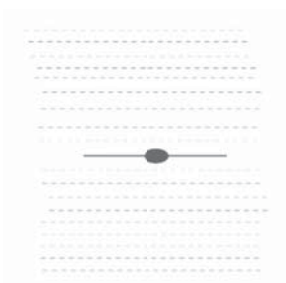
Figure 3-3 The 2x9 "Reflections" Plus the Central Vortex
Generated by a Straight Line

For both abstract and physical lines of about 15 cms length, the separation distances between adjacent reflections is about 1-2 cms. For a line of 2.5 m the separation distance is about 33 cms. The lengths of the reflected lines are about 1.5-1.6 times longer than their source. This number is tantalising close to the golden ratio (1.618) and future research is required to establish if there is an exact connection.

Figure 3-3 invites comparison to Figure 2-3 in the previous chapter, which related to the geometry of 2 lines. As can be seen, the addition of the additional line increases significantly the numbers and complexity of the subtle energies generated by the above single line. It is also interesting to note that the "reflections" referred to in Figure 3-3 are in fact, the same as the cylinders in Figure 2-4, again highlighting the important connection between 2-dimensional abstract geometry and 3-dimensional physical structures.

The centre point of both a straight abstract or physical line also creates a perpendicular dowsable vortex beam, as pictorially represented in Figure 3-3. Interestingly, it is found that the same results are obtained irrespective of the length of the source line. Taken to the limit, the beam pattern observed is identical to dowsing one dot as discussed earlier. Ignoring the above reflections, there would seem to be no difference between dowsing a dot or a line!

Examples of 2-Dimensional Geometry

A Triangle

In the plane of a vertical sheet of paper, a drawn equilateral triangle produces no dowsable patterns! However, coming perpendicularly out of the paper (i.e. horizontally) are 6 lines comprising two pairs of three lines.

As illustrated in Figure 3-4, a vertical cross-section through these 6 lines shows that they form the corners of two triangles which are about 4 and 8 times scaled up versions of the original source triangle.
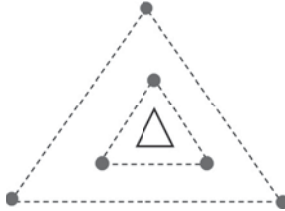
Figure 3-4 Subtle Energies Produced by an Equal Lateral Triangle

Half Sine Wave

The half sine wave, as illustrated in Figure 3-5, is possibly the 2nd most interesting dowsable shape. Irrespective of size, the half sine wave shape appears inert to dowsing. There are no subtle energy lines either horizontally or vertically. Of all the geometrical shapes so far studied, the half sine wave is unique in this respect. This may indicate another example of waves, with interference producing a null effect.

Figure 3-5 Half Sine Wave

The other unique, unexpected, inexplicable, and "weird" phenomenon is that dowsing a half sine wave when the mind's intent is in the 5th dimension gives a strong pattern, even if the mind cannot visualise this scenario. When re-dowsing the half sine wave and specifying the intent in the normal 3- and 4-dimensional space, there is a void as described above. However, if the dowsing intent is asking for a pattern in 5-dimensional space, one obtains 4 lines. These lines are in the plane of the paper, which can be fixed either horizontally or vertically – the effect and pattern seems identical. There are no lines perpendicularly out of the paper.

Although only measured over a distance of 2.**1** metres, these 4 lines appear to be parallel within experimental error, have an outward flow, and seem to go to infinity. Even though the source half sine wave only extended 110mm, the separation distance between the outer lines was 1.35-1.40 metres. These lines have different properties to any other subtle energy so far discussed, such as the 4 types of lines generated by banks and ditches. All 4 of these seem to have the same unique properties, but unlike other lines, they do **not** show a colour on a Mager disc.

These experiments have been repeated with numerous geometric shapes that produce strong patterns in 2, 3 and 4 dimensional space, but all of these produce a void when dowsing in 5-dimensional space. This void is both in the plane of the paper as well as perpendicular to the paper. It makes no difference if the paper with the geometrical shape, is fixed either horizontally or vertically.

Further research is obviously required to explain why a 5-dimensional result is only obtained with a half sine wave.

Examples of 3-Dimensional Geometry

A Sphere

The sphere used as the source object had a 16 cms diameter. Figure 3-6 is an elevation showing the two dowsable lines generated passing vertically through the centre of the sphere. One has a vertical upward flow, whilst the other has a vertical downward flow. The length of these two lines was greater than the height of the room in which the measurements were taken.

As a sphere is, by definition, symmetrical, the fact that the only dowsable lines are vertical suggests that gravity is involved in their production. This is consistent with the findings for other geometrical shapes.

Figure 3-6 The Subtle Energies Produced by a Sphere

A Pyramid

The pyramid used as the source object had a square base 8 cms x 8 cms, with a height of 10 cms. Its base was placed on a horizontal surface. Figure 3-7 is a plan view, and illustrates that ten subtle energy lines are generated.
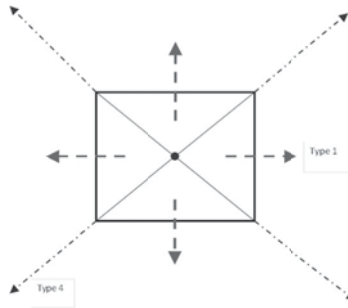
Figure 3-7 Subtle Energy Lines Produced by a Pyramid

These lines comprise:

a. 4 lines originating from the centres of each triangular face, extending horizontally, with a perceived outward flow, and length of approximate 1.53 metres.
b. 1 line from the centre of the square base, extending vertically downward, also with a perceived outward flow, and a length of 1.53 metres.
c. 4 lines originating from the corners of the base of the pyramid, extending horizontally, with a perceived outward flow, and a length that gives the impression of an infinite length, but only measured up to a length of 50 metres.
d. 1 line originating from the apex of the pyramid, extending vertically upwards, with a perceived outward flow, and a length that gives the impression of going to infinity, but, for practical reasons, the length was only measured up to a length of 50 metres.

Generalisations and Conclusions

As mentioned at the beginning of this chapter, due to the lack of space in this book, a far greater number of source geometries and their subtle energies can be found in paper 41 on my website http://www.jeffreykeen.

co.uk/Papers.htm. It must also be emphasised that several local and astronomical forces that include electromagnetic fields, spin, and gravity, affect perceived patterns of subtle energy, and may cause perturbations.

Full mathematical transformations and an explanation of the physics involved in geometry and subtle energies are still required to explain the patterns observed. As an interim, Table 3-1 provides a cross-reference of my findings for each source geometry and the individual components of the subtle energy pattern, and their frequency of occurrence.

It must be stressed that a blank in the table could mean that the factor has not been measured or observed. It does not necessarily mean that the factor is absent. Similarly, to keep the data manageable, several other factors have not been included in Table 3-1. These include arithmetic or geometric series; direction of flow; clockwise or anti-clockwise vortices; Mager colours; etc.

It is apparent from Table 3-1 that short measureable lines are the most common observation, closely followed by very long lines that are too long to measure, but give the impression of extending to infinity. Vortices and diverging beams are equally common. Also frequent is resonance and the occurrence of the scaling of source geometry of 2:1 ratios.

Intriguingly, the fact that 1-dimensional source geometry gives identical observations as a 0-dimensional source, and some 2-dimensional source geometries give identical observations as 3-dimensional objects, reinforces the importance of geometry in the structure of the universe. There is also the possibility of further research explaining the 5-dimensions response.

A final interesting cross reference in Table 3-1 is that the most complex subtle energy patterns are produced by 2 interacting circles, 3 interacting circles, 2 parallel lines, and banks and ditches. These have already been covered, or are covered in much greater detail in future chapters.

	Measureable lines	Very long lines	Vortices	Diverging beam(s)	2:1 ratio	Resonance	n-1 = n dimension	Scaling	137, 131	Gravity	Magnetic influence	5-dimension	Bifurcation	
1 Dot	√			√	√				√					4
A Row of Dots in a Straight Line				√	√									2
A Straight Line	√			√	√				√					4
3 Dots in a Triangle			√											1
4 Dots in a Square	√													1
A Triangle	√					√				√				3
A Square	√					√				√				3
1 Circle				√	√	√					√			4
2 Circles	√			√	√	√	√					√	√	6
Vesica Pisces	√				√	√								3
3 Circles			√		√	√	√	√	√	√	√			7
Half Sine Wave												√		1
Two Parallel Lines	√	√	√			√	√	√				√		7
Angled Cross	√		√											2
Vertical Cross		√				√				√	√			4
Alpha Symbol	√	√	√	√	√									4
Tetrahedral Geometry		√	√									√		3
Banks and Ditches	√	√	√			√	√	√				√		7
A Sphere		√									√			2
A Cube	√	√												2
A Pyramid	√	√												2
Totals	**13**	**10**	**10**	**9**	**6**	**5**	**5**	**3**	**3**	**3**	**3**	**2**	**1**	

Table 3-1 Summary of the Subtle Energy Patterns Produced from a Sample of Common Geometrical Shapes

CHAPTER FOUR

COMMON ON-SITE PERCEIVED GEOMETRIC SHAPES

Introduction

Previous chapters were an introduction into the importance of geometry in creating subtle energy patterns. This chapter concentrates on how the geography and geology of the Earth create their own subtle energy patterns. Also examined is man's influence in creating subtle energies; by either the mind or construction works. The latter could be from Neolithic defensive earthworks and their stone circles, to more modern large buildings, such as cathedrals and domes.

This chapter is a non-technical introduction to the types of geometrical patterns that appear in this book. No detailed analysis or complexity is discussed here. Covered in future chapters is how astronomical events affect these patterns and create perturbations. Both spiral-vortices and mind created psi-lines are very common. They are important and complex topics, each requiring its own chapter, which appear later.

Single & Multiple Lines in 2-Dimensions

Lines are one of the most frequently occurring manifestations of subtle energy, and not necessarily encountered just at ancient sites. Natural lines seem to meander over the countryside, and their widths do not remain strictly parallel. Man-created lines tend to be straighter and tend to keep parallel. The reason is that the mind's intent, when creating subtle energy lines, was usually "please get me from point A to point B as easily as possible".

The simplest detectable geometrical shape is a subtle energy line running along the surface of the earth, the lengths of which may extend from a few centimetres to hundreds of kilometres. However, dowsable lines are rarely simple or straight. There are numerous types, each with their own differing effects, such as colour, direction of flow, and vector properties.

On closer investigation, a "single" subtle energy line often comprises multiple parallel lines, such as groups of 3, 5, 7, or 12. The simplest typical example is illustrated in Figure 4-1. It comprises three parallel lines with the direction of subtle energy flow in the outer two lines going in the opposite direction to the inner line, but as with most subtle energies, these directions reverse over the course of a year, as do the widths of the lines and other characteristics. The field strength of the inner line, when measured on an arbitrary scale of 1 to 100, is double the field strength of each of the outer individual lines. This suggests a conservation of energy, and to achieve this, assumes that the flow lines must join up somewhere. In fact, having detected the end of a line, one finds that a spiral usually terminates it.

Figure 4-1 Typical Subtle Energy Line

These multiple line combinations and subtle energy flows seem to form stable configurations, and appear to exist indefinitely. In addition, subtle energy lines have a width, ranging from a few centimetres up to a few metres.

Fractals

Most subtle energies comprise fractal geometry. For example, each line of the above Figure 4-1 pattern comprises the entire structure repeated smaller and smaller. Figure 4–2 is a simplified generalised version of fractal geometry.
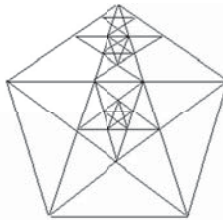

Figure 4-2 A Pentagon and Pentagram Example of Fractal Geometry

The centre of a pentagram is a pentagon, which is also formed by joining the extremities of a pentagram. Figure 4-2 illustrates the relationship between a regular pentagon and a series of pentagrams. The centre of each pentagram is a pentagon in which another, but smaller pentagram, can be constructed. This example, of an inbuilt mechanism to replicate itself progressively either smaller or larger, is one property of fractal geometry, and appears frequently in nature.

Cylinders

As an example of escalating 3-dimensional analysis of observations, it was shown in Chapter 2, that the initial 2-dimensional perception of the surface pattern created by banks and ditches, was the formation of 2 rows each comprising 7 subtle energy lines. On subsequent analysis, this turns out to be 3-dimensional, 7 concentric cylinders, as previously illustrated in Figure 2-2. The 7 lines are where the cylinder meets the ground.

Surface Spirals

A very common shape associated with subtle energies is a spiral. These appear in numerous diverse places; in fact, anywhere on, above, or under the earth's surface. Set out below are some of the more interesting examples where I have found and studied spirals.

1. Ancient sites and burial mounds.
2. Within the auras of solid bodies.
3. Over geological features, including underground intersecting watercourses, and the top of volcanoes.
4. Inside substantial buildings such as cathedrals and domes.
5. Inside underground caves.
6. The mind can generate spirals anywhere.
7. The intersection of two subtle energy lines produces a spiral.
8. Spirals terminate subtle energy lines.

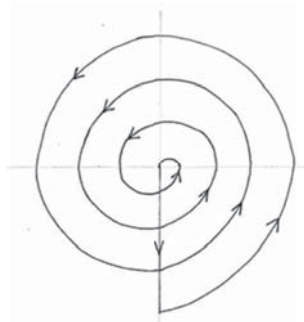All spirals seem to have the same structure, whatever their source.

Figure 4-3 Plan View of an Anti-clockwise Spiral

Figure 4-3 is a typical plan view of a spiral. There is a perceived flow in either a clockwise or anti-clockwise direction. Highly significant is that spirals have 3½ turns, and any line drawn through the origin always intersects the spiral at 7 dowsable points (the origin/centre is not a dowsable point in this context). These 7 points are approximately equally spaced apart, so measurements form an arithmetic series. The fact that in some musical scales a harmonic octave has 7 notes is relevant to subtle energies, and this theme will be developed further.

Ellipsoids & Ovoids

Another common shape is a three-dimensional, ellipsoid or ovoid. These are often associated with auras, and their interesting properties will be discussed in a future chapter. On drilling down further, they comprise 7 or 9 concentric ellipsoids, as illustrated in Figure 4–4.
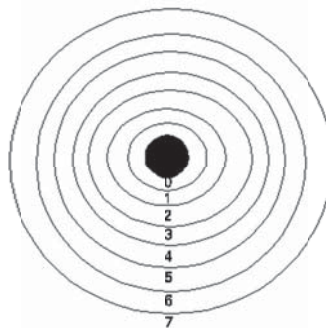

Figure 4-4 The 2-Dimensional Projection of a 7 Shell Asymmetrical Ovoid Aura

Curlicues

Shapes such as those appearing in Figure 4–5 are not so common as previously discussed patterns. They are found in such circumstances as 2-body interaction, are associated with stone circles, and sometimes appear in a field without an apparent cause.

Figure 4-5 A Typical Curlicue Shape

Dowsable Surface Effects of Megaliths

It is well documented that megaliths have horizontal bands, and vertical helices of subtle energy. The usual pattern is one, or sometimes, two helices wrapped around the surface of the stone, although some literature refers to seven turns. Coupled with the helix, as illustrated in Figure 4-6, are seven alternate bands of positive and negative fields (possibly a cause of confusion regarding seven turns of the helix), with five bands above ground and two below ground.
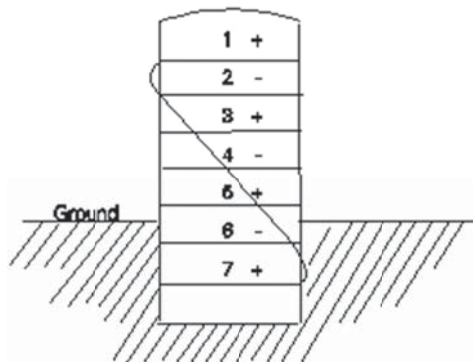

Figure 4-6 Vertical Spiral around Megalith

It is important to realise that this is only a phenomenon within the fabric of a stone, with the subtle energies associated with these helices and bands only extending outwards by up to 120 mm. Megaliths generate other types of subtle energies, but these usually extend much further.

Spider-web Pattern

Figure 4-7 gives an example of a spider-web pattern, which was found in the Rollright Stone Circle (in the Cotswolds, UK). It comprises a complex pattern of 3 components.

1. There are four inner circles, and a fifth circle, which is located about 2 feet outside the ring of stones.
2. Two subtle energy lines forming diameters through the centre, that run approximately north-south, and east-west are possibly associated with water flow.
3. A clock-wise spiral at the centre of the stone circle, which is most probably caused by the interaction of the above two subtle energy lines, as is normal at such points of intersection.
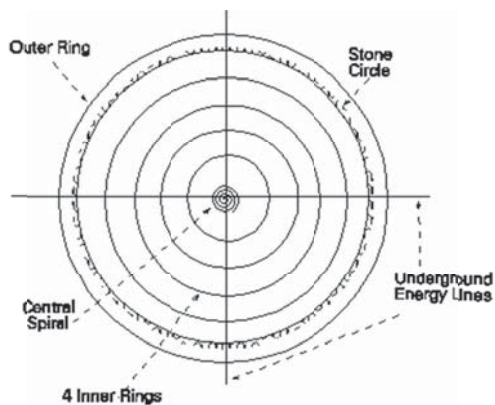

Figure 4–7 Rollright Stone Circle Spider Web Pattern

Diamonds and Cones in front of Megaliths

On a ground plan, 3 dimensional subtle energy diamond shapes appear as spirals. Figure 4-8 is an example of the location of such a pattern, for

example, in front of one of the most southerly stones in the South West
Circle at Stanton Drew (UK). It is on a diameter through the centre of the
circle to the most northerly stone. The same dowsable shape is found in
front of other diametrically opposite pairs of stones. As illustrated in
Figure 4-8, X marks the location of the spiral, which is equidistant (**a**)
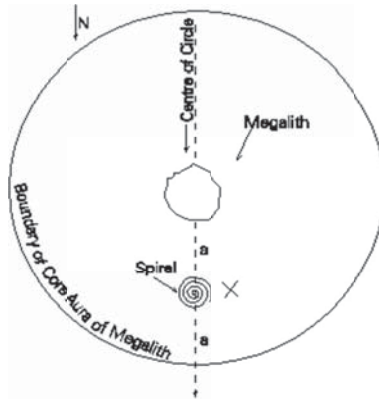between the surface of the stone and the boundary of the core aura

Figure 4-8 Location of a Diamond and Cone Pattern at Stanton Drew
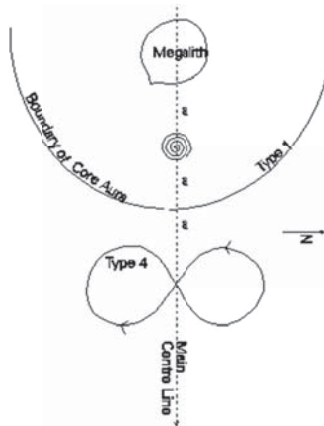
A Figure of Eight Pattern

Figure 4-9 Figure of Eight Pattern at Stanton Drew

Figure 4-9 is again an example from Stanton Drew and relates to the figure of eight pattern. It is located by the most westerly standing stone in the Great Circle (but the effect equally relates to other megaliths and sites). As illustrated in Figure 4-9, the centre of this figure of eight is a distance of **3a** from the surface of the megalithic stone, or a distance **a** from the boundary of the stone's core aura. There appears to be a flow of energy round the figure of eight as shown in the diagram. This pattern is known as the "Lemniscate of Bernoulli".

Torroids

Figures 4–10, and 4–11 conceptually show how a Taurus could be involved with a figure of eight pattern. These Torroids appear frequently in the analysis of subtle energies,
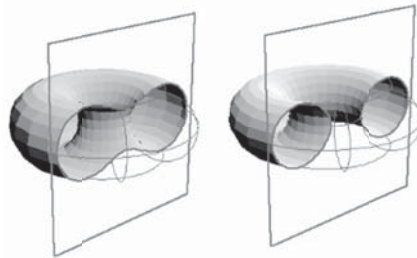
Figure 4-10 Torroid Cross-Sections

Cassinian Ovals

Figure 4.11 illustrates a Cassinian oval, which is a family of curves produced by the intersection of a plane parallel to the axis of a torroid. (Cassini investigated these curves in 1618, when he was studying the relative motion of the earth and the sun.) A special case is where the plane is at a distance equal to the radius of the torroid. This produces a "lemniscate of vernoulli", which is a figure of eight pattern.

The above example of a figure of eight pattern could be generated by toroidal subtle energy generated by stone circles. Cassini Ovals may also be involved in two body interactions.

Figure 4-11 Cassini Ovals

Conclusions

The subtle energy patterns in this chapter form **a** good basis for further development in the rest of this book. For example, it is highly significant that spirals have 3½ turns, and that ellipsoids comprise 7 or 9 concentric boundaries.

CHAPTER FIVE

MATHEMATICS AND UNIVERSAL CONSTANTS

Introduction

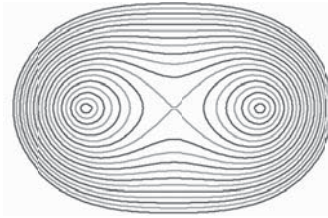Like geometry, mathematics has a profound effect in the understanding of dowsing, consciousness, and subtle energies. This chapter serves as an introduction to this theme and contains extra explanations for the non-mathematician reader. I have endeavoured to make my explanations clear.

What we are seeking are fundamental constants and equations of the universe. These may be pure numbers, ratios, or angles, which are not based on arbitrary or man-made measurements and units. In any scientific research, obtaining universal constants is the ultimate proof of a correct theory. The values discussed in this chapter appear repeatedly, not only in experimental results of consciousness and subtle energies, but reassuringly, in numerous other applications in nature.

Frequently Found Universal Constants in Subtle Energy Research

Mathematical Series

Mathematical series of numbers are very common when measuring subtle energies. These frequently comprise a series of fields such as lines, ellipses, auras, or spirals. Four simple mathematical relationships are often found:

(a) an **arithmetic** series (e.g. 3, 6, 9, 12 ……..) where the **difference** between 2 adjacent measurements/numbers in the series equals the same constant, and have the same units of man-made measurements. Numerous examples of arithmetic series occur in subtle energies generated by ancient sites, and in the composition of auras.

(b) a **geometric** series (e.g. 3, 6, 12, 24 ……) where any number divided by its previous number in the series produces the same constant non-dimensional **ratio**. Geometric series occur frequently in spirals and

mind created dowsable shapes. As dimensionless ratios, they are more useful for generalisations and extrapolations.

(c) an **harmonic series** is a special case of a geometric series. The ratio of the frequency of any tone to the frequency of its lower octave equals 2. Between adjacent octaves there are, depending on which type of scale, intermediate tones e.g. tone, tone, semitone, tone, tone, tone, semitone. (The latter is the well-known series of 7 components. As the number 7 occurs frequently in subtle energies, it is discussed in context later).

d) a **Fibonacci** series which is a series of numbers starting with 0 and 1, where the next in the series is the sum of the previous two numbers i.e. 0, 1, 1, 2, 3, 5, 8, 13 ….. The Fibonacci Constant is obtained by dividing any number in this series by its previous number. This especially applies to higher orders, and is, therefore, a special case of a geometric series. Table 5-1 illustrates how this builds up to a value of 1.618034…..

n	(n+1)/n
0	
1	
1	1
2	2
3	1.5
5	1.7
8	1.6
13	1.625
21	1.615
34	1.619
55	1.6176
89	1.6182
144	1.6180
233	1.61806
377	1.61803
610	1.61804
987	1.618033
1597	1.618034

Table 5-1 The Build-up of the Fibonacci Series

The Golden Ratio, Phi (φ)

The Fibonacci Constant, also termed Phi (φ), is one of the most frequently found universal constants in subtle energy research. It is an irrational number, which goes on forever without a repeating pattern. Strangely, **φ** is seldom taught in schools, even though it reflects the fundamentals of our universe. One can almost say that it has been left to the Dan Brown novel *The Da Vinci Code* to popularise **φ.** Other interesting properties relating to this constant (**φ)** are that subtracting 1

from it (0.618304) also produces its own reciprocal, whilst adding 1 to it (2.618034) gives its own square.
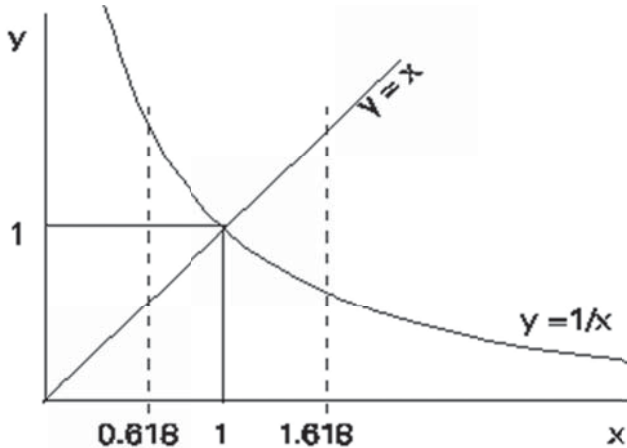

Figure 5-1 The Geometry of Phi (φ)

This leads to another method of deriving (φ), by solving the equation $x - 1 = 1/x$. Phi equals the two solutions of this quadratic equation which are $(\sqrt{5} \pm 1) / 2$. This algebraic solution is also associated with the equation of a hyperbola, which is of the form $y = 1/x$ and the line $y = x$. Figure 5-1 shows this geometric relationship.

Phi is also referred to as the golden ratio, or the golden proportion, because, if the ratio between two dimensions of an object equals phi, the proportions 'feel right'. This applies to numerous situations including the ratio of parts of the human body, a picture height to its width (including TV screens and cinema) as well as to classical architecture, such as the Parthenon. The layouts of many pre-historic and historically built sites are based on a geometry and trigonometry that involves this Fibonacci constant. Dowsable fields associated with the interaction of any two objects also involve φ.

The reason that I have included so much detail about the Fibonacci Series and the φ is because they appear to be fundamental in comprehending subtle energies. Understanding the mathematics of their numerous relationships could help to explain the creation and properties of subtle energies.

Feigenbaum's Constant and Chaos Theory

A second key universal constant and irrational number in subtle energy research is the Feigenbaum's number delta (δ), which equals 4.6692… It is usually found in bifurcations, chaos theory, and fractals. As will become apparent in this book, in nature, chaos can produce order!

Spirals, their Geometry, and Mathematics

Figure 5.2 illustrates an arithmetic spiral, where the gap between adjacent turns is constant (r). This spiral is often called an Archimedean spiral, but this is confusing as there is no obvious connection to Archimedes.
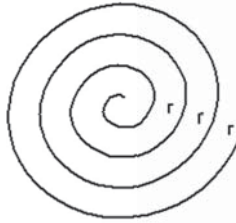
Figure 5-2 Arithmetic Spiral

Figure 5-3 shows a geometric spiral, where the gap between adjacent turns is double that of the previous inner gap; hence a geometric series, as explained earlier in this chapter. Although there are numerous other types of spiral, these are the simplest. Most of the experiments in this book result in spirals that are arithmetical.
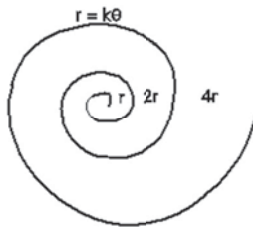
Figure 5-3 Geometric Spiral

Vortices

2-dimensional spirals and 3-dimensional vortices are some of the most common phenomena in subtle energy research. Although the shape in Figure 5–5 is more associated with physical phenomena, such as tornadoes and whirlpools, the simple cone, as in Figure 5–4, mainly appears in subtle energy research, and is found to be an envelope containing a helix. As they are so important, an entire chapter is later devoted to spirals and conical helices
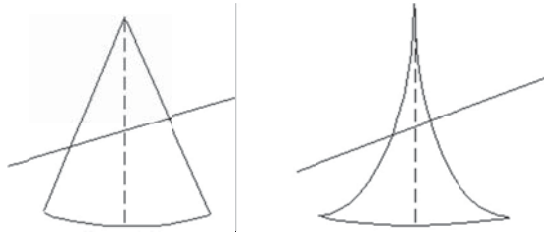
Figure 5-4 Conic Cross Section Figure 5-5 Hyperbolic Conic Cross Section

Cones have interesting properties. Examples include a plane slicing through a cone (a conic section) produces, on the plane, a circle, ellipse, ovoid, parabola, or hyperbola depending on the angle of the plane to the cone. This concept can be extended from a simple cone shown in Figure 5-4 to a hyperbolic cone in Figure 5-5, which is a three-dimensional extension when spun around either axis of Figure 5-1.

Many megalithic sites and stone circles are laid out in a horizontal plane on the ground, with a conic section pattern such as a circle, ellipse, or ovoid. This presents an interesting challenge for future researchers to determine what the connection is between these ground plans, conic sections, and the production of subtle energies.

Pythagoras Theorem

Pythagoras Theorem, as taught in schools, relates to the relationship between the areas of squares drawn on each of the three sides of a right-angled triangle. The simplest right angle triangles have the ratios:

- $1:\sqrt{2}:\sqrt{3}$, (as illustrated in Figure 5-6)
- $3:4:5$,
- $1: 2*\sqrt{2}: 3$, (as illustrated in Figure 5-7) and
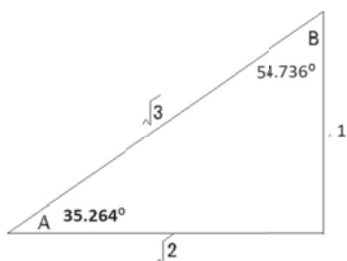- $5:12:13$.

Figure 5-6 1:√2:√3 Right Angle   Figure 5-7 1: 2*√2: 3 Right Angle
              Triangle   Triangle
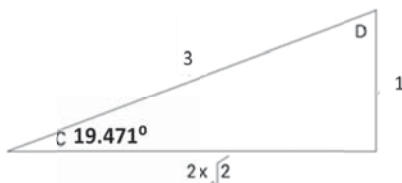
Square Roots

The square roots of 2 and 3 occur frequently in the geometry of subtle energies. The above Pythagorean triangles gives some clues as to why, and again this will be discussed later in the relevant context.

Angles in Subtle Energy Patterns

The angles **19.471°** and **35.264°** occur frequently in subtle energy geometry. Figure 5-6 is a Pythagorean triangle with sides 1, √2 and √3. The angle A is 35.264°. In Figure 5-7, another right angled triangle, has sides 1, a base of 2*√2 and a hypotenuse of 3. Angle C is 19.471°.

A part of future research strategy should be to investigate the connection between angles 19.471° and 35.264° and subtle energies.

Complimentary Angles

One of the useful properties of Pythagorean triangles is that their complimentary angles are also found in subtle energy research and analysis. The following are relevant examples:

- 35.264° = (90° - 19.471°)/2
- 54.735° = (90° - 35.264°).
- 54.735° = (90° + 19.471°)/2
- 109.471° =   (90° + 19.471°)

As is apparent, all the above angles have a relationship with **19.471°.**

The above angles 35.264°, 19.471°, 8.213° are often found in the **horizontal** plane. When one dowses in the **vertical** plane (e.g. apexes of

vertical cones), the following angles are found: 19.471° 11.537° 8.213°. The angle 19.471° is common to both of these series.

Trigonometry and Key Angles

When interpreting findings resulting from subtle energy experiments, it is not very convenient to use square roots of complicated numbers, or even angles whose values are irrational numbers. Using trigonometry is much more practical and useful when interpreting quantified findings. The following two arbitrary examples illustrate this.

On inspection of Figure 5–6, the angle A, opposite the side with a value 1, is 35.264°. By definition, this is the angle whose **sine (**arcsine**)** is $(1/\sqrt{3})$. It is found by experiment that 35.264° is part of a series of angles whose sines are $1/\sqrt{\,}$`n, where n is an odd number equal or greater than 3.

Odd Integer n	Arc Sine1/n			Even Integer n	Arc Sine1/n			Integer n	Arc Tangent 1/n*√2		
	Radians	Degrees			Radians	Degrees			Radians	Degrees	
								1	0.61547971	**35.2644**	°
3	0.33983691	**19.4712**	°	2	0.52359878	**30.0000**	°	2	0.33983691	**19.4712**	°
5	0.20135792	**11.5370**	°	4	0.25268026	**14.4775**	°	3	0.23147736	**13.2627**	°
7	0.14334757	**8.2132**	°	6	0.16744808	**9.5941**	°	4	0.17496905	**10.0250**	°
9	0.11134101	**6.3794**	°	8	0.12532783	**7.1808**	°	5	0.1404897	**8.0495**	°
11	0.09103478	**5.2159**	°								

Table 5-2 Arcsin odd 1/n Table 5-3 Even 1/n Table 5-4 Arctan 1/n*√2

As seen in Table 5–2, the first three key angles:-
19.471°, 11.537°, 8.213° are a series of angles whose sines are 1/3, 1/5, 1/7, 1/9…

In Figure 5–7, angle C, opposite the side with a value 1, is 19.471°. By definition, this is the angle whose **tangent** is 1/2*√2. Once again, it is found that 19.471° is part of a series of angles whose tangent is 1/n*√2, where **n** is an integer equal to or greater than 1. The angle 19.471° is also arcsine 1/3, and is part of a series of arcsine 1/n where **n** is an odd number.

When attempting to analyse the angles found in subtle energy patterns, I have found that Tables 5-2, 5-3, 5-4 are very useful.

The benefits of using trigonometry are apparent from this section. When analysing results from subtle energies, it is easy to identify if values are associated with a series of numbers, and then make predictions for further similar experiments.

At this point, it should be pointed out that there appears to be a lack of symmetry in the geometry of subtle energies. As we have seen earlier, geometric shapes produce subtle energy patterns with very different geometry to their source. But, if we start with that geometry, the subtle

energy generated by that pattern bears little resemblance to the original. Currently we do not know the mathematics of the transformation.

Zero

The concept of zero has two aspects. The first relates to the use of columns to facilitate counting in units, tens, hundreds, etc. The second is more relevant to our quest into consciousness in that it relates to *nothingness, or null*. Concepts such as *phase interference fringes* are key to understanding information and consciousness. These are areas where subtle energy fields cancel each other out to produce voids, and together with fields reinforcing each other, allow a method of storing information such as via holograms or a binary code.

Examples of Universal Constants, and Angles in Science

The above angles, having the trigonometric series of sines and tangents, have a much wider scientific significance than those found in subtle energies. A cursory internet search of academic papers, using Google Scholar, gives numerous other examples where these angles occur.

These include such diverse topics as:- columnar vortices, tornados, torroids, and whirlpools; cosmology; Ampere and dipole force laws and null-points; static and dynamic studies of polyhedral structures, Platonic solids and tetrahedral geometry; astronomical events on the surfaces of Jupiter and Saturn; statistical analysis of the size of birds; flight dynamics; chemistry and molecular structures; fluid dynamics, including bow waves and the Kelvin Wedge; climate studies; aging bone studies; cognitive behaviour; quantum mechanics for spin ½ particles in a magnetic field; etc

The following briefly elaborates on some of the above examples.

Magnetism

Figure 5-8 represents 2 bar magnets. Gauss discovered a neutral position where the north and the south poles cancel each other out. This angle is also 35.264°
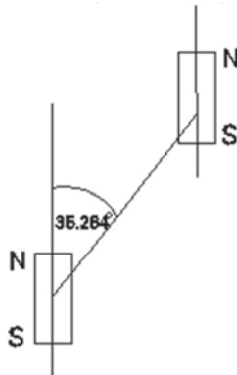
Figure 5-8 Two Bar Magnets

Fluid Dynamics

A ship moving through water produces a bow wave of angle 38.942°, which is twice 19.471°. This is also known as the Kelvin Wedge. Ripples on the bow wave are 35.264° to the direction of travel. A similar angle appears in aero dynamics where the sweep back of some aeroplane wings is 35.264°.

Molecular Geometry

The DNA helix has a slope angle of 35.264°. The bonding angle of the 2 oxygen atoms in the silica molecule is 109.471°. It cannot be coincidence that this angle equals 90° + 19.471°. **109.471°**, is the carbon bond angle in protein molecules.

Vesica Piscis

Any 2 circles that overlap will produce a Vesica: the Vesica being the overlapping area. A Vesica Piscis is produced when the 2 circles are of identical size and whose centres are located on the circumference of the other circle.
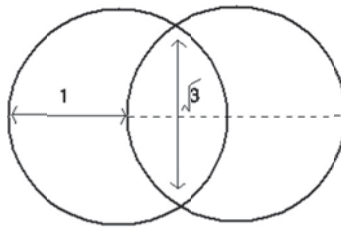
Figure 5-9 Vesica Piscis

This is depicted in Figure 5-9. If the radius of each circle is 1 unit then the vertical line down the centre of the Vesica has a value equal to √3. Ratios involving 1: √3 were discussed earlier. Vesica Piscis occurs frequently in ancient architecture, with the Gothic arch being a well-known example.

Pentagon/ Pentagram

Figure 5-10 represents a Pentagram and Pentagon and was briefly mentioned in the previous chapter. It can be seen that phi and combinations of phi appear on every part of the geometry. This is a simple example of fractal geometry, which is very important in advance studies of subtle energy.
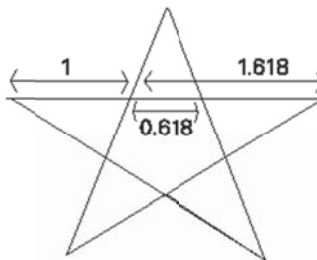

Figure 5-10 Golden Proportion in a Pentagram

Golden Egg

Oval or egg shapes appear frequently in nature. Stone circles are usually not true circles but horizontal ovals. The golden egg is defined as the ovoid where the length of the perimeter divided by the sum of the

lengths of the two axes equals phi. This applies to any cross-sectional plane through the centre of the ovoid. There is also a relationship between the four arcs that comprise a golden egg, the centres of these arcs, and a regular pentagon.

The Number 7 and Other Preferred Numbers

The findings of observations and experiments show a preference for numbers like 3, 4, 5, 6, 7, 9 and 12, which represent the number of subtle energy lines and curves forming a stable group. Examples include psi-lines, and the 9 and 7 shells in auras. As explained previously in Figure 4-1, subtle energy lines appear to possess a flow. To conserve energy, the combined flow in the outer 2 lines equals the flow in the opposite direction in the inner line. One particular example of this mathematical phenomenon is the number 7, which occurs frequently in nature as well as in worldwide cultures, such as the days of the week.

Missing Universal Constants?

However, a worrying unanswered observation is that Pi (π), the exponential or natural logarithmic constant (e), the speed of light (c), the fine structure constant (α) are rarely found in these quantified research results of subtle energies. Added to this concern is that all four of these universal constants are connected by several mathematical equations. This invites a reader to dig deeper!

Frequently Found Formulae, Equations and Graphs

This section is primarily for the non-mathematicians and covers the commonly found graphs and equations derived from subtle energy research. As there are not yet theories of consciousness and subtle energies, the relevant equations cannot be found by prediction, but only empirically. The intention, therefore, is to obtain experimental data as accurately as possible with high correlation coefficients and low error rates, and empirically fit it to the best mathematical curve. Historically, this method has been used to discover famous laws of physics.

It is vitally important, whilst dowsing and collecting the data, not to analyse it at the same time. In practice, this occurs, by necessity, because some of the experiments last many hours, months, or even years. Additionally, other unconnected commitments, or being on-site in remote

locations, result in the data being analysed weeks or sometimes months after it was collected.

The following are samples of using MS Excel to produce graphs that best fit the experimental data by using correlation coefficients. In statistics, the correlation coefficient **r** measures the strength and direction of a relationship between two variables on a scatterplot. The value of r^2 is always between 1 and 0. Very conservatively, I considered that correlation coefficients better than 0.95 were interesting, and above 0.98 I considered exciting! Results coming out at less than 0.90 I treated with suspicion. This is a much stricter criteria than is usually adopted in science.

Four types of scales for the x-y axes of the best-fit graphs that were produced, were found to be: linear, log, log-log, and polar diagram. Similarly, the 5 most frequent trend line formulae produced by Excel, for the resulting graphs, were linear, exponential, power, logarithmic, and quadratic. Examples of each of these are shown in Figures 5–11 a-j.

Figure 5-11-a is an increasing straight line, having an equation of the general form **y = a.x+c**. (where x and y are the variables and a & c are constants). Figure 5-11-b is a decreasing straight line, having an equation of the form **y = -a.x+c**. Both axes are simple arithmetical, with values increasing in equal increments.
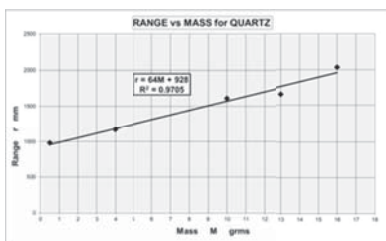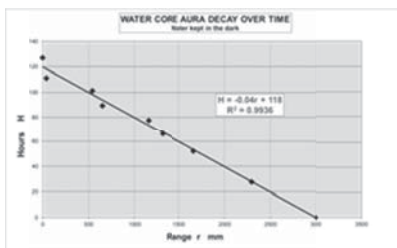

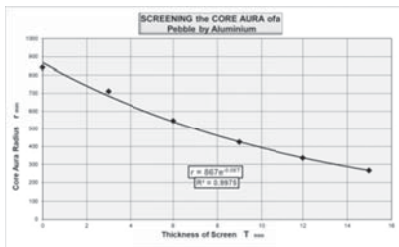Figure 5-11-a Increasing linear   Figure 5-11-b Decreasing linear

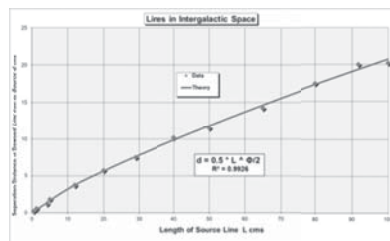Figure 5-11-c Decreasing exponential Figure 5-11-d Increasing exponential

Both Figures 5-11-c & d have similar simple arithmetical axes, but the data for both produce curves. Figure 5-11-c has a decreasing exponential curve of the form $y = a.e^{-cx}$. Figure 5-11-d is an increasing exponential curve of the form $y = a.x^c$.
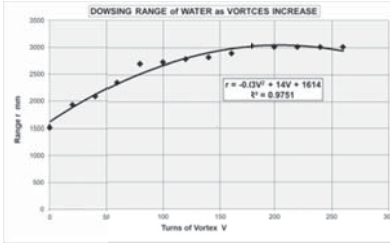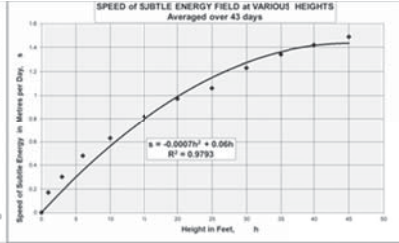
Figure 5-11-e   Figure 5-11-f
Increasing asymptotic curves approximating to quadratic equations

Both Figures 5-11-e & f also have simple arithmetical axes. However, they are both increasing asymptotic curves that approximate to a quadratic equation (of the form $y=a.x^2+b.x+c$) but only in the relevant data range.

Figure 5-11-g is increasing in a linear fashion (with a logarithmic form $y = a. \ln(x) + c$) but has a horizontal logarithmic scale, whereby the values escalate rapidly. Figure 5-11-h has both vertical and horizontal axes with logarithmic scales, and a power index curve is produced in the form $y = a.x^c$
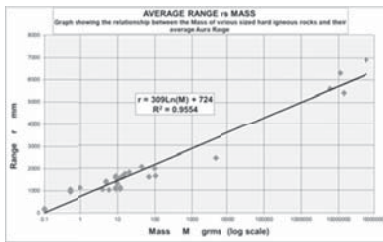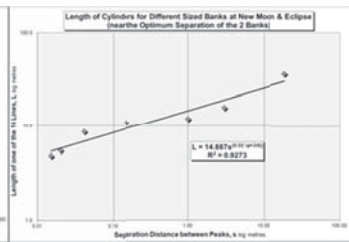
Figure 5-11-g   Figure 5-11-h
Increasing linear - logarithmic equation.   Increasing linear-power index equation

The objectives in both Figures 5-11-i and 5-11-j is not to produce equations and curves, but to plot the obtained data to assist interpretation of what had been discovered. Figure 5-11-i represents a sharp resonance trough, and is frequently found when exploring the subtle energies

involved with 2 or more body interactions. The corollary of this graph is a similar shaped sharp resonance peak, which is equally frequent.

The curve associated with Figure 5-11-j has been plotted with polar axes, and depicts the aura of a spinning object. It is readily seen that, in this specific experiment, the aura reaches a sharp maximum in the vertical N-S plain, and it decreases to zero in the E–W plain.
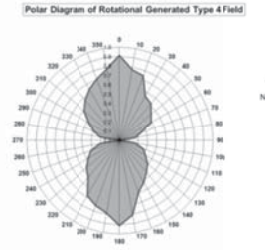
Figure 5-11-i   Figure 5-11-j
Sharp Resonance Trough   Polar Aura of a Spinning Object

Conclusion

In any scientific research, obtaining universal constants is the ultimate proof of a correct theory. As will become apparent, one of the objectives of this book is to find universal constants and key angles, resulting from the experiments and measurements discussed.

A long list of topics, unrelated to subtle energies but containing the same universal constants and angles was discussed in this chapter. It is, therefore, very reassuring that the study of consciousness, the mind, subtle energies, and the structure of the universe all lead to the same mathematics, geometry and universal constants.

Stone-age man probably had the ability to detect subtle energies, and understood instinctively many of the concepts in this book. For example, ancient man intuitively believed that the stone rings in a golden egg shape form an optimum configuration to remove detrimental earth energies, and increase the strength of the subtle energies that provided beneficial effects to improve their lives, crops, and their animals. This was the possible motivation for ancient man to build such large complex structures, as the perceived benefits for a rural based civilisation must have been considerable

However, during the course of this chapter there were numerous questions raised. It is hoped that these will provide specific challenges for

future research. For example, is it relevant for subtle energies, that all universal constants are also an irrational number?

The Way Forward

1. What is the connection between conic sections, and the production of subtle energies?
2. Investigate the connection between subtle energies, and the angles 19.471° and 35.264°.
3. The main two universal constants found empirically in subtle energy research, are the golden ratio, ϕ, and Feigenbaum's constant, δ. As subtle energy probably involves the structure of the universe, a theory for subtle energy cannot just involve these 2 constants. Existing data should therefore be reviewed, and new experiments performed to find additional universal constants.
4. Is there a connection between subtle energies and irrational numbers?

CHAPTER SIX

AURAS OF INANIMATE OBJECTS

Introduction

Auras are a very exciting and unique phenomenon that involves subtle energies. They surround every object on earth: be it inanimate, a life form, or even a shape of abstract geometry. There are no comparable phenomena in conventional science.

The size of an aura is a function of its source object's shape, size, composition, and mass. For example, as highlighted in Chapter 2, the subtle energy aura from a sharp or pointed end of an object has a longer range than the blunt or flat part of the surface of the same object. As with all subtle energies, auras are only visible in the normal sense by a few gifted people, but many more people can detect them noetically. When they are initially perceived and measured, experience dictates that they are interpreted as emissions from the source object.

However, on further investigation, the researcher gradually discovers that for many reasons they are unlike any other natural phenomena. For example, personal experience throughout one's life is that any emissions from an object reduce in intensity as one moves further away from the source object. This applies to heat, light and other electromagnetic fields as well as to gravity or even odours.

However, unlike the emissions described above, subtle energies and auras in particular, possess a constant field-strength with a very unnatural sudden sharp boundary. There is no gradual fade-in or fade-out, nor does the dowsing reaction obey the inverse square law.

The researcher now becomes even more curious about auras, and starts thinking about external factors. However, in practice, this precise delimiting boundary is very useful when making accurate scientific measurements.

Seven Concentric Boundaries

The simplest auras are those for solid inanimate source objects, such as stones and crystals. Fundamentally, dowsing solids produces a pattern centred on the source object, comprising seven distinct fields.

A dowser walking along the ground, away from, or towards an object from different directions, initially obtains the impression of 7 dowsable sensations, and builds up a two-dimensional impression of 7 rings each approximating to an asymmetrical circle, or ellipse. These 7 concentric rings are centred on the source object, as shown in Figure 6-1.

Figure 6-1 The 2-D Projection of an Aura of a 7 Shell Asymmetrical Ovoid

On further investigation, it is eventually discovered that auras comprise 7 sets of 3-dimensional ellipsoids of subtle energy, inside each other, expanding outwards giving the impression of 7 shells. In attempting to understand the physics of auras, and search for clues, it may be helpful to compare these discreet rings to other phenomena in nature.

The simplest analogy is to planetary orbits around the sun, but these are in a 2-dimensional plane. Perhaps even more relevant are electron orbits around the nucleus of an atom. These are restricted to precise shells, which are determined by quantum physics. Another analogy is circular waves, such as those produced by a stone thrown into water. These waves move outward if the pond is open, but standing waves are produced in, say, a closed circular vessel, where the waves reflect from the boundary towards the centre. Other examples of standing waves include those produced when vibrating a membrane, such as a drum skin. None of the above physical alternatives seem to explain auras, and this leaves the possibility of extending quantum physics, so it applies to the macro physical world.

Figure 6-1 also defines the numbering system used. In this definition, the core aura is the innermost subtle energy shell nearest to the surface of

the source object, and is numbered Field 1, whilst the other components can be referenced as Fields 2 to 7. Table 6-1 clarifies the convention of the terms used.

More detailed measurements (using a needle as a pointer and the mind's-eye to detect subtle energy, rather than relying on the slow response of rods or pendulums), confirm that sharp boundaries are being detected. Figure 6-2 is a polar diagram of the 7 fields within the aura produced by an arbitrary pebble taken from a beach.

Boundary Number	Field Number	Comment
0-1	1	Core aura
1-2	2	
2-3	3	
3-4	4	
4-5	5	
5-6	6	
6-7	7	Outer most field

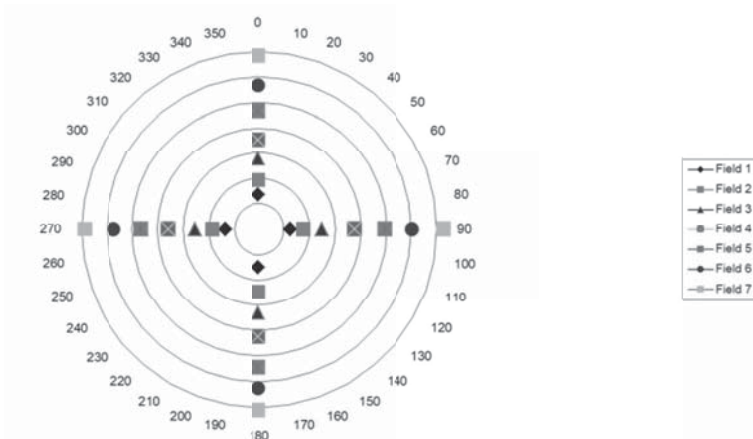**Table 6-1 Referencing Aura Fields**

Figure 6-2 Accurate Measurements of a Pebble's Aura in a 2-D Plane

As is apparent from Figure 6–2, distances were measured in four horizontal directions - north, south, east, and west. As the source is an irregular stone, the aura is not perfect, nor are the concentric circles evenly spaced. For example, the north and the west 0º and 270º points for field 4 lie within the 3rd & 4th circle, whilst the easterly point lies 90º on the edge of the 4th circle and the southerly point 180º is outside the 4th circle. As will be discussed later, this asymmetry is normal.

Ignoring environmental perturbations, that will be discussed later, from these and other examples based on observations and measurements, the mass and the substance of the source object determine the overall **size** of its aura, whilst the **shape** of the core aura i.e. Field 1, is significantly determined by the shape of the source object. However, the geometrical shape and pattern of the remaining series of 6 Fields, although approximating to ovals, are not so dependent on the source object. In fact, rotating any source object through 360º does not seem to change the aura's pattern, as Fields 2-7 retain the same geometrical shape with the identical separation distances. Again, this suggests external factors

Colours

Each shell of an aura is associated with a colour, which can be ascertained by using a Mager disc. Of all the scientific measurements of auras, colour is by far the most subjective and contentious. At best, people see colour differently. As an example of this, Table 6-2 gives the colour components of the aura of the same hematite crystal, as observed by 3 different people; one who unaided could actually see the colours; one who could perceive a sensation when using a Mager disc; whilst the third person used L shaped rods with a Mager disc.

Ring Number	A Visual 5 May 03 14:00	B Dowsed - Mager Disk 29 June 03 22:00	C Dowsed - Mager Disk 19 July 03 11.00
1	Yellow	Mauve	Yellow & Red
2	Yellow & Green	Green	Yellow & Green
3	Orange	Yellow	White
4	Red & Purple	Ultra-violet	Ultra-violet
5	White	White	Ultra-violet
6	Dark Blue	Red	Blue
7	Twinkling Lights	Blue	Ultra -violet

Table 6-2 Hematite Aura Colours

It is apparent from Table 6-2 that there is a moderate correlation between the three sets of measurements. Five out of seven rings have two out of three of the colours very similar. The correlation would probably have been greater if it was not for the fact that the measurements were taken independently, at different times, by different people, in different locations with local environmental influences, and probably differing states of charge of the hematite crystal.

However, the main conclusion of this section on colour seem to reinforce the view expressed earlier that auras do not comprise 7 thin shells but are 7 distinct fields - like a set of Russian dolls, one inside the other. This means that auras are not analogous to interference fringes.

Arms and Spirals

The 7 elliptical fields discussed so far are only part of auras. In addition, there is an outer series of spirals lying on 6 arms. Figure 6-3 is a pictorial representation of this outer pattern. Each arm contains a series of spirals, which seem to extend to infinity (this is obviously difficult to prove, but in practice these spirals seem to extend well beyond 100 yards without any diminution). Along each arm, the spirals are alternatively in a clockwise and anti-clockwise direction. Similarly, they are alternatively spiralling upwards and downwards. All 4 combinations of up or down and clockwise or anti-clockwise are possible.

Figure 6-3 Spirals on 6 Arms of an Aura

.
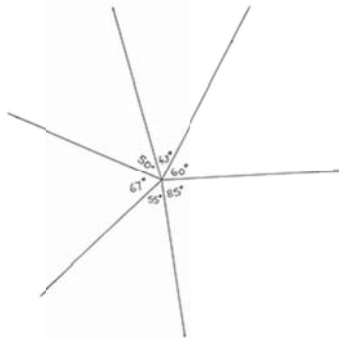
Figure 6-4 Angles between the 6 Arms Containing the Spirals
of a Hematite Crystal

The orientation of the 6 arms (with reference to, say, north) seems to be determined totally by the local environment and not by the source. Further research is required to establish what determines the orientation and geometry of these 6 arms with respect to, say, the north. Is it simply the geographical location, or the composition of the earth locally, or local man-made constructions?

As before, if the source is rotated through 360° there seems to be little impact, if any, on the geometry of the spirals. Moreover, the angles between the arms are not regular. As seen in Figure 6-4 each of the 6 angles are not exactly 60°, possibly a consequence of the source not being a perfect sphere

Figure 6-5 is the superimposition of the above 3 Figures giving the overall effect, and to illustrate the geometry of the "spider web" pattern. As also can be seen from Figure 6-5, the 6 arms radiate from the centre of the source object. The spirals start between the third and seventh boundary but depend on the substance and asymmetry of the pattern of ovals.

Figure 6-5 Inner Ellipses and Outer Spirals of an Aura

Decay

If any source object is deprived of light (i.e. kept in a sealed box in a dark drawer), the core aura, followed by the associated ovoids, disappear gradually at first but completely within about 3 days. Figure 6-6 illustrates this decay to zero, over a 120-hour period, from a 3-metre core aura produced by 1.0 litre of water. (When dowsing this decay, it is important to phrase the dowsing question to ensure one is not detecting remanence, i.e. mind's intent must be to ask for the state of the aura now, not as it was in the past). After the core aura has disappeared, the other boundaries are still detected until they too gradually disappear. As the aura collapses the relative distances of the component ovoids stay approximately the same, i.e. the aura gives the impression of being sucked into the centre analogous to a black hole. During decay, the colours comprising the aura may change.

As is apparent from Figure 6-6, the graph of water decay is a linear relationship of the form

$$r = -0.04H + 120 \qquad\qquad (i)$$

where **r** is the range of the core aura, and H are the Hours.

There is a very high correlation coefficient of

$$R^2 = 0.9888$$
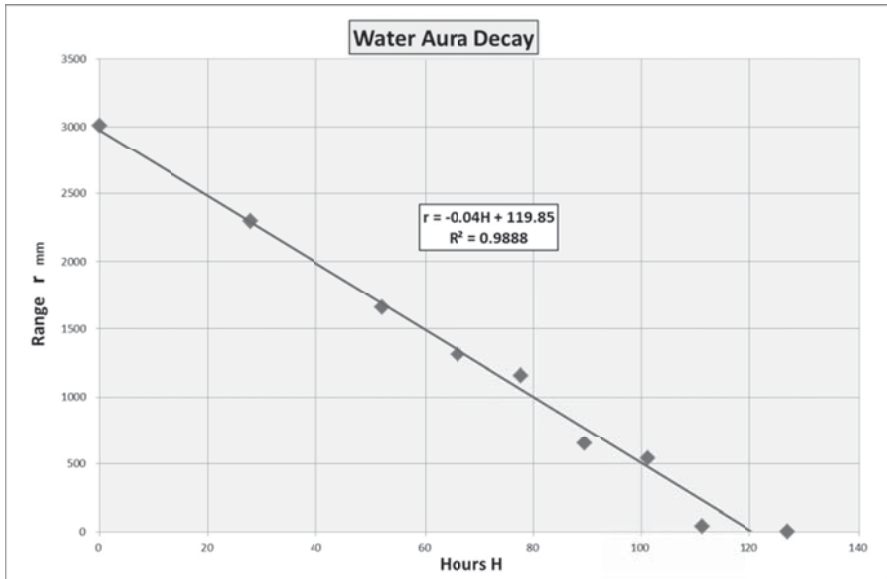
Figure 6-6 The Decay of the Aura of Water Kept in the Dark

Recharging an Object's Aura

The corollary of the above decay is that it is relatively easy to re-charge an object so its aura returns to its original dimensions and properties. One way is to place the object in direct sunlight for a day, especially on bright days when there is plenty of ultraviolet light.

Table 6–3, and Figure 6–7 illustrates how the aura of a fluorite crystal expands from the surface of the crystal with an initial value in the shade of 7.13 mm, to a value in bright sunshine of 51.25 mm, asymptotically in 105 minutes. This is an expansion of 619%.

Another way is to place an object in close proximity to another object, which already has a large aura. The fastest recharge I have achieved is with a selenite crystal, by placing it between the palms of one's hands and place it on the crown or solar plexus. Interestingly, this can take just a few seconds, but the selenite can completely discharge in minutes!

Time in Bright Sunshine	Distance of Core Aura from Surface				Average Distance	Deviation	% Deviation
Minutes	mm	mm	mm	mm	mm	mm	%
0	7.5	6.5	7.0	7.5	7.13	0.38	0.053
15	26.0	25.5	25.0	24.5	25.25	0.50	0.020
30	35.0	35.5	35.0	35.0	35.13	0.19	0.005
45	39.0	39.5	41.0	40.0	39.88	0.63	0.016
60	45.0	45.3	45.0	45.0	45.08	0.11	0.002
75	48.0	47.5	48.5	48.0	48.00	0.25	0.005
90	51.0	50.0	50.5	50.0	50.38	0.38	0.007
105	51.0	51.5	51.0	51.5	51.25	0.25	0.005

Table 6-3 Expansion of a Fluorite Aura in Increasing Sunshine
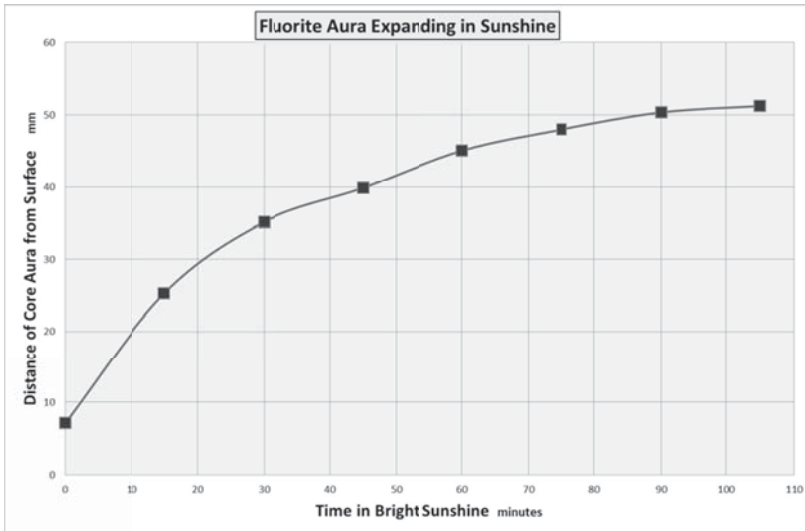
Figure 6-7 Fluorite Aura Expansion from Shade to Sunshine

Stability of the Spirals on the Arms

An interesting result of this decay experiment is that although the 7 ovoids disappear after approximately 3 days of darkness, the outer spiders-web of spirals is unaffected. After the 7 ovoids of an aura have decayed to nothing, all properties of the remaining spirals appear to stay the same, i.e. the dimensions in Figure 6-3 remain the same after the aura's ellipsoids decay, as do their locations, their field strengths, their colours and their

spin directions. This has been confirmed for many different objects. In one case, even after total decay of the aura, up to 20 spirals on an arm have been measured over a distance of about 100 yards.

A further interesting phenomenon can be demonstrated with the outer spiral structure, by taking two similar sized stones (e.g. green moss agate each of mass 6 grams). If these two stones are separated by multiples of 100mm apart, the pattern of spirals cancel out, and the entire spiders-web disappears. This phenomenon may be easier to see if the source stones have been kept in light-proof containers for over one week, so that the seven ellipsoids part of their auras have decayed, and only the outer spiral structure remains.

Attenuation, and Screening by Metals
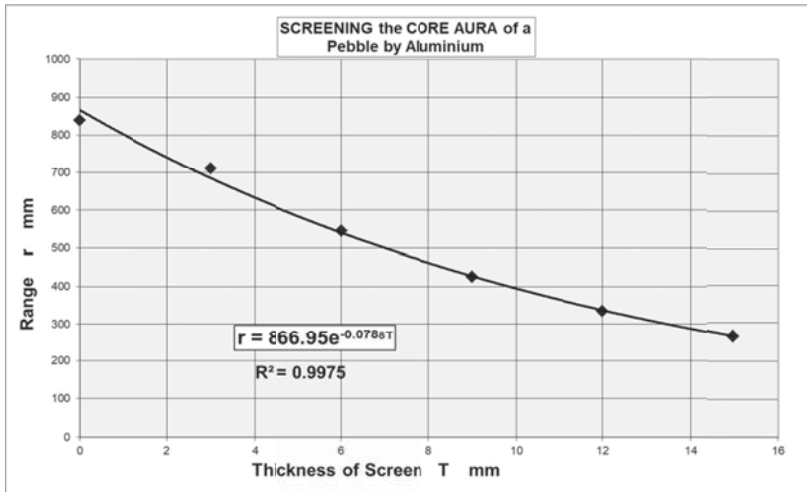
Figure 6-8 Screening of a Pebble's Aura by Aluminium

Although auras pass through air or walls without significant attenuation, metals may attenuate and shrink all seven-aura fields significantly. Figure 6-8 illustrates for a core aura, the effect of placing a charged pebble in aluminium containers of different thickness. As the thickness increases, the range of detectable subtle energies, **r,** decreases towards zero i.e. **r** decreases as a function of the screening metal's thickness **T**. A similar effect occurs with stainless steel. This suggests a generalised equation of the form:-

$$r = r_a.e^{-sT} \qquad\qquad\qquad (ii)$$

Where r = Range; r_a = Range in air without any screening; T = Screening thickness; s = the screening constant for different materials.

Spin and Rotation

Spin is a fundamental property of the universe, be it galaxies, or down to the interiors of fundamental particles. Spinning an object increases the size of its aura. In one particular experiment, a small hematite crystal at rest had a core aura radius of 460 mm. If this was kept spinning on its own axis at the rotational speed of, say, a food processor, the aura increased by about 300 mm to 760 mm, i.e. an increase of 65% in the size of the core aura. Interestingly, the source object does not retain this extended aura; it returns immediately to its rest size as soon as rotation ceases.

Pressure

The INCREASE in CORE AURA of a FLUORITE CRYSTAL vs APPLIED PRESSURE
Log P and log r scale. Log Log Curvilinear relationship

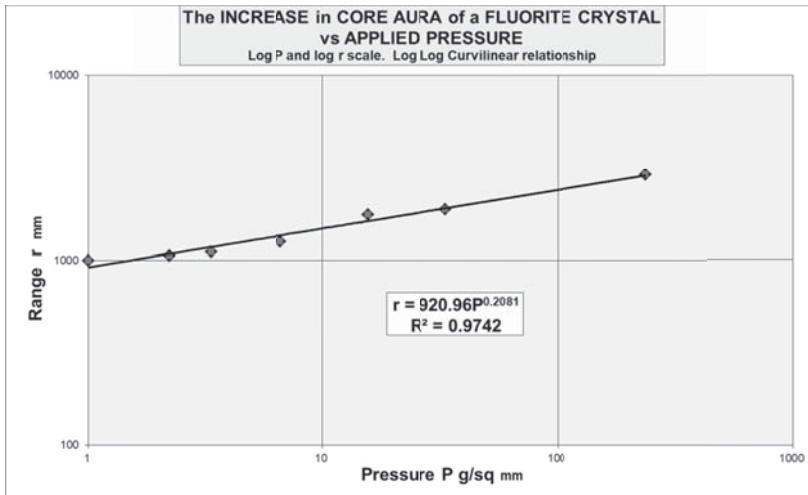$$r = 920.96P^{0.2081}$$
$$R^2 = 0.9742$$

Figure 6-9 Effect of Pressure on an Aura

Squeezing source objects extends their auras. For a core aura of a fluorite crystal, Figure 6-9 is a graph showing that the log of Pressure P, vs. the log of Range r, gives a straight line. The generalised equation is of the form, where "a" is a constant dependent on the source material:

$$r = a.P^{0.21} \qquad\qquad \text{(iii)}$$

with a very high correlation coefficient of 0.97.

This illustrates that pressure has a significant effect on auras, and can increase their size exponentially. In this example, the radius of the core aura of 1,000 mm at normal atmospheric pressure is increased three-fold, to 3,000 mm, when the pressure is increased from 1 gram per sq. mm to about 240 grams per sq. mm, i.e. a 3 times increase of pressure results in a 240 times increase in the aura size! This invites the question "is this aura increase happening at the molecular or atomic nucleus level".

The Aura's Source and Dual Representation of Auras

This section discusses the dowsable structure attached to the surface of any solid source object, and how this relates to the object's aura. It is well know that megaliths consist of 7 horizontal dowsable bands linked with an associated vertical up or down spiral(s). This was discussed in Chapter 4, Figure 4–6. It would seem this structure applies to most solids. This is a different concept to the seven ellipsoids, outer arms, and spirals comprising the source object's aura, as discussed above. This is an additional set of subtle energies, and is a key part of the source object's aura.

In order to obtain a sufficiently long source object on which to perform this experiment, a bamboo cane of about 1 metre in length was used. Figure 6-10 illustrates a typical structure. This comprises 7 bands (marked a-g) of alternate positive and negative subtle energy, coupled with a different type of field that forms one turn of a spiral along the object's length. To avoid complexity, this is not shown in Figure 6-10
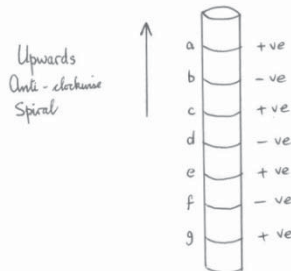

Figure 6-10 The Distribution of Subtle Energies Over the Surface of Objects

In this example, the externally detectable spiral within the source is upwards and anti-clockwise when looking down from the top, and it is assumed that this spiral field returns downwards inside the solid fabric of the source object. The subtle energy associated with the 7 bands and a spiral are confined closely to the object's surface. Each of the 7 bands only extends to a maximum of about 5mms from the surface, whilst the single spiral does not even extend from the surface.

As already discussed, a source object deprived of light loses the ellipsoidal part of its aura after a few days but retains its outer spirals. An analogous phenomenon applies to the 7 bands and spiral on the surface of the source object. When the ellipsoids have vanished, so have the 7 bands. However, like the outer spirals, the surface spiral remains unaffected and intact. This suggests that the 7 bands are closely linked (a) to the 7 aura ellipsoids and (b) to photons and electromagnetic forces. Furthermore, the outer "spider-web" of spirals would seem to be closely linked to the surface spiral on the source object. The latter two phenomena would seem to be produced by non-electromagnetic forces or fields.
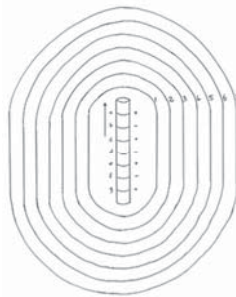
Figure 6-11 Aura Source Fields and Ellipses

Rotating Figure 6-11 around its vertical axis shows the 3-dimensional composition of the 7 ellipsoids of the bamboo cane. (It is easy to rotate a bamboo cane to check the 3-dimension structure of the aura). This shows that the centre (foci) of all 7 ellipsoids is at the physical centre of the rod. It is **not** like Figure 6-12 which would apply if each of the 7 bands separately produced an aura boundary. Table 6-3 gives a relationship between the aura number, 1-7, and the bands, a-g.

Figure 6-12 Wrong Model for the Interaction Between a Source and Its Aura

Aura Ovoid Number	Source Field Band
1	g
2	f
3	e
4	d
5	c
6	b
7	a

Table 6-3 Relationship between aura fields and source bands

Further proof that this relationship exists is obtained if the cane is turned through 180º around a horizontal axis, as shown in Figure 6-13. As expected, the fundamental subtle energy structure of the source remains unchanged with the upward anti-clockwise spiral (as illustrated in Figure 6-13 becoming a downward clockwise spiral, with the positive and negative bands remaining the same. The aura relationship is the same as Table 6-3.
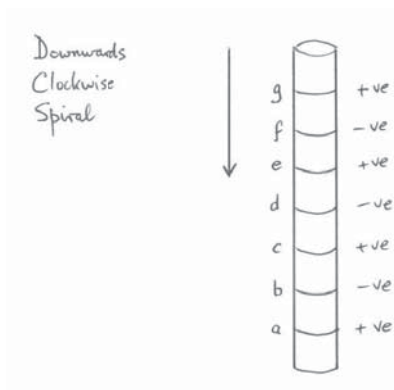
Figure 6-13 Inverted Source

Auras of Water and Vortices

The auras associated with water are, in general, the same as for stones and crystals as discussed above. However, being a liquid, vortices can be created. This results in the aura being more complex. The graph in Figure 6-14 illustrates this and shows that spinning water can double the size of its core aura, in this case from 1.5m to 3.0m asymptotically. Shaking the water in any direction has no effect – only creating vortices does.

Figure 6-14 Increase in Water Aura when in a Vortex

The Weird Effect of an Arrow

An arrow (irrespective of how it is produced, the medium used to create the arrow, and the medium on which the arrow is drawn, are irrelevant). The direction of the arrow will affect the size of any aura: whether the aura is from a crystal, a coin, a plant, or even a television. An outward pointing arrow produces a larger aura in the direction of the arrow. An inward pointing arrow reduces the size of the aura and appears to "push" the aura away from the viewer.

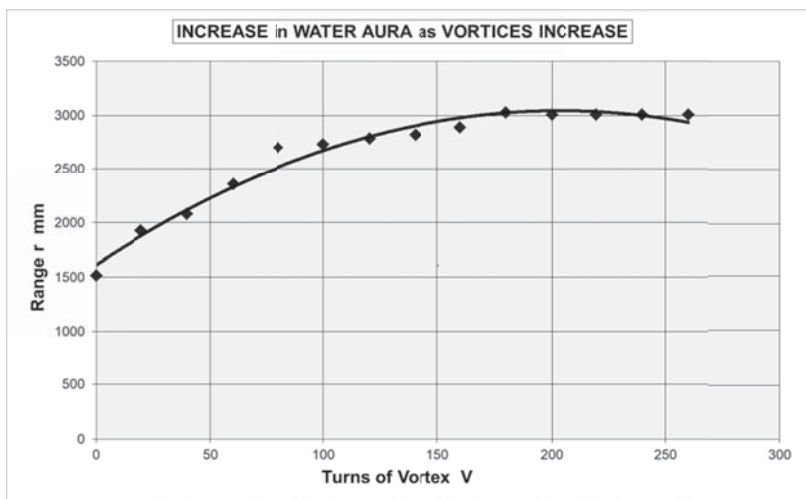The obvious question is "how does the geometry of an arrow, either in the form of a solid object or abstract drawing, affect an existing aura?"

Summary and Conclusions

Nature seems to have created auras of inanimate objects that comprise at least 5 complementary but differing fields.

1. The first field clings closely to the surface of the object, which manifests itself as 7 horizontal bands.
2. These 7 bands are linked by at least 1 vertical spiral having a differing form of subtle energy.
3. The middle part of an aura manifests itself as seven concentric approximate ellipsoids, the shapes and sizes of which can readily be changed by both the source object itself and its environment.
4. An outer pattern of six arms, which appear to be extending from the centre of the source to infinity.
5. On each of these 6 arms are a row of vortices that also seems to go on to Infinity.

Auras have a complex system of colours with each shell comprising different colours, which is further complicated because one shell is inside another shell, like Russian dolls.

Auras can shrink in darkness with a relationship $r = -0.04H + 120$, and can totally decay after about 5 days in darkness. On the other hand, light can "recharge" and expand auras, typically within 2 hours, and similarly can be recharged, when objects are placed adjacent to another strong existing aura.

Another property of some auras is that they can be attenuated, and screened by metals, with a formula of the form $r = r_a.e^{-sT}$. When 2 objects are close enough, their auras can interact, and as they are separated, null points are produced, where their auras disappear.

When objects are spinning on their axis, or by rotation in, say, an elliptical path, their auras increase. Auras of liquids have an additional property caused by their ability to form vortices, where stirring them can relatively quickly double their aura size. When an object is put under pressure its aura expands with the relationship $r = a.P^{0.21}$.

Yet a further complication is that auras can be affected by external geometry. An example of this is an arrow pointing towards an aura tends to push it away, while an outward pointing arrow expands the aura.

Fields in paragraphs 1 and 2 above, involving 7 components, are fundamentally affected by light, but the spirals in fields 1 and 3 above are not. The entire complex three-dimensional geometrical patterns of auras further demonstrate that intuition may be wrong, as source objects are not necessarily "radiating" subtle energy. This is apparent because there is no inverse square law being obeyed, and an "infinite" number of spirals are produced by an "infinite" amount of radiating energy.

The fact that auras readily respond to so many influences, makes them an excellent tool for scientific research purposes. Complexity and manifestations of auras lead to the conclusion that they are created by the interaction between any object, with the cosmos.

The Way Forward and Suggested Research Areas

1. What are auras?
2. What do colours represent?
3. Why 7 rings?
4. Why 6 arms?
5. What determines the orientation, geometry, and angles between these arms?
6. If the source is rotated, why is there no impact on the geometry or orientation of the object's aura?
7. Is there a theoretical reason why this spirals on the arms start between the 3rd and 7th boundary of the auras ellipsoids?
8. What is physically happening between electromagnetic light radiation/photons and atoms or molecules of the source object?
9. After the 7 ovoids of an aura have decayed to nothing, why do all the properties of the remaining spirals appear to stay the same?
10. If 2 objects are separated, at certain separation distances the pattern of spirals cancel out, and the entire spiders web pattern disappears. Even if the source has been kept in a lightproof container, so that all the 7 ellipsoids in their auras have decayed, why does the outer spiral structure still remain

11. Although auras pass through air or walls without significant attenuation, metals can attenuate and shrink all 7-aura fields. Why?
12. What is happening at the molecular or atomic nucleus level, when the pressure (P) increases the aura size (r) in a log **P** log **r**, curvilinear relationship?
13. How does an arrow, irrespective of how it is produced, and the medium used, affect the size of any aura, depending on which way it is pointing?

CHAPTER SEVEN

AURAS OF PLANTS AND HUMANS

Auras of Plants - Introduction

The auras of plants are similar to solid objects and water as discussed in the previous chapter, but with additional and interesting factors. Such an example is that the size of a plant's aura will depend on the plant's own size and health, including its hydration. However, much more profound findings suggest that plants can show signs of consciousness. An initially unbelievable example is that the size of a plant's aura expands significantly if, say, a sealed glass container of water is brought close to, but not touching the plant. It is apparent that plants as well as animals appear to have paranormal powers and can interface with subtle energies and the cosmic information field.

Communicating with Plants

Although counter intuitive, this section contains the background and protocol for what could be called a basic 2-way communication between the human mind and plants via their auras.

Numerous instances of plant-plant communication have been recorded over the last few years. Relevant searches in Google produce over 7 million results! Most reported research relates to plants being under attack, such as, by insects, and the plant communicating with and warning other plants of the danger. One of several communication methods is by plants producing certain chemicals as a defence mechanism, that other plants subsequently produce in anticipation of attack. However, this could be interpreted as normal evolution.

Research into plant-human communication is much rarer. Examples include the use of lie-detectors, or inserting probes into the stem of a plant and measuring potential differences. Physical stimuli that have been used include drought (e.g. depriving the plant of water), incisions (e.g. cutting into a plant's stem or a leaf), or chemical intrusion (e.g. adding abnormal levels of acid or alkaline to the roots' compost). These examples cannot

really be classified as 2-way communication as they are primarily 1-way passive observations of a change of state.

The advantage of using auras in quantitative scientific research into conscious communication is that measurements of aura size are not only easy to make, but can even achieve an accuracy of a few millimetres. At present, machines are unable to do this as well as the mind. In the previous chapter, we have seen that animals can expand their auras when in positive conditions, and contract their auras when threatened. Is it possible that plant auras possess a similar capability?

Experiments, Protocol and Findings

For over 20 years, I have both witnessed and given demonstrations to numerous people of the mind's ability to communicate with plants via their auras. Initially, it is preferable to use a yes – no binary interaction. It is important in these experiments that several independent people partake, witness, and make measurements to avoid dowsing one's own thoughts! As usual, it is essential to calibrate one's dowsing response by asking un-ambiguous questions and note the response. For example, an expanding aura means yes, while a contracting aura means no. Some of the experiments that have been demonstrated, using the above findings, include the following:-

The aura of a plant expands significantly when water is brought towards the plant: seeming to imply "pleasure". The adopted protocol must eliminate the possibility that a simple chemical or physical reason is involved. For example, the plant could be detecting molecules of water from evaporation. This can easily be eliminated by containing the water in a sealed bottle, placing it in a black container, and keeping the water at least half a metre away from the plant. Significantly, this added protocol makes no difference to the original "pleasure response" of an expanding aura. It is not obvious how the plant knows about the presence of water; creating apparent telepathy.

If a person gently strokes the leaves of a plant, or is thinking soothing thoughts, or even saying how attractive the plant looks, the plant's aura immediately expands significantly. Similarly, applying fertiliser to the plant increases its aura.

On the other hand, if a person approaches a plant carrying, say, secateurs or a knife with the intent of damaging the plant, the plant's aura immediately collapses, implying "fear" and a defensive mode. However, if that person moves away, the aura recovers. How does the plant know?

These examples illustrate that plants possess not only a basic sense of consciousness but also a greater awareness of their environment than previously thought, including the human or animal mind's intent. It is, therefore, possible to have rudimentary communications with plants using similar techniques. Elementary but extensive communication with plants can involve asking such binary questions as:

- Do you need watering?
- Do you need fertiliser?
- Are you receiving sufficient light in your current position?
- Is your present position too drafty?
- Is your present position too hot?

Human Auras

This section is confined to scientific three-dimensional geometry of the human aura, not to the higher levels of spiritual or emotional aspects of human thought and behaviour. In general, the auras of humans are the same as solids, crystals, water, and plants as discussed above, plus the following additional factors.

People (and probably most animals) have conscious control over the size of their auras. For example, someone wishing to become introvert can collapse all 7 of their ovoid fields into a small aura extending over a few feet. However, an extrovert can extend their auras for distances possibly over 100 feet. An example of this is a performer in front of a large audience who can extend the realms of their aura to the back of the auditorium. I have witnessed this on many occasions, and taken measurements to prove this phenomenon is genuine. This is an example of consciousness affecting auras.

Similarly, being ill can significantly contract one's own aura. Some people, who can see colours and patterns between the 7 ovoid boundaries, are able to relate this to the person's state of health, such as blood pressure, or depression. At a meeting, I witnessed a person unexpectedly being told that because a certain ovoid in his aura was a specific non-standard colour, he probably had cardiac problems. Subsequent hospital tests confirmed this diagnosis was correct, which eventually lead to heart surgery!

The ellipsoids of the normal human aura are concentric to the spine. If someone has had, for example, a car accident or fallen over badly, their aura may become displaced so that it is, say, in front or behind them. The mind can be used to centralise displaced auras.

A person positioned over a subtle energy line is another factor affecting the size of a person's aura: detrimental energy may cause an aura to shrink and have an adverse effect on health. Just by using the mind to move the detrimental subtle energies, I have witnessed several people's health improve as a result.

Chakras

As mentioned earlier, for inanimate objects, the seven internal bands only extend a few millimetres from their surface and are alternatively positive and negative. For humans, however, the chakras seem to radiate outwards in a conical shape, which can be influenced by consciousness and intent. For example, the angle of divergence and distance of detection and influence can be readily changed by differing emotions. The shape of chakra "radiation" can simply be drawn by placing both horizontal and vertical 2 dimensional surfaces at different distances from the spine, and using a pen as a pointer, dowse the shape of each chakra field.

Table 7-1 illustrates the connection between the chakra and the aura number. As a cross-check, a search of the traditional spiritual orientated literature relating to chakra and aura colour confirms this Table. The colour connection between chakras and auras is very subjective, variable, and may only be relevant to a "normal healthy person". It is, therefore, surprising to a sceptical scientist that all the literature refers to identical chakra colours, which may simply imply that everyone is copying the same source texts!

Although I may obtain slightly different colours when dowsing, the connection between chakra name and aura number is the same. Moreover, assuming a vortex flow, the dowsable field around the outside of the spine is upwards, and by inference downwards inside the spine, making Table 6-2 compatible with Table 7-1. This is further supported by the fact that the colour of the chakra matches the colour of the associated aura field.

Chakra Name	Chakra Colour	Aura No.	Aura Colour
Crown	Mauve/ Indigo	7	Violet
Brow	Dark Blue/Violet	6	Dark blue/Violet
Throat	Blue	5	Blue
	Green	4	Yellow-Dark blue
Solar Plexus	Yellow	3	Yellow
Sacral	Orange	2	Orange
Base	Red	1 Core	Red- Yellow

Upward Flow

Table 7-1 The Connection Between Chakras & Auras

It is a sobering thought, subject to the above qualifications, that the basic structure of the human aura and chakras are no different in principle from, say, a bamboo cane! However, unlike inanimate objects, humans possess consciousness and intent that enables them to alter their own and other peoples' auras and chakras.

The Tree of Life - Brief History

The Tree of Life pattern is usually associated with Kabbalah and is often thought to be between 500 - 1000 years old. But it could have been developed from Jewish mysticism originating from the time of Ezekiel and Isaiah, making it nearer 2,500 years old.

Figure 7-1 below is a medieval example, and Figures 7-2 and 7-3 are two more modern examples of tree of life patterns, which have been selected at random from the internet. They all have a similar geometric shape of 10 linked circles. The examples in Figures 1 and 2 have their Hebrew names in the circles, whilst the Tree of Life in Figure 3 has circles numbered for convenience.
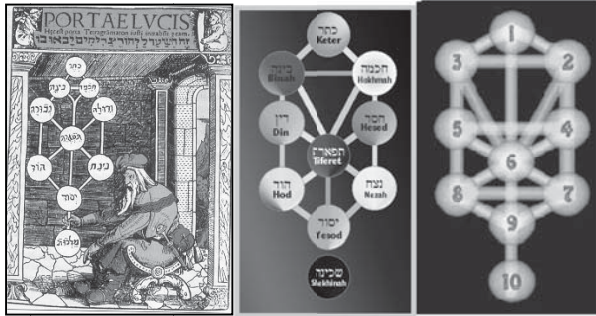
Figure 7-1   Figure 7-2   Figure 7-3
Examples of tree of life patterns through the ages

Producing a Tree of Life - Theory

But where does this Tree of Life pattern come from? Not many people are aware that it can be obtained by dowsing any living plant or animal. The Tree of Life geometry is yet another manifestation of the phenomenon of auras, which only life-forms have, in addition to all the other aura properties discussed so far in this book.

Usually, the Tree of Life pattern can be plotted horizontally on the ground, whilst Chakras are a vertical concept, but are a manifestation of the same aura phenomenon. Using the numbering in Figure 7-3, Table 7-2 shows the transformation between the seven chakras and the Tree of Life circles, which more accurately, have a spiral and vortex structure. Note the *Chokmah,* on the top right numbered 2. This is produced by the Brow chakra and the mind. Interestingly, Kabbalah correctly associates it with wisdom. This is supported by some of the following experiments.

Chakra	Vortex Number(s)
Crown	1
Brow	3, 2
Throat	5, 4
Heart	6
Solar Plexus	8, 7
Sacral	9
Base	10

Table 7-2 Connection Between Chakras and the Tree of Life

Producing a Tree of Life - Actual

For any particular person, living animal, or plant, an easy method of producing a specific Tree of Life is to start by detecting the location of the base circle, 10, as illustrated in Figure 7–3. As will eventually be discovered, the person whose Tree of Life is being plotted is standing between circles 1 and 6, and facing circle 1 in Figure 7-3. The first observation is that circle 10 (like all the other circles) dowses as a spiral. Standing at the centre of each spiral one can pick up the interconnecting lines, and follow them to the adjacent spiral. The horizontal size of the Tree of Life is about twice the height of the associated person.

On further measurements and analysis, the "circles" superficially appear to be Archimedean spirals comprising 3½ turns, but more correctly are 3-dimensional conical helices, in which the helix forms an envelope around an inverted cone. As spirals are so important and complex, they are treated in detail within their own Chapter 18.

Mood/Thought Transference

The Tree of Life has interesting properties, one of which is the apparent ability to transfer moods/thought between people. A simple demonstration, involving three people, is for person A to set out the Tree of Life for person B. Person C stands away from the Tree of Life. Establish the normal strength of an outstretched arm of person C, by person A measuring the resistance to downward pressure on person C's arm. Person C then stands on spiral 2 (Chokmah) of person B's Tree of Life. If person B has a strong negative thought, such as a bereavement, bad health, financial stress, etc., it seems to affect adversely person C, both mentally and physically, as muscle testing now shows weakness and little resistance to their outstretched arm. When person B returns to normal, or has happy thoughts, the reverse happens.

This demonstration suggests the existence of thought and mood transference when standing on a certain spiral of someone else's tree of life pattern. Without realising this, people must experience this many times each day. It suggests that we may all interact with each other, we are all connected by the structure of the universe, and one should avoid negative people as quickly as possible, so not to be affected by their negativity, even inadvertently.

Case Study Measurements

Figures 7-1, 7-2, and 7-3 are theoretical representations produced by graphic artists who have possibly never experienced a Tree of Life, nor measured it accurately. This section is based on an accurate Tree of Life of an eighteen-month-old female child. Figure 7-4 is a photograph of disc markers placed on the spirals of this of Tree of Life pattern: the camera being vertically above at ceiling height. A Tree of Life only has 10 spirals. The large circle in the top centre is where the person was standing. It is **not** part of the Tree of Life. In Kabbalah, this is referred to as *Da'at.*

Figure 7-4 An Actual   Figure7-5 19.5°   Figure 7-6   35°
    Tree of Life
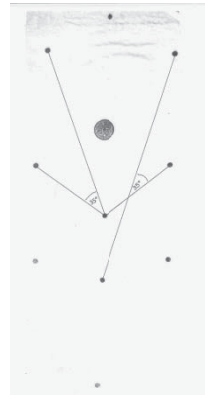
On measuring a Tree of Life by joining up the dots, some important universal angles are found, which excitingly equal the universal constants and key angles itemised in Chapter 5, within experimental error. To assist comprehension, Figures 7-5-9 show these angles separately.

Figure 7-5 shows examples of the angle 19.5°. This is a good approximation to **19.471°**.

Figure 7-6 shows examples of the angle 35°. This is a good approximation to **35.264°**, which, for example, is the angle between the diagonal of a cube and the diagonal of its base.

Figure 7-7 shows examples of the angle 55°. This is a good approximation to 54.735 °, which is the complimentary angle to 35.264°.

Figure 7-8 shows examples of the angle 109.5°. This is a good approximation to **109.471°**, which, for example, is the carbon bond angle in protein molecules.

The above angles have all been in the **horizontal** plane. When one dowses in the **vertical** plane, and plots the boundaries of the conical envelopes, the following angles are found: **19.471° 11.537° 8.213° …..**

As explained in Chapter 5, all these angles, both horizontally and vertically not only occur in numerous other situations, but also form part of the series of angles whose sines are 1/n, where **n** is an odd number equal or greater than 3, or tan1/n*√2.

Figure -7 55°   Figure 7- 8 109.5°

Summary and Conclusion

The auras of plants, animals, and humans possess all the characteristics detailed in Chapter 6. Importantly, in addition, various levels of consciousness affect their auras. In particular, fear, ill-health, or detrimental energies can cause an aura to shrink, whilst pleasure or an extrovert performance can significantly expand an aura. Although inanimate objects have chakras and auras, they cannot control their chakras or aura colours like living entities.

The Tree of Life geometry, which only lifeforms have, is yet another manifestation of the phenomenon of auras. This is in addition to the 5 other manifestations discussed in Chapter 6, making a total of six different manifestations of an aura.

Living plants and animals have a Tree of Life, which comprises ten vortices/conical helices in a horizontal plane. It remains the same geometry if a person stands vertically or lies horizontally. The ten helices are connected by lines, along which seem to flow subtle energies. The

helices are linked by key universal angles, both in the vertical and horizontal planes. When standing on certain of these spirals, limited thought and mood transference is possible.

The probability of finding universal constants by chance is virtually zero. This is proof for the sceptics that in certain controlled circumstances, not only does dowsing work, but also can be used for fundamental scientific research.

As a philosophical conclusion, why have we a left-right symmetry, and 10 fingers and toes? Darwin's theory of evolution and the survival of the fittest, does not explain questions like these, and possibly is, therefore, incomplete. The Tree of Life, which is created as a result of the structure of the universe, has left / right symmetry and 10 vortices. By implication the structure of the universe, is involved in guiding evolution.

The Way Forward and Suggested Areas for Research

1. How does a plant "know" that a sealed bottle of water is nearby, or the intentions of a human? Is there some form of telepathy?
2. More research is required into the connection between auras and consciousness in plants, animals, and humans.
3. What is the lowest form of life with a conscious aura?

CHAPTER EIGHT

THE AURAS OF CIRCLES AND OTHER ABSTRACT GEOMETRY

Introduction

Previous chapters have examined auras originating from inanimate objects, and life forms. Also covered was an introduction to the concept of subtle energies that are associated with abstract geometry, where the mind's intent is on pure geometry and not associated with the more usual physical tangible objects. This chapter develops all of these topics and examines how the study of auras associated with abstract geometry can enhance our knowledge of subtle energies.

To summarise the previous chapters, physical bodies have the following components to their auras:

1. Their surface has a 7 horizontal bands of subtle energies clinging close to the source.
2. A spiral links and wraps around these horizontal bands.
3. The external aura comprises 7 ellipsoids.
4. 6 arms emanate from the centre of the source.
5. Each of these arms comprise vortices apparently extending indefinitely.
6. Life-forms have a horizontal plane of 10 spirals, which are the footprint for 10 vertical conical helices.

Table 8-1 Components of Auras Associated with Physical Bodies

We discussed the unexpected and non-intuitive equivalence of the same geometric shape, from any source, solid or abstract, producing the same subtle energy pattern.

Also touched upon was the fact that local space-time variables and physical forces such as magnetism, spin, pressure, and orientation, not

only affect these subtle energies, but also these factors affect the mind's perception.

One of the benefits for dowsing pure abstract geometry is that it eliminates the variable of mass. This enables fundamental comparisons to be made between solid and abstract sources possessing identical geometry. Another important benefit is that dowsing pure geometry generates different types of subtle energies, which is beneficial for researching consciousness. This chapter analyses the simple case of an abstract circle.

Perception in 2-Dimensions

The same subtle energy pattern is obtained when dowsing an abstract 2-dimensional circle, such as one drawn on paper or a circular depression in a carpet, or even the impression left on a lawn after removing an inverted cup. It makes no difference if the circle is an entire disc or an open ring.
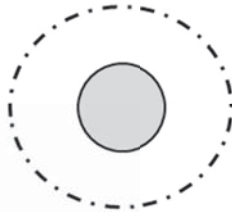

Figure 8-1 One Circle and its Core Aura

The geometry of a 2-dimensional circle has a perceived concentric circular core aura, which is in the same plane as the surface on which the circle is drawn. The aura has a radius greater than the source circle. Figure 8-1 represents this, where the central circle is either a disc or a ring, and the dotted outer line represents the boundary to the core aura.

So, how does the aura in Figure 8-1 compare to the properties of a generalised aura for tangible objects as set out in Table 8-1?

1. When the source circle is placed vertically, the internal open area of the ring has **9** horizontal bands of subtle energy. When this circle is placed horizontally, it has **0** bands.
2. A 1-turn spiral, around a vertical diameter, links these horizontal bands.
3. The external aura comprises **9** ellipsoids.
4. 6 arms emanate from the centre of the circle.

5. Each of these lines comprises vortices apparently extending indefinitely.
6. As expected, there is no Tree of Life Pattern.
7. From the centre of an abstract ring a beam emerges, which is different if the ring is held horizontally or vertically.

Table 8-2 Components of Auras Associated with Abstract Geometries

When comparing Table 8.1 with Table 8.2, it is apparent that items 1 to 3 are significantly different. Auras from pure geometry differ from auras from physical bodies. The latter have a preference for a series of 7, but the pure geometry auras prefer a series of 9. Another new factor is that only vertical sources have horizontal bands. An additional new property is that a subtle energy beam emerges from the centre of the circle, but different subtle energies are produced if the source is horizontal or vertical.

This suggests that gravity is involved in subtle energies in general, and in one component of auras in particular. Let us now investigate these factors in further detail, and highlight several other important differences.

Scaling

For different sized source circles, the noetic aura radius is a linear relationship in the form *aura radius (a) = constant * circle radius (r)*, with the constant in the range 1-10. However, in finer detail, the findings are more complex.

Figure 8-2 is a graph showing how the radius of a circle's aura increases with the increasing radius of the circle creating the aura. The top line is measuring the aura from the centre of the source circle, whilst the bottom line is measuring the same aura from the circumference of the circle. The latter is useful for 2-body experiments.
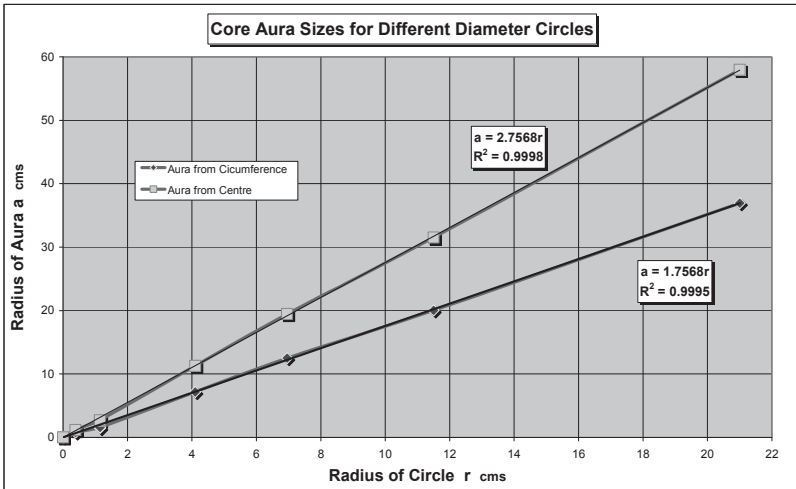
Figure 8-2 Relationship between a Circle's Radius and its Aura

The formulae for the core aura size, **a**, are

a = 2.7568 r when measured from the centre of the source circle   (i)
a = 1.7568 r when measured from the circumference of the circle.   (ii)

Both of these formulae have a very high correlation coefficient of 0.995.

Simple mathematics of the geometry between the circle's radius and its aura explains why the difference between the two coefficients is exactly 1.

The measurements for Figure 8-2 were taken at the time of a new moon. As will be detailed in a future chapter, it is well known that a new moon shortens measurements, whilst a full moon expands measurements. The above constant **1.76** is, therefore, not unique, but depends on the time and date of the measurement. For comparison, at a last quarter moon, equation (ii) becomes **a = 5.78 r**, whilst at full moon (Sat 19th Mar 2011 at 17:00) the formula becomes **a = 9.89 r**.

A very important finding affecting all subtle energy research is that not all constants are permanent constants! For example, in Figure 8-2 the equation **a** = constant*r will always produce straight lines, but their slopes may change. If similar experiments are repeated within, say, one hour, the same constant value will be obtained. Because of local environment and astronomical factors, some constants are time dependent.

7 or 9 Rings?

Ring Number	Radius of Aura Ring	Arithmetic Progression n - (n-1)
n	metres	metres
1	0.305	
2	0.808	**0.503**
3	1.496	**0.688**
4	2.014	**0.518**
5	2.508	**0.494**
6	3.020	**0.512**
7	3.600	**0.580**
8	4.136	**0.536**
9	4.748	**0.612**
Average		**0.555**
Variation		**0.053**
% Variation		**9.60%**

Table 8-3 The 9 Aura Rings for a Circle of Radius 4.5 cms

Abstract circles produce 9 aura rings extending outwards from the core aura, but solid discs (both 3-dimensional and 2-dimensional) only produce 7 rings. This seems counterintuitive, as a solid disc has more information than an abstract circle drawn on paper, and, for example, a 3-dimensional metal source has even more information than a 2-dimensional paper cut-out. However, having more information does not produce more rings!

The field strength across the entire aura decreases from an arbitrary 100 at its centre, to 0 at the aura's outer boundary. This suggests that the aura comprises 9 concentric ellipsoids, decreasing in size like a Russian doll, and not 9 discreet rings.

Table 8-3 summarises the findings for the 9 aura rings of an abstract circle having a radius of 4.5 cms, drawn on paper, and placed horizontally. The measurements were made in the same horizontal plane as the source circle, with the origin of the rings at the centre of the source circle. These measurements were made when it was a last quarter moon. As is apparent, the core aura was 0.305 m, and the 9 rings formed an arithmetic progression with an average separation distance of 0.555 m, with a 10% variation.

Perception in 3-Dimensions

Dowsing a source geometry circle also produces a 3-dimensional subtle energy beam coming perpendicularly out of the paper. This phenomenon does not occur in solid physical source objects. Interestingly, the subtle energy produced in this beam and its properties, depends if the source object is vertical or horizontal.

Horizontal Source Ring Drawn on Paper

When a circle drawn on paper is positioned horizontally, its core aura is as depicted in Figures 8-1, 8-2, and 8-3, with the extended aura comprising **9** concentric ellipsoids, centred on the centre of the source ring. All these aspects of the aura have the same type of subtle energy (Type 1).

As before, this aura has 6 arms, but in addition to the usual Type 1, these arms have different subtle energies (Types 4 and 9). These arms are parallel beams with constant field strength along their entire length. The orientation of these 6 arms remains constant even when the source is rotated. This suggests that the Earth's environment is involved in their creation. This could include the Earth's magnetism, gravity, and its spin.

Along each arm, there are an indeterminate number of spirals with 2 different types of subtle energy (Types 3 and 9**)**. Each spiral has a vertical axis, and, alternatively, spirals clockwise and anticlockwise.

So far, the above auras have a similar pattern to auras emanating from solid objects except they are based on a repeating pattern of 9 instead of 7. They also have different energy types, but as these are a complex subject, they have their own chapter later.

What is a new phenomenon, that does not occur in physical discs/circles, is that a vertical beam emanates from the centre of the horizontal circular ring source with a spiral of Type 3 and 9 subtle energies.

Vertical Source Ring Drawn on Paper

When the same circle drawn on paper, as above, is positioned vertically, a horizontal beam is produced. The diameter of a vertical cross-section through this beam at its source (i.e. at the sheet of paper with the circle) equals the diameter of the core aura. Typically, the diameter of the core aura is 1.6 times the diameter of the source circle. An important

finding is that this horizontal beam is not produced with physical discs or circles.

The beam comprises a diverging Type 5 subtle energy, with reducing field strength along its length. Measurements of vertical cross sections show that the envelope of the beam is a cone with an elliptical cross-section. The vertical major axis is greater than the horizontal minor axis. Drilling down further, and like the ellipsoids in the aura, the cone comprises 9 equally spaced subtle energy cones, inside each other like Russian dolls. The cones have the same horizontal axis that passes through the centre of the source circle. The beam diverges, with the apex of the outer cone having a half angle of approximately 1.0°.

Analysis and Theory

It seems remarkable that the above relationship in equations (i) and (ii) is not only linear, but is very simple, and has an unusually high correlation coefficient of 0.999. The similar formula for masses of increasing sizes is logarithmic with auras decreasing pro rata.

However, it is not immediately obvious in the specific example of equations (i) and (ii), as to what the one-time constant 1.7568 relates. Nor is it obvious why or how the mind's intent interfaces with

a) the structure of space-time
b) the earth's environment in its widest sense, and
c) a geometric image

to produce an aura involving 1.7568 times the radius of the geometric image.

Aura Shape and Orientation

On closer inspection, the auras of abstract circles do not have a smooth envelope, but in 2-dimension appear as irregular circles. This has been quantified for 3 circles of radii 1.15 cms, 4.1 cms, and 21 cms, and is illustrated in Figures 8-3, 8-4, 8-5, and 8-6. To obtain a meaningful measure of an aura's radius, e.g. as required in the data for Table 8-2, the average of about 10 measurements of these polar values for each source circle was used. The average deviations were between 6.8% and 8.9% for the 3 circles, implying that the causes of the perturbations only have a relatively small effect.
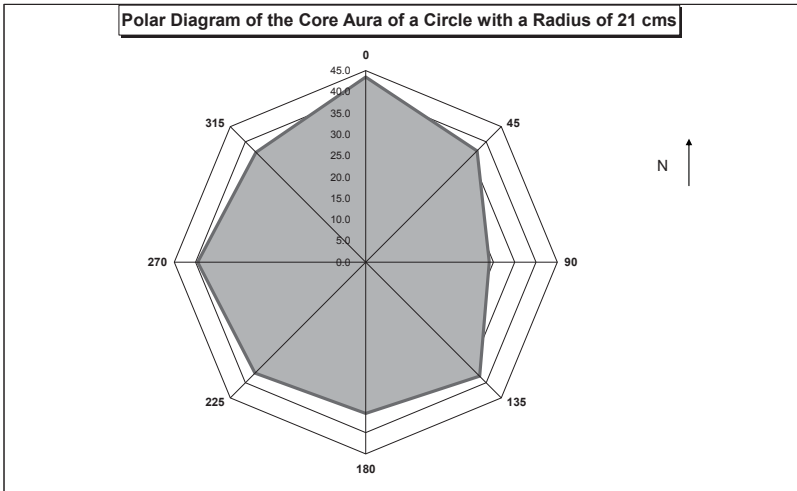
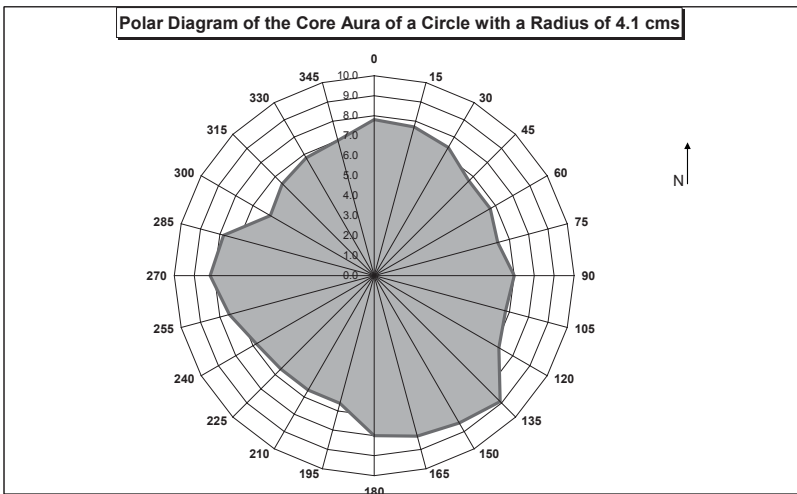Figure 8-3 The Orientation of the Aura from a 21 cms Circle

Figure 8-4 The Orientation of the Aura from a 4.1 cms Circle

It is apparent from all 3 graphs that the size of an aura depends on the orientation of the measurement. Aura maxima occur at 0°, 135°, and 270°. i.e. north, south-east, and west. This suggests that the earth's magnetic

field extends auras towards the North Pole, and the earth's rotation on its axis from west to east extends auras to the west. It is not immediately obvious what resultant vector forces cause the south-east maxima, but suggestions are made in the Postulations section later.
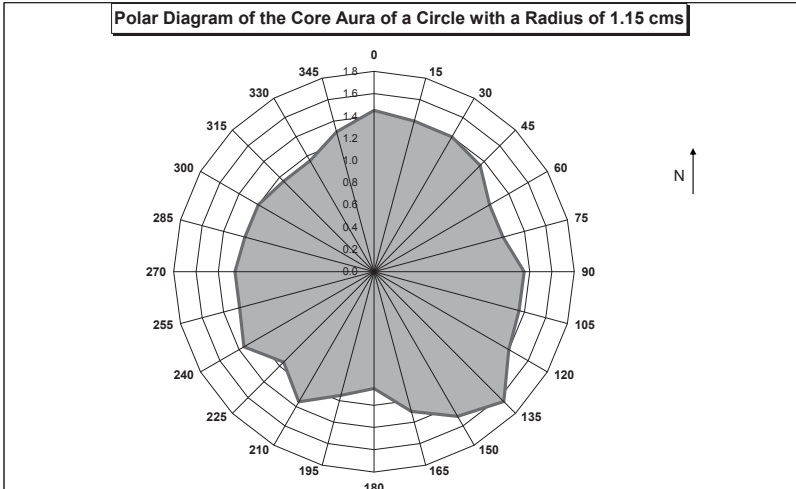
Figure 8-5 The Orientation of the Aura from a 1.15 cms Circle

The Effects of Magnetism

To further study the possible effects of the earth's magnetism, one of the above experiments was repeated in an artificially created magnetic field. Figure 8-6 shows the effect on the aura depicted in Figure 8-5 when a reversed north-south magnetic polarity was created around the source circle of 1.15 cms.
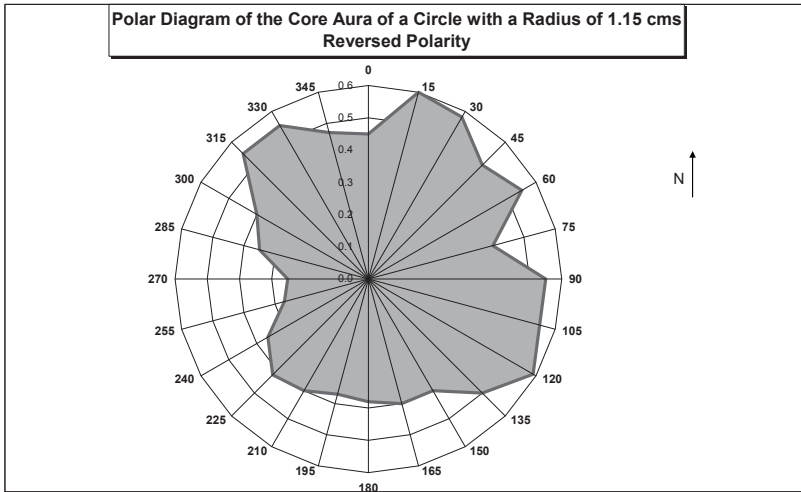
Figure 8-6 The Effect of Magnetism on the Aura of a 1.15 cms Circle

The most significant changes are:

1. The 270° (west) measurement changes from a maximum to a minimum.
2. The other maxima have rotated by ±15°. The due north maximum changes eastwards to 15°, but the south-east maximum reduces by 15° to 120°.
3. The average aura radius shrinks in size from 1.29 cms to 0.48 cms.
4. The average deviation changes from 8.56% to 23.26%.

These findings suggest that locally reversing the earth's magnetic field reverses the effects of the earth's vorticity on auras, and seems to produce "stressed" auras with more chaotic subtle energy flows. It is apparent that magnetism affects the mind's perception.

The Effects of Bright Sunlight

As we have seen in Chapter 6, auras and subtle energies are affected by several factors, such as vorticity, and pressure. Usually an increase in pressure or vorticity increases the aura size. Electromagnetic radiation also affects subtle energies. It was shown, in Chapter 6, that sunlight can

recharge some solids. Shown graphically was the example of the core aura of a fluorite crystal, increasing by a factor of 5 in under 2 hours.

	Diameter of Coin and Circle	Aura of Coin in Shade	Aura of Circle in Shade	Aura of Coin in Sunshine	Aura of Circle in Sunshine
	mm	mm	mm	mm	mm
	2.30	5.10	6.40	4.00	3.20
	2.35	5.30	6.00	2.50	3.00
	2.40	4.50	5.10	2.30	3.50
	2.40	4.80	5.70	2.50	2.70
	2.40	5.00	5.60	2.50	3.10
	2.45	6.30	5.50	2.50	3.10
	2.44	4.50	4.60	3.00	3.00
	2.40		5.50	2.90	3.50
	2.35		4.80	2.90	
	2.40		5.90	3.10	
	2.42		6.00	3.00	
	2.44			2.90	
				3.80	
Average	2.40	5.07	5.55	2.92	3.14

Table 8-4 Aura of a Coin in Shade and Sunshine

However, unexpectedly, for some metals and abstract geometry, auras shrink in bright sunlight and expand in shade. A simple demonstration of the phenomenon is to place a coin on a sheet of paper and measure the core aura size in in a dark room, and mark the extent of its core aura on the sheet of paper. Also draw a circle around the same coin, remove the coin, and measure the core aura of the circle drawn on paper. For additional accuracy, measurements should be made by approaching the core aura boundary, both outwards and inwards. This experiment should then be repeated in bright sunshine.

Tables 8-4, 8-5, and 8-6 shows the results of this experiment done in Israel with a 10 shekel coin with arbitrary strong sunlight, and followed by repeating the experiment in dark shade. As we have seen in the above polar diagrams, the auras are not symmetrical, but affected by perturbations from the earth. Therefore, several measurements were made of the auras in different directions around the circle's perimeter.

Aura Diameter of Coin in Shade mm	5.07
Aura Diameter of Coin in Sunshine mm	2.92
Shrinkage of Aura in Bright Sun mm	2.16
Percentage Shrinkage	**42.51%**

Table 8-5 The Shrinkage of Auras in Sunlight

Table 8-5 shows that the shrinkage of the aura in sunshine compared to its size in the shade. This arbitrary example has a significant 42.51% shrinkage. Table 8-6 shows the difference in aura size between the coin and the circle drawn round the coin, which is removed before the aura of the drawn circle is measured.

Aura Diameter of Coin in Shade mm	5.07
Aura Diameter of Circle in Shade mm	5.55
Difference in Auras in Shade mm	-0.48
Percentage Shrinkage	**-9.53%**
Aura Diameter of Coin in Sun mm	2.92
Aura Diameter of Circle in Sun mm	3.14
Difference in Auras in Sun mm	-0.22
Percentage Shrinkage	**-7.62%**

Table 8-6 Discrepancy Between Diameters of a Circle's Aura

These 2 experiments should give identical results, but as is apparent, there is about an 8% difference. Subsequent experiments showed that this discrepancy is caused by the thickness of the pencil line drawn round the coin, which had the effect of increasing the diameter of the drawn circle by about 8%. As seen in Figure 8-2, the relationship between a drawn circle's radius and its aura is linear, which is a reassurance that the 8% discrepancy does not affect the main findings.

As the above results were unexpected, I repeated the above experiments back in England with different metal objects, and circles drawn with a compass to produce the identical radii to the metal objects. The extremes of light intensity were from a very dark cupboard to a hazy English sunshine. The findings were identical to the original Israeli experiments, even though different protocols and materials were used.

The positive results of these experiments is that it is now necessary to create a research project on why electromagnetic radiation should have different effects on crystals, compared to pure geometry, and metal sources. Another positive outcome is that a by-product of these

experiments is yet another confirmation of the equivalence between abstract geometry, and a physical object with identical geometry and dimensions.

Conclusions

A major achievement of these experimental results is that for the first time, auras of abstract geometries have been measured, analysed and documented. The findings here have not only been shown to be repeatable, but have demonstrated a strong link between subtle energies, consciousness, magnetism, gravity, and spin.

A major finding is that the unexpected and non-intuitive equivalence of matter and geometry. The same geometric shape produces the same subtle energy aura results, irrespective if the source is a tangible physical object, or pure geometry. This result has significant benefits for subtle energy research, as it eliminates the variable of mass, and, therefore, reduces the number of causes of perturbations in experiments.

A simple linear relationship with a high correlation coefficient has been discovered between the radius of a pure outline of a circle and its aura. The other main achievement is producing a constant with a high correlation coefficient, and understanding that this "constant" changes with time due to local and astronomical factors. The practical effect of these changes is negligible. Plotting results of experiments will always produce straight lines, but their slopes may change.

Having more information does not produce more rings! Solid discs of either 2, or 3-dimensions only have 7-fold geometry, but abstract drawn circles produce 9-fold geometry in their ellipsoidal auras, spirals, bands, and rings.

A pure geometry source produces a 3 dimensional subtle energy beam coming perpendicularly out of the paper. This phenomenon does not occur in solid sources. What is also new is that a vertical beam emanates from the centre of a horizontal pure geometrical source.

Gravity, pressure, and sunlight have been shown to affect auras significantly. However, a significant finding is that sunlight can have opposite effects on crystals, compared to metals, and pure geometry sources. This phenomena requires a further research project.

The Way Forward and Suggestions for Future Research

1. Using pure geometry sources, experiments should be repeated to isolate the factors and their effects on the constant in the equation relating source size to its subtle energy size.
2. The diameter of a core aura is approximately 1.6 times the diameter of the source circle. With more accurate experiments, and allowing for known perturbations, is this the universal constant, the golden ratio, 1.618?
3. Similar experiments should be repeated with a positive intent to see if the mind can separate the perceived perturbation effects of spin from gravity.
4. The findings in this chapter, only relate to circles up to 21 cms diameter. Further experiments are required for larger circles.
5. Discover if there is common mathematics that transforms the geometry of the source to the pattern of subtle energy that is perceived. For example, we know that dowsing an abstract 2-dimensional circle produces an aura
   a. that is a linear function of the radius of the circle being dowsed
   b. which contains a 3-dimensional perpendicular vortex having a small divergence angle, and
   c. with each of the above involving 9 components,
      What is the mathematical transformation that converts a 2-dimensional circle $x^2+y^2 = r^2$ into the above observed model? This may be used as a starting point to apply to other geometries.
6. Further research is required to understand the physics of the experiments involving the effects on auras of orientation, vorticity, magnetism, and reversed polarity.
7. Create a research project on why electromagnetic radiation should have different effects on crystals, compared to pure geometry, and metal sources.
8. Further experiments are required to see if there are exceptions to the equivalence between abstract geometry, and a physical object with identical geometry and dimensions.
9. Research why the aura of crystals expands in sunlight, but the auras produced by metals and pure geometry shrink in sunlight. Demonstrate if this phenomenon is because of the crystal lattice structure, with the lattice angles being the same as the preferred angles in the structure of the universe.

CHAPTER NINE

THE BRAIN AND SUBTLE ENERGIES

Introduction

The words *dowsing, divining, noetics,* apply to many different para-normal events that the mind, in its widest sense, is capable of achieving. For some of these activities, tools amplify the sensation. If a dowser is using L-rods, pendulums, or the traditional willow \ hazel Y-rods, it is not one of these tools that is detecting information, but the mind. Conceptually there are 4 forms of dowsing; passive detection, seeking information, sending requests, and a combination of all 3 of these.

Passive Detection examples are on-site or physical dowsing, such as examining the aura of an object, or investigating a linear earth energy field, or an up or down spiral on an archaeological site. Here the brain is passively detecting the subtle energies being perceived. In this category of dowsing, there must not be any intent by an observer, or any other person, to influence the fields being detected, by such mind activities as moving, bending, or changing the nature of the field.

Seeking Information where the brain can be considered as interacting with a cosmic information field in a passive way. An example of this is "lead me to an underground source of tin ore", or when viewing a remote location or building.

Sending Requests can be considered as interacting with the cosmic information field in a pro-active way. Examples could include such activities as projecting geometrical shapes to remote parts of the world, or requesting a car parking space – a common request!

Combination is the fourth practical use when incorporating all or any of the above other forms of dowsing: i.e. when both seeking information and passive detection. In practice, dowsers seamlessly move between the different categories. Examples of this include map dowsing, or creating a psi-line, and then passively measuring its dimensions and properties.

Where in the brain are these activities and subtle energies perceived? Is the same area responsible when sending and receiving noetic information, or are different areas involved? Is the process of sending information in

the same area of the brain as when, say, creating a psi-line, or requesting information?

At the time of writing, it is not possible to answer any of these questions with certainty. Historically, quoted areas in the brain responsible include the pineal gland, the pituitary gland, or the hypothalamus. More recently, published scans of the brain purport to show relevant brain activity when meditating or dowsing.

These scans are usually based on recording either heat or magnetic activity in the brain. However, many years ago I found to my cost, that magnets placed close to the head not only produce headaches, but also disable all dowsing activity. In fact, a powerful magnet closes down the brain for up to 24 hours! Hence, I am not convinced at the time of writing, that brain scans can provide a definitive answer for either where, in the brain, paranormal activities are performed, or what mechanism is involved.

Practical Experiment

The reader may wish to attempt the following simple, non-invasive quantitative experiment, to find the part of the human anatomy that detects "dowsing". This requires no complex, expensive, or electronic equipment, but can give very accurate answers. It just involves the researcher walking towards a small dowsable object and noting when its aura is first detected. As always in science, it is satisfying to start with some theory, and then demonstrate its truth by experiment.
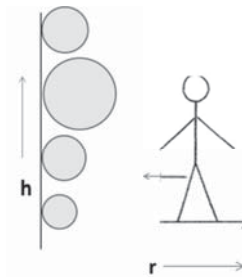
Figure 9-1 Height of Aura vs Distance

Figure 9-1 is a sketch of the protocol. A source object such as a small crystal, stone, or ball should be as spherical as possible so that its aura is also spherical. In practice, if the orientation of this source is kept constant

towards the researcher, small deviations from a spherical aura are irrelevant. The adjustable height of this source is defined as (**h**). The objective is for the researcher to walk towards the subtle energy source and mark (using a measure on the floor, with its zero under the source object) where the aura is first detected (**r**). It may be easier to start detecting the outer shell of the aura, as this is larger, and then progress to detecting the inner or core aura, which is much smaller, and, therefore, produces results that are more accurate.

The theory for this experiment is explained in the Appendix to this chapter, but the results are summarised in Figure 9.2. This illustrates an actual experiment where a dowsable source object (in this example a rose quartz crystal) is suspended at various heights, as depicted on the h-axis. The r-axis depicts the furthest the dowser can detect the core aura from the source, after it has been adjusted to the various heights. The reference point for measurements should be made from a consistent part of the body, such as the leading edge of a foot, and using a tape measure resting on the floor.

This experiment's basic assumption is that the height of the source object that corresponds to the furthest distance the researcher can detect the core aura, equals the height of the part of the anatomy that is associated with dowsing. It is seen in this example that the optimum height of the source is 1735 mm, which corresponds to the forehead part of the brain of the person undertaking the measurements. The secondary peak interestingly occurs at the height of the person's heart. In this experiment, when asking for a dowsing response no assumptions were made of the location in the body of the "dowsing detector".

A corollary experiment, in which the source is approached both backwards and forwards, can indicate whether the front or back part of the brain is involved in dowsing. In the above example, towards the back of the brain rather than the forehead seemed to be the location of the dowsing detector.

So how does theory compare to an actual experiment? Figure 9.2 superimposes the theory with actual results. A close fit occurs where the brain is the prime detector, but with some interesting perturbations and deviations that deserve comment.
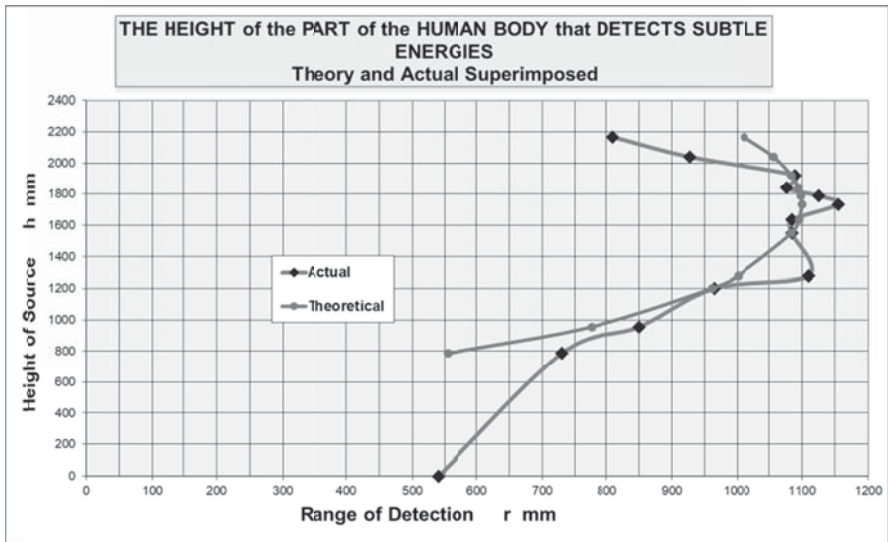
Figure 9-2 Where Subtle Energies are Detected

    Although the perturbations near the peak of the parabolic curve suggest there may be more than one dowsing detector in the human anatomy, more probably, what is being perceived by the brain comprises not only the core aura field from the crystal source, but also fields augmented by the dowser's own bionic fields. The latter may originate from the observer's heart, forehead and crown chakras, plus the local background fields interacting with the dowser and the source object.

Appendix

Two extreme cases of dowsing models of the human body are considered.

Postulate 1. If **all** parts of the human body have equal sensitivity to detecting dowsable fields, then Figure 9-3 illustrates graphically a person walking along the horizontal r-axis towards the vertical h-axis, which represents the height of the small source of a dowsable field, etc. A point source object is essential for this experiment, in order that the geometry is theoretically correct. The theory of this experiment is invalid, if the experiment is attempted with a large source object or megalith – assuming their heights can be adjusted!
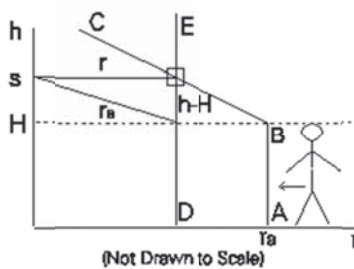
Figure 9-3 Dowser Approaching an Aura of Variable Height

The r-axis represents the floor along which the dowser is walking when approaching the source object. The Range, **r** mm, is the distance the dowser is away from the source object when he first perceives the aura.

r_a is the furthest point a person can detect the core aura of the small source. For each source, this is a fixed distance representing the extent of its aura. If postulate 1 was true, that all parts of the human anatomy were equally sensitive to dowsing, then whatever height the source is placed above the ground, the person approaching the source will always detect it at $r = r_a$. If the height of the person is H mm, the vertical straight line AB in Figure 9-4 extends to **H** mm.

As the source is raised higher than H, in this postulated model, it is assumed that the top of the head will be the part of the anatomy first detecting the dowsable field associated with the source object. The relationship between **h** and **r** will form a curve as in Figure 9-4, i.e. the person will have to approach the source closer to first detect its aura as it is moved further higher away from him. If the source is placed at height **S,**

the dowser will have to stand on the line DE before he detects the dowsing field from the source above his head.

The shape of this curve can be determined by some simple geometry, using Pythagoras Theorem (something one does not often use after leaving school!). The right-angled triangle in Figure 9-3, the height **H**, comprises the hypotenuse r_a, which is always the constant Range of the core aura. (Please note, Figures 9-3 and 9-5 are not drawn to scale to facilitate clarity.) The height of the source above the top of the dowser's skull is h-H, whilst the apparent range r, is the distance of the dowser from the h-axis. Consequently:

$$r_a^2 = r^2 + (h\text{-}H)^2$$
$$r^2 = r_a^2 - (h\text{-}H)^2$$
$$r = \pm\,(\,r_a^2 - (h\text{-}H)^2\,)^{0.5}$$

This curve will obviously be symmetrical below the feet of the dowser as well as above his head, and is illustrated in Figure 9.4.

WHAT PART of the HUMAN ANATOMY DETECTS SUBTLE ENERGY
Theory - Whole Body

Height of Source h mm (vertical axis: 0 to 2200)

Range of Detection   r mm (horizontal axis: 0 to 1200)
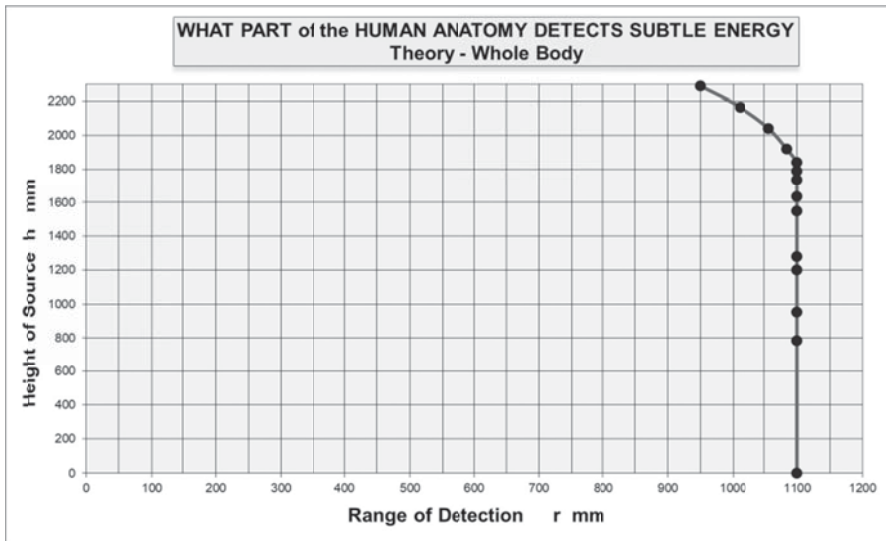
Figure 9-4 Graphical Depiction of why Postulate 1 is Wrong

Postulate 2. The second extreme postulate is that only one very small part of the human body detects dowsing. Figure 9-5 illustrates this graphically, where the point X marks an arbitrary anatomical point that is

responsible for dowsing. When the source is at the same height from the ground as point X, h_x, the dowser will detect a field at the furthest point from the source on the h-axis, i.e. $r = r_a$. As the source is raised or lowered from this optimum position, the dowser will have to reach a closer point to the source, such as line DE, before detecting the source.
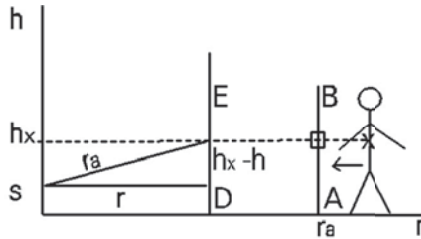
Figure 9-5 The Part of the Body Detecting Subtle Energies

As before r_a is the hypotenuse in the right-angled triangle, so that:

$$r_a^2 = r^2 + (h_x - h)^2$$
$$r^2 = r_a^2 - (h_x - h)^2$$
$$r = \pm (r_a^2 - (h_x - h)^2)^{0.5}$$

A parabolic type of curve is obtained which is symmetrical about the dowsing point, **X**.
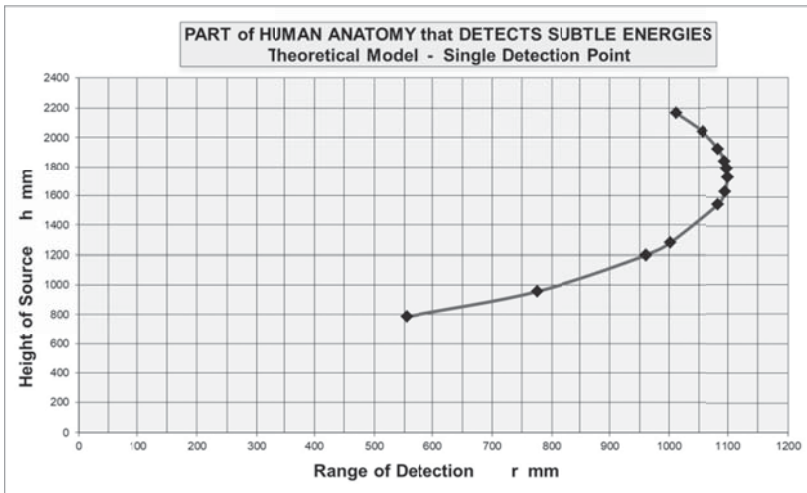
Figure 9-6 Graphical Depiction if Postulate 2 is Correct

If Postulate 1 is correct, the graph of the experimental results of the height-range relationship should look like Figure 9.4 (where the Range of a source is 1,100mm, and the height of the person is 1,840mm).

If Postulate 2 is correct, the height-range relationship should look like Figure 9-6 (where the human dowsing detector is 1,735mm from the ground, and the Range for the source is 1,100mm). As discussed above Figure 9–6 has a good fit to the data.

Summary and Conclusion

There are four methods of using dowsing and interacting with subtle energies.

A simple "low-tech" method is available for determining what part of a person's anatomy is responsible for researching subtle energies. Figure 9-2 suggests that it is at forehead level towards the back of the brain.

The Way Forward and Suggested Research

The obvious next step is to arrange brain scans to find the exact location(s) where the brain interfaces with subtle energies. The appropriate medical equipment must be non-intrusive and avoid any magnetism that would invalidate this experiment. These scans need to be undertaken using subjects who are expert dowsers, and can see, or strongly feel subtle energies. While the scans are in progress, the subjects should be:

1. Undertaking the 4 methods of dowsing discussed in this chapter.
2. Investigating if there is any difference between local and remote activities.
3. Detecting if the 9 affect different parts of the brain.

As part of this research, discover what is occurring in the brain, to explain why children under the age of about 11 years old are better than adults at seeing and feeling subtle energies. Similarly, establish why elderly people, over about 70 years old lose their sensitivity in detecting subtle energies.

CHAPTER TEN

A MODEL OF CONSCIOUSNESS

Introduction

Historically, major scientific advances have occurred by probing the boundaries of knowledge and exploring radical ideas. From the earliest civilisations, one such boundary is the understanding of consciousness and the mind. On a seemingly different subject, current scientific theories have difficulty in explaining observations and issues such as dark energy, dark matter, as well as quantum physics. This article explores the possibilities of turning conventional explanations of the universe "on its head" by elevating the role of consciousness to see if this gives a better understanding of quantum physics and other observations of the universe.

For example, if consciousness is a driving force in the universe, then such concepts as the anthropic principle; objects seeming to be in two places at the same time; the ability of anticipation; observers affecting the results of experiments; and other "mysteries" of quantum physics may be easier to explain without resorting to such devices as eleven dimensions or an infinite number of parallel universes.

In-bred into the evolution of mankind is a psychical, mystical, or spiritual element. A characteristic of most civilisations are priests, "magicians", diviners, etc. attempting to answer "why?", explore the paranormal, predict the future, or report alleged supernatural events. Science has treated spirituality as an alien topic, and associated concepts such as shamans, witches, voodoo, oracles, dowsing, faith healing, or even prayer have been derided. To illustrate the approach adopted in this chapter, if, for example, a person can achieve a high success rate as a water diviner, and fulfil a useful need, it does not matter if dowsing or any other of the above techniques cannot be understood by the current level of knowledge within orthodox science. What is important are results. Healthy scepticism is justified, but not dismissive doctrine.

Over the last few hundred years, mainstream scientific thought has considered that the universe is a physical entity comprising matter, and that consciousness is only a consequence of a minor part of living matter.

More recent science, in attempting to interpret the quantum world, has tended to move towards ancient Eastern traditions, whereby matter may be a consequence of consciousness. In developing this approach, a key concept is that consciousness involves information.

To assist in developing this theme, a combination of conventional scientific tools, as well as long established spiritual beliefs, are utilised to probe a model that may help to explain consciousness, including some paranormal phenomena.

Outline of the model

In the model about to be developed, the mind is not just a brain in a skull. It comprises, at one end, cosmic consciousness, (sometimes referred to as an information field or the Akashic record), and a physical body at the other. This concept reflects the overlap between the quantum universe at the micro level, and the large-scale physical world, with consciousness straddling both. Figure 10-1 depicts this as a block diagram of the concepts involved.

Quantum universe

Consciousness

Access
Influence

Communicate
Intent

| Information Field | Mind | Physical Body |

Akashic History
Future
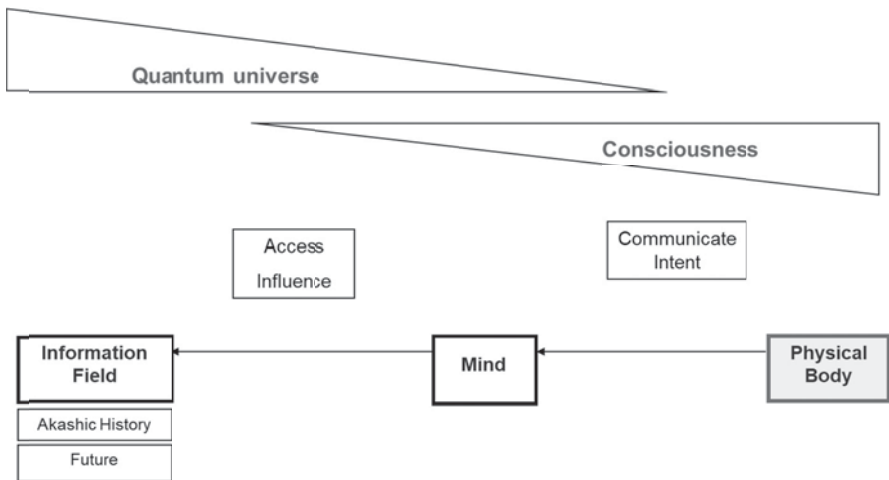
Figure 10-1 Information Flow from Physical Bodies, via the Mind
to the Conscious Universe,

Let us work our way through this model, starting with the Information Field.

Concepts associated with the Cosmic Consciousness

Cosmic consciousness may currently be the best working model that helps to explain numerous observations and phenomena. In an ideal world, equations, mathematics, and quantifiable repeatable experiments would fully define and explain this concept. However, we are not there yet. As an illustrative analogy, our current level of understanding of consciousness and cosmic consciousness is possibly where astronomy was about 600 years' ago when it was "obvious that the Sun went round the Earth", or before physics could "see" atoms and fundamental particles. This book adds to the vast amount of existing circumstantial evidence.

The main feature is that the cosmic consciousness reflects the structure of the universe and stores information. Current thinking is that the cosmic consciousness is more than Akashic information (a concept originating several thousand years' ago) which is just a complete and faithful record of history. It seems to be pro-active, comprising past, present, as well as some future information, and thus influences the evolution of history. The Akashic record can, therefore, be considered as a sub-set of the cosmic consciousness. However, some theories of physics consider "time" to be an illusion to avoid the simultaneity of the past, present and the future. Accordingly, when accessing the information field, one has to relate the information required to "now" or other known events.

It would seem that within cosmic consciousness there would need to be an organisation of events. For example, the concentric ripples on a pond's surface will not occur until a stone has been thrown into it. Thus, it would seem that handling sequential organisation would have to be a property of the information field. With this qualification regarding the concept of time, the stored information may be millions of years' old, so the information field must be self-organising and stable.

Not only must theories of the structure of the universe obey quantum physics, but also they must explain it. An alternative consideration is that the conscious universe / the information field and the consciousness of living beings may be the reason for our perception of quantum physics, dowsing, intuition, and all the universal constants, angles, and mathematics described in Chapter 5 of this book.

Send Mode

Consciousness is both passive (when just observing events) and pro-active (if deciding to do something). Information is involved in both of these situations. Starting with the pro-active case when sending

information, let us now trace the path of the information flow through the model postulated in this article. Figure 10-2 depicts this flow.

Logically following the information flow clarifies how this model helps in explaining various phenomena. The physical body (represented at the bottom right of Figure 10-2) has to communicate intent to the mind. The mind has to access and sometimes influence the information field. Considering each element in turn, starting with the physical body:-
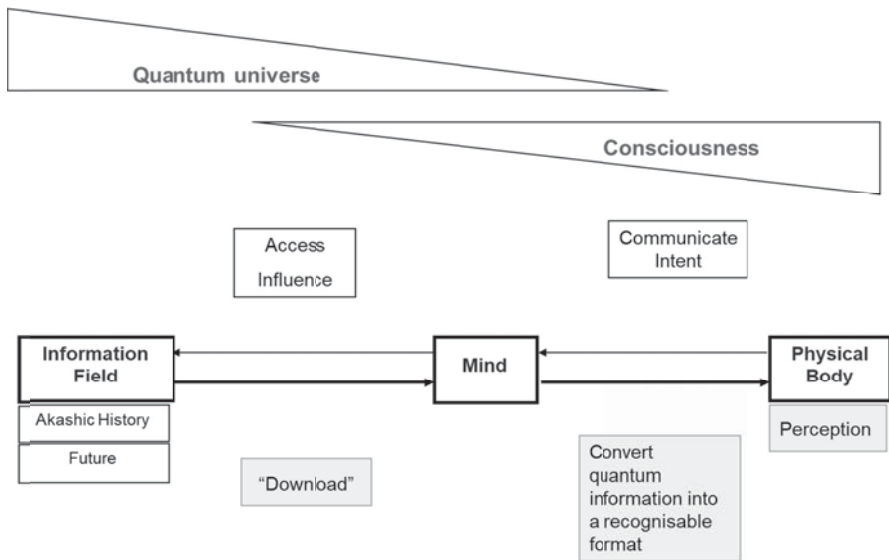

Figure 10-2 Depiction of Information Flow to the Mind and Body.

The Physical Body and Intent

Before discussing some relevant examples of intent, it is first necessary to discuss free will. If we assume that we have some free will, is this in conflict with the previous statement that cosmic consciousness or the information field holds future information? For the following reasons, I do not feel that everything in the future is pre-determined:

a) Everything being pre-ordained does not reflect reality. If everything was pre-determined, there would be no motivation to do anything. Although not very scientific, the attitude of *"Why bother"* does not build civilisations.

b) Intent would only reflect the information field. Therefore, there would not be much of an information flow, and not much to discuss about a model of consciousness.

c) If the information field does not hold all future information, we limit the messy concept of an infinite number of parallel universes.

However, if the cosmic consciousness is a fundamental part of the structure of the universe, it provides a mechanism to influence or steer evolution in general; of physical objects, life, and thought. Perhaps one can change one's destiny within the "basic plan" set out by genetics and circumstances, etc. One has the opportunity to change it, but one has to make that conscious decision to do so. For about 2,500 years, this has been a complex and on-going philosophical topic with no simple answers.

With the above qualifications, examples of intent are as follows. There obviously are an infinite number of intents by a vast number of people and other sentient beings. Expanding on the analogies mentioned earlier, major breakthroughs in astronomy are made when striving to find the boundaries of the observable universe. Similarly, significant scientific findings are made in delving deeper into ever smaller boundaries in particle physics. Adopting this type of approach, the vast majority of intents are dismissed in this article, as only unusual intents relevant to the boundaries of consciousness are considered here.

The desire to drink a glass of water probably does not help us to research the information field. However, one common desire that does help us in our quest is to seek information; the simplest being a binary question with a "Yes/No" answer. A relevant example when dowsing would be "is there drinkable water beneath my feet?" Another common, but non-complex intent, is to find a lost object, or to search for subtle energies. As we have seen in Chapter 4, an effective tool for researching consciousness is using intent to create remote mind generated dowsable geometric shapes with the purpose of comparing them to the original intended geometrical shape in an attempt to understand differences, perturbations, or distortions.

A more sophisticated intent is to seek information in general, not just a "Yes/No" answer to a question. For example, having found drinkable water, it is possible to determine its depth and flow rates. Intents that are more ambitious may be for someone to try to influence events, making things happen, or even in these days, a non-trivial desire such as finding a car parking place. A further extension to an objective of intent is to influence people. Adopting a positive approach to life seems to work, and even helps to build multi million pound businesses. Apparent telepathy,

such as pre-empting a phone call is a similar example of influencing people, especially between close family members. Other complex, but common intents, include the desire to perform faith healing, or to remote view places for military and intelligence purposes.

Choose a Technique

If the initial part of intent is a desire to do something, the next part of intent is to choose a technique that hopefully will lead to implementing the desire. Intent has to be conveyed to the mind. There are several well-established techniques to achieve this. Determining a protocol is a primary starting point, and the following techniques are in common usage.

The use of visualisation and images is very powerful, and can be a more concise and accurate tool to convey intent, than using just words. Extending this concept to quantifiable techniques is to visualise precise geometric shapes with specified dimensions, and project these shapes, say, from an aircraft flying at several thousand feet to a specific location several thousand miles away. An independent remote observer can detect these shapes by dowsing, and record their location, geometry and dimensions. It is then possible to compare the accuracy of the two sets of images, and hence the accuracy of this model. Visualisation techniques can be relevant for most situations.

On-site dowsing; map dowsing; information dowsing; or photograph dowsing are well established techniques for clarifying and focusing intent. Similarly, ancient desires, such as telepathy, and remote viewing can also be explained using this model. In fact, apart from the ethical implications, there has been significant recent interest in developing protocols to improve the accuracy of these intentions.

It must be stressed that not all of the above intentions will have the desired outcome with 100% certainty. Like quantum physics, the outcomes have different probabilities. Different people have varying skills and success rates. "Simple" items at the top of the above list, such as detecting underground water, may, with certain people, have over a 90% success rate. Whilst items towards the latter part of the list, such as influencing people, may only have less than a 10% hit rate, or only slightly better than random. Apart from the obvious fact that people have differing levels of ability, training, and practice, one possible reason for low hit rates is that there may be an inadvertent intent to interfere with the "universal system" or "destiny", or not allowing sufficient time for events to unravel, thereby creating a conflict, in which case one cancels out the other.

Techniques for Preparing the Mind

The mind now needs to action the intent. Conceptually, this is a separate step from creating intent, and selecting a technique, as discussed above. However, these two processes could be concurrent within this phase of preparing the mind. To achieve this, the mind prepares to access the information field, possibly using one of the following well established relevant techniques: - meditation, trance, sub-conscious deliberation, dowsing, prayer, or positivism. As these are well covered in existing literature they are not expanded upon here.

Action the intent

We now need to action the intent by accessing the information field. In doing so, it would seem necessary to convert the macro intent to micro action. This would possibly involve an interface with quantum information. Fractal or self-replicating geometry could be the conceptual mechanism for converting macro intent to micro action. In other words, geometrical images, or observations, are automatically and endlessly repeated smaller and smaller, to produce a reduced sized copy of the whole visualisation that the quantum part of the brain can action. Analogies could include the ever growing boundary of a Mandelbrot set (a famous example of a fractal), or fractal pentagrams/pentagons ever decreasing inside each other like a set of Russian dolls. This self-similarity can be exact as in the pentagram example, or quasi and not totally identical as, for example, a fern leaf. As discussed earlier, dowsing is sometimes not precise, or different dowsers making the same measurements obtain slightly differing results but still produce the same ratios and angles. Fractals involving quasi self-similarity could be relevant in this context, and dowsers improve with experience.

In some cases of intent, it may be necessary to modify the information field, as opposed to just accessing it "passively". A simple example of this is planting information in the information field, such as setting down dowsable geometric shapes, earth energy lines, or spirals in a specific location. An independent person could then detect them with the results used to research the universal consciousness model. It should be remembered that in some cases there could be an elapsed period of time between the original intent being initiated, and arranging the correct circumstances necessary to action that intent.

Receive Mode

Having accessed the Information Field, let us now consider the flow of information back to our physical bodies. This is depicted in Figure 10-3, and can be conceived as a "download" of information, which, in turn, involves converting quantum information into a recognisable format. The final step is an individual's perception of what the converted quantum information means, and often relates to personal experiences. This is why it is possible for different people to obtain varying answers when assessing the same event or fact. Let us look at each element of this process, starting with the "download" analogy.
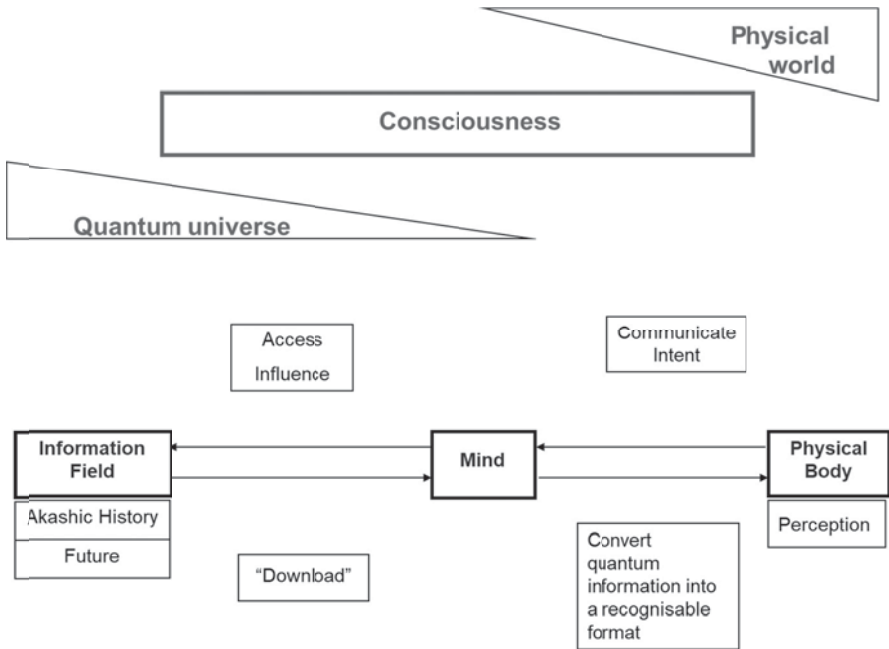
Figure 10-3 Consciousness Embracing both the Quantum and Physical World

Techniques for "Downloading" the Information Field

The following are a sub-set of the previous techniques for accessing the information field, plus some additional methods and observations. As before, the following well-established list does not require further

elaboration. Downloading can occur whilst in meditation or a trance, or whilst deeply engrossed in the "sub-conscious". One often experiences out of the blue "Eureka" moments, or having premonitions, whilst dreaming or waking up during the night, reaching an answer to a problem. Alternatively, this mental state is a natural part of the process of dowsing. It is also possible to utilise various other protocols.

Conceptually, and thinking in classical physical terms, **access** is initially a searching concept, and is different to **"downloading"** information after having first obtained the access point. However, in the quantum world, these processes could be combined or are instantaneous. On the other hand, there is often a delay between worrying about a problem, and receiving inspiration sometime in the future, possibly unexpectedly.

Process Information

Having accessed and downloaded quantum information, the mind now has to process and interpret it. In doing so, it has to filter from an infinite sea of data in the information field, the one piece of relevant information. As already explained in the Introduction, non-psychics or non-dowsers may not appreciate that the mind naturally has a "switched-off" state. The reason being is that people would literally be driven mad by having to process an infinite amount of information. A specifically defined intent is essential to "switch-on" the mind to a specific "channel". Similarly, people would not necessarily be aware of a psychic phenomenon or an earth energy line unless they are specifically advised to look for it.

The mind, in its widest sense, has to convert micro information into macro comprehension. As before, fractal geometry could be the mechanism for this, whereby quantum information is converted into a recognisable tangible format. A further ability of the mind could be to detect changes in the information field, which could be necessary for someone to be aware, for example, of a newly created dowsable earth energy line, or a mind created psi-line. It is debateable whether the "dowsable line" exists physically, or, as elaborated later, is a perception in the mind.

Measurement is key to scientific research. As discussed earlier, when measuring identical dowsing phenomena (such as the width or length of a line), it is well known that different dowsers obtain different results. This is an important factor as it not only enables a scientific study of the factors involved in dowsing, but also supports the theory that quasi self-similarity fractals may be involved in converting micro to macro information. The simplest interpretation of downloaded data is for the mind to create

geometric shapes (which has the advantage of providing quantifiable research experiments), whilst the more general process is for information to be visualised resulting in complex images being created, possibly in the "mind's eye".

It is now appropriate to consider the perception by individuals of the downloaded information or created images.

Perception

The simplest case of perception of downloaded information is a "Yes/No" answer. This is the most frequent use of dowsing, whether using tools, or the more sophisticated use of "device less dowsing", whereby one has a sensation in the mind's eye, throat, or solar plexus for a "Yes/No". At a higher level of complexity, one builds a model of the downloaded information in the brain. A common interpretation of information when dowsing is as geometric shapes, such as spirals, lines, or angles. In general, people interpret information based on their personal experiences.

As discussed in Chapter 1, sight is a good analogy to perception as postulated in this model. Essentially, the eyes optics are converted in the observer's mind/brain into a coloured, three dimensional resultant model of the original image. This model forms a perception in which the person observing believes that he or she is "seeing directly" what is being looked at. This analogy is also appropriate, as not only do some people seem to have to dowse with their eyes open to obtain better results, but more fundamentally, as has been demonstrated in this book, an important research tool is to dowse pure geometrical shapes, for which sight is obviously essential.

Information or remote dowsing is obviously "all in the mind". Recent experiments in dowsing local geometric shapes suggest that some perceived subtle energy fields are not physically there, so they cannot be detected or measured locally by, say, a "conventional scientific" meter. Adopting the concepts of the model of consciousness discussed here, subtle energies or images are a construct of a perceived model in the observer's brain cells, as a result of the mind interaction with the information field. Moreover, it is relatively easy to superimpose a physical background or object, such as a tape-measure, on these dowsed images, to form a combined seamless perception. This is a further suggestion of a link between the way the mind processes sight and dowsing.

Conclusions

In researching consciousness, the handling of information by the mind is key. It would seem that the mind is more than just a brain in a skull. Experiments, observations, and measurements lead to developing the universal consciousness and information field theory, together with a preliminary attempt at striking the appropriate balance between mind and matter. There are good logical reasons for elevating consciousness in the scientific understanding of the structure of the universe. If substantiated, this approach may enable an easier interpretation of such concepts as the anthropic principle, and other philosophical and scientific conundrums.

This has started to highlight many links between consciousness, and seemingly unconnected physical concepts such as geometry, gravity, magnetism, and astronomical factors. For example, it has been shown that gravity can affect the perception of what is being observed – both in its dimensions and/or its composition. Similarly, magnetism can affect what is being observed, but differently from gravity. It is well proven that astronomical factors, which are obviously non-local, and probably in connection with gravity, also affect what is being observed. It has also been shown that the mind appears to interact with pure geometry. The latter not only produces dowsable patterns that may resemble those from diffraction gratings or x-ray crystallography, but in some cases when viewing a 2-dimensional source object (e.g. a short pair of parallel lines drawn on paper), the observer perceives the same image as viewing a totally different 3-dimension object (e.g. a massive pair of sand dunes).

The model for consciousness being developed in this book, provides possible answers to some of the mysteries of quantum physics. For example, the often-quoted Copenhagen interpretation can be reworded as "what one observes depends on the question being asked" or "the act of observation affects the result". As we have seen, this is the starting point of dowsing where the language and objective is "intent, the mind in its widest sense, and consciousness". If one is looking for waves, one finds waves. If one is looking for particles, one finds particles. Hence, wave-particle duality and conscious observation actually creating physical reality are less of a conceptual problem. Similarly, remote interaction, an object being in two places simultaneously, and large objects as well as small obeying the rules of quantum mechanics are all compatible with the model described in this chapter.

Summary

Using a combination of reviewing the extensive relevant literature, the author's original scientific research, and exploring the boundaries of human experiences, this chapter develops a model for consciousness. Consequently, consciousness is elevated in the scientific understanding of the structure of the universe, possibly enabling easier interpretation of such concepts as the anthropic principle and quantum physics. The handling of information is a key, leading to a review of the information field theory, together with a preliminary attempt at striking the appropriate balance between mind and matter.

The Way Forward

Much of this chapter can be classified as philosophical, as many of the ideas are difficult to test. To make this model more scientific, mathematics, measurements, and comparison to observations are necessary. A vital component of any scientific theory is that the theory can make novel testable predictions. In this case, an acid test could be that the mathematics for the cosmic acceleration be re-worked, but with a structured zero point field, as discussed here, and see if this produces results that are 120 orders of magnitude less than the current interpretations of the zero point field and quantum physics, and, therefore, tie up with observations.

What is consciousness? As is apparent, this is a vague term, and this chapter has avoided defining it. It is suggested that only after all the concepts presented here are better understood, can a robust definition of consciousness be produced.

Future research into dowsing and consciousness could be directed in two parallel streams. Either top down, by possibly contributing to the development of the "theory of everything", quantum gravity, and establish that mass and the laws of physics are inter-related to consciousness, or bottom up by performing numerous simple experiments such as those touched upon in this book. The latter includes bringing matter into this model by measuring such things as the size of an object's aura against its mass, and exploring consciousness and the information field by dowsing simple geometric shapes. Using the analogy of X-ray crystallography, this latter technique could be used to investigate the structure of the conscious universe / information field. Either way, these are exciting times.

CHAPTER ELEVEN

HOW NOETICS AND DOWSING WORK

Introduction

For thousands of years people have wondered how noetics and dowsing work. We are fortunate in living at a time when the answer is accessible: thanks in part to living in the information age; the appreciation of the importance of geometry in the structure of the cosmos; the ascendency of ancient Eastern philosophy; and after 100 years, still not understanding the weird effects of quantum mechanics; science is beginning to accept the non-orthodox.

Based on a plethora of experimental evidence, this chapter explains an understandable model on how dowsing works. To simplify the discussion and avoid the reader reverting to other chapters, this chapter includes a recapitulation of relevant topics that were covered earlier, resulting in some minor duplication.

As already discussed, it is not the rods or pendulums that produce the dowsing response - they only amplify the sensation. As this book demonstrates, the mind and its interaction with the cosmos are paramount. Coupled with this concept is that local and astronomical forces significantly affect the mind-cosmos relationship, resulting in what is being perceived.

Device-less dowsing pure geometrical shapes is a powerful technique in simplifying scientific research into dowsing. For example, the effects of gravity, magnetism, photons, spin, and orientation have been quantified experimentally. It has also been proven that these forces do not affect the dowser, only what is being dowsed.

This model applies to all types of dowsing and associated techniques, such as information dowsing (including health, and searching for objects, minerals, or water), earth and subtle energies, map dowsing, dowsing photographs, archaeological dowsing, telepathy and remote viewing.

The Optical Model

The first step in some forms of dowsing requires seeing an image, especially when not on-site, or the dowser has not ever been to the location. For example, without visualising a map or photograph when map or remote dowsing, or the local topology when archaeological or earth energies dowsing, or when searching for minerals or objects, or investigating the colours and structure of a person's aura, it is difficult to connect the dowsed perception to physical reality. Some aspects of consciousness and dowsing, therefore, involve vision.

Stereo information is communicated via the eyes, retina, rods and cones, and along the optic nerve to the brain. A 3-dimensional optical model is then created in the brain cells. It is important to stress that one does not "see" a physical image on a retina. These concepts are paramount when explaining dowsing, "reality", and perception. This conceptual input phase is depicted in Figure 11-1, with subsequent figures in this chapter adding additional information to build the final figure depicting the entire model.
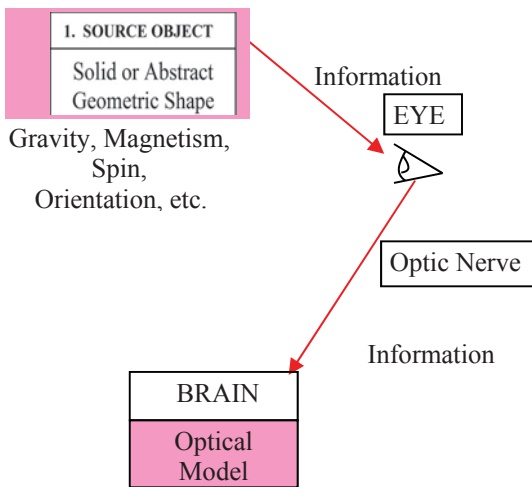
Figure 11-1 Creating an Optical Model in the Brain

The Mind

Via intent, the relevant optical model and associated information is transferred to the mind – the "greater" brain that can link to the structure of the cosmos. This is depicted in Figure 11-2.

There is a second source of input for many people. The input is "sensed" by the body, or intent is created, and information goes straight into the mind, not via the eye. Examples include dowsing subtle energies but not possessing the ability to "see" energy lines, or when information dowsing abstract concepts, or dowsing subtle energies, or visualising intent.
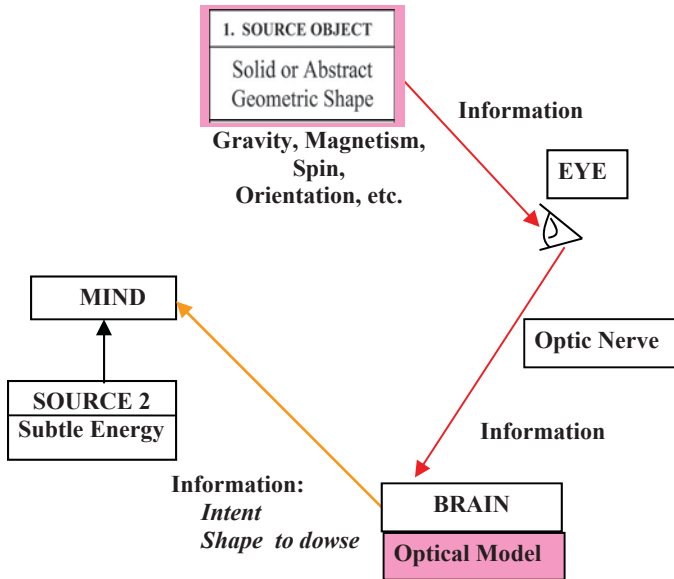
Figure 11-2 The Brain, Intent, and the Mind

The Information Field

The conceptual logic of the next phase is shown in Figure 11-3. The mind transmits the intent and relevant information to the information field, which is postulated as part of the structure of the universe. For example, the dowsed object has a specific orientation, and may be immersed in local

gravity, electromagnetism, or the earth's spin on its axis or around the sun. Conceptually, for physical objects, communicating this information is easy, as the relevant part of the cosmos is in the centre of, surrounds, and creates the dowsed subject. For dowsing intangibles, it seems that the information is communicated by specific types of subtle energy and standing waves to a "relevant" part of the information field.
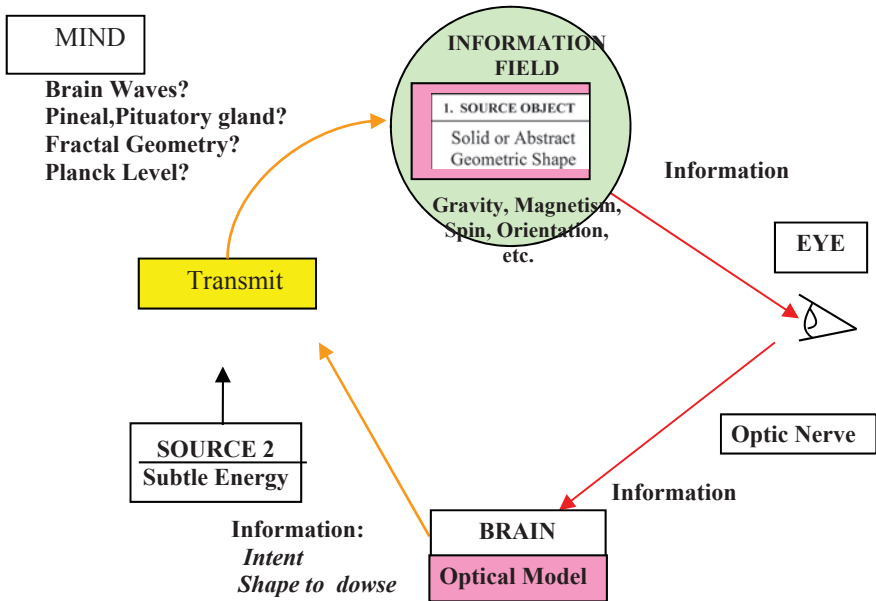
Figure 11-3 The Mind Communicates to the Information Field

The postulation is that dowsed information is sent down to the Planck level, which is the smallest level of physical and quantum reality. However, this mechanism is currently the great unknown, and is the subject of extensive research. For example, there are at least 5 steps in the brain involved in producing speech, starting in an area of the brain dealing with initial non-verbal thoughts.

Some current suggestions as to the mechanism for the brain interacting with the information field, but currently without solid scientific evidence, include brain waves and electrocorticography, or the involvement of the pineal or pituitary glands. As will be demonstrated in future chapters, communication speeds greater than the speed of light are involved.

Therefore electromagnetic waves, limited to the speed of light, cannot be involved or are only part of the story.

The brain, like all matter in the universe, is made up from relevant constituents of the cosmos starting at the Planck level. Conceptually, the brain's neuron system has both a macro and sub microscopic components giving "access" to the quantum world. This combination gives rise to consciousness. It is not possible, therefore, to completely distinguish between the mind, matter, and consciousness. Present developments suggest that the structure of space-time incorporates a holographic storage of information in at least 5-dimensions. Dowsing could involve these higher dimensions. Is fractal geometry involved in converting the brain's macro visualised intent to micro quantum information? Could the conscious universe / information field even be involved with the brain's initial non-verbal thoughts?

Download Information

The mind then accesses the information field, and downloads the relevant information – possibly in a geometric form. The latter could incorporate a transformation of the source geometry into a version based on the structure of space time, plus the effects of local forces. This is illustrated in Figure 11-4.

As probabilities are an inherent part of the quantum world, accessing the information field is not always a 100% certainty. Dowsers may be better at different types of dowsing, with varying success rates, but practice can increase hit rates.
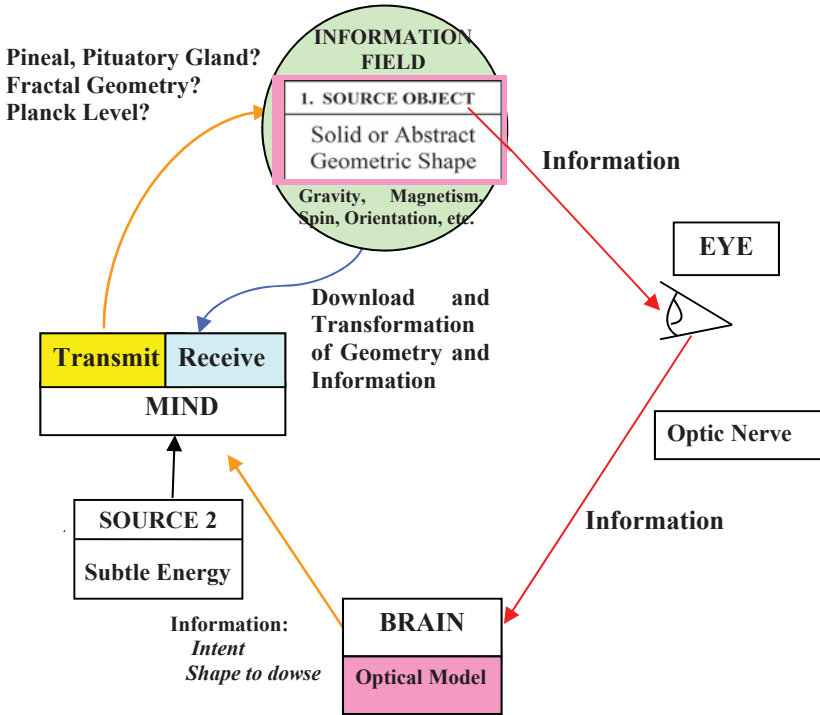
Figure 11-4 Download Information to the Mind

Dowsing Model

The brain having built a model based on its received and perceived noetic information, interprets it, and superimposes it onto the brain's optical model. For example, when archaeological dowsing, or dowsing subtle energy lines with a measuring device, the mind needs to superimpose the perceived dowsed geometry on to a tape measure. This is illustrated conceptually in Figure 11-5. People perceive noetic images slightly differently, which partially is explained by this personal superimposition process, together with the uncertainties of the quantum world.

Pineal, Pituatory Gland? Fractal Geometry?

INFORMATION FIELD

1. SOURCE OBJECT

Solid or Abstract Geometric Shape

Gravity, Magnetism, Spin, Orientation, etc.

Information

EYE

Transmit **Receive**

MIND

Transformation of Geometry and Information

PERCEIVED DOWSABLE PATTERN

Optic Nerve

SOURCE 2

Subtle Energy

Dowsing Model

BRAIN

Optical Model

Information

Information: *Intent Shape to dowse*

Figure 11-5 Perception of Received Information

Conclusions

This model of how dowsing works explains, in principle, all forms of dowsing and associated techniques. It is compatible with a plethora of experimental evidence. The mind is a conceptual entity existing between the brain and the structure of the cosmos. The latter is believed to comprise at least a 5-dimension, holographic, quantum universe that is based on information, geometry, fractals, ratios including harmonics, irrational numbers such as phi (φ), chaos theory, and yin-yang properties (e.g. male/female, positive/negative, dipoles, abstract/physical, matter/anti-matter, etc. Possibly these may be different manifestations of the same basic structure). This mix, together with free-will and intent creates consciousness and dowsing.

The Way Forward and Further Research

In order to improve comprehension of noetics and dowsing, further research is required into interrelated topics which include a universal consciousness, a possible 5-dimension, holographic, quantum universe that is based on information, geometry, fractals, ratios including harmonics, irrational numbers such as phi (φ), chaos theory, and yin-yang properties (e.g. male/female, positive/negative, dipoles, abstract/physical, matter/anti-matter, etc.)

Chapter Twelve

Categorising Different Types of Subtle Energies: Part 1

Introduction

Why Categorise

Previous chapters have hinted at different types of subtle energies. To date, nine different subtle energy types have been identified and itemised together with some of their properties. These all have a connection with the earth's environment, geometry, and the laws of physics. Each of these fields, or what is perceived as a subtle form of non-physical energy, seem to display differing properties. So why categorise?

Historically, progress has been made in understanding science by such analysis. Categorising the ninety plus elements occurring in nature into the Periodic Table helped in comprehending that each element was simply determined by the number of protons in its nucleus. Chemistry could then be explained by the latter being balanced by the corresponding number of orbiting electrons forming shells, which reflected the structure of the Periodic Table.

Another historical example was cataloguing the plethora of discovered "fundamental particles". This led to the understanding of the standard model of sub-atomic particles, which, in turn, led to a much smaller number of more fundamental particles, such as quarks. Even in biology and botany, categorising living matter into 3 or 4 levels of similar plants and animals has proved invaluable in research, and furthering the study of evolution.

Similarly, when dowsing, I believe it is beneficial for scientific research to categorise sensations into different forms of perceived subtle energy. With a little practice, it is readily possible to compare identical perceptions to other situations. Professionals, academics, and amateurs, of

whatever branch of subtle energy research, are invited to see how many different types of subtle energy they can detect.

It is anticipated that eventually this categorisation will lead to a simplification of the nebulous subject of dowsing and subtle energies. This should produce greater insight and further comprehension of consciousness, perception, and the mind interacting with the structure of the universe.

Approach Adopted

Where possible, each perceived subtle energy is analysed by comparing the following properties and characteristics:

1. Where each subtle energy field is found.
2. The source for each field type.
3. The associated geometry of the source.
4. The geometric pattern of the subtle energy field.
5. Linear or ellipsoidal fields.
6. The length, width, and height of each field.
7. The perceived flow and its direction.
8. If the subtle energy has vector effects on measurements.
9. Any associated mathematical equations that describe the patterns produced.
10. Clockwise or anti-clockwise flows of spirals.
11. Whether gravity, photons, magnetism, or spin affect the field.
12. The stability or decay of the field over periods of time.
13. The attenuation of the field by metals, rocks, or organic material.
14. The field strength.
15. If the concept of male or female can be associated with the field type.
16. The associated wavelength, if applicable.
17. The associated velocity of communicating information.
18. Conversions of one type of field to another.
19. The associated Mager colour.

Table 12-1 Perceived Subtle Energy Characteristics and Properties

As explained in previous chapters, perceiving subtle energies, by their nature, is not like conventional science where, say, it is possible to get universal agreement to a meter reading. In practice, the consequence of this apparent limitation is that most dowsers will perceive similar effects of such physical influences as gravity, spin, magnetism, or light. However,

some may perceive varying colours or wavelengths. They all will perceive slightly different measurement of length, depending on the time of day, lunar month, and the year of observation.

In this context, these variables are not important, as the various properties that are perceived by each observer are being used to compare, contrast, and categorise the subtle energy as it is experienced. They should always perceive the same category for a given subtle energy.

The following types of subtle energies are listed together with their properties. Very occasionally, a subtle energy type or its colour, may appear to change. However, there is no firm evidence of this, but if it does exist, it could be caused by several factors. There could be an undetected change in the environment in its widest sense.

More likely though, in the early days of detecting different types of subtle energies, it is easy to confuse an unknown subtle energy that one has not yet identified and experienced. Alternatively, confusion is easily caused by a combination of several different types of subtle energies emerging from the same source, or occurring in the same psi-line or conical helix. The other complication is that some energy types appear in more than one form. For example, Type 1 subtle energy occurs in a straight line form, or ellipsoidal, such as in auras.

Once again, I learned all the above lessons the hard way. As I found new types of subtle energy, I have had to revise some of my earlier classifications! The numbering that I have given to the different types of subtle energies is based on the chronology in the order that I discovered them.

Mager Colour

As a simplified introduction to identifying different types of subtle energy fields, the concept of colour can be used. The Mager rosette is a disk containing various colours. It is a well-established technique that helps the mind to associate different types of subtle energies as a tangible colour on the disk. Although it is very simple to use and it quickly gives a result, it is "unscientific". It is personal because each person may see different colours. It is not infallible, but seems consistent for each individual, and helps the observer to identify different types of subtle energies

Type 1

Type 1 subtle energy is very common and is primarily found associated with inanimate and physical objects such as stones, crystals, or water. It is also found on ancient and archaeological sites. Abstract geometrical shapes, such as triangles and circles, can also produce Type 1 lines, some of which form very complex patterns.

The location and size of Type 1 fields change in time, and are influenced by cosmic factors such as seasons, eclipses, and the phases of the moon. This suggests the involvement of the earth's and moon's gravity, coupled with the earth's spin on its axis and rotation around the sun.

In Chapter 7, it was shown that if a source object, such as a crystal or seed, is kept in the dark, the Type 1 fields associated with its aura gradually decay to nothing over a period of a few days. This suggests that an electromagnetic component is involved in Type 1 fields. Apart from the above effects of photon deprivation, Type 1 fields are remarkably stable and free from decay over long periods of time.

However, as already discussed in Chapter 6, metals can attenuate Type 1 fields. Figure 6-7 illustrates how different thicknesses of aluminium can reduce the size of the Type 1 core aura of a pebble. The formula that best fits the data is exponential, with a very high correlation coefficient.

The sex of an inanimate object is an oxymoron. A Type 1 field may appear to reflect the sex of a person. It may dowse male or female dependant as to who created the field, or who was the last person associated with the source object.

Like most subtle energy lines, Type 1 appears to have a flow of subtle energy. The velocity of communicating information along Type 1 fields can be very slow, and not much greater than human running speeds, say 6 meters per second. Similarly, in several examples, the wavelengths for Type 1 fields are relatively long, and can vary between 10 mm and 15 metres. A simple example is that the Type 1 aura of some megaliths oscillates at a low frequency, with a period of a few seconds between each oscillation.

Type 1 fields could be perceived as a mixture of Mager colours, such as shells in multi-coloured auras. In contrast, Type 1 fields emanating from an abstract geometrical source can have a more specific colour.

Type 2

Type 2 subtle energy is primarily found associated with all life forms; large or small, plant or animal. Pre-life forms, such as seeds, as well as previous life forms, such as wood and leather, also produce a lesser powered Type 2 subtle energy.

In addition to the Type 1 aura produced by the life form's physical presence (i.e. its mass, shape, and substance) a Type 2 aura is also created. This is usually smaller than, and fits inside, the Type 1 aura. Ellipsoids and lines are the 2 main dowsable geometric forms of Type 2. Life forms produce a seven shell aura, which are driven by their seven chakras.

The size of an object's aura depends on the objects size and mass. For example, the size of the aura of a seed is less than that of a fruit, which, in turn, has an aura less than the aura of a tree. However, the size of a human or an animal's aura can also be easily controlled by the mind of the involved animal. Interestingly, under stress, plants can reduce the size of their auras and vice versa.

As discussed in Chapter 7, the chakras of life forms, as well as producing ellipsoidal auras, produce the tree of life pattern. The 10 Kabbalah vortices are connected by Type 2 lines.

Type 2 subtle energy may also be associated with inanimate tangible sources, such as the top of banks and ditches around ancient sites, or emanating from certain geometric shapes, such as along one of two parallel lines drawn on paper. These Type 2 fields are perceived as 3-dimensional lines often having a diamond shaped cross-section.

Type 2 fields do not appear to be influenced by gravity nor are they affected by photons. The latter is demonstrated in Figure 12-1, where a sunflower seed has been kept in the dark for a few days. The line with square data markers plots the size of the Type 2 aura, which, over a period of one week, does not diminish in size. As expected, the seed's life force is unaffected by being buried underground! In contrast, the line, with circular data markers, plots the decay of the seed's Type 1 aura over the same period of time.

SUNFLOWER SEED DECAY in Darkness
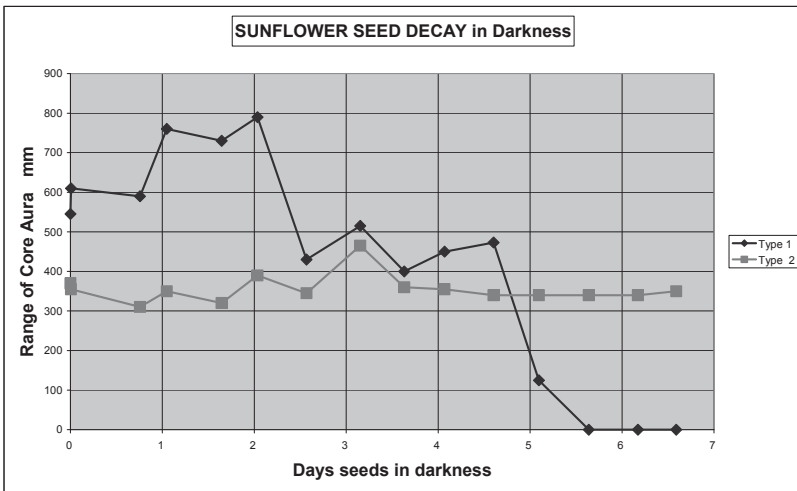
Figure 12-1 Comparison between Type 1 and Type 2 Reaction to Darkness

Type 2 fields do decay over a period of time, as all associated life forms eventually die. Figure 12-2 illustrates the decay of a daffodil flower over a period of a week. This shows that the Type 1 aura (circular data points) remains approximately constant, as the physical stem remains constant, but the Type 2 aura decays as the flower fades. Note that the life force producing Type 2 subtle energy is still present, to a lesser extent, after the flower has died. This is compatible with "dead" items such as leather, or wood emanating Type 2 fields.

Metals do not attenuate or screen Type 2 fields. The perceived field strength of a Type 2 field is a function of the size and mass of its source. The sex of an animal can be dowsed even after death. Most seeds and plants fields have been observed, nor does it seem possible to convert Type 2 fields to another type. Type 2 auras are multi-coloured.
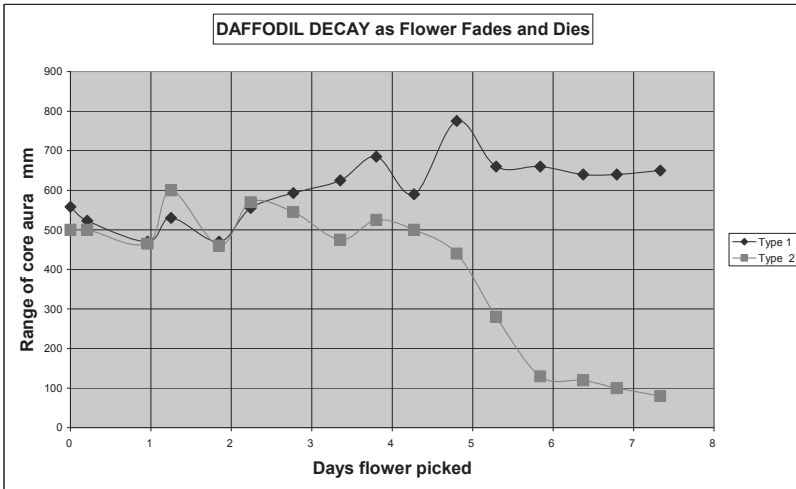
Figure 12-2 The decay of a daffodil flower's Type 1 and Type 2 fields

Type 3

Type 3 subtle energy is very common and is always associated with spirals, Cornu spirals, and vortices. I have experienced Type 3 fields occurring in the following situations:

(a) in association with the outer structure of auras of both inanimate and animate objects,

(b) at the top of banks at ancient sites, or between 2 parallel lines,

(c) the vortices in the Kabbalah tree of life pattern,

(d) terminating dowsable lines,

(e) at the intersection of two Type 1 or two Type 4 linear fields,

(f) created by "domed chambers" be they in underground caves, or within buildings,

(g) occurring frequently as earth energies, including their possible creation by underground water flows, or volcanic activity and vents,

(h) Type 3 spirals have also been used to determine the optimum location for building ancient sites, burial mounds, and temples and

(i) terminating mind created psi-lines.

Although the initial impression at ground level is a 2-dimensional spiral, the Type 3 subtle energy structure is 3-dimensional. Usually, the Type 3 spirals are a series of conical helices stacked 7-fold several metres high. Type 3 fields are always helices, and often have a conical vertical cross-section.

 As the helices associated with Type 3 fields seem to have a vertical axis, gravity would seem to be involved in their production. Type 3 fields are not affected by photons. The aura of an object that has been kept in the dark for several days does not lose its outer Type 3 spirals (even though the aura's inner Type 1 ellipsoids have decayed).

The entrance of the Type 3 spiral usually points due north from the centre of the spiral. This indicates that the spin of the earth is a factor in the creation of spirals. Type 3 produces outward flowing bifurcation lines starting at the northern spiral entrance. Interestingly, after bifurcation, the resulting lines are Type 1 Mager white, which terminate in a much smaller Type 3 spiral continuing in ever decreasing sized bifurcations.

Type 3 fields are remarkably stable and free from decay over long periods of time, and are not screened by metals or rocks. Type 3spirals usually have a perceived Mager colour of green.

As spirals and conical helices are so important and appear so frequently, Chapter 18 is dedicated to them, where more information can be found.

Type 4

Type 4 subtle energy is primarily found associated with, and as a result of, thought or prayers. It is an example of a tangible manifestation of intent. Type 4 fields appear in sacred scrolls, and are particularly strong around the ark of synagogues or the altar of cathedrals. They also seem to be associated with remote dowsing, and are usually manifested as lines and geometric shapes created by the mind, including shapes floating in the air or projected remotely. Type 4 subtle energy, usually indicates mauve/violet on a Mager disc.

As discussed in Chapter 8, abstract geometry sources and other virtual dowsable objects also produce Type 4 auras having nine shells, separated in an approximate geometric series.

Physical and abstract sources that produce Type 4 subtle energy lines include 2-body interactions. These usually end in a Type 3 green spiral. Type 4 is a short-range subtle energy that often has a flow. Sometimes it could become confused with Type 8 subtle energy (which is discussed later in Chapter 21) but this is long range and linear.

Another source of Type 4 subtle energy occurs between banks and ditches, as discussed earlier. These lines appear to have a rectangular

shaped cross-section. Another Type 4 field is a figure of eight pattern, which appears in some ancient stone circles. In summary, there seems to be many "flavours" of Type 4 fields. The most common manifestations are amorphous fields clinging around sacred objects, extensive parallel beams, ellipsoidal fields, and cones.

The size of a Type 4 field produced around a physical source is a function of its mass, as well as the intensity of intent or prayer. For example, the Type 4 field of a small sacred scroll has a smaller range than a cathedral altar. Table 12-2 is an example of a religious artefact of composite materials, having different ranges for each of its subtle energies.

Subtle Energy Type	Comparative Detection Distances
Type 1	430mm
Type 2	300mm
Type 3	5,370mm
Type 4	775mm

Table 12-2 Comparison of the Extent of Subtle Energy Types

As is apparent from Table 12-2, the Type 3 field extends the furthest, followed by the Type 4 and then the Type 1 with the Type 2 field extending the shortest distance. This is obviously an arbitrary example, but is a fair representation of relative strengths.

Type 4 fields do not appear to be affected by gravity. Nor are they affected by photons, or electromagnetic fields. They are remarkably stable and free from decay over long periods of time. They are not screened or attenuated by metals or any materials: they seem to pass easily through buildings. Several researchers have confirmed that the colour of Type 4 fields is perceived as predominantly blue/indigo/violet.

Type 5

Some types of subtle energy are mainly produced by geometric shapes, not matter. Type 5 is such an example, and is a rare form of subtle energy that is not immediately obvious.

One example discussed earlier, is the subtle energy beam emanating from the centre of an abstract circle, or from a simple cross drawn on paper when held vertically. This form of Type 5 subtle energy is a diverging beam comprising 9 coaxial cones, with its field strength

decreasing as it leaves its source. This beam is usually white, Type 5, with an outward flow, irrespective of orientation of the source or observer.
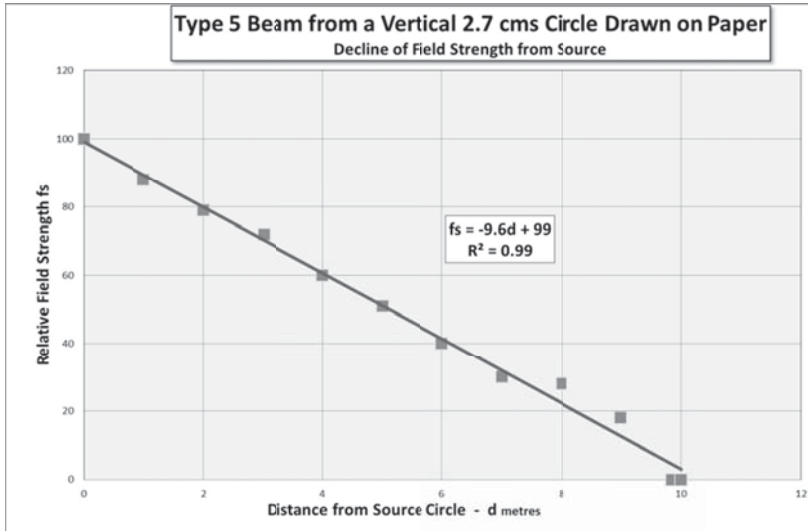
Figure 12-3 The Reducing Field Strength of Type 5 Subtle Energy

The graph in Figure.12-3 is linear with a very high correlation coefficient. It shows the decline in the field strength of a Type 5 beam emanating from a vertical circle drawn on paper as it leaves this source. The lower 3 data points appear to have a slightly greater error, probably due to the difficulty in detecting accurately weak subtle energies.
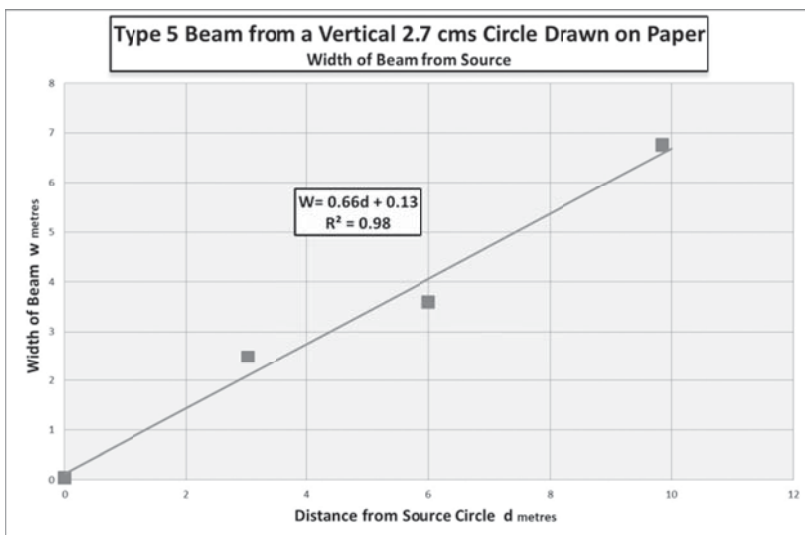
Figure 12-4 The Divergence of a Type 5 Subtle Energy Beam

This straight-line graph is unusual for 2 reasons. It does not decline in an inverse square relationship, as say, an electromagnetic field. Also, as we have already seen with other types of subtle energy, such as auras, it is "normal" for a subtle energy to stop suddenly at a boundary without any warning.

The linear graph in Figure 12-4 also has a high correlation coefficient. It shows how a Type 5 subtle energy beam diverges as a linear cone, whose apex is at the centre of the source circle. For this particular example, the base of this cone does not extend past approximately 10 m from the source circle.

The initial results suggest that the cone's half apex angle can vary from about 1° to 20° and is a function of the lunar month: a new moon producing greater divergence. However, this requires further research.

Type 5 subtle energy is detected at the entrance to most spirals; in particular spirals that terminate energy lines, such as at the end of radials in a peace grid, or in 2-body interactions, or Psi-lines. A small ellipsoidal portal (about 10 x 20 cms) exists at these entrances from which bifurcations commence, and where, intriguingly, a 5-dimension noetic response is obtained. This is the same response obtained when dowsing source geometry of half a sine wave. The Mager colour for Type 5 is usually violet/ultra-violet. It is not known how to interpret this 5-dimensional response to Type 5 subtle energy.

Summary

The easiest way for a researcher to fine tune their minds into detecting different subtle energy types is to refer back to Figure 2-3, using the simple source geometry in Figure 2-5. The white lines are Type 1, the line through the upper bank is Type 2, the spirals between the 2 banks are Type 3, and the line going through the lower bank is Type 4.

Further Subtle Energy Types

Only 5 of the 9 detected subtle energies are discussed here. Comprehension of the remaining 4 subtle energies may be easier after first studying multi-body interactions, psi-lines, conical helices, the structure of subtle energies, and the effects of tetrahedral geometry on the mind's perception. These are covered in the following chapters, after which follows Chapter 21, "Categorising Different Types of Subtle Energies – Part 2".

Chapter Thirteen

Photographing Subtle Energies

Introduction

It is well known that photographing dowsable fields captures most, if not all, of the characteristics of the actual subtle energies at the scene being photographed. When such a photograph has been subsequently printed, dowsing the photograph produces identical geometric subtle energy patterns to those when on-site. Even if this seems incredible, the following research experiments, using basic photographs, produce findings that are not only unexpected, but help in understanding the interactions between the mind and the cosmos.

Practical Examples of Photograph Findings

Examples of several very interesting effects that I have witnessed and performed include the following:

1. Placing several photographs on top of each other presents no problems with regard to interactions. If the observer's intent is on the top photo all the others are ignored.

2. It is instructive when on site, to place an inverted photograph of a subtle energy pattern, on top of the actual original dowsable field that has been photographed. If a linear subtle energy field was photographed, the inverted photograph can be placed anywhere along the actual energy line. All that is necessary is to align the photograph so that the north on the photograph is orientated to true north on-site. The amazing thing is that whilst the photograph is on top, the inverted photograph cancels out all trace of the subtle energy lines. Removing the photograph immediately restores both the original dowsable field and the dowsable effects from the photograph! Why this should occur is subject for further research.

 (This experiment could upset the balance of subtle energies, especially on important or sacred sites, or when other researchers are experimenting on the same site. Only after asking permission should disturbing subtle energies be undertaken, but never on a major site. Only use a minor site, or

a mind created field that will have no consequences, and always restore afterwards to the original state.)

3. If the original dowsable field is moved to a different location by using thought (as discussed earlier) the photograph of the original dowsable field also loses all its original dowsable characteristics. It does not matter how far away the photograph is located from the original field. If the original dowsable field is moved back to its original exact location, the dowsable characteristics return to the photograph. These counter intuitive phenomena, between the photograph and the information field, appear to be analogous to entanglement and coupled pairs in quantum physics.

4. Earth energies change in time. In a photograph, these changes are also recorded. The intent/question can be "give me the information of the dowsable field at the time of the photograph", or "give me the state now", or "at any time ".

5. Photographs can cause remanence. For example, a spiral can be "copied" from the photograph to the ground or the surface on which the photograph is resting. The remanence can be deleted by intent when the photograph is removed.

6. All nine types of dowsable fields (as discussed in this book) equally give this photographic effect.

7. Some people claim that the photochemical coating on the film "contains" the dowsable image, and hence the dowsable effect is electromagnetic in nature. However, digital photographs, even with low bit density, low-resolution printing, and black and white printing produce an identical dowsable effect. (It would be an interesting experiment to determine the lowest possible bit density information to retain the ability to dowse photographs). This suggests that it is the actual image of the photograph interacting with the information field that produces the same effect as the actual original site's interaction with the information field. Once again, the concepts, shape, pattern, and geometry occur when interpreting the interface with the information field.

8. Even with small photographs, the observer obtains full sized dowsable fields – the same as on-site.

9. It is equally possible to "map dowse" a photograph. This is true whether dowsing on the actual scale and size of the photograph, or placing the photograph on the ground. The same scale is obtained as if on the real site. This phenomenon is comparable to a virtual reality experience, whereby one can walk around a large field that is located remotely from the subtle energies that were photographed, and using the photograph as if on the actual site that had been photographed.

10. Photographing mind generated subtle energies gives identical results to photographing naturally occurring subtle energy patterns.

Protocols for Photographing Subtle Energies

In this section, photographs of actual dowsable sites are shown, each with reference to diagrams of the subtle energy patterns and geometry perceived by the observer when on-site. These have been independently confirmed by numerous other people.

After making sure that no strong naturally occurring dowsable fields are present in the vicinity, this book should be placed on the ground, open at the photograph being dowsed. Usually, the orientation of the photograph is important as it should be pointing in the same direction as the original subtle energy field. Apart from photographing spirals, there is often no reaction if the orientation is wrong.

The reader should then dowse the photographs naturally using his or her preferred device. I prefer rods for this exercise as I feel they give results quicker than other methods; they easily point in directions to walk; they provide direction of flows; and spirals are easily followed. The photographs can also be used to improve the skills of the reader in using device-less dowsing such as 'feeling' the field in one's mind's eye, when one may perceive a sensation of pressure in the brain.

Apart from checking the orientation of the photograph, the measurements taken should include the type(s) of subtle energy detected, the direction of flow, the Mager colour, and the pattern of the subtle energy geometry. It is also important to realise that in the time difference between when the photograph was taken, and the time the photograph is subsequently dowsed, the subtle energies on-site have probably changed. It is, therefore, instructive when visualising dowsing intent to specify both the state of the subtle energy when the photograph was taken, and then subsequently request the subtle energy fields that exist now. The two results can then be compared and the differences noted.

Several of the photographs in this chapter are from parts of Hengistbury Head, Bournemouth, UK. As well as being a very interesting Neolithic and Bronze Age site, it contains most of the subtle energies discussed in this book. I have frequently visited this site to check changes to the properties and details of subtle energies. Several other locations and non-UK sites are covered in other parts of this book.

Seven Type 1 Lines, Avebury stone circle

Figure 13-1 is a photograph of a very small part of the Avebury stone circle in Wiltshire, UK taken on 8th July 2001 at 14:53. The photograph was taken at the bottom of the ditch looking upwards.

Figure 13-1 One of the Banks at Avebury

Dowsing this photograph produces identical subtle energy patterns to Figures 2-2, 2-3, and 2-4 in Chapter 2 in relation to the banks and ditches at Hengistbury Head. Type 1 fields of the 7 parallel lines generated by the ditch and banks can be detected. The 7 separate horizontal lines are parallel with the top of the ridge, and should be found to extend over approximately 16 feet, similar to the actual separation distances on site.

One Type 1 Line, Hengistbury Head

The photograph in Figure 13-2 is one of the 14 Type 1 parallel lines created by the double dykes at Hengistbury Head. This photograph was taken on the 24th September 2001 at 19:00.
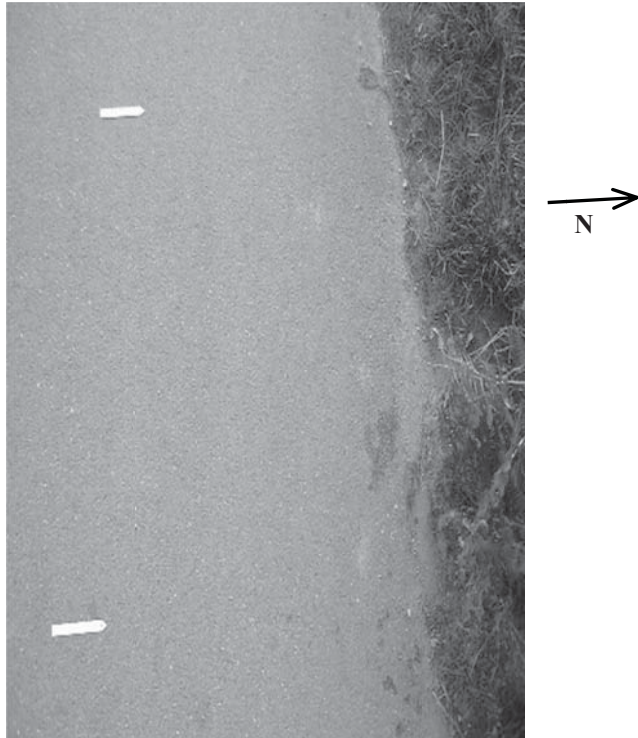
Figure 13-2 Section of a Type 1 Subtle Energy Line

The Type 1 field comprises a single 4 ft width band with a perceived flow from south to north i.e. from left to right across the page.

Seven Horizontal Bands on an Avebury Megalith

Figure 13-3 is a photograph, (best held vertically facing east), of Type 1 fields comprising seven horizontal bands on the surface of a megalith at Avebury. This photograph was taken on 8th July 2001 at 16:50. As the megalithic stone has subsided over the years, the lines are no longer

horizontal but parallel to the top surface i.e. these lines were possibly horizontal when the stone was vertical.

Figure 13-3 A Megalith at Avebury

Five parallel lines can be detected above ground, and two below ground. This is the normal arrangement for standing stones. Figure 4-6 in Chapter 4, illustrates this effect. A Type 4 field in the shape of a vertical spiral can also be detected on this Figure 13-3 photograph. This spiral clings closely to the surface of the megalith, and runs diagonally upwards from a few feet above the bottom left hand corner towards a point about 2 foot below the top right hand corner. The spiral continues in both directions behind the stone.

A Type 1 Line Comprising 3 Bands

Figure 13-4 A Type 1 Line of 3 Bands

The photograph in Figure 13-4 is best viewed when placed on the ground pointing due north. It comprises 3 linear parallel bands of Type 1 subtle energy. The photograph was taken at Hengistbury Head on 9th September 2001 at 13:38. The six white markers in an imaginary diagonal line, located in the middle of the photograph, indicate the boundaries of the three bands.

Even though the photograph is relatively small, dowsing the photograph gives similar dimensions to those found when actually dowsing on-site. The width of the three bands is about 14 feet with the middle band having a northerly flow towards Christchurch Priory and St Catherine's Hill. As always with earth energies, both the widths of the

fields and direction of flow varies over time, but I could not determine what events trigger reversal of the lines' perceived flow.

A Type 2 Line
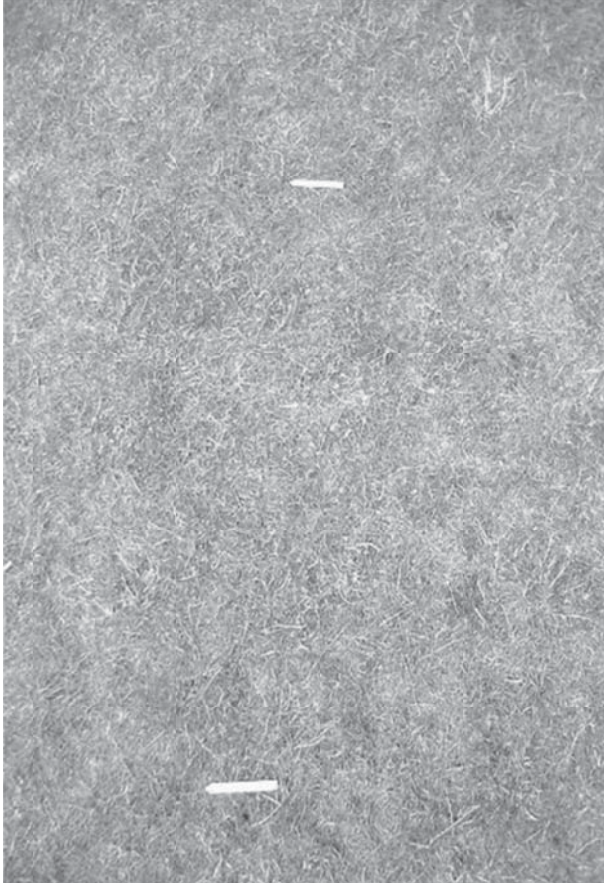
Figure 13-5 A Type 2 Line

Figure 13-5 is a photograph of a Type 2 subtle energy line that runs along the easterly dyke at Hengistbury Head. The photograph was taken on the 9th September 2001 at 11:56. The characteristics of this Type 2 line are a diamond shaped cross-section, and showed green on a Mager disc.

A Type 3 and Type 8 Spiral
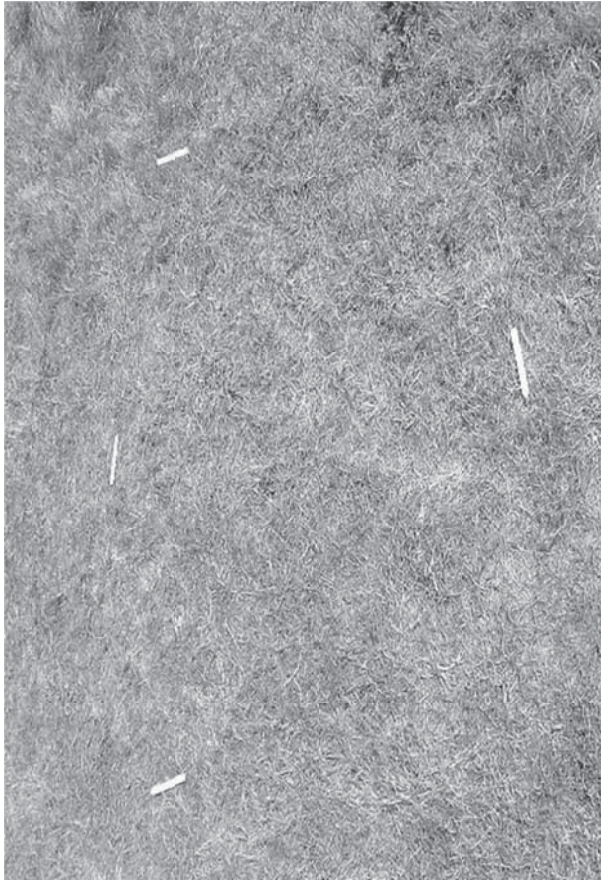
Figure 13-6 A Double Spiral

The photograph in Figure 13-6 is a combination of two spirals generated by the double dykes at Hengistbury Head. The photograph, which can be viewed with any orientation, possibly because it is a spiral, was taken on the 9th September 2001 at 12:20. When the photograph was taken, the Type 3 spiral had an upward flow with the observer feeling a sensation of being lifted. The spiral was in a clockwise direction, with a maximum width of approximately 6 feet. However, when viewed at the

end of December 2017, the spiral had a downward flow and was combined with a Type 8 spiral with an upward flow.

An ancient burial mound

Figure 13-7 is a Type 3 spiral associated with an ancient burial mound at Hengistbury Head. Two white markers at the centre of the photograph indicate the location of the spiral's centre. This field may be perceived as downwards spiralling in a clockwise direction, with a 7 turn geometric constant of approximately 2. This photograph was taken on the 26th October 2002 at 11:02, and can be viewed from any orientation.

From information dowsing, it would appear that the burial mound is less than 4,000 years old. The dowsable spiral does not seem natural, as it was not there 5,000 years ago. Two Type 4 subtle energy lines, intersecting at the centre of the spiral, possibly determined the location for building this burial mound.

At the entrance of this spiral, which is on the outer rim, is a small Type 9 field, from which bifurcates a Type 1 and Type 4 subtle energy line at 90° to each other. However, this latter effect cannot be associated with the original ancient burial mound, and has probably been added much later, as a result of corruption by smugglers' own psi-lines.

Figure 13-7 A Type 3 Spiral at an Ancient Burial Mound

A Type 4 Subtle Energy Line

Figure 13-8 is a photograph of a Type 4 subtle energy line generated by the double dykes at Hengistbury Head. The photograph was taken on the 9th September 2001 at 12:06. The easiest way to dowse this photograph is to lay it on the ground with the top of the page facing north and approach the photograph from the east i.e. from the right hand side of the page. At the time of the photograph, the flow of this subtle energy line appeared to be from north to south i.e. from the top of the photograph to the bottom of the page.

Figure 13-8 A Type 4 Subtle Energy Line

Complex Subtle Energy Patterns at Rollright Stones

Figure 13-9 is a photograph of the centre of the Rollright stones, which is an ancient Neolithic and Bronze Age site near Chipping Norton in the UK. Once again, the interesting phenomenon is that this small photograph gives the full spider web pattern for the entire site. This photograph was taken on 31st August 2002 at 11:48.

Figure 13-9 Complex Subtle Energy Patterns at an Ancient Site

    This photograph should produce a dowsable field similar to that
illustrated in Figure 4-7 in Chapter 4. Two Type 1 lines pass through the
centre of the site, and as an observer walks outwards, the spider's web
pattern is detected which incorporates four circular Type 1 lines. At the
centre is a Type 3 spiral, which at the time of the photograph was
clockwise in an upward direction.

Peace grid

After ensuring there were no subtle energies on a floor, a mind generated peace grid was created. Figure 13-10 is a photograph of part of this subtle energy peace grid, taken at 3 pm on 29 December 2017. It is Type 4, and indicates mauve or violet colour on a Mager disc. The pattern perceived is like a chessboard with squares of approximately 830 x 830 mm. The orientation of the grid is north and west. The subtle energy flow changes direction for alternate squares, as shown by the pointers situated on the grid lines. As usual, where two of the chessboard lines intersect, a spiral is formed indicating Type 3 and green. Peace grids are discussed in more detail in the next chapter.

Figure 13-10 A Mind Created Peace Grid

Mind generated Psi-line

The photograph in Figure 3-11, taken at 2 pm on 29 December 2017, is a standard psi-line comprising two Type 3 spirals terminating either end of the psi-line: 2 small coins at the top right of the photograph, mark the spiral's centres, which are approximately 825 mm apart. These spirals are connected by 3 linear Type 4 subtle energy lines having a violet Mager

colour. Three markers have been placed on these lines, with their pointers in the direction of flow of the subtle energies. The width of this band of 3 lines is about 215 mm.

A marker in the photograph (centre left) indicates the direction of north. A small circular marker indicates the entrance to the spiral. The radius of the spiral at this point is about 570 mm, and as is apparent from the photograph, this entrance is due north of the centre of the spiral. This entrance is a small area of Type 9 subtle energy with a Mager colour of ultra violet.
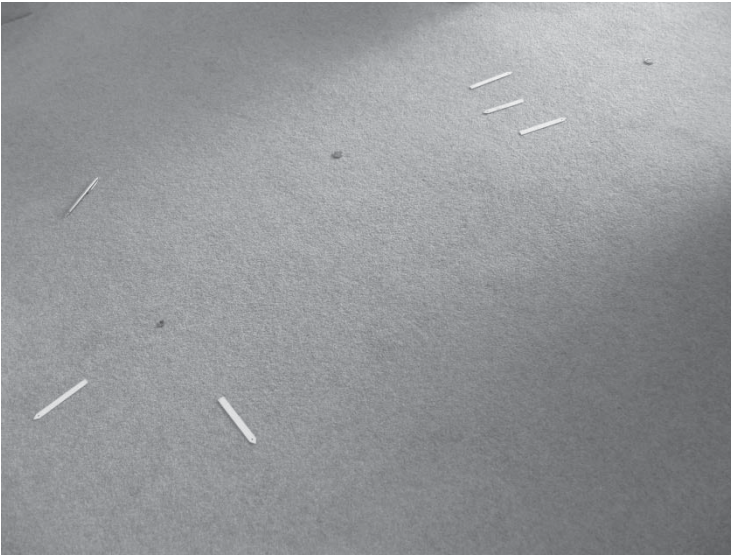
Figure 13-11 A Mind Created Psi-line

At this point, the spiral bifurcates into 2 white Type 1 lines perpendicular to each other, with outward flows, and aligned north west. Each of these short lines terminates into a smaller bifurcating spiral in a fractal fashion. Psi lines are discussed in more detail in Chapter 22.

Conclusion

All the photographs in this chapter were obtained using basic digital cameras. The information obtained was transmitted electronically and stored on hard disc drives, SD cards, or data sticks. No other physical bodies have been involved, only bytes of data. In addition, this information

had a very low bit density. In the printing process, all colours have been removed leaving only black and white images. The results are identical even using basic printing on low quality paper.

More than one person has independently confirmed the subtle energies detected on all these photographs. So, how do the subtle energies reach and then become attached to these photographs, and how can one explain the "weird" findings in this chapter?

The findings in this chapter suggest connections to the ancient theories of the Akashic record. However, this chapter leaves two counter-intuitive and "uncomfortable" alternatives as to the nature of subtle energies, when attempting to explain their photography.

a) Do subtle energies have a connection to "normal" information that can be handled by conventional technology? However, most people cannot see or feel subtle energies, machines cannot yet detect them, and the subtle energies in the photographs are without their generating geometry, geology, or their creating mind. This book shows that subtle energies exist. The problem with this explanation is that it is not compatible with some of the findings in this chapter, such as going back in time.

b) The alternative is that there are no subtle energies in any of these photographs; they remain in the locations where they were observed. The mind becomes entangled with these photographs to the actual site that was photographed. Having gained this remote viewing ability, the mind's intent can subsequently be modified to the time the photograph was taken, or to go back in time to interrogate the cosmic records.

In attempting to rationalise the findings in this chapter, as well as in the rest of this book, the most probable explanation of this photographic paradox is that the mind can connect a visual image to its source, where-ever that is on earth. My preference for this alternative is because

1. If a subtle energy line in a photograph that was taken in the past, no longer exists, or has moved from the scene in the photograph, it no longer appears in the photograph, even if it did originally.

2. It is compatible with the long-standing discovery in quantum physics, that observations involving the mind can affect the results of experiments.

The Way Forward and Suggested Research Topics

It will be a great challenge for future researchers to produce a theory of consciousness that explains the findings in this chapter. Questions to be answered include:

- Why does placing an inverted photograph of a subtle energy pattern, on the actual subtle energy that has been photographed, cancel out all trace of the original subtle energy line?
- Determine the lowest possible bit density of a photograph, that provides sufficient information to enable entanglement to take place between the mind and the actual location where the photograph was taken.
- Why does using a photograph assist the observer to access historic Akashic records?
- Where and how is the historic information stored?
- How does the mind access this information?
- Explaining why time only goes forward has defied science for centuries. To this, must now be added how is it possible to go back in time?

CHAPTER FOURTEEN

QUALITATIVE PRACTICAL EXAMPLES

General Introduction

Having established in Chapter 13, the power of photographing subtle energies as a tool in scientific research, the relevance and importance of universal constants in Chapter 5, and the definition of different types of subtle energies in Chapter 12, it is appropriate to apply and combine these concepts and develop them further. This chapter discusses some actual examples from locations around the world, where I have found good scientific evidence that has been incorporated into this book. The text is mainly qualitative and, therefore, is a break from any new mathematics, geometry, and philosophical concepts!

Angkor Wat

Introduction

A study of the dowsable fields at the centre of Angkor Wat (in Cambodia), results in the discovery of universal constants and angles. Angkor Wat, is part of a complex of constructions comprising numerous temples, with extensive irrigation canals and lakes. The 'site' is about 40 miles wide and most of the temples are vast. The complex was built between 800AD – 1,300 AD, mainly in sandstone. Appropriate adjectives include *enormous, impressive, imposing, and awesome.*

Figure 14-1 The Jungle around Angkor Wat

Unfortunately, centuries of neglect has resulted in nature taking over, with the majority of the site being over-run by the jungle, so that the trees merge with masonry. Figure 14-1 is an example of this, where the trees seem to be living off the displaced masonry creating a very eerie feeling.

Figure 14-2 represents only a small part of the overall complex, and gives the layout of some of the temples. The 2-mile scale at the bottom left provides an indication of the vast area involved. It took me about 12 hours to walk around just this one temple. Angkor Wat, the main temple, and the subject of this article, is located at the bottom centre.
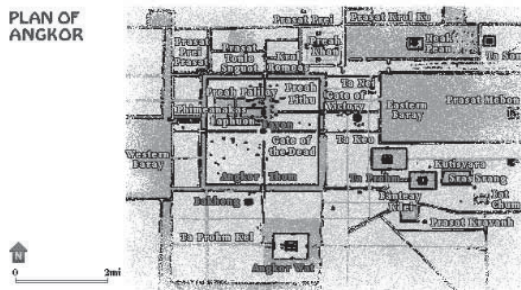
Figure 14-2 Plan and Scale of Angkor Wat

Figure 14-3, is one of a series of photographs that I took of the main entrance at dawn, at 6 am sunrise, and sunset at about 6 pm, whilst facing east. This illustrates the iconic east-west orientation of the temple.

Unlike most of the rest of the site, as the main temple at Angkor Wat has been a continuously active Buddhist temple, the monks have kept the

jungle out, and maintained the local site and buildings in an excellent state of preservation.

Figure 14-3 The Main Entrance of Angkor Wat Facing East

Figure 14-4 is a plan of the main temple at Angkor Wat. As is apparent, the building is rectangular with an east - west main axis, and is surrounded by a large rectangular moat. The scale at the bottom left shows that the distance is about 1 mile from the main entrance on the left of Figure 14-4, to the east of the exit on the right of the moat. Along the east-west centre-line, there is a dowsable linear field along the whole of its length (over 1 mile long), together with a similar central north - south dowsable line. As we will see, the subtle energies are particularly interesting where these two lines meet at the centre.
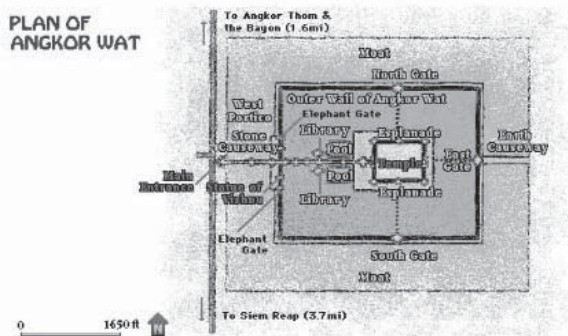
Figure 14-4 A Plan of the Main Temple, at Angkor Wat

Angkor Wat has a strong Indian influence. Its builders wished to create an "open" design to encourage earth energies, which was the philosophy adopted in Indian architecture.

It is apparent that the builders felt and understood these subtle energy fields. This view was reinforced by one of the local guides, who volunteered the information that his family had lived in the area for over 500 years, and that feeling these fields was normal. This is probably identical to European Stone Age man, who built their numerous megalithic structures that produced similar fields.

The Centre Marker Stone

As mentioned above, the point at the centre of the temple has very strong and easily noticeable fields. Our local guide, who could see these subtle energy fields, warned us in advance exactly where they were. Many people standing at this point are aware of strong sensations. Rods or pendulums are not required to feel them.

The original builders of Angkor Wat must have known what subtle energy fields they had created, and inserted a small rectangular marker tile in the floor at this centre point, where the east – west, and north – south lines mentioned earlier crossed. Figure 14-5 is a photograph of this centre marker.

It may be significant that I took about 200 photos of Angkor Wat, all of which were crisp. This photograph is blurred. Either there was camera shake from the effects of the field, or the fields were interfering with the digital camera. However, as shown in the previous chapter, this apparent loss of information, and degradation of the photograph, is not detrimental in proving the power of the technique adopted. As often in life, a negative can be turned into a positive.
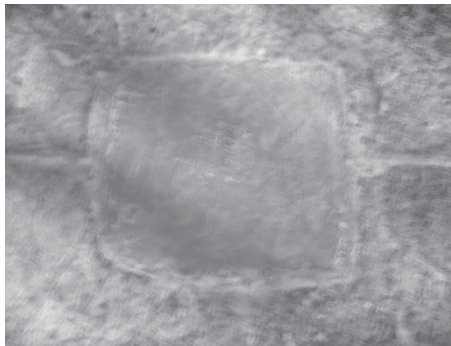
Figure 14-5 The Centre Marker Stone

Possibly the reason for the fields feeling so powerful, is that six interwoven dowsable fields are present at this centre point, each with strongly different characteristics. This can be confirmed by dowsing Figure 14-5, which gives identical results, on a one-to one scale, as if the dowser was on-site.

Four Subtle Energy Lines N-S, E-W

The first of these 6 interwoven dowsable fields comprises the previously mentioned linear fields in a north - south and east – west direction. These are Type 1 fields, which are usually associated with physical objects. As illustrated in Figure 14-6, there is an outward perceived flow from the centre. At the time of my visit, the length of these lines was about 250m, with a height of about 50 mm and a width of about 120 mm.
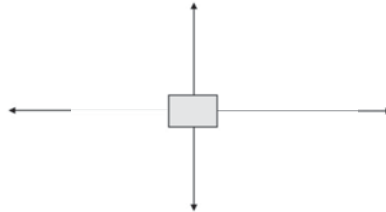
Figure 14-6 Four Lines N-S, E-W (Type 1)

Four Subtle Energy Diagonal Lines

The second field, perceived to be emanating from the corners of the rectangular centre tile are four diagonal lines, which also have an outward perceived flow, and are depicted in Figure 14-7. Unlike the previous lines, these are Type 4 fields, which are often associated with spiritual, prayer or mind generated actions (e.g. religious scrolls, church altars, a worshiped Buddha).
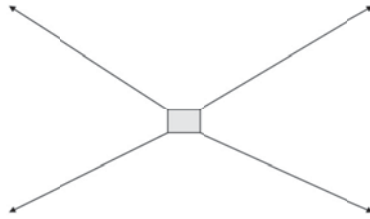
Figure 14-7 Four Diagonal Lines (Type 4)

Energy Conical Subtle Spiral - A

The third field, where the Type 1 lines in Figure 14-6 intersect, appears as a downward flowing anti-clockwise conical spiral, as discussed in Chapter 4, that is usually associated with the intersecting Type 1 lines. This Type 3 cone has a 19.5° half-angle, which is a universal angle, as discussed in Chapter 5.

Conical Subtle Energy Spiral - B

The fourth field, where the Type 4 lines in Figure 14-7 intersect, appears as an upward flowing clockwise Type 3 conical spiral. This type of spiral is usually associated with the intersecting Type 4 lines. To facilitate detection, intent can be focussed by approaching the centre marker along any of the Type 4 lines. Again, the envelope of the spiral is an inverted cone, which is concentric with the previous spiral, also having its apex at the centre of the rectangular marker where the Type 4 lines intersect.

Significantly, the apex of this spiral's conical envelope has an 11.5° half-angle, and as this spiral is smaller than the previous one, it sits inside the previous one. As will be recognised from Chapter 5, the above 2 angles form part of the series of angles having an arc sine $1/\mathbf{n}$, where $\mathbf{n}$ is an odd integer. On further analysis, this trigonometric series of cones continues smaller and smaller giving the impression of fractal geometry.

On an analysis of the turns in this conical spiral, the separation distances between adjacent turns form a geometric series. (As is commonly found, a perturbation affects the first and last term of the series. This may form an interesting subject for future research).

Series of Subtle Energy Spirals – A
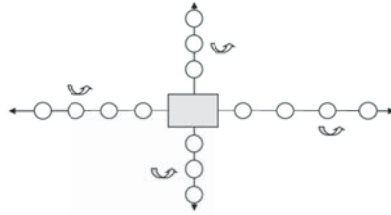
Figure 14-8 Arithmetic Series of Spirals along Type 1 Lines

As depicted in Figure 14-8, which is a plan of the pattern, the fifth subtle field comprises a series of Type 3 spirals, which extend for about 250m along the entire length of each of the four Type 1 lines. These spirals all reflect the central spiral, with similar properties. Therefore, they are downward flowing, anti-clockwise spirals with an inverted cone, all having the same height, and the same vertical cross-section. It is the identical pattern for all four Type 1 lines, with the same separation distances for all four Type 1 lines. This is an example of reflections, or self-replicating geometry.

Series of Subtle Energy Spirals - B
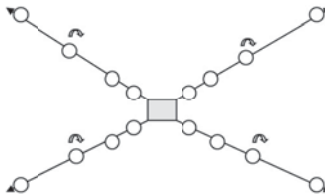
Figure 14-9 Geometric Series of Spirals along Type 4 Lines

As illustrated in Figure 14-9, there exists a sixth field comprising a series of Type 3 spirals along the length of all four diagonal Type 4 lines. These spirals all reflect the central spiral associated with the Type 4 lines, each with similar properties. i.e. they are upward flowing, clockwise spirals, with an inverted cone the apex of which touches the Type 4 line on the ground, with the same vertical cross-section. As before, the spirals extend along the whole length of the line, which is about 250m. All four Type 4 lines produce the same geometric series separation distances between adjacent reflected spirals.

Peace grids

Peace Grids in S.E. Asia

Whilst visiting such countries as Thailand, Vietnam, Cambodia, and China, it appeared to me that some Hindu and Buddhist Temples seemed peaceful and tranquil, even though there were throngs of people, noisy ceremonies, and hordes of tourists. In these Temples, I noticed many subtle energy lines, both inside and outside, but it was difficult to dowse because of the crowds or the security guards. Was it the architecture, the location, or man-made spirituality that created this tranquillity?

Whilst in India I had a brief opportunity to research this phenomenon: starting at Sarnaath, where Buddha preached his first sermon. Figure 14-10 shows a part of this site that includes the tower. Sarnaath is about 10 kms from Varanasi, and was built from 249 BC. Muslims destroyed it in the 11th century AD. The vast site is now mostly in ruins.
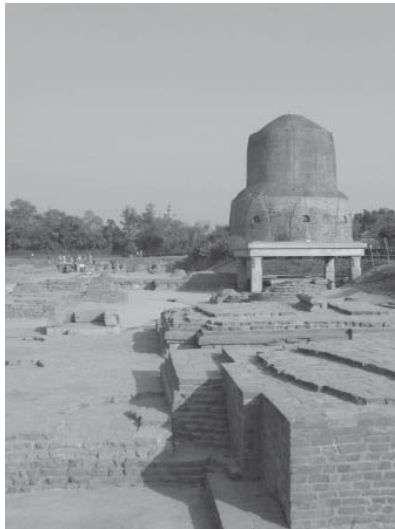
Figure 14-10 Sarnaath

Even so, there are many subtle energy lines in a grid pattern, with alternate lines having opposite flows. Where the terracotta paths cross a subtle energy line, the line is highlighted on the ground with thin rectangular tiles. Therefore, these lines would appear to be permanent, do not move significantly, and the builders must have been aware of them.

These lines are very straight, and indicated mauve on a Mager disc, similar to psi-lines. When asking their age through dowsing, it transpired that possibly this grid did not exist before the temples were built, and are about 2,000 years old.

Natural subtle energy lines meander. They do not form regular square grids, and they move about daily, over lunar months and during eclipses etc. These temple lines have none of these characteristics. The evidence suggests they are man-made.

As well as the grid, there are radial lines from the tower extending to the outer 7th shell of the tower's aura. These are characterised as white on a Mager disc, and each line ends in a spiral.

Peace Grids and Prayers

The site is still used for prayer. Our guide was well educated, and as a devout Hindu, he was immersed in Hindu philosophy and traditions, and meditated daily. However, he had never heard of dowsing, subtle energy lines, or sensing energy lines and spirals. After showing him dowsing rods, and how they reacted, he requested to borrow them. Not only did they work immediately, but also after less than 10 seconds, he said he did not need the rods as he could now see the lines and feel them.

Independent Confirmation

My initial scepticism was quickly overcome as we walked around the site. By device-less dowsing he was correctly telling me the location of each line, but more impressively, he could feel that alternate lines had different directions of flow. Previously I had not told him about this. I could only do this with rods. This is an excellent example of the power of intent switching on dowsing.

The next site I visited in India was the Chandela Temples, which is in pristine condition with superb architecture and workmanship. It was built in the 10th century AD, and is a world heritage site. Hundreds of erotica and pornographic Karma Sutra carvings cover the walls of some of the temples.

A "peace grid" could also be dowsed in parts of this site. Some of the external terracotta floors were laid so that the joins between the slabs were along subtle energy lines. As before, radial lines from the buildings were also marked in the floors.

Producing a Peace Grid

So, how did the builders produce these tranquil "peace grids"? That evening I found some parkland adjacent to our hotel, which had no energy lines and was inert when dowsing. Using intent and visualisation, I endeavoured to create a peaceful area similar to Buddhist temples. On subsequent dowsing, I found I had created a 5ft x 5ft square grid, as depicted in Figure 14-11. The size and area covered by the peace grid could also be specified as part of the original intent.

Adjacent lines had alternate directions of flow. This grid was similar to Psi-lines, and dowsed mauve on a Mager disc. It was orientated to true North-South, East-West, not magnetic north. Unexpectedly, this suggests that the earth's spin on its axis, as well as the mind, is a factor in creating a peace grid. This is opposed to a magnetic north influence that has been found in several researched earth energy lines.
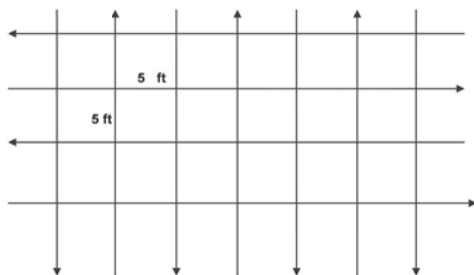
Figure 14-11 Mind Created Peace Grid

Mind and Matter Experiments

I then experimented by seeing what happens when superimposing matter on the mind-created spiritual grid. As the nearest object was a garden chair, I placed it in the grid. This created 4 subtle energy diagonals at 45° to the grid, as shown in Figure 14-12. These lines had an outward flow, but have different properties to the mauve psi-lines, and they dowse white on a Mager disc.

Further investigation showed that 4 diagonals are created for small objects, but more diagonals are created by larger objects, such as the tower at Sarnaath. These diagonals extend to the outer 7th shell of an object's aura, and end with a spiral. However, these spirals seem to have unusual properties, including an extra dimension, which is discussed in a future Chapter 32. The mind-created peace grid and diagonals was identical to

the findings in the Buddhist temples. The pattern in Figure 14-12 conjures up visions of General Relativity, where matter distorts the geometry of adjacent space.
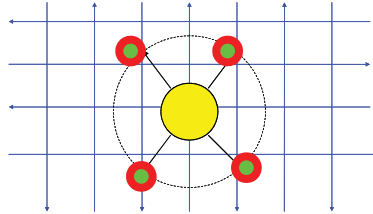
Figure 14-12 Mind and Matter

But was I just dowsing what I believed? I needed independent proof, so without telling our "non-dowsing" guide what I had done, I asked him to see if he could detect anything on this area of parkland. He quickly detected my grid with its alternate directions of flows. He also picked up the diagonals from the chair. I had my proof!

As is my usual practice, I deleted my grid when the experiments were finished. What is tranquil for me may be harmful for the many plants, birds, animals, and insects in the created grid. On the next day, without any prompting, I asked our guide to see what he could find. Interestingly, our guide automatically went into the Akashic Record and could still detect the grid. However, after I told him to change his intent to "Now" he confirmed he could not detect the grid. This is yet another example of dowsing the correct question.

World-Wide Peace Grids

There was an interesting postscript to this story. Over an Easter week-end my family went for a picnic at the stately home, Kingston Lacey, near Wimborne, Dorset, which is owned by the National Trust. There is much Egyptian and oriental material on display, which was collected by the previous owners, the Banks family, over a hundred years' ago.

The large picnic area in the grounds was very peaceful. The many visitors, including the children were well behaved and very friendly. I was surprised to find the same peace grid pattern, but the squares at 10ft x 10ft were twice the size of my original. Moreover, the same diagonals were present where an ancient Egyptian sarcophagus was situated in the grid. I

am not aware who created this grid. Was it the builders, owners, or tourists?

I subsequently requested several other people to independently create a peace grid after hearing the lecture of my discovery. Interestingly their grid was also 10ft by 10ft at creation, which is twice the size of my grid, and suggesting frequencies an octave lower or higher. It is also interesting that the dimensions were Imperial and not metric, both in India and in England.

On my travels around the world, I have seen numerous peace grids, not only outdoors in gardens and fields but inside buildings in specific rooms. These have ranged from Royal palaces, stately homes, drawing rooms of prime ministers and presidents, down to bedrooms and lounges in ordinary people's apartments.

So, what is the answer to my original question? How do Buddhist temples obtain peacefulness and tranquillity? The conclusion seems to be that tranquillity is not necessarily a consequence of location, nor is it caused by temple architecture. It is mind-created, as a result of intent, meditation, and visualisation. Perhaps this technique can be used for peaceful crowd control in such emotional and heated situations as political demonstrations, protest marches, rallies, or football matches. This could be yet another application of a dowsing Special Interest Group!

Fairy Rings, Psi-lines, Smugglers, and Venus

This practical example brings together the following six seemingly unconnected events:

1. the power of dowsing photographs
2. fairy rings
3. the effect on plant growth by a combination of subtle energy lines and an astronomical alignment
4. mind generated psi lines
5. the use of psi lines by smugglers
6. verifying the findings by historical documents

Intersecting Psi Lines

Although there is much ancient folk lore and horticultural documentation regarding Fairy Rings, they are not often associated with textbooks on physics, mind science, and astronomical events. Fortuitously, Figure 14-13 is a photograph I received by email of a fairy circle that suddenly appeared

one morning in a friend's garden. On dowsing this photograph, I detected that the centre of this fairy circle was located at the intersection of 2 psi-lines. Moreover, as I detected other interesting effects I immediately went on site to take some accurate measurements, including the orientation of the 2 psi-lines. A compass reading gave one line as 80°, so it was nearly east-west, and the other line was 345-350°, which is nearly north-south.

Figure 14-13 Photograph of the Fairy Circle

Astronomical Trigger

On referencing a horticultural text, the event that triggered the fairy circle must have occurred several days previously to allow sufficient spores to grow and send roots radially outwards underground from the centre of the circle. When these threadlike mycelia, which are hidden in the soil, have a sufficiently large "infrastructure" the mushrooms suddenly appeared above ground.

On further investigation, the date could be calculated on which this essential trigger occurred that created this particular fairy ring. On investigating recent astronomical events, I discovered that the fairy circle's creation coincided with a rare combination of the intersection of the 2 psi-lines, coupled with a conjunction of Venus at the time of a new moon.

Subtle Energy Spiral

As illustrated in Figure 14-14, the fairy circle had a diameter of about 1.5 metres, with its centre located at the intersection of 2 psi-lines. Also

illustrated in Figure 14-14 is a permanent spiral that is located at the intersection of the 2 psi-lines. As discussed previously at Angkor Wat, it is common for a spiral to appear when subtle energy lines intersect.
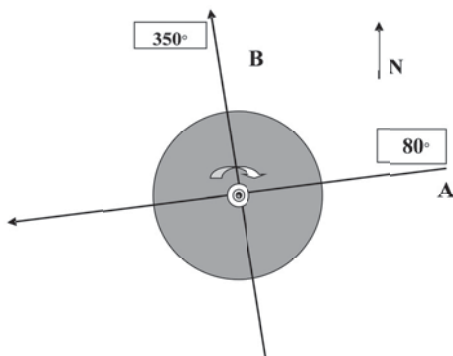
Figure 14-14 Fairy Circle Geometry and its Subtle Energies

Map Dowsing

Knowing the location where these 2 psi-lines intersected, and their orientation, enabled me to extrapolate on a local map where they originated and terminated. Map dowsing also suggested that these lines were straight. Over several weeks, these lines were physically followed outwards over many miles, and their precise locations were plotted on a map, as shown in Figure 14–15. These accurate lines were a good fit to the theoretical extrapolations. It was discovered that these lines are not only ancient and permanent, but are very straight, and, therefore, man-made, as natural subtle energy lines meander.

Smugglers

On information dowsing for the age of the lines, one line is about 375 years' old whilst the other line is about 415 years' old. Over the last 20 years, I have found many similar lines across Dorset and Hampshire. Most of them start on the sea, with easy beach landing places. This suggests that both of these 2 lines were created by smugglers. The South Coast of England was well known for being a major area for smugglers, with much literature on the subject. It turned out that Figure 14-15 gives locations that tie up with historical literature detailing local smuggling.

The four smuggling locations relevant to this story are Poole Harbour (from Lilliput, where there are still landing jetties today), Middle Chine, Pug's Hole, and Kinson (which was a major centre for the smugglers' trade). These are all well-known places in Bournemouth. These subtle energy lines are no different to mind created Neolithic "Sat. Nav." lines produced thousands of years' ago for direction finding, especially useful in the dark or in fog.

Figure 14-15 Psi-lines Marked on a Map of Bournemouth and Poole

Verification Using Historical Documentation

Figure 14-15 shows that two of the smugglers' psi-lines intersect at Pug's Hole in Talbot Woods, Bournemouth; a natural wooded depression. Figure 14-16 is a 3-part psi-line, strongly indicated on the beach-landing site, leading to a flat path that curves quickly to the left and provides tree cover, which is very convenient for hauling contraband! As is apparent, the paths still exist between the trees, and are slightly elevated. Figure 14-17 is a photograph of the actual point of intersection, which is highlighted by the canes and sticks, placed on the psi-lines.

Figure 14-18 is a photo of the local Council information board that was unexpectedly found on-site, giving the history of Pugs Hole, and stating that "Isaac Gulliver brought smuggled goods through this location and on to Kinson". This confirms the original postulation based on a dowsed photograph that the psi-lines extended on the map through to Kinson.

Figure 14-16 Psi Line's Beach Landing Starting Point

Figure 14-17 Pug's Hole   Figure14-18 The Local Council Information Board
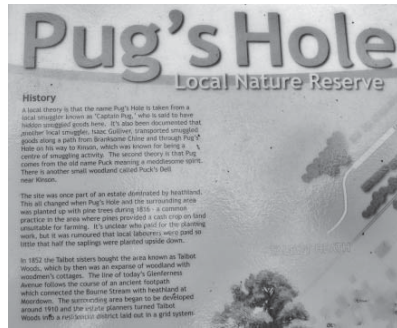
Figure 14-19 follows one psi-line that was found to go through Kinson Common towards Gulliver's properties in Kinson. On further investigation, it was found that the local Council have even signposted the psi-tracks as Gulliver's Trail.

Figure 14-19 Smugglers Psi-line Marked by Local Council

This research invites the question "What is the connection between Jonathan Swift's book Gulliver's Travels, and the psi-track that leads from Isaac Gulliver's properties in Kinson, to the landing jetties for contraband at Lilliput, Poole?"

In conclusion, dowsing a photograph of a fairy circle suggested the initial postulation that smugglers created and used psi-lines for navigation - especially useful at night. This has been demonstrated as correct. This is excellent proof that dowsing in general, and dowsing photographs in particular, can be a useful technique for accurate scientific research.

Conclusion

Events described here highlight the power, accuracy, and application of dowsing in general, and dowsing photographs in particular. The numerous initial postulations obtained from dowsing a low-resolution photograph sent by email were eventually found to accurately agree with historical documented evidence, and on-site physical observations.

Further information can be found on my website at
http://www.jeffreykeen.co.uk/Papers.htm Paper 42

Chapter Fifteen

Two-Body Interaction

Introduction

This chapter discusses the interaction of any 2 bodies (be they physical, geometrical shapes, abstract, or living entities) and their effects on the subtle energies they produce. Initially, we analyse the apparent simple case of two abstract circles drawn on paper, and then develop this to generalise the findings to any two physical bodies.

Chapter 8 discussed the complexity of auras associated with single bodies, but as we will see, the auras of 2 simple bodies are even more complex. As adopted earlier, eliminating the variable factor of mass is a great advantage in subtle energy research, and enables fundamental comparisons to be made between solid and abstract sources possessing identical geometry.

Summary of Findings

An interaction between 2-circles, or any two objects, occurs if they are in close proximity: but how "close" is critical. Figure 15–1 shows how complex the subtle energy pattern is for an interaction between 2 circles or objects. This bears little resemblance to the simple basic pattern from 1 circle, as previously discussed in Figure 8-1.
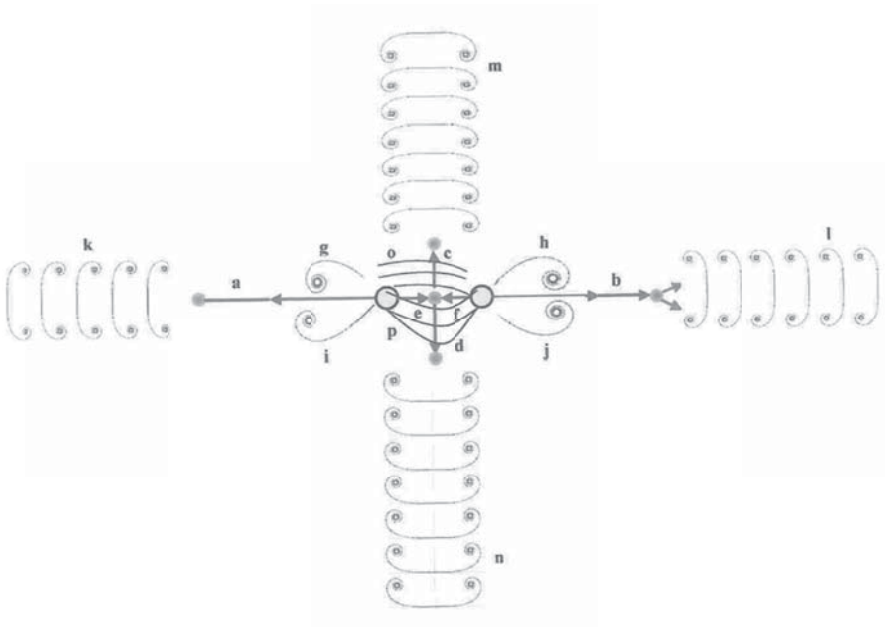
Figure 15-1 The Subtle Energy Pattern Produced by 2-Body Interaction

The size of the pattern in Figure 15-1 is a function of the dimensions of the source objects and their separation distance. This perceived pattern comprises a complex arrangement of straight lines, dipole "lines of force", subtle energy beams, vortices, Cornu spirals, curlicues, and bifurcations, which have complex dynamics and null points that are now detailed.

Straight Lines

2-circle interaction produces six straight dowsable subtle energy lines in 3 groups of symmetrical pairs, as follows:

- As shown in Figure 15-1, two linear subtle energy beams, **a** & **b**, are on the axis through the centres of the 2 circles. They are Type 4 subtle energy with a violet Mager colour. In general, for any separation, the lengths of lines **a** & **b** are equal and have a perceived outward flow.
  Their length is variable and is a function of the separation distance between the 2-circles. As an example, Figure 15-2 is a graph of the length of this beam plotted against the separation distance between

two 3.85 mm diameter circles. This curve is sinusoidal with perturbations. No beam is produced if the two bodies are touching and if their separation distance is greater than 6 cm. The maximum beam length is when the separation distance is 3 cm. The theoretical aspects of Figure 15-2 will be elaborated later.
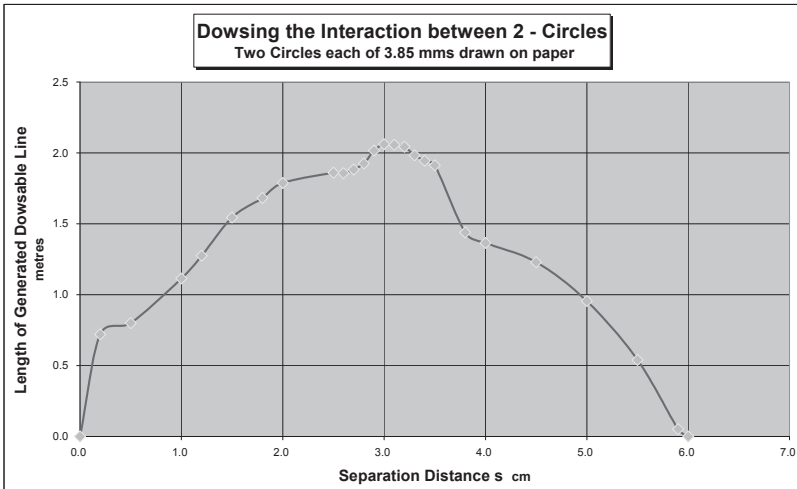
Figure 15-2 The Subtle Energy Beam Length when Separating 2 Circles

- The two lines **c & d** are at right angles to the lines a & b, and are equidistant between the centres of the 2 circles, if the circles are of equal size. If not, the point where **a & b** cross **c & d** is closer to the larger circle Lines **c & d** also have a perceived outward flow, but, unlike lines **a & b**, are almost fixed in length as the circles separate. In general, the lengths of lines **c & d** are equal. They also are Type 4 subtle energy with a violet Mager colour.
- The two lines **e & f** have an inward flow toward the geometrical centre point between the 2 circles. They also are Type 4 subtle energy, but with a "higher energy" ultra-violet Mager colour.

Curved Lines

Also depicted in Figure 15-1, are 3 types of curved lines: - "lines of force", curlicues, and Cornu spirals. The Cornu spirals, the 6 curved "lines of force", and the 12 curlicues and their terminating spirals, are a green

Mager colour. Unexpectedly, the curved bifurcating lines are white, but their terminating spirals are green, and where they bifurcate there seems to be a small ultra-violet portal. The curved lines, Cornu spirals, terminating spirals, and single spirals can all be categorised as Type 3 subtle energy.

"Lines of Force"

Between the 2 circles, 6 curved lines, marked **o** & **p**, emanate inwards from the 2 circles. These look similar to a conventional bipolar magnetic lines of force pattern. They consist of 2 pairs each comprising 3 curved lines either side of the central axis.

Cornu Spirals

Outside the ends of lines **a** & **b** and **c** & **d** are 4 coaxial sets of Cornu spirals marked as **k** & **l** and **m** & **n**. The number of Cornu spirals in each set is discussed later.

Curlicues

Figure 15–3 depicts two Cornu spirals. Four sets of curlicues marked as **g**, **h**, **i** & **j** emanate outwards from the 2 circles. Each set comprises 3 curved lines, making 12 in total. These possess a flow away from the 2 circles, on either side of the straight central axis. As illustrated, the lengths of these curlicues are less than the straight lines **ab** and **cd**. *(However, due to lack of space, Figure15-1 only shows 4 of the 12 lines emanating from the 2 circles).*

These curlicues and Cornu Spirals are well known in optics and occur when studying interference patterns and diffraction. Lines **ab** and **cd** seem to act as mirrors, so the observed patterns are symmetrical about these lines.
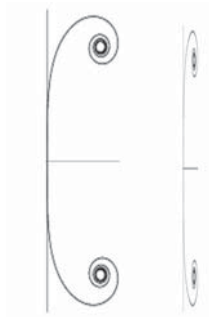
Figure 15-3 Cornu Spirals

Conical Helices

There are 17 spirals, or more accurately, conical helices in the Figure 15-1 pattern, which are categorised as follows:

Terminating Beams

When looking downwards, 4 clockwise spirals, indicated in Figure 15-1 as circles, terminate the straight lines.

Curlicues

12 spirals terminate the curlicues. Those 6 positioned above the central axis of the 2 circles are also clockwise, but the 6 below the central axis are anti-clockwise.

Central Spiral

Between the 2 circles, where lines **e f** and **c d** meet, a clockwise spiral is formed (looking down). If the 2 circles have equal sized auras this spiral, also marked with a circle, is midway, but if they are unequal this spiral is closer to the largest circle. When the paper on which the source circle is drawn is horizontal, this spiral is more accurately, a perpendicular vertical vortex.

Null Points

Whilst separating any 2 objects, a series of null points are created. As the null points are being approached, the curved lines become flatter, as illustrated in Figure 15-3. Eventually, at these null points, all 16 terminating spirals, the central spiral, the Cornu spirals, the 12 curlicues, as well as all the 6 lines of force disappear. The pattern at these null points is depicted in Figure 15-4.

All that remains are the straight lines **ab** and **ef** through the central axis and the perpendicular lines **cd** which are not affected, nor are the directions of perceived flow. All the lines in Figure 15-4 are Type 4 subtle energy.
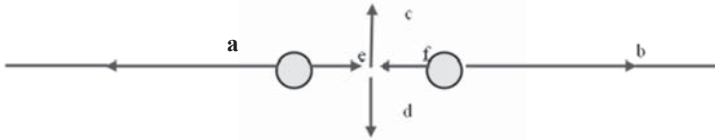
Figure 15-4 Subtle Energy Pattern for 2-Circles at Null Points

Physical or Abstract

Usually, the observed dipole subtle energy pattern, as in Figure 15-1, is the same for abstract source geometry, such as 2 circles drawn on paper, as it is for any identical solid source geometry. The observed patterns and dynamic effects are identical. This is compatible with Chapter 8. However, as the two objects are separated, there are three significant quantitative differences between abstract and physical source geometry. These relate to null points, Cornu spirals, and auras.

Null Points

Paper drawn circles produce 6 null points, whilst solid discs only produce 4 null points.

Cornu Spirals

Abstract objects generate 4 sets of Cornu spirals, each set comprising **9** separate Cornu spirals (i.e. 36 in total). Solid objects produce 4 sets of Cornu spirals, each comprising **7** separate Cornu spirals (i.e. 28 in total).

Auras

As discussed in Chapter 8, abstract circles produce 9 aura rings extending outwards from the core aura, but solid discs (both 3-dimensional and 2-dimensional) only produce 7 rings.

Analysis and Theory

The above findings for 2-body experiments suggest that there are 2 different phenomena; one for the creation and control of straight lines and another for the curved lines.

Straight Lines

The variable length subtle energy beam, which is a straight line passing through the axis of 2-bodies, can be explained by pure resonance of 2 sine waves, each with a half wavelength, λ, which equals the maximum separation distance between two interacting bodies.

$$\lambda = 2 \cdot S_{max} \qquad\qquad (i)$$

If L = the length in metres of the generated subtle energy beam, and
     S = the separation distance between the two circles.

The heuristic formula based on this theory is:

$$L = L_{max} * \sin(S / S_{max} * \pi) \qquad\qquad (ii)$$

Substituting actual values from the graph in Figure 15-2,

$$L_{max} = 2 \text{ and } S_{max} = 6$$

$$L = 2 * \sin(S / 6 * \pi) \qquad\qquad (iii)$$
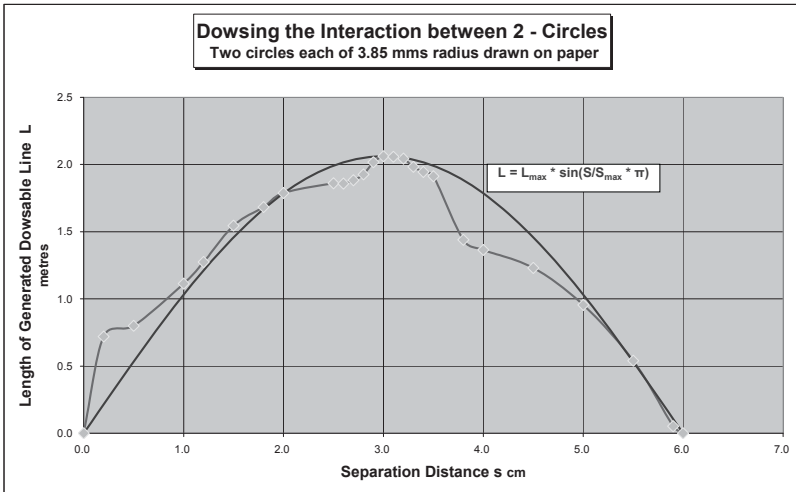
Figure 15-5 A Theoretical Equation c.f. Actual Experimental Results

Figure 15-5 supports this theory where the theoretical equation (iii) is superimposed on the actual experimental results as depicted in Figure 15-2. Equation (iii) is a very good fit to the observations, even allowing for the perturbations.

What is causing the perturbations between the theoretical equations and the kinks in the Figure 15-5 curve of actual data? In the real world, and from my other research work, the perturbations are caused by the earth's gravity, spin and magnetic field; factors that were not considered in the above theoretical resonance equations.

As an example of these perturbation factors, orientation of the 2 circles to true or magnetic north does not seem to make a significant difference, but a strong artificial E-W magnetic field produces the same results as detailed above, but with increased separation distances by about 10%. This reinforces the view that magnetism is one of the causes of the perturbations.

A further clue is that the apparent perturbations seem to occur at the same separation distances as the null points, and these distances form a series with a similar geometric constant as the null points. The implication is that null points are also caused, or affected, by the earth's gravity, spin and magnetic field, etc.

Equations (ii) and (iii) are not absolute, as they rely on experimental parameters, not universal constants. Can we eliminate these parameters and perturbations, and have a relationship that only relies on the radius of

the two circles, their separation distance, and universal constants? The radius of a circular object's aura is a function of the object's radius, and determines the maximum separation distance and maximum line length.

The solution to this problem is given in Chapter 30. A powerful technique is adopted whereby the actual experiment can be visualised as taking place in deep intergalactic space; there being no perturbation effects from the Earth's magnetism, gravity, or spin etc.

Curved Lines

The above explanation of a resonance effect that creates or controls the straight lines does not apply to the vortices, curlicues, and Cornu spirals. These must be produced by a different effect, because a similar resonance model based on 2 shorter sine waves with a half wavelength equal to 1/6 or 1/4 of the maximum separation distance would produce 4 or 6 negative areas, but these would equal the positive areas. This is illustrated in Figure 15-6.
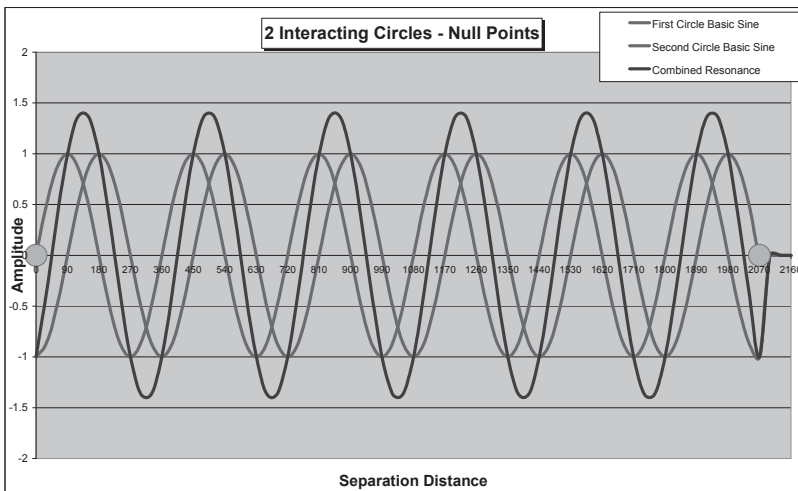
Figure 15-6 Illustrating that the above Model Fails at Null Points

The findings show that this model is incorrect, for two reasons. There are no multiple resonance peaks; only one resonance peak is observed. As also observed, the null points are sharp troughs that only extend over a few

mms of separation, and are comparable to the fine tuning of radio stations. The model in Figure 15-6 does not produce either of these effects.

It would, therefore, seem that the derived equations suggest that the linear parts of the dowsable pattern are determined by the geometric structure of space-time, whilst all the curved lines, which disappear at the null points, are produced by, yet unknown, earth-based forces such as spin, magnetism, and gravity.

Conclusions and Summary

Without any equipment, the mind can readily detect 2-body interactions. An interaction between any two objects occurs if they are in close proximity. Provided their auras overlap, the interaction of any 2-bodies (such as 2 pure abstract geometry circles drawn on paper, or 2 physical objects) instantly generates a complex pattern. As *any* two bodies separate, independent observations have confirmed the creation of a consistent, repeatable pattern comprising subtle energy beams, vortices, Cornu spirals, null points, resonance effects, entanglement, and bifurcations.

This complex pattern is affected dynamically during the separation process. Esoteric differences have been quantified, and interesting comparisons made between identical abstract and solid geometries. The observed pattern created by 2 separating *abstract* bodies includes 6 null points and a total of 36 Cornu spirals, whilst 2 *physical solid* bodies of the same size, only produce 4 null points and 28 Cornu spirals.

The subtle energy "laser beams" have a short variable length, which is a function of the separation distance between the 2 objects and the size of their radii. These beams terminate in spirals.

This interaction can be explained if the maximum separation distance between two objects equals ½ the wavelength of the waves involved in the communication of information between them. If this condition is satisfied, a strong resonance effect is produced, with the maximum effect at half the maximum separation distance. As will be demonstrated in Chapter 30, after the effects of local perturbations have been eliminated, the maximum separation distance between 2 objects of radius r is $S_{max} = 2.r^\varphi$. This is a significant finding; the dynamics of 2 separating bodies only involves their size and a universal constant.

As also found in several occasions in this book, the structure of the universe has the ability to treat abstract geometric sources similarly to physical objects, with respect to the creation of subtle energies. But, intriguingly physical bodies, that one would have thought would involve more information than an equivalent abstract geometrical pattern, produce

less subtle energy. This is a counter-intuitive property of the cosmos that requires an explanation.

The following 2 phenomena are a foretaste of topics covered in later chapters. At least 16 different sets of bifurcations were discovered in this chapter. These emanated from the terminating spirals associated with the straight lines and curlicues. Obtaining a bifurcation ratio of half of Feigenbaum's constant indicates a strong connection to standard chaos theory, and that the mind is tuned into the universal laws of physics.

By increasing the pressure on one of the two interacting objects, entanglement was demonstrated when observing the significant increase in the aura size of the other interacting object instantly. Four different types of subtle energy are involved in the 2-body pattern generated, with three different perceived colours.

Consciousness seems to play an important part in 2-body interactions. There are probably an infinite number of potential short-range 2-body interactions. The conscious mind has the ability to eliminate all of these and concentrate on just 2 selected objects. The main subtle energy beam generated by the interaction of 2 bodies, is only observed when the observer's intent is looking at the 2 source objects. Intent and the act of observation of the source geometry seem to determine the number of layers in an aura, or the number of Cornu Spirals in an interaction pattern. This is comparable to observations affecting experiments in quantum physics.

Combining all the above findings, with previous findings in this book, suggests that the total pattern produced by 2 objects (as illustrated in Figure 15-1) is a combination involving:

1. The geometric structure of space-time.
2. Consciousness and observation.
3. An interaction or entanglement of subtle energy.
4. Chaos and bifurcation.
5. Nodes and standing waves.
6. Resonance.
7. Local gravity.
8. The earth's local vorticity.
9. The earth's local magnetic field.

At the null points, the latter 3 factors seem to cancel out the effects of the first 5 factors.

At the next level of detail, there are 2 mechanisms involved in 2 body interactions:

1. The straight subtle energy lines are mainly as a result of the structure of the universe, which is also responsible for the creation of these subtle energy lines, and the dynamics of separating the 2 bodies.
2. The curved lines and spirals are produced by local forces such as spin, magnetism, and gravity, which are also involved in the production of null points that do not affect the straight lines.

The consequences of these discoveries are far reaching. The findings support that chaos theory, bifurcations, and entanglement are not only built into the physical world, the laws of physics, and the structure of the universe, but are also equally built into the mind's perception and consciousness.

The Way Forward and Suggested Future Research

1. What is the mathematical transformation that enables 2 circles (whose simple equations are in the form $x^2 + y^2 = r^2$) when in close proximity, to produce a complex mathematically described pattern such as in Figure 15-1? This mathematics has to explain the, complex arrangement of straight lines, dipole lines of force, vortices, Cornu spirals, curlicues, bifurcations, together with the complex dynamics of 2-body separation and null points.
2. Why do 2 abstract circles produce 9 Cornu spirals whilst solids produce 7? This is similar to abstract circles producing 9 aura rings, but solid discs only produce 7 rings
3. What is the mechanism that produces 6 null points for abstract geometry, but 4 for solids?
4. What do the null points tell us about the creation and destruction of Cornu spirals?
5. Why do the null points destroy all spirals, Cornu spirals, and curlicues, but not the straight lines?
6. Why do null points only extend over a few mms of separation of the two objects?
7. What is the connection between the null points and the perturbations caused by magnetism?
8. Does abstract thought of a geometrical shape, require more or less information than physical objects with identical shape?
9. Could the null points be caused by the outer auras of each of the 2 interacting circles cancelling out the associated information?

10. An interesting future research project would be a study of how the subtle energy pattern depicted in Figure 15-1 changes as the separation distance between the 2 bodies decreases to zero, and then as they touch. Similarly, what happens as the 2-bodies stop interacting because their separation is too great?

11. Some of the characteristics of 2-body separation can be explained by information communicated by waves, whose wavelength determines their maximum separation distance of the 2 bodies. What is the theory of this?

12. What is it in these waves that enable the 2 bodies to be aware of each other's separation and size? "Hoping" to find an interacting partner, each body must either
   a) be radiating standing waves with wavelengths that are a function of their radius/size and separation distance, or
   b) only after the auras of the 2 bodies overlap can the relevant information be communicated.

   The latter option seems more probable. How else would 2 bodies "know" where each other is, their radii and when within interaction range?

13. Experiments are required to find the factors involved leading to a formula for L_{max} the maximum length of a 2-body subtle energy beam.

14. There is only 1 optimum separation distance between 2 objects that produces a resonance peak. If this is 30cms as in the example in Figure 15-2, the half-wavelength that causes the resonance is also 30 cms. These are relatively large wavelengths and imply a macro cause, not a mechanism at the quantum level.

As there is insufficient space here to cover all the theoretical aspects of 2-body interaction, further details can be found on my website at http://www.jeffreykeen.co.uk/Papers.htm in a published paper numbered 48.

CHAPTER SIXTEEN

THREE-BODY INTERACTION

Introduction to Near Perfect Alignment Properties

Having investigated the subtle energies involved with 1-body, and then with 2-body interaction, the next logical step was to investigate 3-body interaction. The initial answer to this investigation was nothing fundamentally special to report, if the 3 objects were arranged randomly. However, whilst experimenting with 3 stones, I discovered that if these 3 stones were in a perfect linear alignment, a significant subtle energy beam was produced.

After much experimentation, it became apparent that, with a conscious intent on **any** three aligned geometric shapes, a subtle energy beam was always produced with the same interesting properties. After a gradual escalation of relevant experiments, I could demonstrate that these aligned bodies may be any 3 objects: 3 grains of sand, 3 pure geometric circles drawn on paper, 3 coins, 3 pebbles, 3 trees, or 3 megaliths. Figure 16–1 represents these findings.
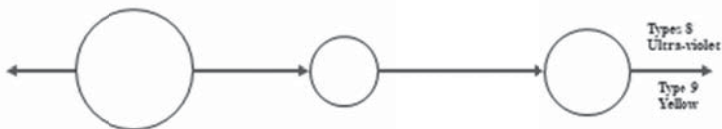
Figure 16-1 Subtle Energy Beam Produced by any 3 Objects in Alignment

Many subsequent experiments and measurements indicated that this alignment beam not only had a very long range, but also was a parallel subtle energy beam. Using this information, I eventually demonstrated that the alignment beam exists even for 3 astronomical bodies. For example, measurements showed that the sun, earth, and the moon created identical subtle energies when in geometric astronomical alignment (such as at new and full moons, or during eclipses). As will be discussed in future chapters,

this subtle energy phenomenon has been demonstrated to extend from the earth to the outer planets!

In order to create this alignment subtle energy beam passing through 3 aligned objects, the following criteria need to be satisfied:

1. their centres are in a straight line, and
2. are separated by a distance greater than the sum of their auras, so the auras of the 3 objects do not overlap, and
3. there is no 2-body interaction between any pair of the objects.

If so, then a subtle energy beam is formed as in Figure 16-1. In practice, these criteria are easy to satisfy, because auras are measured in cms, and the separation of the 3 objects is usually measured in metres and kms. This alignment beam has a "flow" emanating outwards from the largest object, and its length is not limited, or affected by how far the circles are separated.

After many years of experiments, I discovered that the alignment beam is a complex combination of Type 8 and Type 9 subtle energy: the Type 8 having a perceived Mager colour of ultraviolet, whilst the Type 9 has a perceived Mager colour of yellow. In fact, this complexity requires two later chapters of this book for explanation.

The Geometric Limits for a Subtle Energy Beam

Alignment Beam Tolerances

How accurate must the alignment of the 3 bodies be to produce the Type 8/9 alignment beam? The answer to this question is not straightforward – it depends on the location of the observer. For ease of explanation, it is useful to utilise the analogy of the observer being on earth, and observing either an eclipse of the moon or the sun, as illustrated in Figure 16–2.

The experimental protocol is to use 3 small objects (physical or circles drawn on paper) to simulate the new and full moon situations, but ensuring that their auras did not overlap, thereby avoiding 2-body interaction. Two of the objects were fixed, whilst the third was moved around one of the others as in Figure 16-2.

In Figure 16-2, α = the angle from perfect alignment ($\alpha = 0°$ for perfect alignment); p = the perpendicular distance of the object from perfect alignment; R = the radius of "orbit" of the moveable object. The objective of this experiment is to measure the elementary trigonometry of sine α =

p/R, and hence discover the greatest value of α that still produces the 3-body subtle energy beam.
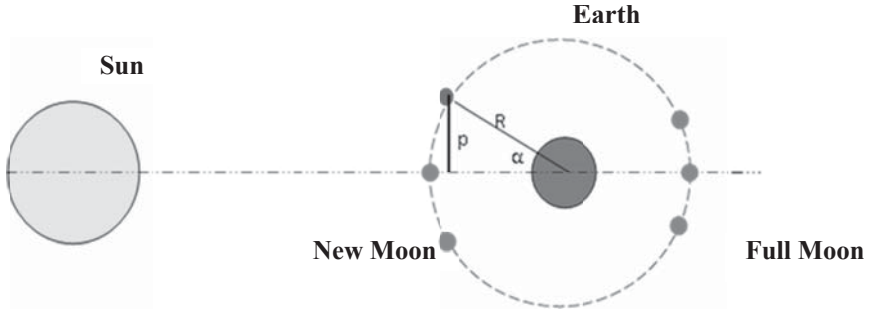
Figure 16-2 The Location of Observers to Detect an Alignment Beam

A standard yardstick and its protocol was adopted for this research. As explained in more detail in Chapter 24, this involves dowsing pure geometry - a dot, whilst simultaneously maintaining the conscious "intent" of focusing on the 3-bodies. The dot transforms into a perceived variable beam of subtle energy, the length of which is defined as **L**. Conveniently, **L** not only takes on the properties of the alignment beam, but is affected by the "field strength" of the alignment subtle energy beam created by the 3-bodies. For each position of the "orbiting" object, **L** was measured. This method is a useful quantification of subtle energy "field strength" of the alignment beam. As we have previously shown, the effects are identical to the actual astronomical phenomenon.
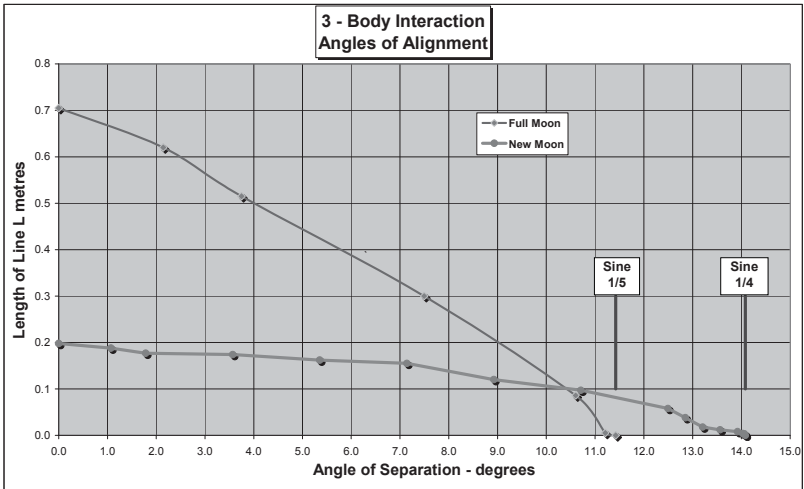
Figure 16-3 How the Length of the Beam Reduces with Poor Alignment

Fig 16-3 is a graphical representation of the experimental results. The subtle energy is present when the line length is greater than zero. The top line in the graph represents measurements taken by an observer in a full moon position i.e. the observer is located on the outer of the 3 bodies. The lower line in Figure 16-3 plots the measurements obtained by an observer located on the middle of the 3 objects i.e. the new moon position. As is apparent, the length of the yardstick decreases (because of the reduced field strength of the 3-body alignment beam) when only a few degrees out of alignment, and then its length reduces rapidly.

As is apparent from Figure 16–4, the alignment subtle energy beam is created if the maximum angle out of perfect alignment is arcsine 1/5 for full moon simulation, but arcsine 1/4 for new moon simulation. As we will see throughout this book, sine 1/n is common in subtle energy research.
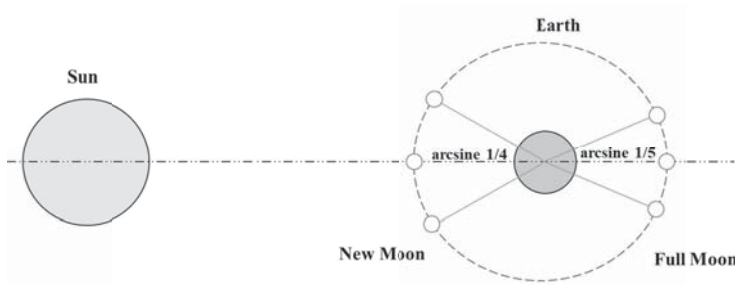
Figure 16-4 The Angular Limits to Produce a Subtle Energy Beam

It is important to point out that the measurements in Figure 16-2 were taken with 3 small objects, so the divergence from the creation of an alignment beam reduces rapidly. In the case of 3 astronomical bodies, as there are enormous diameters involved, a much greater tolerance is possible in alignment, before the beam disappears.

Non-alignment

What happens if alignment is outside the above limits? There are several possibilities. If all 3 objects are in perfect alignment, but sufficiently close, so they form 2-body interactions, then Figure 16-5 illustrates the result. The beam emanating from the 3 objects has a very short range, and is Type 4 subtle energy, indicating a Mager blue. The end of this beam bifurcates into two Type 1 white lines, with a half-angle of about 16°.
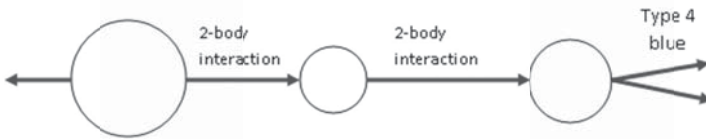
Figure 16-5 Any 3 Objects in Alignment, but only 2-Body Interaction

Figure 16-6 illustrates that when the 3 objects are **not** in alignment, and with **no** 2-body alignment, the end beam, after a relatively short distance, also divides, but with a half-angle of about 31°, which is about double that in Figure 16-5. The split exit beam is Type 5 with a blue Mager colour.
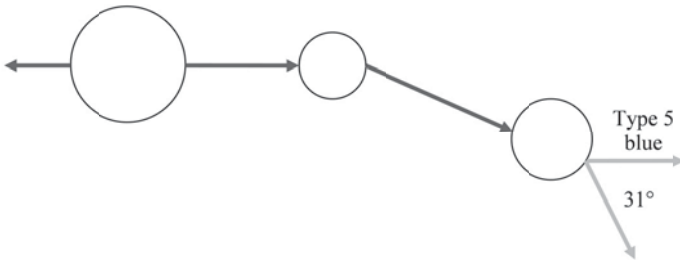
Figure 16-6 Any 3 Objects not in Alignment, but no 2-Body Interaction

If one of the 3 objects (A) is too far separated to be in a 2-body interaction, but B and C are, Figure 16-7 illustrates the geometry when all 3 objects are in alignment. The 2-body interaction between B and C is different to when they are isolated. The beam emitted from C does not divide into 2, is very long, can be classified as white Type 5, and has an outwards flow, as in Figure 16-7.

Figure 16-7 3 Objects in Alignment, but B and C in 2-Body Interaction

If, however, the 3 objects in Figure 16-7 are **not** in alignment, as depicted in Figure 16-8, the single very long emitted beam can also be classified as white Type 5.

Figure 16-8 Any 3 Objects not in Alignment, but only 2-Body Interaction

The logic for these combinations of alignments and subtle energy types is not immediately obvious, but it should be useful data in the discovery of a full theory of subtle energies.

Shape of the Subtle Energies Close to the 3-Bodies

We have seen that an alignment beam can be exceptionally long. At the other extreme, we now discuss experiments to determine the shape of the subtle energy beam clinging to the 3 source objects. The properties of the alignment subtle energy are different near the central object, compared to one of the outer objects. Figures 16-9 and 16-10 illustrate the shape of the subtle energy beam around the 3 interacting bodies.
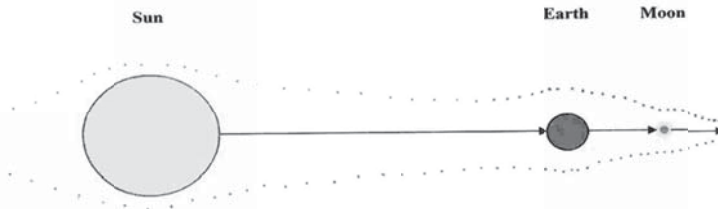
Figure 16-9 Full Moon Simulation

In Figure 16-9, the central object is larger than the outer object. This configuration is equivalent to the full moon analogy. Note the width of the beam, which can be readily obtained by dowsing the beam's boundaries. It expands around the middle object to about twice the latter's diameter, but about 7 times the diameter of the outer object. The latter is the last to receive the "flow" via the larger object. The vector effect (to be discussed later) increases the value of measurements around the middle object.

In Figure 16-10, the middle object is now the smallest, and the beam's width becomes very narrow round the middle object. It is about the same as the middle object's diameter. The vector effect shrinks measurements near the middle object. Further research is required to understand these vector effects
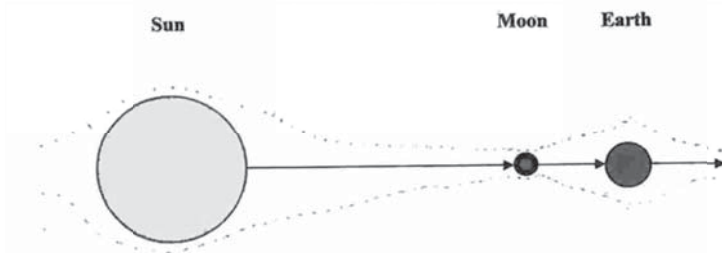
Figure16-10 New Moon Simulation

Differences Between 2-Body & 3-Body Interaction

It is instructive to contrast the above 3-body effects to the 2-body case discussed earlier. These differences are summarised in Table 16-1, and as is apparent, every property observed for 2-body interaction is different or absent in 3-body interaction. This example is only one of many that demonstrate that there are different types of subtle energy beams. This approach can be generalised as a method to determine which type of subtle energy is under investigation.

Observation	2-objects	3-objects
Auras must overlap	√	x
Short range interaction	√	x
Beam length dependent on the separation	√	x
Very long beam length	x	√
Vortex produced	√	x
Bifurcations	√	x
Type-4 subtle energy beam	√	x
Type-8 subtle energy beam	x	√
Type-9 subtle energy beam	x	√
Lengths measured are not invariant to direction	√	x
Mager colour when aligned	White	Ultra-violet

Table 16-1 Comparison between 2 and 3-Body Interaction

Unlike the relatively short beams produced by 2-body interaction, the length of the alignment beam produced by 3-body interaction tends towards infinity, does not possess any spirals, nor does it bifurcate. This beam affects dowsing measurements in a different way to earth energy lines, psi lines and a 2-body beam

It is instructive to measure all the above properties at actual new and full moons and during eclipses, thus emulating the above 3-body experiments with small stones and drawn circles. All the eleven properties measured are identical to the 3-objects column in Table 16-1. This confirms that the 3-body alignment phenomenon applies equally across all scales of measurement, from grains of sand to planets.

Postulations on Intent or Observation

Is this alignment beam produced as a result of the 3 bodies own action, or the observer's conscious intent, or as a result of the act of observation, or is it a combination of all of these? What seems undeniable is that the alignment beam is the result of three effects of geometry.

1. Not just the physical alignment itself, but also
2. The actual geometry of the 3 interacting objects, together with
3. Cosmic consciousness and/or the structure of the universe recognising, and reacting to, the above 2 geometries.

There are 2 options to explain this phenomena. Either, the very act of conscious intent when looking at 3 aligned geometric shapes creates the beam. However, it is possible to detect this beam without observation, or unexpectedly, or when looking away from the 3 objects. Alternatively, as there are probably an infinite number of 3-body interactions, it seems more likely that there are an infinite number of the above subtle energy alignment beams formed as a consequence of the structure of the universe. As already discussed, the mind naturally switches off to avoid information overflow. It seems that all but the strongest subtle energies, together with the observer's intent, just selects the appropriate subtle energy beam.

Conclusions of this Chapter

A major achievement of this and the previous chapter, is that experimental results for geometric alignments have, for the first time, been measured, analysed, and documented. The findings here have not only been shown to be repeatable, but have demonstrated a strong link between geometry, consciousness, and the creation of subtle energies.

These findings confirm findings in other chapters, and lead to the following deductions:

1. The structure of the universe, from the Planck level to galaxies, enables 2 or more geometrical bodies to be "aware" of each other's existence and precise location.
2. Similarly, the structure of the universe enables 3 geometrical bodies to "know" instantly when they are in perfect alignment.
3. On measuring 11 different properties of subtle energy alignment beams, it has been confirmed that the 3-body alignment phenomenon applies equally across all scales of measurement, from

      grains of sand to planets, and from physical bodies to abstract geometry. These findings support Global Scaling Theory (GST).

4. The unexpected conclusion, from comparisons between 2 and 3 body interactions, is that actual full and new moons have identical properties to interacting small stones or mass-less geometric shapes. Again, there seems to be an equivalence between pure geometry, and matter without the effects of mass.
5. Perception, even by the sub-conscious mind, is affected by subtle energies, which originate both terrestrially and astronomically.
6. Although it is well known that some subtle energy beams affect both mental and physically health, the beams discussed here are only transient, lasting a few minutes. All life forms have been exposed to subtle energies for millions of years. It is, therefore, unlikely that this form of subtle energy is detrimental.
7. The 3-body alignment beam could be the trigger at full or new moon, that causes fish to spawn, or baby turtles to emerge from their eggs, or the menstrual cycle, and many other documented biological events.

The Way Forward and Suggestions for Future Research

As always, discoveries in research generate more questions than answers. Interesting questions and suggested topics for future research include the following:

1. Any 2 interacting objects, be they solid bodies or pure geometric shapes, produce identical effects. The same applies to 3 aligned circles drawn on paper or 3 solid bodies. There seems to be an equivalence between pure geometry, and matter without the effects of mass. *Why?*
2. Irrespective of size or material, how do any 3-bodies know when they are aligned? Is this a consequence of the structure of the universe?
3. Why does alignment produce a subtle energy beam?
4. To produce a subtle energy alignment beam, why has the alignment to be better than arcsine 1/5 for full moon simulation, but arcsine 1/4 for a new moon simulation?
5. 4 examples were given of 3 objects not meeting all the criteria for the production of a subtle energy alignment beam. However, each of these incorrect geometries of the 3 bodies, produce different subtle energy beams, with different Mager colours, and different

divergence angles. Discovering the logic for these findings could help in understanding the theory of subtle energies.

6. The subtle energy beam produced by 2 interacting objects has very different properties to the subtle energy beam produced by 3 aligned objects. *Why?*

7. Unlike earth energies, or the subtle energy produced by 2 interacting bodies, yardstick measurements made in the 3-body subtle energy beam are invariant to the direction of flow. *Why?*

8. In 3-body alignment, measurements are decreased if made near the outside of the 3 objects, or increased if measured near the middle of the 3 bodies. This effect is identical to dowsing at new moon or at full moon, or an eclipse of the sun. The reason is possibly the shape of the subtle energy beam. *Why?*

9. How does the moon know it is about to align with the sun and earth, and is touching the subtle energy beam, if this beam has not yet been created!

10. To produce an alignment beam, why must the 3 objects not be in 2-body interaction, (i.e. their auras not overlapping)?

11. How and why do 3 aligned geometric objects "switch on" a subtle energy beam?

CHAPTER SEVENTEEN

MIND CREATED SUBTLE ENERGIES

Introduction

Up to now, most of this book has covered the ability of the mind to detect subtle energies. This chapter, however, covers the important subject of the mind creating subtle energies, not only locally, but also remotely. As we will see, this ability of the mind leads to techniques for quantifying scientific research into the nature of subtle energies, and the vast distances over which the mind extends.

Mind Produced Patterns of Subtle Energy

Locally

It is appropriate to commence this section with caution. Although the mind can create and destroy complex geometrical subtle energy patterns, there are challenges. The relevance here is to demonstrate that the use of geometry is an excellent scientific tool to research subtle energies. For example, this research can quantify the mind's remote powers. However, it is also a warning to anyone attempting to detect subtle energies and then interpret his or her findings. It shows how the act of creating or observing subtle energies can degrade information and affect the pattern observed. This is an analogy to observations in quantum physics.

The reader might like to try generating simple shapes such as lines, rectangles, cubes, circles, and spirals as illustrated in Figure 17–1. Initially the mind's intention should be to create locally these 2-dimensional patterns on the ground. Visualising the geometry of intent is a good way to learn the technique.

Figure 17-1 Easily Produced Mind Generated Shapes

Remotely

Figure 17–2 depicts my first attempt, many years' ago, with the above experiment. The shapes on the left were mind created locally, and were very similar to those specified. I then attempted to place the same shapes remotely, but the shapes on the right of Figure 17–2 were those detected on subsequent actual visits to the intended remote locations. As is apparent, the geometry became degraded in "transmission", presumably because of information loss.
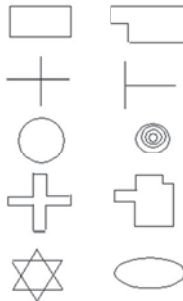
Figure 17-2 Mind Generated Shapes; Local and Remote

Subsequently, to increase complexity, I created one, two, and three-dimensional remote subtle energy patterns, with specified dimensions, on the ground, in buildings, or floating in the air. In all cases, when creating these patterns, I was situated:

a) at distances from a few feet to over 5,000 miles away from the remote location.

   b) at differing heights including in an aircraft flying at 36,000 feet;
      inside tall buildings; standing at ground level; and within
      underground caves.
   c) in the open air, indoors, or in screened metal cages

   For all these locations, the results were identical, and demonstrate that
the mind's intent can "pass through" any obstacle. Remotely projecting
geometrical shapes for these experiments was relatively easy, as I knew
what all the remote locations looked like and could, therefore, visualise the
intended placement of the remote subtle energy pattern in relation to
nearby buildings, trees, lakes, and other identifiable objects. (This differs
from remote viewing where, by definition, the observer is attempting to
ascertain the remote geography).

   Subsequently, for each experiment, on-site measurements were made
of the actual geometric pattern created, and by comparing these results to
the measured dimensions of the geometrical pattern originally specified,
the degradation of the information could be assessed. Initially the results
were similar to the right hand column in Figure 17-2, but as usual, practice
improves accuracy.

   This simple, practical technique using geometry is a very powerful tool
for not only demonstrating the existence of subtle energies, but also their
creation and detection by the mind, as well as researching their interaction
with the laws of physics and the structure of the universe.

Mind Generated Subtle Energy Across the Atlantic

   Figure 17-3 is a photograph of a Type 3 spiral that I remotely mind
generated to a precise location in Sarasota, USA, from about 3,000 miles
away, when in an aircraft flying over the Atlantic at 35,000 feet. The
mind's intention was specified by drawing an accurate pattern with
dimensions of what was to be created, together with the required distance
from adjacent buildings. This photograph was taken on 9th December 2002
at 21:09 (UK time). Subsequently, when on-site, the specified pattern was
within an accuracy of 1 foot! This spiral had a maximum diameter of
about 5 feet, and flowed in an upward clockwise direction.

Figure 17-3 A Type 3 Spiral, Remotely Mind Generated

It is important that this photograph is best viewed with both the reader and the top of the photograph facing westwards. There are several very interesting lessons to be learnt from this photograph, in addition to the demonstration of remotely sending complex information using a visual protocol.

When attempting to dowse this photograph in December 2017 it was completely inert, whatever the orientation of the observers or the photograph. This is pleasing, because following good practice I deleted all traces of this subtle energy pattern a month after creating it and after finishing my experiments.

However, what is very instructive is that when the mind's intent was set to the above date and time of creation (in December 2002), it is possible to obtain the subtle energy patterns exactly as they were in the original specification. This has been independently confirmed.

When the original creation and experiments were performed, subtle energy types had not been categorised nor psi-lines researched. However, the interesting finding is that when dowsing back in time to December 2002, there is, as well as the Type 3 spiral, Type 8 and a weaker Type 9 subtle energy; the latter 2 types were unknown at the time of creation. These subtle energy types have subsequently been found to be associated with psi-lines. This suggests a postulation that mind created psi-lines are the mechanism for transmitting or viewing information remotely.

Mind Generated Psi-lines

Since ancient times, psi-lines have been perceived and used (e.g. for tracking), and are even created by animals and birds to assist in their migrations. We know this, as psi lines can be permanent and our ancestors have left numerous examples around the world. They are subtle energy lines that are easily created and destroyed by the mind, without any physical equipment.

As they can also be readily detected, destroyed, or modified by others, it not only proves that they actually exist, but are a rare documented example of mind to-mind interaction. Psi-lines can either travel along the ground or they can float in space. Although there is no constraint on their maximum length, they must have a minimum length. It seems impossible to create psi-lines less than about 1 m.

The easiest way to learn how to create psi lines is to visualise a straight line such as at the top of Figure 17-1, and implant this thought onto the ground nearby. In doing so, using the mind, specify on the ground where the psi-line starts and finishes. When moving to the specified location, you should be able to detect the 2 spirals at either end of the line. It should then be possible to detect the energy types of the spirals and of the line itself. The next step is to detect that, in fact, the line is of a fractal nature and starts as comprising 3 lines.

Psi-lines are discussed in more detail in Chapter 22.

Properties of Mind Created Subtle Energies

Over many years of experimentation, the following properties, in addition to those above, have been discovered for mind generated subtle energies, both locally and remote.

1. If a dowser is "transmitting" from within a metal cage, the latter does not screen thought created subtle energies. This suggests that remote dowsing does not involve electromagnetism.
2. Time delay does not appear to be a factor. Subtle energy fields seem to be created faster than measurements can be taken, and deleted instantaneously. This can be confirmed by a remote observer at the end of a telephone.
3. There appears to be little information loss for created subtle energy fields comprising simple geometric shapes or spirals such as those illustrated in Figure 17-1. Similarly, there appears to be little information loss for such characteristics as subtle energy type, Mager colour, etc.
4. However, as illustrated in Figure 17-2, sometimes there is partial information degradation on both the simple, and the more complex geometrical shapes.
5. Mind created geometric shapes are also very stable in **time**. The dimensions and the shape of a dowsable field remain constant. For example, a rectangle remains the same size rectangle after 3 or more years. They are permanent unless erased intentionally.

Reflection number, n	Created field 0	1	2	3	4	5
Distance between reflections in Feet	0.000	13.917	27.917	50.667	96.000	177.000
Ratios of adjacent reflections (n+1)/n			2.01	1.81	1.89	1.84

Table 17-1 Reflections of Mind Created Dowsable Fields

6. The field strength of created subtle energy appears to be the same whatever its distance from the creator.
7. Mind created subtle energy fields seem to have 9 reflections in a geometric series, which has a geometric ratio of about 2, as shown in Table 17–1. This table only covers the first 5 reflections.

Floating in Space

The above discussions assume that subtle energies are either connected to the earth's surface, or to material objects, including buildings. Possibly more interesting though is that the mind can create one-dimensional, two dimensional and three-dimensional subtle energy fields above the ground suspended in space. These "floating" fields can just as easily be produced by the brain, similar to subtle energies placed on tangible surfaces.

Mid-air created subtle energy fields are not part of, nor associated with, the molecules of the atmosphere. Both the location and dimensions of such created subtle energy fields are remarkably stable over a long period of time. The wind, convection, or Brownian motion would dissipate the dowsable field rapidly if it were associated with tangible matter such as the gases in the atmosphere. On the other hand, as the created fields remain constant with respect to an observer on the ground, they must be locked by some mechanism into the Earth otherwise they would drift off into space or move around the Earth as the Earth spins. But, the height of the subtle energy field created above the surface of the earth remains constant in time.

Several experiments have confirmed that subtle energies created in "space" drift westwards at varying rates, depending on the height of the subtle energy. Figure 17-4 is a graphical representation of one such experiment. On the date and time of this experiment, the height versus speed of drift approximates to an exponential relationship and asymptotically approaching a speed of 1.4 m per day. In addition, the maximum height was about 50 feet and the correlation coefficient was of a very high accuracy at 0.98. (The mixed metric and imperial units were for practical experimental reasons). However, as will be discussed later these results vary significantly depending on the time of the year.

What is the force that is pulling the subtle energy field westwards, and why is the direction always westward? The "obvious" suggestions are that the earth spinning on its axis, or the earth orbiting the sun, or the moon orbiting the earth, or even the Coriolis force is involved. The challenge for researchers is to determine the mechanism and the reason for such slow drift. Of these alternatives, with the slow subtle energy drift of only 1.4 m per day, the moon orbiting the Earth once a month is a possible candidate.
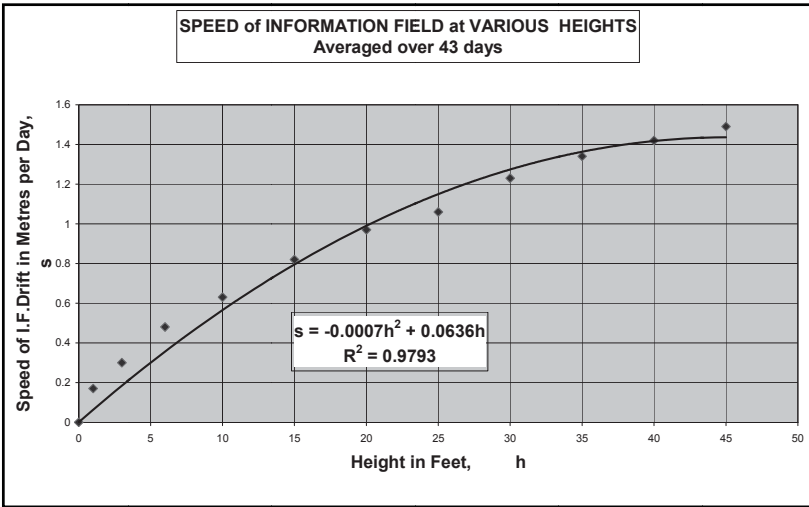
Figure 17-4 Speed of Subtle Energy at Various Heights

As we have just seen, mind created subtle energy fields move faster the higher they are from the ground. However if this were true for conventional physics, geometric shapes would become distorted because they would be sheared at a faster rate at their top compared to their bottom, in relation to the ground. For example, a vertical two-dimensional rectangle, as illustrated in Figure 17-5, would become a more and more stretched trapezoid. However, this does not happen: the field's geometry does not change. The conundrum is that as no friction is involved, what "grips" the subtle energy to make it move, when we know that subtle energies pass through physical barriers without any apparent attenuation. Is there some very weak coupling with the ground?
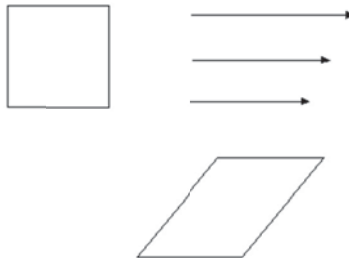
Figure 17-5 Theoretical Subtle Energy Distortion with Height

Summary

The mind can create subtle energy fields of almost any pattern, either locally or remotely. We have seen that the conscious mind extends over, and can affect vast distances. It is much more than just a physical brain within a skull. A further conclusion is that time span and separation distance appear to be irrelevant when creating remote subtle energies, whilst the location of the latter can be pinpointed accurately. Greater complexity is usually associated with increased degradation. Interestingly, 9 multiple images are created in a geometric series, unlike the 7 for physical objects, which are often in an arithmetic series.

The dimensions and characteristics of thought created dowsable fields seem inherently very stable, except that, although they drift westwards at a constant height above the ground, they are permanently fixed on the ground if they are created there. This drift rate depends on height at which they were created, the phases of the Moon, and the time of day. A combination of these findings demonstrates that mass and the moving earth are factors in the mechanism(s) - but how?

The Way Forward and Suggested Research Topics

1. Investigate the reasons for information loss for both local and remotely generated subtle energies.
2. Confirm if mind created psi-lines are the mechanism for transmitting, or viewing, subtle energy information - either locally or remotely.
3. Why is it impossible to create psi lines less than about 1 m.?
4. Why does mind created subtle energy have 9 reflections, each separated in a geometric series?
5. Investigate why mind created subtle energies, that have been specified as resting on the ground, remain "locked" to the ground, but subtle energies specified to float in space, do not remain constant but drift to the west?
6. As the speed of a floating subtle energy increases asymptotically with height, as illustrated in Figure 17–4, explain why floating subtle energies behave like a flowing fluid near the ground, analogous to friction or viscosity slowing the fluid's flow rate. This phenomenon is not compatible with subtle energies passing through physical barriers without any attenuation.
7. Why is this effect asymptotic, and relatively short ranged?
8. However, why does the geometry of a floating subtle energy field remain constant, when its height is flowing at different speeds? This

suggests that a floating pattern of subtle energy is not affected by its flow rate. However, this contradicts Figure 17–4.

CHAPTER EIGHTEEN

SPIRALS AND CONICAL HELIXES

Introduction

Rotation of objects in orbit, or the spin of objects around their axes seem to be an important feature of the universe, at whatever scale one chooses – be it rotating galaxies, planets revolving in solar systems, planets spinning on their own axes, electrons spinning around nuclei of atoms, or the spin associated with fundamental particles. The latter particles, that carry the fundamental forces of nature, such as the photon and the gluon are bosons, which have integer spin, whilst the quarks and leptons that make up matter are fermions, which have half-integer spin (1/2, 3/2).

As spirals are one of the most common subtle energy patterns, preliminary research suggests that a study of these topics is important in understanding consciousness, the structure of the universe, and the mind's interaction with the structure of the universe.

Scope

Spirals appear in numerous diverse places; in fact, anywhere on, above, or under the Earth's surface. Set out below are some examples of where spirals are found.

- Ancient sites and burial mounds.
- Within the auras of solid bodies.
- Within the auras of geometric patterns.
- Within the subtle energy generated by geometric patterns.
- Spirals form a major part of the Tree of Life subtle energy.
- Over geological features.
- Underground intersecting watercourses.
- Inside substantial buildings, particularly those with domes.
- Inside underground caves.

- Mind generated spirals (anywhere).
- The spiral produced at the intersection of two subtle energy lines.
- Spirals terminating subtle energy lines and psi-lines.
- Vents in volcanoes.

Complexities of the Real World

To facilitate an introduction to the following concepts of the ubiquitous "spiral", there are additional complexities and perturbations, which are only discovered qualitatively i.e. by the standard scientific method of measurement. Before proceeding any further, it may be instructive to examine the experimental techniques adopted, together with some of the locations where the research for this article was undertaken.

To illustrate the diversity of the phenomena associated with conical helices, and the extensiveness of the measurements undertaken during my travels around the world, I have examined numerous substances, and assembled on-site measurements, together with relevant supporting photographs, from the following situations and sources.

1. Part of the aura of a solid body comprising an outer series of spirals. In particular, the following crystalline solid objects were used in these experiments: 0.1grams of Quartz, 0.6g of Hematite, 4g of Quartz, 8g of Moss Green Agate, a Pebble weighing 34g, a piece of Granite weighing 1,090g, and an Amethyst of 4,425g.
2. Subtle energy lines terminating in a spiral. In this case, two interacting pebbles from a beach in Turkey created a subtle energy line, as discussed in Chapter 15.
3. Man-made prehistoric sites are a well-known source of spirals. In this case, a series of spirals were measured that were created by the linear double dykes at the ancient site of Hengistbury Head (in Bournemouth, UK), and the rings of banks and ditches at Avebury. These were discussed earlier in Chapters 13 and 14.
4. Isolated spirals, such as those associated with a burial mound at Hengistbury Head (as mentioned in Chapter 13) were analysed. Whilst in Greece, Crete, and Sicily spiral measurements were taken at the centre of an ancient Greek temple, and an ancient Greek Offering Table.
5. A small vent near the summit of Mount Etna caused an isolated spiral.

6. As discussed in Chapter 6, at the centre of the Rollwright Stones, there is a spiral possibly caused by underground intersecting watercourses.

7. Spirals created by the geometry of a building's architecture are very common. Examples used in this chapter include those in domed rooms in St Petersburg palaces; in the auditorium in the Kirov Theatre, and at the centre of Angkor Wat in Cambodia.

8. Domed chambers in underground caves generate spirals, and a study was made of one in Majorca.

9. As we have seen, the mind can generate spirals. For the research described in this book, these were formed locally a few feet away, as well as created remotely 3,500 miles away whilst in an aircraft at 32,000 ft.

10. The intersection of two dowsable lines generates a spiral. In item 2 above, two interacting crystalline stones created one dowsable line. In this extension of the experiment, the two Type 4 lines were created in laboratory conditions by four stones, i.e. two pairs of interacting stones.

I will now return from a travelogue around the world, and come back to academic science!

Experimental Techniques

Several months were spent analysing data resulting from the above observations, and this has led to some interesting results and conclusions. However, before detailing results, it is appropriate to describe the experimental techniques adopted, in order to encourage duplication of these experiments, and for others to confirm and refine the findings. This is good science, and should be useful for (sceptical) readers!

How does one obtain the following measurements? As already elaborated, nearly all spirals are 3-dimensional helices, which have conical envelopes. Seven basic measures helped to prove this conclusion.

Angle of Cone

A simple, but effective technique for measuring a cone's angle is to dowse for the vertical axis of the conical helix, and mark its location on the ground. After fixing a sheet of paper vertically above this mark (i.e. along the axis of the helix), a line may be drawn on the paper along the vertical axis. It is preferable (being faster and more accurate) to "device-

less" dowse the envelope of the conical helix with a pencil, mark the cone on the paper, and then draw and measure with a protractor the half-angle of the cone.

Diameter of the Base of Cone

The easiest way to dowse the size of the spiral (which more correctly is the diameter of the base of the conical helix), is by projecting the base of the conical helix on to a floor. The intent is to visualise looking down on the helix, thereby projecting the 3-dimensional helix as a 2-D image of a spiral on flat ground. The spiral can then be marked out.

The Height of the Cone

Usually, the height of the cone is often too high, or physically inaccessible, to dowse directly. If so, calculating the cone's height by trigonometry is easily done using the radius of the base (half the diameter) and the half-angle of the cone, as determined above. Alternatively, it can be measured by having the intent of turning the height of the cone through 90°, and projecting it on to level ground. This is analogous to "The Bishop's Rule" for measuring the depth of water – a century's old proven technique.

Spiral Turns

Whilst the plan of the spiral is projected on to the ground, it is possible to dowse the trajectory and flow of the spiral. Measurements can then be recorded of three more properties that are important. These are the number of turns of the spiral, the direction of the perceived flow, and the separation distances between the turns.

Orientation

When attempting to build up an accurate 2-dimensional and 3-dimensional model of spirals, it is essential to adopt more advanced measurements. This involves not only measuring distances and angles, but also their direction with respect to north. The easiest way to record orientation is to use a magnetic compass. Orientation is also important, when, for example, measuring spiral diameters. Because of the shape of the spiral, its diameter varies in different directions.

Overview of Findings

Findings Common to all Conical Helices

Location	Source	Spin Direction	Number of Turns	Flow Direction	Entry Path
Mind from 3,500 miles - Actual	Actual	a/c	3.5	Down	N to S
Mind from 3,500 miles - Intent	Specified	a/c	3.5	Down	N to S
Quartz 0.1g	Actual	a/c	3.5	Down	N to S
Hematite 0.6g	Actual	a/c	3.5	Down	N to S
Mind - Local	Actual	a/c	3.5	Down	N to S
Line Termination (2 crystals 24g)	Actual	a/c	3.5	Down	N to S
Kirov Theatre	Photo	a/c	3.5	Down	N to S
Quartz 4g	Actual	a/c	3.5	Down	N to S
Moss Green Agate 8g	Actual	a/c	3.5	Down	N to S
Quartz 100g	Actual	a/c	3.5	Down	N to S
Mind - Remote 120 miles	Photo	a/c	3.5	Down	N to S
HH D/D Spiral - on-site	Actual	a/c	3.5	Down	N to S
HH D/D Spiral - photo	Photo	a/c	3.5	Down	N to S
Granite 1,090g	Actual	a/c	3.5	Down	N to S
Pebble 34g	Actual	a/c	3.5	Down	N to S
Domed Cave Floor - Majorca	Photo	a/c	3.5	Down	N to S
Amethyst 4,425g	Actual	a/c	3.5	Down	N to S
St Petersburg Palace	Photo	a/c	3.5	Down	N to S
HH Burial Mound	Photo	a/c	3.5	Down	N to S
Rollwrights - centre	Photo	a/c	3.5	Down	N to S
Mount Etna Vent	Photo	a/c	3.5	Down	N to S
Ancient Greek Offering Table	Photo	a/c	3.5	Down	N to S

Table 18-1 Upper Spirals and their Properties

Table 18-1 summaries the results of observations of the conical helices associated with the sources just detailed. As is immediately apparent, all spirals investigated have 3½ turns, with upper cones possessing an anti-clockwise downward flow, and a north-south radial entry. There was no difference between on-site or photograph measurements.

Overview of External Dimensions

Figure 18-1 gives an indication of the size of the spirals associated with the sources **in** Table 18-1**.** The smallest spirals are mind generated or from very small solids. The largest are from large domed architecture, large ancient sites, earth energies, and volcanoes. This is only indicative of spiral diameters because each measurement was taken at different times of

the day, on different days, on different months, on different years. As always, subtle energies are constantly changing.

Although the largest spiral diameter in Table 18-1 is about 3 m, some spirals, such as those covering an entire ancient site, can extend to over 100 metres. As these measurements require specialist equipment, they have not been included in the quantitative analyses of this chapter. However, their qualitative properties are similar to smaller spirals, possibly displaying properties of fractal geometry, i.e. the larger patterns being self-replicating versions of the smaller ones, and vice versa.
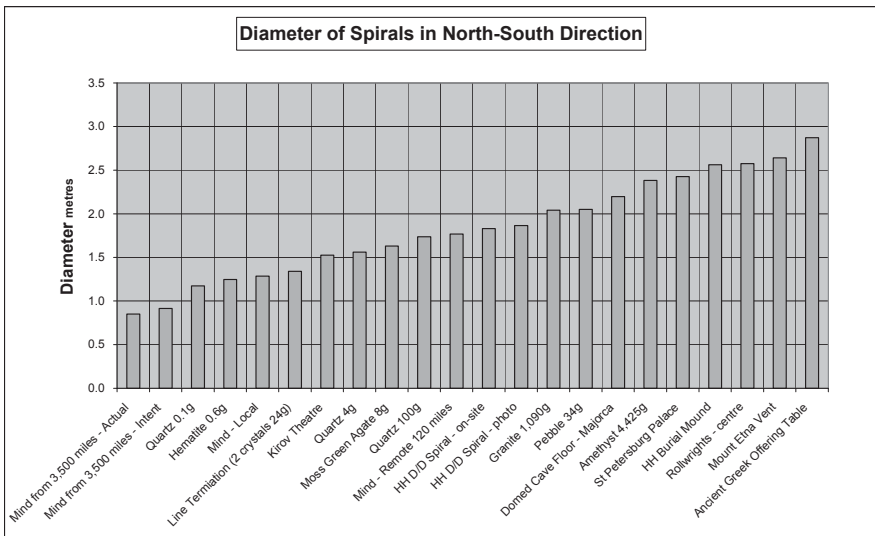
Figure 18-1 Sources of Spirals and their Size

Findings Common to all Spirals, Irrespective of Source

All spirals seem to have the same structure, whatever their source. Elevations, plans, and cross-sections in the following diagrams give a general indication of the geometry involved.

Anti-clockwise spirals

Figure 18-2 is a typical plan view of a spiral. Several features are immediately apparent. There is a perceived flow in an anti-clockwise

direction. This seems to start from the centre of the spiral, flows in a straight line due south, and then makes a right-angled turn to start the spiral. The spiral finishes where it started, at the centre.
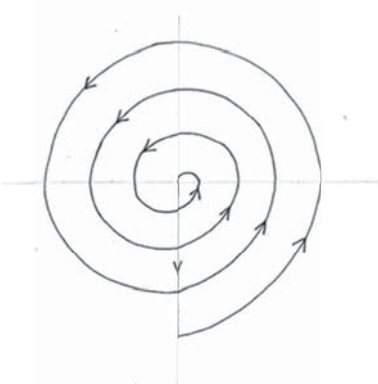
Figure 18-2 Plan View of an Anti-clockwise Spiral

Both clockwise and anti-clockwise spirals exist, which will be elaborated on later. The separation distance between adjacent turns of a spiral is approximately the same, implying that spirals are more closely related to arithmetic rather than geometric.

Highly significant is that all spirals have **3½** turns, and any line drawn through the origin always intersects the spiral at 7 dowsable points (the origin/centre is not a dowsable point in this context). These 7 points are approximately equally spaced apart so measurements form an arithmetic series. The fact that, in some scales, a harmonic octave has 7 notes, is relevant.

Figure 18-3 is a typical side elevation view of a spiral. As is apparent, spirals are 3 dimensional. An observer tracing a spiral on the ground will initially perceive a pattern similar to Figure 18-2. Only after further investigation will the observer realise that the "spiral" is not just 2-dimensional. As illustrated in Figure 18-3, vortices/spirals are perceived to possess an outer conical envelope. Hence, the correct name for this phenomenon is not *a 2-D spiral*, but *a 3-D conical helix*. In this case, the apex of the cone is pointing downwards.

In fact, Figure 18-2 is Figure 18-3 projected on to the ground, or in other words, the intent of the observer in Figure 18-2 is to look down and view the conical helix from above its central axis. It is now possible to understand the flow pattern initially perceived in Figure 18-2. This flow starts at the apex of the cone, and goes vertically upwards, along the

central axis of the cone. On reaching the base of the cone it flows due south along a horizontal radius until it reaches the edge of the cone. It then descends with 3½ turns back to the apex.
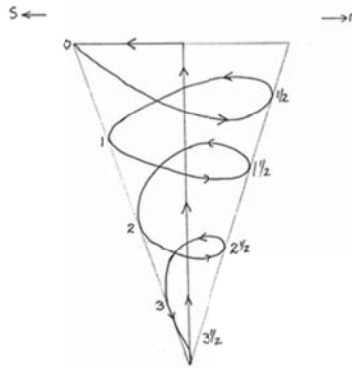
Figure 18-3 Side Elevation View of an Anti-clockwise Spiral
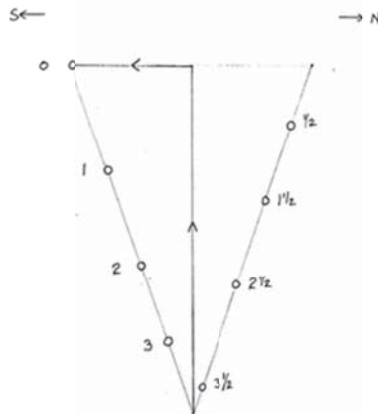
Figure 18-4 Cross-Section View of an Anti-clockwise Spiral

Figure 18-4 is a typical cross-section view of a conical helix, where the cross-section is a vertical north-south plane through the central axis. In Figure 18-3, the observer is viewing from the outside, whilst in Figure 18-4 the view is from the inside. Both figures depict the same helix. For an anti-clockwise helix, the flow of the helix on the left hand side of the cone is coming out of the paper, and the perceived flow goes into the paper on the right hand side.

Practical Examples of Anti-Clockwise Spirals

Two examples of anticlockwise spirals from Angkor Wat, are shown in Figures 18–5 and 18-6. These conical helices are important examples, because their half-angles are 19.5° and 11.5° degrees. Within experimental error, these angles are arcsine 1/3 and arcsine 1/5, exactly as highlighted in Chapter 5 Table 5–2.
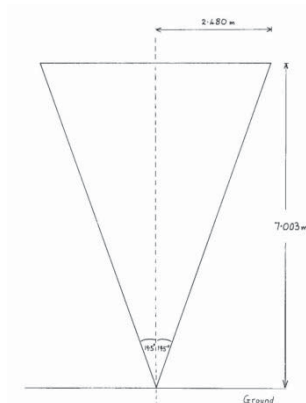
Figure 18-5 Type 3 Conical Spiral (Type 1 lines) at Angkor Wat

These angles were produced manually, as described above in the earlier section labelled experimental techniques. These figures were obtained on my first attempt at measuring the dimensions of a conical helix and its cone apex half-angle. About six colleagues watched as I made these measurements, and they checked the accuracy. I am, therefore, amazed that Table 18–2 highlights experimental errors of only -0.152% and 0.315%. Table 18-2 is another confirmation of the series **sin1/n**, where **n** is an odd integer, and validates the accuracy of the technique to observe and quantify conical helices of subtle energy.
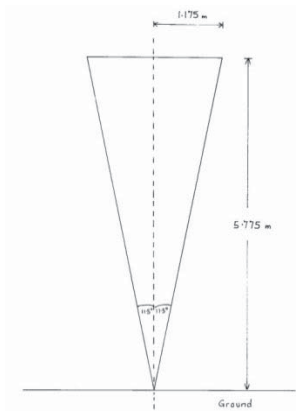
Figure 18-6 Type 3 Conical Spiral (Type 4 lines) at Angkor Wat

Type of Spiral	Height metres	Radius of Base metres	Apex Half Angle ArcTangent Degrees	sine 1/3 sine 1/5 Degrees	Degrees Difference	% Difference
Type 1	7.003	2.48	19.5008	19.4712	-0.0296	**-0.152%**
Type 4	5.775	1.175	11.5006	11.5370	0.0364	**0.315%**

Table 18-2 Examples of Conical Helices Apex Half Angles

Clockwise Spirals

Superficially, clockwise spirals are the same as anticlockwise spirals, apart from the direction of the "flow" of their subtle energy. For completeness, and to simplify describing the geometry when we combine conical helices in the next section, clockwise spirals are set out below.

Figures 18-7, 18-8, and 18-9 are identical to Figures 18-2, 18-3, and 18-4, except they depict a spiral with a clockwise flow. An important difference between the two spirals is that the flow along the vertical **axis** of an anti-clockwise helix is nearly always upwards, which naturally leads to the actual downward flowing **helix** clinging to the surface of the cone envelope. This is depicted in Figure 18–3. However, the vertical flow along the cone's **axis** is nearly always downwards for a clockwise helix, and leads naturally to the perceived upward flowing **helix**. This is shown in Figure 18–8.
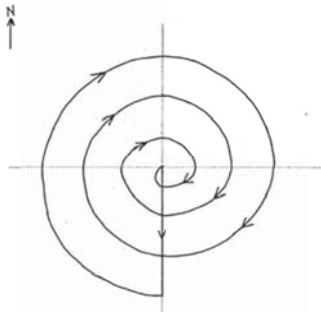
Figure 18-7 Plan View of a Clockwise Spiral
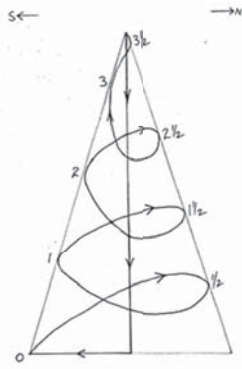
Figure 18-8 Side Elevation View of a Clockwise Spiral
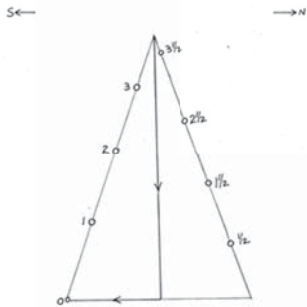
Figure 18-9 Cross-Section View of a Clockwise Spiral

Linked Conical Helices

A fundamental feature is that most "spirals" seem to comprise two linked conical envelopes. Conceptually, these two cones are linked apex to apex, with an X-shaped cross-section. The top cone points down whilst the bottom cone points upwards; in other words Figure 18-3 sits on Figure 18-8, as depicted in Figure 18-10.

As is apparent, passing through the touching apexes is a horizontal plane of symmetry; the lower conical helix is a mirror image of the top one. Looking down, if the top spiral is anti-clockwise, the bottom is clockwise, and vice versa. Upper cones have a propensity for a perceived anti-clockwise downward flow, whilst the lower cones have a clockwise upwards flow. These flows can readily be felt; the observer's body has a strong sensation of being lifted off the ground, and vice versa for a downward flowing spiral. But there is no evidence of a connection between the top and bottom flows – they seem to be independent reflections. Being reflections, the cones have the same sizes, and in particular, the diameter of the base of the top cone equals the diameter of the bottom cone's base.
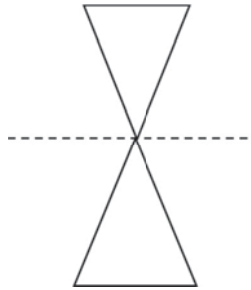
Figure 18-10 Side Elevation View of a Pair of Conical Helices

For those cases where the top cone is clockwise, Figure 18-11 illustrates the flow when looking down. It has the same orientation as Figure 18-2, but an opposite flow.

To avoid confusion, it is important to adopt two practical conventions. The first is when visualising conical helices; the viewer should, by convention, always be looking down (i.e. along the direction that gravity is pulling). The second convention is that the definition of whether a conical helix is upwards or downwards depends on the perceived flow of the spiralling part of the helix, not the upwards or downwards perceived flow

along the cone's central vertical axis. The obvious reason for these two arbitrary conventions is that an observer whose intent is to visualise conical helices standing on the ground looking upwards, will perceive the opposite flow to an observer looking down.
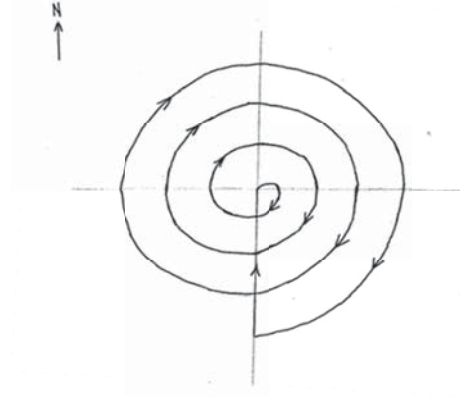
Figure 18-11 Plan View of a Top Clockwise Spiral

Figure 18-12 Side Elevation View of a Series of 7 Conical Helices

As always in science, when someone believes they understand a subject, subsequent data can lead to new insights. Having determined that "spirals" are really a pair of conical helices, on further investigation it is discovered that "spirals" are more accurately a series of seven pairs of conical helices, stacked vertically, one on top of each other, sharing a

common axis. This is depicted in Figure 18-12, where the column can be erroneously construed as a series of diamond patterns, not as reflections of pairs of cones of the same size and the same separation.

Traditionally, people associate perceived upwards spirals as positive, beneficial, or "healing", whilst downwards spirals are negative or associated with, say, burials. Initially, this presents a challenge because the findings of this research suggest that all spirals have both an upwards and downwards component. A possible explanation is that the positive or negative sensation could all be in the observer's mind, depending on whether the observer's intent is focused on the top or bottom conical helix.

As is apparent, every conical helix has a vertical axis. This suggests that gravity is a fundamental factor in the production of conical helices.

What spirals have in common is that they are all Type 3 fields. Unlike other types of dowsable fields, they and their source, are unaffected by light or electromagnetic fields in general, and are not diminished by a Faraday Screen, or attenuated by being enclosed in by a thick metal container. This and gravity are discussed elsewhere.

The limitation of analysing measurements, such as those in Figure 18-1, is that the measurements are in one dimension. As discussed earlier in this chapter, the measurement of orientation is essential to study three-dimensional conical helices. This leads to the use of polar diagrams to represent results. As a result of extensive studies of polar diagrams, it is found that, in general, all spirals look similar.
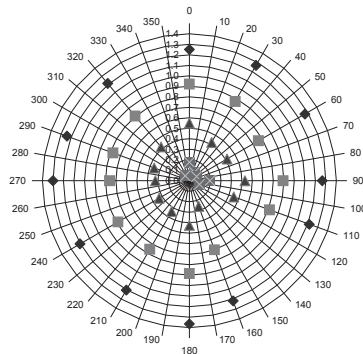
Figure 18-13 Polar Diagram of an Architectural Created Spiral

The polar diagram in Figure 18-13 was produced from taking measurements from a photograph of the spiral on the floor at the centre of a large domed room in one of the palaces in St Petersburg, Russia. This

polar diagram only provides a snapshot at specific co-ordinates; it does not give a continuous line. Figure 18-14, shows an idealised interpretation of the geometry.
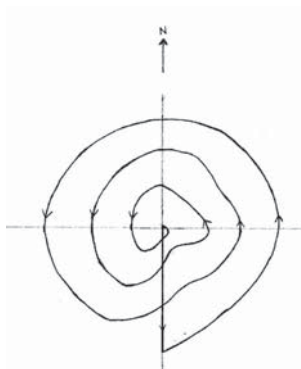
Figure 18-14 Spiral Turns and Flow

As is apparent from Figure 18-14, spirals are not always symmetrical. This should be treated positively, and used to find the cause of this perturbation. This also illustrates the importance of recording orientation with respect to north when taking measurements. As in all subtle energy studies, there are the usual perturbations caused by the spin of the earth on its axis, the rotation of the earth around the sun, the rotation of the moon, and other cosmic activity. It is interesting to note that these causes of perturbations to subtle energy fields are, in turn, caused by spin!

Bifurcation

All conical helices that terminate linear subtle energy fields bifurcate into a symmetrical pair of subtle energy lines, which end in another helix, which also bifurcates, and the process continues with ever decreasing lengths of lines. However, some spirals, such as the centre spiral between 2 interacting bodies, do not bifurcate. The reason for this is as yet unknown.

The classical representation of bifurcations is shown in Figure 18-15, but, as we shall see later in Chapter 32, subtle energy bifurcation does not involve "parabola like" shaped lines, but more like straight lines at right angles.

The bifurcations process starts at the entry points of the conical helices, which, as we have seen, is at the northern most part of the spiral. At this

point, there is a small portal of interesting and a rare form of subtle energy (Type 9) perceived at the points of bifurcations.

$$x_n = r\,x_{n-1}\,(1 - x_{n-1})$$
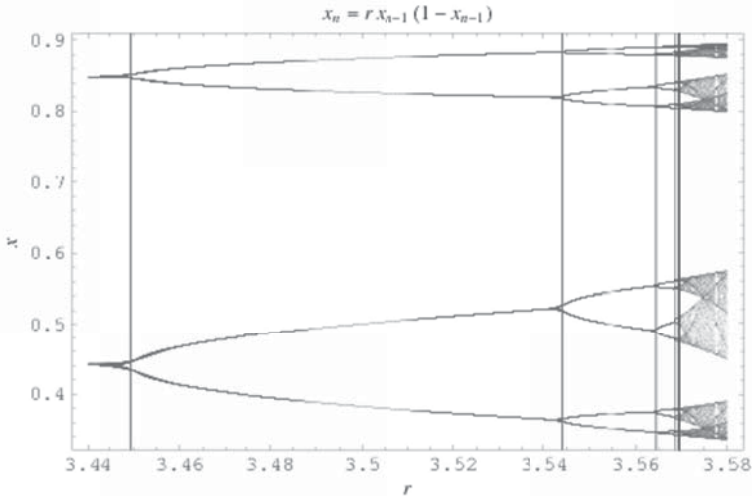
Figure 18-15 An Illustration of Bifurcation in Standard Chaos Theory

Conclusions and Summary

1. The strong north-south orientation of spirals suggests that the earth's spin is also involved in the generation of conical helices. The position of the north pole is determined by the spin of the earth on its axis with respect to the plane of the earth's orbit around the sun. An additional component of conical helices is, therefore, a cosmic and rotational influence.

2. In contrast to the previous point, it does not seem to affect the nature, the geometry, or the location of the "spirals" associated with physical matter, if the latter is spinning or not. The mechanism that produces conical helices is, therefore, non-physical (in the normal accepted meaning of the word), and has the property of being unaffected by spin.

3. As stated earlier, an important feature of conical helices is that they always have a vertical axis. It would, therefore, seem that gravity has a fundamental influence in producing them.

4. All the "spirals" display the characteristics of Type 3 fields, even if they are produced by the intersection of a Type 4 and Type 1 or other subtle energy lines.

5. Type 3 fields seem permanent, and are impervious to electro-magnetic fields. Unlike some other types of subtle energy fields, conical helices, and their source, are unaffected by light/photons, electromagnetic fields, in general, and are not diminished by a Faraday screen, or attenuated by being surrounded by a thick metal container.
6. It cannot be co-incidence to have found, in conical helices, key angles (universal constants), of arcsine 1/3 = 19.4712° arcsine 1/5 = 11.537° arcsine 1/7 = 8.213°. This implies that subtle energies, in general, and conical helices, in particular, seem inherently connected to the structure of the universe – not just an isolated random phenomenon.
7. The validity of dowsing relevant photographs is again well demonstrated by the consistency with on-site measurements. It makes no difference if the photographs are thousands of miles away from their subject matter, on the other side of the world. Using the vocabulary of quantum physics, this would seem to be an example of non-local entanglement, with instant connectivity.
8. Many conical helices are slightly asymmetrical due to perturbations caused by the spin of the earth on its axis, rotation of the earth around the Sun, and the rotation of the moon.. This is ironic because all these perturbing factors are involved with spin, as are the conical helices themselves!
9. This chapter, therefore, adds yet more evidence of the commonality between the structure of the universe, information, geometry in general, polyhedral, and vortex structures in particular, and how all of these link with connectivity and consciousness.

Owing to lack of space, the following list of topics relating to conical helices is not covered here:-

Experimental errors, perturbations, the asymmetry of vertical cone overlap, the distance of spirals from their source, the analysis of spirals resulting from the intersections of 2 subtle energy lines, and the effect of varying this intersection angle to produce null angles. However, all of these can be found at http://www.jeffreykeen.co.uk/Papers.htm.

Relevant papers are numbered 13, and 14.

The Way Forward and Suggested Research Projects

1. Why are there 3½ turns in a conical helix, and what is the connection to musical octaves comprising (2 x 3½) 7 notes?
2. Conical helices of subtle energy always seem to appear as inverted pairs, like reflections that appear as touching apexes. Why?

3. Moreover, these pairs of conical helices are stacked vertically above each other as pairs. Why?
4. What causes conical helices to appear the same, if they originate from differing sources?
5. Why is there a mirror image between pairs of conical helices? This seems to apply to both vertical and horizontal "reflections".
6. Most conical helices involve bifurcations. However, some spirals, such as the central spiral between 2 interacting bodies, do not bifurcate. Why?

CHAPTER NINETEEN

VORTICITY, PRAYERS, AND DIPOLES

Introduction and Scope

The previous chapter related to the concepts of spin and rotation with regard to intangible subtle energies. This chapter investigates vorticity, spin, and rotation in relation to tangible physical bodies. Four different situations are now considered for both solids and liquids. These are:

a) Static Solids
b) Rotating Solids - special
c) Rotating Water - special
d) Non-physical Rotation

The measurement of auras is the optimum property used to quantify comparisons. Each is now examined in turn.

Static Solids

Starting with the aura of static objects, such as crystals, enables a benchmark to be set against which observations of rotational experiments can be compared. A brief recapitulation of an aura associated with tangible matter is a useful starting point.
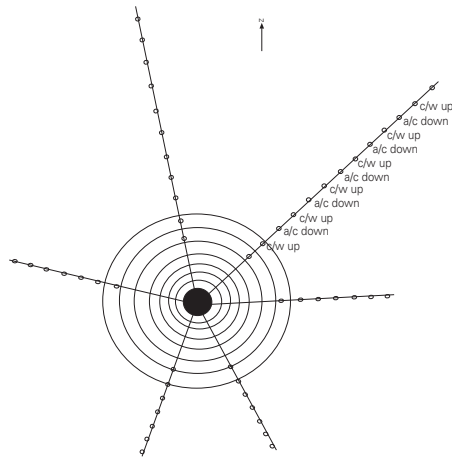
Figure 19-1 Inner Ellipses and Outer Spirals of an Aura

To prevent readers having to search backwards, Figure 19-1 is the same as Figure 6-5. This figure represents a horizontal cross-sectional plane through any object, and illustrates auras associated with solids, the properties of which may be briefly summarised and quantified as follows.

1. Auras comprise a series of ellipsoidal shaped inner fields.
2. These ellipsoids are concentric with the centre of the source object.
3. These ellipsoid fields have 7 boundaries. i.e. there are seven different fields, with each field enclosing the adjacent smaller field.
4. The separation distances between these boundaries form an arithmetic series.
5. These ellipsoids comprise Type 1 fields.
6. These auras are present in all 3 dimensions.
7. The size of the core aura (the innermost field) is a function of **mass.** For a static body, the formula for the Range of the core aura (the distance of the core aura boundary to the centre of the source object) is given by:-
   R = a log M + b   (i)
   Where **R** = Range; **M** = Mass; **a & b** are constants.
   In other words, a megalith has a larger aura than a grain of sand.
8. An aura's outer arms comprise a series of conical shaped helices.
9. These arms seem to extend to infinity.

10. The separation distances between adjacent spirals also form an arithmetic series.
11. The spirals are Type 3 fields.
12. Finally, natural every-day objects, untouched by humans, do not possess Type 4 fields.

The following sections compare the above static aura and field properties with those observed and measured in rotational experiments.

Rotating Solids

If any solid, such as a crystal or stone is spun, even at high speeds, there is **no** change in its aura's dimensions, location, orientation, or structure.

- The aura, as described above, is not affected by either spinning the object on its axis, or by its rotation in a circle.
- Type 1 boundaries stay the same.
- Type 3 spirals stay the same.

This is counter intuitive, and seems very strange. The obvious question is "Why do auras and their fields appear static when their source is rotating?" As apparent from the equation (i) above, the property of mass is a main factor in determining the size of auras. This observation suggests that

- an aura is not strongly coupled to the object creating it, and
- the property of mass is involved with other external non-local factors.

This observation could be most profound, and is discussed further in the conclusions of this book.

Water Vortices

This section moves on from spinning solids to rotating liquids. Unlike solids, liquids can form vortices. What happens with the simplest and commonest liquid – water? When a bottle of water is moved vigorously in a circular motion to form a vortex, the range of its aura is increased. This is illustrated in Figure19-2.
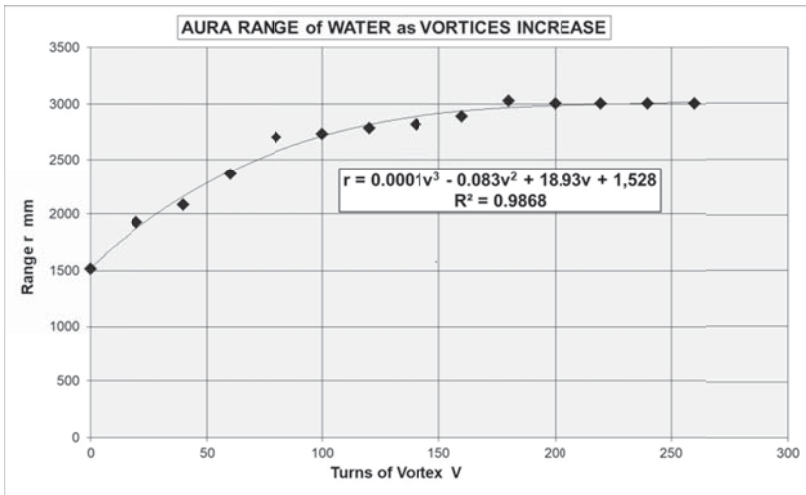
Figure 19-2 The Aura of Water in a Vortex

Figure19-2 relates to one experiment, where the size of the water's core aura eventually doubled. After 200 turns of a plastic bottle containing the water, the core aura increased from 1.5m to 3.0m. The aura's size has an asymptotic relationship to the number of turns of the water to create a vortex. Within the data range, the relationship is third order polynomial, with a very high correlation coefficient of 0.986. A theory is required that explains these findings.

It is not just the core aura that increases. All 7 ellipsoidal fields expand in unison, together with the associated Type 3 spirals. The other interesting finding is that the expanded aura retains its increased size after the spinning stops. These observations only occur for rotating liquids and are discussed further in the conclusions of this book.

Non-Physical Sources of Rotating Subtle Energies

The previous sections discussed the rotation of physical solid and liquid bodies. This section discusses the fourth category of rotation, where the observer's intent is purely on rotational generated fields and their effect on subtle energies. As will become apparent, every property observed and measured is different to all the previous results. The following experiments and findings are numbered to facilitate referencing and for making comparisons.

1. Spin generates its own aura of Type 4 fields. An easy experiment to detect Type 4 rotational fields is to switch on an electric fan. Type 4 fields are not there before the fan is rotating.

2. This Type 4 field can then be compared experimentally to, say, a mind created floating subtle energy line, or mind created energised water. This comparison shows that the rotational generated fields are the same as mind created fields. This suggests a connection between torsional waves, subtle energies, and the mind.

3. As already discussed in Chapter 17, Type 4 fields are also associated with spiritual concepts such as prayers. They can, for example, be detected in religious scrolls, altars in active cathedrals, or a worshipped Buddha.

4. Using an electric fan, the reader may like to try the next simple experiment, to detect that rotational fields comprise nine Type 4 field boundaries, and not seven as with static objects.

5. This experiment can then be followed by measuring the separation distances between the nine boundaries to demonstrate that they form an approximate geometric series. A practical challenge here is that as spin generated auras can act like dipoles, it is not always obvious from where the origin of measurements should be taken.

6. Unlike the Type 3 spirals discussed in the previous chapter, a simple observation establishes that there are no Type 3 fields being generated from a rotating fan.

7. When the rotation stops, the Type 4 aura disappears.

8. A very heavy spinning object generates exactly the same Type 4 aura as the same sized light object. A rotating object's mass is, therefore, irrelevant to the size of the created aura. This is opposite to auras of solid objects, and invites the question why?

9. Simple experiments prove that faster and larger spinning objects produce bigger auras. Range (**R**) is a function of revolutions per minute (**ω**) and radius (**r**). The concept of vorticity is relevant here, where

$$\textbf{Vorticity, V} = \textbf{½ . r}^2 \textbf{. ω} \qquad\qquad \text{(ii)}$$

The aura size increases as the radius of the spinning object is increased, and as the revolutions per minute are increased.

10. Unlike the aura of static solids, rotational auras are not present in all 3 dimensions. This is easily shown by means of a simple experiment to measure the range of, say, the 9th (outer most) field boundary along a horizontal axis of rotation. The maximum range is found to be along the axis of rotation ($\theta = 0°$). If the fan is turned around a vertical axis through 90°, or by laying the fan on its back,

(so that the axis of rotation is vertical, not horizontal), there are no observable Type 4 fields. In other words there is a zero field at 90° to the axis of rotation ($\theta = 90°$). It would, therefore, be expected that a normal cosine relationship exists.

Range, $R = Fn(V) = ½ . r^2 . \omega . \cos \theta$ (iii)

To prove if this is true, a series of readings were taken for different angles of spin **(θ)**, but keeping **r** and **ω** constant in equation (iii). The results appear in Figure 19-3. Between 0° and 90° the findings adhere closely to a fourth power relationship between **R** and **θ** with a correlation coefficient of better than 0.99.
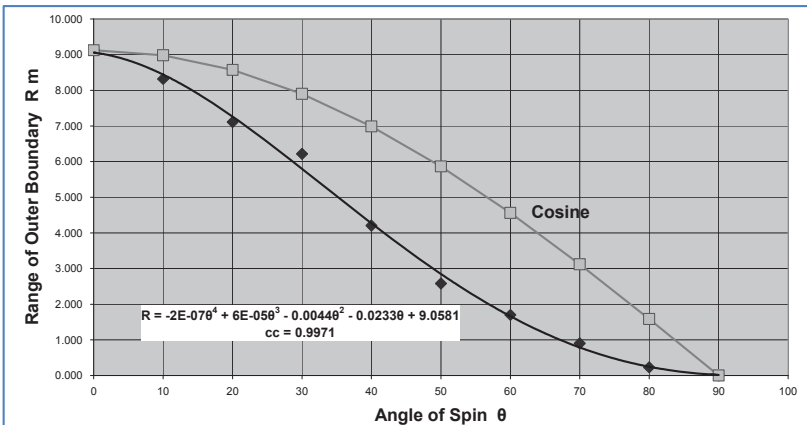
Figure 19-3 Size of Aura against Angle to Direction of Spin

The observations do not adhere to the expected cosine relationship, as in equation (iii) above, which is superimposed in Figure 19-3. Once again, there is a perturbation effect. This creates a challenge to determine the cause of the perturbations.

11. To see if this anomaly is a result of a directional background effect, the horizontal range was measured through 360°, by keeping both the vertical axis, and the horizontal axis of rotation constant. Once again, the range does not adhere to the expected cosine relationship, as illustrated in Figure 19-4.
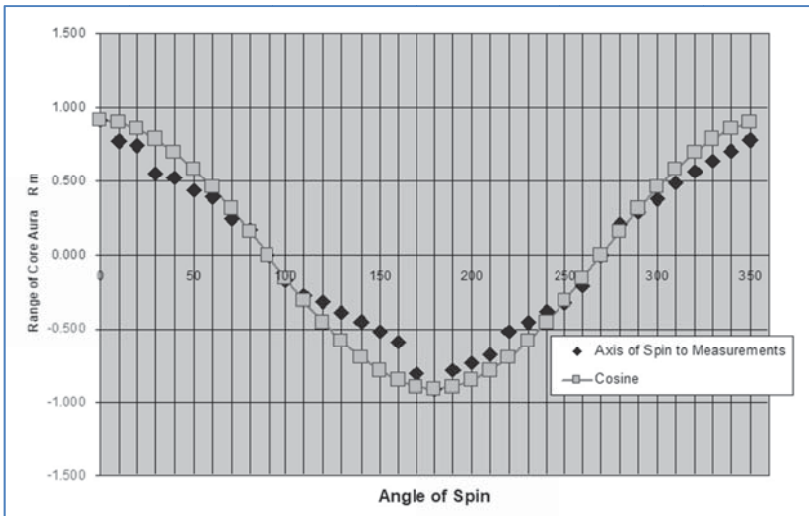
Figure 19-4 Size of Aura against Angles to Direction of Spin

Figure 19-5 represents a Polar diagram of the Type 4 fields perceived to be emanating from a rotating object, where the horizontal axis of rotation is pointing north i.e. the north-south 0° to 180° line. The 3-dimensional representation of the aura can be obtained by visualising this diagram being spun around this axis of revolution. It is similar to two back-to-back "pears". The aura is not very symmetrical. Is this due to experimental error, background effects, or are more perturbations present?
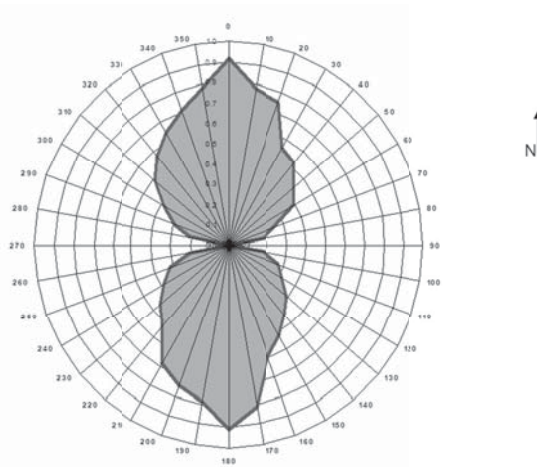
Figure 19-5 Polar Diagram of Rotational Generated Type 4 Field

Summary

Table 19-1 summarises the findings in this chapter and in particular, the differences between static and rotating objects.

Property	Static Object	Rotating Object
Field Types	1 and 3	4
Number of Field Boundaries	7	9
Boundary Separation Distances	Arithmetic	Geometric
Permanence	Always present	Only whilst spinning
Range Dependence	R = Fn (M)	R = Fn (r,ω)
3-D Aura shape	Uniform	Directional
Source of aura	Matter	Rotation

Table 19-1 Comparison of Aura Characteristics

Conclusions

The properties of auras generated by spinning objects, or liquid vortices, are very different to auras associated with static objects. This statement seems to apply to all of the characteristics as elaborated above.

From experiments involving spinning solid objects, the auras produced do not spin with the associated source object. Conceptually, if a sphere or

an ellipsoid is spun, its shape could appear the same as when static. There may be an element of doubt. However, in auras the arms of the Type 3 spirals are not spinning with their source object, and remain static. There can be no confusion about this observation. These arms, therefore, cannot be **physically** connected to the source object, even though the latter is creating the observed aura. And, by inference, the Type 1 ellipsoids are also not physically connected to the source object producing them. The implied conclusion is that the auras we perceive are not physically present – "they are all in the mind", or they are very loosely coupled to their sources.

This is further evidence that supports the theory that auras of physical objects seem to be a result of matter interacting with a universal consciousness. As we have discussed earlier, the latter concept has numerous names ranging from the Akashic Record from thousands of years ago, to the Zero Point Field, or more recently to the Information Field. We are looking for the mechanism that produces auras, which also has the property of being invariant to rotation? i.e. a mathematical transformation of axes that is invariant to rotation.

Experimental results suggest that rotation affects liquids differently to solids. For example, unlike solids, liquids retain their enlarged auras resulting from spinning. Why? The most tempting reason is because of the vortices created. After the macro and visible effect of these vortices have subsided, due to friction and viscosity, these vortices seem to leave a permanent effect at the micro level. It would appear that a permanent impression is left on the molecular vibrational or spin states of the water molecules, that, in turn, enlarge auras. Once again, there is a strong hint that vorticity has its own special relationship with the information field.

The preference for arithmetic series in Type 1 fields (associated with physical bodies), and for geometric series in Type 4 fields (associated with mind and vortex generated activities) is consistent with other reported general observations and laboratory experiments.

Non-adherence to a simple cosine relationship for the angular pattern of a rotationally generated field is possibly because the perceived radiated field pattern is not emanating from a single source, even though physically the source is a single rotating object. Allowing for experimental error, the 3-dimensional polar diagram of rotational generated Type 4 fields is very similar to the radiation pattern associated with a dipole antenna, which possibly has a separation distance of a half wavelength. Further theoretical research is justified, as this connection could lead to a fundamental discovery.

Mind generated fields (that would include prayers) have similar properties to rotationally generated subtle energy fields. Experiments with Tibetan Spinning Prayer Wheels reinforce this view. These prayer wheels comprise a cylinder holding an inserted written prayer. The cylinder can be made to rotate on a spindle attached to a handle, assisted by a swinging chain and weight attached to the cylinder. Typically, the Type 4 field, emanating from the prayer when static, extends for about 0.5 metres. When spun, the field extends to several metres.

The implication of this research is that consciousness, intent, the mechanism of dowsing, the associated phenomena of remote viewing, and subtle energies are all linked to vorticity, dipole antenna radiation patterns, and the structure of the universe.

This chapter, therefore, adds yet more evidence of the commonality between the structure of the universe, geometry in general, and polyhedral and vortex structures in particular, and how all of these link in with connectivity and consciousness. We are indeed living in exciting times. This conclusion suggests that further research is warranted. It would appear that vorticity is not only involved in consciousness, but also has wider implications in understanding our universe, and, therefore, the subject warrants further research.

The Way Ahead and Suggestions for Further Research

This chapter has generated a significant number of questions, and hence a prolific source of research projects. The following are suggested areas of future research.

1. Why do auras and their component fields appear static when their source is rotating, and, therefore, suggest auras are only loosely coupled to their rotating source? Why is this opposite to auras of physical objects, where their size is mainly a function of the source's mass?
2. Is there an aura producing mechanism, with a mathematical transformation of axes, which has the property of being invariant to rotation?
3. What is the theoretical reason for a fluid's aura size having an asymptotic relationship to the number of turns of the associated vortex? Why is this a relationship involving a 3rd order polynomial with a high correlation coefficient?

4. Why does a fluid's aura, expanded by a vortex, retain its expansion after the spinning stops? Why is this opposite to an aura associated with a spinning solid object?
5. Investigate why rotational generated fields have the same Type 4 subtle energy as mind created fields.
6. Investigate why rotational fields comprise 9 Type 4 field boundaries, and not 7 as with static objects. Why do the distances between the 9 boundaries form an approximate geometric series?
7. Investigate why physical bodies are associated with Type 1 fields with a preference for arithmetic series, whilst mind and vortex generated subtle energies are associated with Type 4 fields in a preferential geometric series.
8. Unlike auras associated with solids, which are 3 dimensional, why are auras associated with rotation mainly 2-dimensional?
9. Investigate why rotational auras are not very symmetrical, and ascertain what perturbations cause this asymmetry.
10. What perturbations cause the discrepancy in the cosine relationship and the angle of spin? Is the fourth power relationship in Figure 19-3 the same as would be expected from a field radiated by a dipole antenna?
11. What effect, if any, does the earth's rotation have on the above experimental results?
12. What is the connection between Tibetan spinning prayer wheels, Type 4 fields, vorticity, and cosmic consciousness? Is there any measurable difference between spinning the wheel clockwise, as opposed to the preferred traditional anti-clockwise motion?
13. The 3-dimensional polar diagram of a rotational Type 4 subtle energy is similar to the radiation pattern associated with a dipole antenna. Investigate whether this analogy is useful in finding a theoretical explanation for the perceived rotational generated fields observed in this book.

CHAPTER TWENTY

POLYHEDRAL GEOMETRY
AND THE MIND'S PERCEPTION

Introduction

Chapter 5 introduced the concept of universal constants and angles, which occur in many branches of science. Examples include common angles such as in DNA; Kelvin wedge; carbon molecular bond and polyhedral geometry. Table 20–1 gives an explicit example of such a common trigonometry series that occurs in general science, as well, as in subtle energies.

Integer	Arc Tangent 1/n*√2	
n	Radians	Degrees
1	0.615	35.2644 °
2	0.340	19.4712 °
3	0.231	13.2627 °
4	0.175	10.0250 °
5	0.140	8.0495 °

Table 20–1 An Example of Common Universal Angles

Frequently finding these angles cannot be a coincidence, but reflects the structure of space-time, in which geometry is a fundamental part. This chapter explores what happens when the mind gives positive feedback to space-time, via dowsing source geometry of common angles, to see if a positive feedback response provides further insights.

Overview of Experimental Protocols and Findings

Figure 20-1 is the tetrahedral source geometry that was used in these experiments. This geometry comprises 8 superimposed Pythagorean (right-angled) triangles with a simplified version of Table 20-1 containing the basic angles 35.264°, 19.471°, 90°, and 109.471° (i.e. 19.471°+ 90°).

Observations made by several independent experienced researchers have confirmed the creation of a complex pattern of subtle energies comprising subtle energy beams, subtle energy cones, energy flows, vortices, as well as geometric and arithmetic separation distances. Interesting comparisons are made between identical abstract and solid geometries.

Subsequent observations show that results are affected by magnetic fields, the orientation of the source geometry, and whether the latter is made from solid wire or an abstract shape drawn on paper. These facts are used to research why and how these perceived patterns are produced. Figure 20-2 illustrates the findings, and suggests an analogy to patterns from a diffraction-grating, or X-ray crystallography that, for example, produced the structure of DNA.
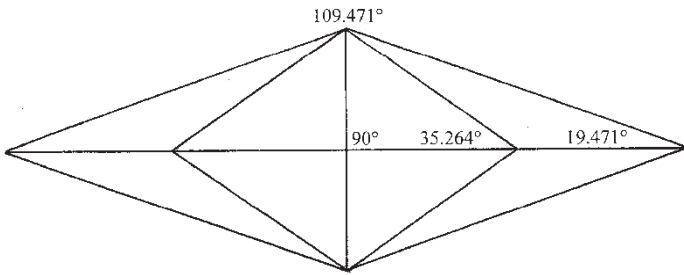
Figure 20-1 Tetrahedral Source Geometry

Detailed Findings

Abstract Source

When an abstract version of Figure 20-1 that has been drawn on paper is

a) laid **horizontally** on the ground, and
b) with its major axis aligned **north-south,**

Figure 20-2 gives the complex perceived pattern of subtle energies. This pattern comprises 8 subtle energy lines (which have a perceived outwards flow), 16 arithmetically spaced vortices, 16 geometrically spaced vortices, and 4 isolated vortices. There is also a central vertical conical vortex with a height of about 14 metres comprising the usual 7 sub-vortices.
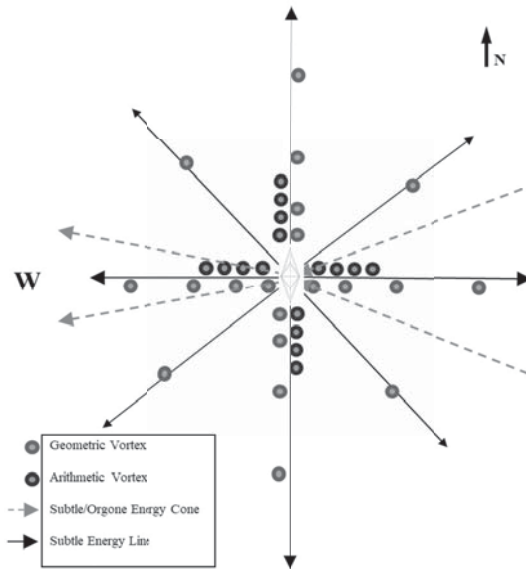
Figure 20-2 Subtle Energy Pattern with Abstract Source Geometry

It could bring significance to comprehending the theory of these findings, that all the vortices are attached to subtle energy straight lines.

Figure 20-2 also shows a diverging subtle energy cone emanating from the westerly apex of the tetrahedral source geometry with an outward flow. Also in Figure 20-2, there is a similarly converging subtle energy cone giving the impression of being "sucked" into the easterly apex of the source geometry, and being converted into a different subtle energy that exits the source geometry.

Figure 20-1 depicts possibly the only source geometry pattern that creates/emits all these subtle energy cones and associated effects; each having a different type of subtle energy. (This is a complex subject that is further developed in the next chapter.) The reasons for this finding are not yet known, and further research is required to determine if the optimum alignment is to magnetic or true north. In other words, is the effect due to the earth's magnetism or the earth spinning on its axis?

As is apparent, the eastward and inward flowing subtle energy cone's apex half-angle is significantly greater than the apex of the outward flowing cone on the opposite side of the source geometry.

Physical Source
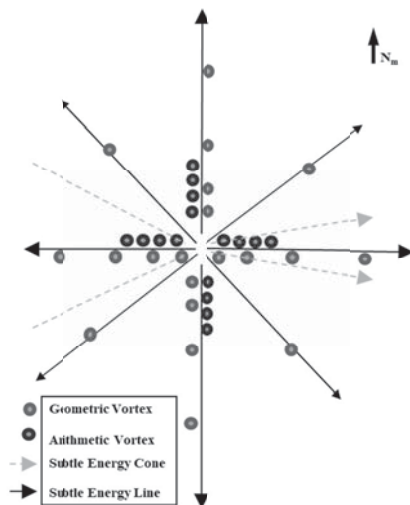
Figure 20-3 Subtle Energy Pattern with Solid Source Geometry

As expected, a solid version of the geometry in Figure 20-1(for example using wire), produces an identical perceived pattern as the pure geometry source. However, a significant exception is that the larger converging subtle energy cone enters from the west, and is emitted from the eastern apex and flows towards the east, as illustrated in Figure 20-3. This finding is significant. As previously discussed; pure abstract geometry usually gives identical subtle energy as solid objects.

The reason for this lack of symmetry is currently unknown. It would seem that there may be a left hand rule for subtle energy from solids, but a right hand rule for abstracts, with the three possible variables being subtle energy, gravity, and the earth's spin. These are exciting findings as studying chirality and symmetry often leads to major findings in physics

Orientation

For both abstract and solid versions of Figure 20-1, when the major axis is aligned **east-west** all the vortices and subtle energy disappear, leaving only the 8 subtle energy lines and the central vertical vortex. Figure 20-4 is the dowsed pattern in the horizontal plane. It is important

for future research to determine if the earth's spin (indicated by true north) or magnetism (indicated by magnetic north) creates and destroys the missing 36 vortices and the subtle energy cones.
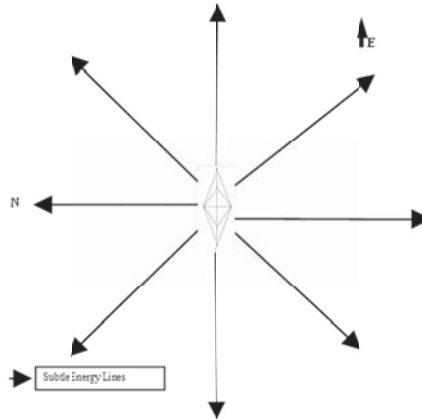
Figure 20-4 Dowsed Pattern with East-West Orientation

As just described, if one turns a sheet of paper containing Figure 20-1 through 90°, these 36 vortices and the subtle energy cones disappear. Alternatively, if turned another 90°, 36 vortices and the subtle energy cones reappear. What does this tell us about the mind, consciousness, and how positive feedback of common geometry interacts with the cosmos?

For example, a horizontal rotation of Figure 20-1 does not change the vertical force of gravity that acts on the geometry. However, the orientation of this source geometry to the earth's spin and magnetic field does change. This suggests gravity is not involved in the production of Figures 20-2, 20-3, and 20-4, but the earth's spin and magnetic field are responsible.

Orgone Energy

There is much unscientific hype on Orgone energy that has been published. The subtle energy cones as described in Figures 20-2 and 20-3 possess some of the claimed properties of Orgone energy that do have scientific evidence. Orgone energy, Ormus, and Organite are sometimes associated with organic matter or material from the Dead Sea. One relevant property of Orgone energy is that it significantly enhances auras such as those for glasses of water or the aura of humans. For example, the

radii of auras can increase by over 4 times, and this property may be used in research to confirm the presence of Orgone energy. As the source geometry is rotated away from north, the apparent strength of the Orgone energy is reduced, the angle of the cone increases, and eventually there is a cut-off angle at about 22.5°.

As the 22.5° cut-off angle of alignment is similar, within experimental error, to the 23.5° angle of the earth's tilt on its axis, it could suggest that the earth's spin (and true north) is important in producing Orgone energy. Alternatively, as the cut-off angle of 22.5° is simply ½ of 45° this could suggest that Orgone is produced by the geometry of space-time and spin is not involved. The following section is aimed at developing this theme.

Analysis and Theory

Factors Affecting the Subtle Energy Pattern

The above findings suggest that the earth's magnetic field, the earth's vorticity, the earth's gravity, as well as conscious observations are all involved in producing the complex subtle energy pattern. The analogy with X-ray crystallography was mentioned earlier. With this in mind, the following builds on this concept in an attempt to understand the physics of the above phenomena. The objective is to alter each of the above variables to see how the results are affected.

So far, horizontal source geometry has been discussed. What happens when we make the source vertical? There are 2 options: either the major axis or the minor axis is vertical. It is also instructive to experiment with artificial magnetic fields. However, this creates numerous combinations of variables: there are six different orientations of the source geometry, a choice between solid source geometry and abstract source geometry such as drawn on paper, coupled with the introduction of artificial magnetism with a different polarity to the earth's magnetic field. We are looking for clues as to the role of gravity, spin, and magnetism in producing subtle energy. It, therefore, becomes very complex in attempting to comprehend the changes to the patterns. Tables 20-2 and 20-3 summarise the findings with the intention of finding hidden patterns. In these tables, the solid source data is on the right hand side, whilst the data for the abstract source is on the left hand side.

Table 20-2 summarises different orientations of the source Figure 20-1 in the earth's natural north-south magnetic field. The 8 energy lines are always present. The central vortex is only present when the source is horizontal, and as the central axis is vertical, these two facts suggest the

involvement of gravity. All the other vortices are absent only when the major axis is orientated east-west with the source horizontal, or when the major axis is orientated north-south, with the source vertical.

The Orgone energy is emitted in several different combinations.

1. As already discussed, it is emitted from the west apex, for a horizontal abstract source (with a flow towards the west), but
2. From the east apex, for a solid physical horizontal source (which produces a flow towards the east).
3. Orgone is also emitted from the top apex for both an abstract or solid source positioned in a vertical plane (with the flow upwards).

The Effects of Artificial Magnetism

Table 20-3 has the same orientations as Table 20-2, but an artificial magnetic field was superimposed on Figure 20-1. The earth's natural magnetic field is replaced by a stronger magnetic field having an east-west polarity. It does not seem to make any difference to the results if the north polarity points to either true east or true west. The main differences with Table 20-2 are as follows:

1. The characteristics shown in Table 20–3 of the abstract source are identical to the solid source geometry, unlike Table 20-2 where there is asymmetry between abstract and physical.
2. The results summarised in Table 20– 3 are invariant to orientation for each of the 3 possible positions of the source geometry: horizontal, vertical minor axis, vertical major axis. This is unlike Table 20-2 where the east-west results are different to north-south (apart from when the major axis is vertical).
3. As in Table 20-2, the 8 subtle energy lines are always present, even though there is the unnatural east – west magnetism, suggesting that magnetism is not involved in these 8 subtle energy lines. The central vortex is only present when the source is horizontal, suggesting the involvement of gravity.
4. All the other 36 vortices are always present.
5. For both abstract and physical sources, Orgone energy is only present when the minor axis is vertical and a superimposed east-west magnetic field is present.
6. As in Table 20-2, Orgone is emitted from the top apex for both an abstract or solid source positioned in a vertical plane (with the flow upwards). This also suggests gravity being involved.

Dowsed Pattern	Abstract/Drawn Source Geometry						Matter/Physical/Solid Source Geometry					
	SHAPE ON HORIZONTAL PLANE		SHAPE with Minor Axis IN VERTICAL PLANE		SHAPE with Major Axis IN VERTICAL PLANE		SHAPE ON HORIZONTAL PLANE		SHAPE with Minor Axis IN VERTICAL PLANE		SHAPE with Major Axis IN VERTICAL PLANE	
	Major axis N-S	Major axis E-W	Major axis N-S	Major axis E-W	Minor axis N-S	Minor axis E-W	Major axis N-S	Major axis E-W	Major axis N-S	Major axis E-W	Minor axis N-S	Minor axis E-W
8 energy lines (in plane of source)	√	√	√	√	√	√	√	√	√	√	√	√
16 arithmetic vortices (in plane of source)	√	×	√	×	√	√	√	√	×	√	√	√
16 geometric vortices (in plane of source)	√	×	√	×	√	√	√	√	×	√	√	√
4 isolated vortices (in plane of source)	√	√	√	×	√	√	√	√	×	√	√	√
Central vortex x 7	√	×	×	×	×	×	√	√	×	×	×	×
Apex subtle/orgone energy cones emitted from	W	×	Top	×	Top	×	E	×	×	Top	×	×
Apex where auras increased 2-4 times	W	×	Top	×	Top	×	E	×	×	Top	×	×
Direction of subtle/orgone flow towards	W		UP	×	UP	×	E	×	×	UP	×	×

Table 20-2 The Earth's Natural North-South Magnetic Field

Dowsed Pattern	Abstract/Drawn Source Geometry						Matter/Physical/Solid Source Geometry					
	SHAPE ON HORIZONTAL PLANE		SHAPE with Minor Axis IN VERTICAL PLANE		SHAPE with Major Axis IN VERTICAL PLANE		SHAPE ON HORIZONTAL PLANE		SHAPE (with Minor Axis) IN VERTICAL PLANE		SHAPE (with Major Axis) IN VERTICAL PLANE	
	Major axis N-S	Major axis E-W	Major axis N-S	Major axis E-W	Minor axis N-S	Minor axis E-W	Major axis N-S	Major axis E-W	Major axis N-S	Major axis E-W	Minor axis N-S	Minor axis E-W
8 energy lines (in plane of source)	√	√	√	√	√	√	√	√	√	√	√	√
16 arithmetic vortices (in plane of source)	√	√	√	√	√	√	√	√	√	√	√	√
16 geometric vortices (in plane of source)	√	√	√	√	√	√	√	√	√	√	√	√
4 isolated vortices (in plane of source)	√	√	√	√	√	√	√	√	√	√	√	√
Central vortex x 7	√	√	×	×	×	×	√	√	×	×	×	×
Apex subtle/orgone energy cones emitted from	×	×	Top	Top	×	×	×	×	Top	Top	×	×
Apex where auras increased 2-4 times	×	×	Top	Top	×	×	×	×	Top	Top	×	×
Direction of subtle/orgone flow towards	×	×	UP	UP	×	×	×	×	UP	UP	×	×

Table 20-3 An Artificial East-West Magnetic Field

   Table 20-4 is a summary for both solid wire or paper drawn source geometry. It is an attempt to correlate the data in Tables 20-2 and 20-3 and to query whether gravity, magnetism, or spin is involved in each component of the patterns in Figures 20-2 and 20-3.

Dowsed Pattern	When Present	Gravity	Spin	Magnetism
8 energy lines	Always present	x	x	x
16 arithmetic vortices **16 geometric vortices** **4 isolated vortices**	**Absent** only when the earth's natural N-S magnetic field is present - plus major axis E-W and horizontal source or Major axis N-S and vertical source	√	√	√
Central vortex x 7	Only present when source is horizontal Vortex has a vertical axis	√	x	x
When is Orgone energy emitted?	Horizontal source geometry: plus major axis N-S, Vertical minor axis: plus major axis N-S plus magnetic E-W Vertical minor axis: plus major axis E-W, with or without magnetism, Vertical major axis: plus minor axis E-W	√ √ √ √	√ ? √ √	x √ √ x
Apex from which orgone energy emitted **Direction of subtle/orgone flow**	West for horizontal abstract source (flow towards the west), but East for solid horizontal source (flow towards the east) Top apex for vertical solid or abstract source (flow upwards)	x x √	√ √ x	? ? ?

Table 20-4 The Effects of Orientation, Gravity, Spin, and Magnetism

Conclusion

   The objective at the start of this chapter was to see if the feedback of the cosmos's own geometry had an effect on the production of subtle energies created by the mind. As is apparent, there were many unexpected and interesting discoveries. These can be summarised as the involvement of the following factors:

1. The geometric structure of space-time.
2. Consciousness and observation.
3. Local gravity.
4. The earth's local vorticity.
5. The earth's local magnetic field.
6. The orientation of the source geometric pattern.

Identifying frequently found angles common in tetrahedral geometry, vesica pices, and in many branches of science could not be a coincidence, but reflect the structure of space-time.

The 8 straight lines are always present and are not affected by gravity, spin, or magnetism. This would seem to imply that these 8 straight lines are created by, and reflect, a combination of consciousness and the geometric structure of local space-time, causing a mathematical transformation of Figure 20-1 geometry. The obvious question is what is this transformation?

As the central vortex is only present when the source geometry is horizontal, and the vortex's axis is always vertical, the inference is that this vortex is mainly affected by gravity, but there is no evidence from this data as to how the vortex is created. The 36 other vortices all involve gravity, as well as spin, and magnetism.

The emission of Orgone energy seems to involve gravity plus spin or magnetism. Further research is required to determine which of the latter two factors is involved.

The Way Forward and Suggested Research Projects

As hoped for, the plethora of data resulting from the numerous experiments in this chapter should provide an exciting source of research projects. Some of these questions and suggestions for further research are summarised as follows:

1. Why does source geometry, which comprises Pythagorean triangles containing tetrahedral angles, produce a complex pattern involving most types of subtle energy?
2. Why does an east-west magnetic field create a symmetry that is absent from a north-south magnetic field?
3. Why does the earth's north-south magnetic field make solid geometry respond differently from abstract geometry, but not when there is an east-west field?
4. Why are all the vortices, both geometric and arithmetic, appear to be attached to straight subtle energy lines?

5. Why should a converging subtle energy cone give the impression of being sucked into the easterly apex of the abstract source geometry, and being converted into a different form of subtle energy cone that exits the source geometry?
6. Why should the physical version of the same source geometry produce a chirality effect that only affects the 2 subtle energy cones, changing their entry and exit directions from left to right?
7. How does the mind / cosmic consciousness combination interact with spin, gravity, and magnetism?
8. By just turning a sheet of paper through 90° and loosing 36 vortices and Orgone energy, what does this tell us about consciousness, the mind and how geometry is transformed by the cosmos?
9. Is the optimum alignment of the tetrahedral source geometry to magnetic or true north?
10. Is the 22.5° cut-off angle the same as the earth's tilt? Alternatively, is it ½ of 45°?
11. What is the mathematical transformation that enables simple, but very common angles, to produce a complex mathematically described pattern such as in Figures 20-2 and 20-3?
12. It would seem that the observer needs to look at the source geometry to be able to perceive the intricate subtle energy patterns. Does consciousness create the dowsable pattern, or is it there all the time, but intent is required to perceive it? However, if intent is present, but the dowser is not looking at the source objects, the dowsable pattern is not always detected.

CHAPTER TWENTY ONE

CATEGORISING DIFFERENT TYPES OF SUBTLE ENERGIES: PART 2

Introduction

Chapter 12 started to categorise the first 5 types of subtle energies, whose basic characteristics are very briefly set out in Table 21-1.

Subtle Energy Type	Associated with
Type 1	Inanimate objects
Type 2	Life forms
Type 3	Spirals
Type 4	Thought and prayer
Type 5	Produced by abstract geometry

Table 21-1 The Basic Characteristics of the First 5 Subtle Energies

Chapter 12 also explained, that currently, I have identified 9 different types of subtle energies. However, I deliberately left this chapter until after the discussions on Pythagorean triangles and polyhedral generated subtle energies, as the Types 6, 7, 8, and 9 subtle energies discussed now are easily created from this source geometry.

Type 6

Type 3: Geometric Vortex
Type 8: Arithmetic Vortex
Type 6: Diverging Cone
Type 7: Converging Cone
Type 1: Line
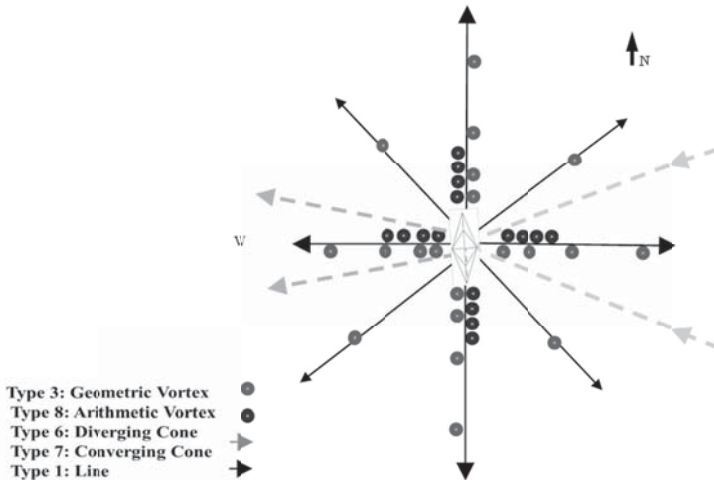
Figure 21-1 Subtle Energy Pattern with Abstract Source Geometry

For convenience, I have relabelled as Figure 21-1, the complex pattern previously illustrated as Figure 20-2. It contains numerous subtle energy lines and vortices, but the two cones are new. The cone depicted on the left with dashed lines, emanates Type 6 subtle energy from the westerly 109.471° apex of the source geometry illustrated in Figure 21-1. This has an outward flow, and a green Mager colour. Inexplicably, as previously explained, if Figure 21-1 is made of physical rods (instead of abstract geometry drawn on paper) the Type 6 cone is emitted from the easterly apex.

Therefore, Type 6 creation involves a complex combination of mirror symmetry, the different treatment by the mind between physical and abstract objects, as well as magnetism, gravity, and spin vectors

Type 7

In Figure 21-1, there is a Type 7 subtle energy cone depicted on the (easterly) right hand side, giving the impression of being "sucked" into the source geometry, and being converted into a different subtle energy, Type 6, coming out. The reason for this is not known, nor whether the optimum alignment of the source geometry is to magnetic or true north. As in the case of the Type 6 cone, the right hand cone is a mirror image for the Type

7 produced by a non-abstract, but physical source geometry. Type 7 has an inward flow, and a yellow Mager colour.

Type 8

Type 8 subtle energy fields usually occur in 2 forms of geometry lines and conical helixes. They may also be associated with other forms of subtle energy. Typical examples are set out below.

Tetrahedral Source Geometry

As is apparent from Figure 21–1, there are four north – south and east – west lines. Along these lines are groups of 4 vortices, spread out in an arithmetic series. These comprise Type 8 subtle energy. As commonly found, these Type 8 vortices share the lines with the Type 3 vortices, but these are in a geometric series.

Alignment Beams

As already discussed in Chapter 16, one way of generating Type 8 subtle energy beams is by the geometric alignment of any 3 objects. They have an indefinite length, possess an ultraviolet Mager colour, and allow instantaneous communication of information.

Psi-lines

Type 8 fields are also found in mind created psi-lines. Psi-lines comprise a 3 dimensional series of parallel tubes of a specified length. Figure 21-2 represents a cross section through one of these elliptical tubes. The lighter coloured areas in the centre are Type 8 subtle energy.

Figure 21-2 Vertical Cross-Section Through a Psi-line's Oval Tubes

Along the length of a psi-line are a series of Type 8 nodes. Figure 21-3 is a simplified representation of a psi-line where the dots are the nodes. There appears to be about a 1 cm gap in psi-lines at their nodes, with this gap filled with Type 8 subtle energy. Psi-lines are terminated by Type 8 conical helices, and the circles in Figure 21-3 represent the terminating spirals.

Figure 21-3 A Simplified Representation of a Psi-Line

Conical helixes

Conical helixes have already been discussed in relation to Type 3 spirals. However, Type 3 spirals usually exist in combination with a coaxial Type 8 conical helix, as illustrated in Figure 21-4, which is a simplified 2-dimensional footprint. As discussed in Chapter 14, the centre of Angkor Wat is an example of this.

Although the entrance to the Type 3 spiral points due north, the default entrance to the Type 8 spiral is due west, but, in general, is determined by other factors (not necessarily involving the earth) such as the direction of any associated energy line. As with Type 3 spirals, at the entrance of the Type 8 spiral is a small Type 5 portal from which bifurcation commences.

Type 8 conical helices are shorter than their Type 3 partners. In all the above examples, the Mager colour for Type 8 is ultra violet. Type 8 fields do not seem to be affected by the earth's spin, gravity, or magnetic fields. It is, therefore, postulated that Type 8 fields are created by geometry and fundamental cosmic properties.

Type 3
Entrance

Type 8
Entrance
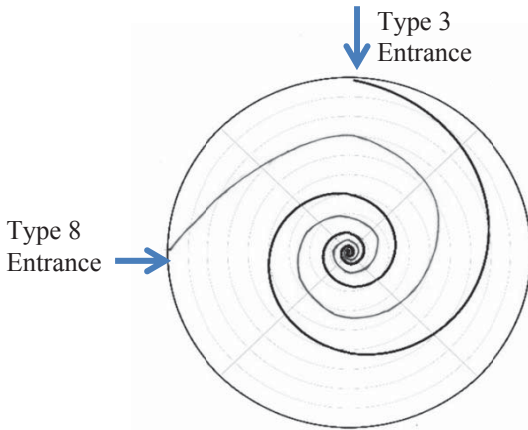
Figure 21-4 Footprint of the Double Spiral

Type 9

Sources and Structure

Type 9 subtle energy is a more recent discovery. It is found in columnar vortices and nodes. Columnar vortices can be produced by many sources, such as mind created psi-lines; the apex of cones; and sunspots. Nodes occur in many subtle energy lines as well as in columnar vortices.

Node

Perceived flow
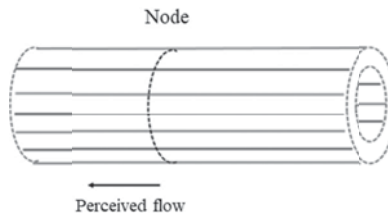
Figure 21-5 The External Appearance of a Section of a Columnar Vortex

Very complex structures are involved in columnar vortices, and the role of Type 9 subtle energy is important. The external appearance of a columnar vortex is illustrated in Figure 21-5. It is perceived as a cylindrical tube comprising 7 or 9 parallel lines of either Type 4 or Type 8 subtle energies, or a combination of both. This envelope pattern is

identically repeated in 2, 3 or 4 coaxial cylinders, together with a core of subtle energy along the central axis. These "lines" comprise even smaller diameter lines which repeat ad infinitum the overall columnar vortex pattern; an example of fractal geometry.

An example of columnar vortex complexity is illustrated in Figure 21-6. It comprises 4 rings, each ring having 9 x Type 4 lines plus 9 x Type 8 lines, thus making 72 subtle energy lines in total, plus a fractal core. This columnar vortex is made by an amethyst geode lying on its back.

| 4 x Rings |
| 9 x Type 4 lines |
| 9 x Type 8 lines ● |
| Type 9 Web ...... |
| Fractal core |
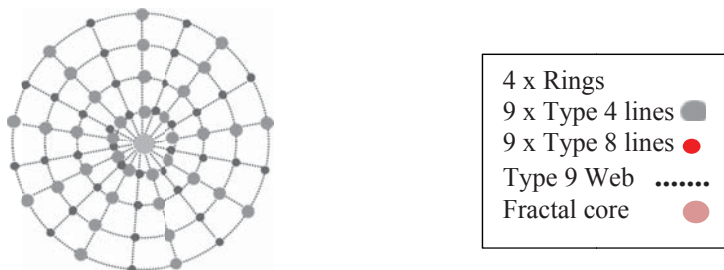
Figure 21-6 A Cross Section of Vertical Vortex from an Amethyst Geode

Type 9 Summary

Type 9 subtle energy appears to provide the necessary "scaffolding" and "cross bracing" that enables columnar vortices to retain their tubular and parallel structure over very long distances and extensive periods of time. The entire complex structure is held together by a Type 9 web. The latter is quark-like in that it does not appear in isolation but only embedded deep in nodes or vortices.

Simultaneously Producing All Types of Subtle Energies
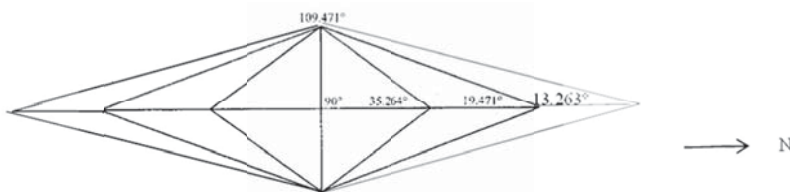
Figure 21-7 Pythagorean Triangles with Angles as in Table 20-1

Extrapolating from the above, it has been found possible to obtain simultaneously all 9 types of subtle energy fields from one source geometry. Extending Figure 20-1 by superimposing additional Pythagorean triangles from Table 20-1, a source pattern is produced, as in Figure 21-7 that produces all 9 types of dowsable subtle energy fields.

 Interestingly, if these triangles are drawn separately no dowsable pattern is obtained in the plane of the triangle. They must be superimposed as in Figure 21-7, with the long axis orientated north-south.
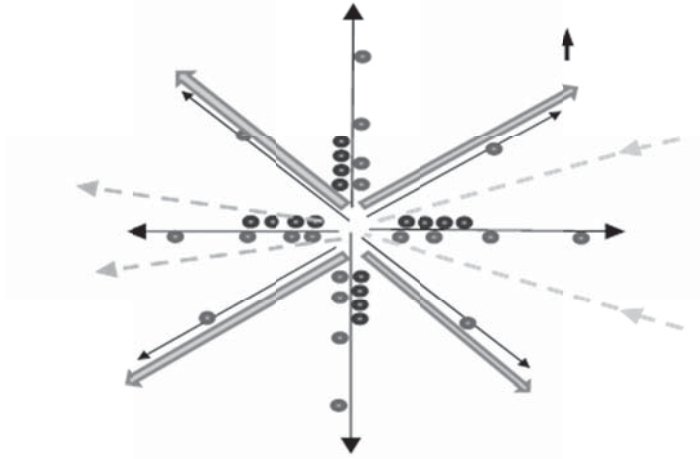
Figure 21-8 Subtle Energy Pattern Generated by Figure 21-7

Dowsing Figure 21-7 produces Figure 21-8, which is the same as Figure 21-1, but 4 additional Type 2 lines are produced. These new lines are at the centres of, and perpendicular to, the 4 outer lines in the source Figure 21-7. This Type 2 subtle energy is depicted in the 4 thick diagonal lines with arrows in Figure 21-8. Type 5 portals appear at the helix entrances of all of the Type 3 geometric and Type 8 arithmetic vortices.
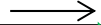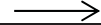
Subtle Energy Type	Description	Legend for Figure 21-8	Comments	Mager Colour
1	Lines	⟶	When alignment is N-S	White
2	Lines	⟹		Green
3	Geometric Vortex	⦿		Green
4	Lines	⟶	When alignment is E-W	Blue
5	Portal	Embedded	5-D in Vortex Entrances	No colour
6	Cone	– – →		Green
7	Cone	← – –		Yellow
8	Arithmetic Vortex	⬤	In nodes & vortices	No colour
9	Web		In nodes & vortices	Yellow

Table 21-2 Identification of Subtle Energy Types

When the source pattern is turned through 90° so the major axis points east-west, inexplicably all the lines and vortices disappear and are replaced by 4 Type 4 lines emanating from the 4 corners of the major and minor axes. Type 9 fields, together with Type 8, can be detected in the regularly spaced nodes in the Type 4 lines.

Table 21-2 gives the legend for the 9 energy types, illustrated in Figure 21-8 as generated by the source Pythagorean geometry as in Figure 21-7.

Conclusion and Summary

It is demonstrated that an abstract geometrical source of a combination of certain Pythagorean triangles allows the mind to create the 9 subtle energy types. This technique enables the reader to fine-tune his or her noetic or dowsing skills.

Whatever discipline is the reader's speciality, one objective of this book is to help him or her improve the sensitivity and scope of their noetic research, intuition, or dowsing. Utilising the paper drawn geometries discussed here is a practical and convenient simulation of their specialities, but avoiding the need for any specimens, complex apparatus, or external conditions of rain, wind, and cold! Hopefully the reader's on-site experience will then be enhanced.

As always in research, the findings provide more questions than answers. A prime question is why should an abstract geometrical design provide all the types of subtle energies that are encountered in the numerous specialities in noetics research, as well as in practical dowsing? Why do certain Pythagorean triangles and polyhedral geometry not only reflect the structure of the universe, but also strongly interact with the mind and consciousness.

Each of the above 9 types of subtle energy fields should be subjects for further experimental and theoretical research. Most likely, additional types of subtle energy will be discovered. All the dowsable fields discussed above probably result from the same basic mechanism which involves an interaction of the mind with its cosmic and earth environment. Hopefully, pursuing this line of research should lead to a greater understanding of how the mind interacts both locally and remotely with physical objects, abstract geometry, the earth, and the structure of the universe.

Way Ahead and Suggested Research Projects

1. There are probably more than 9 different types of subtle energies. It is, therefore, important to find if there are more new subtle energies. To assist in this quest, and based on the findings in this book, researching different source geometrical patterns is a powerful tool that could be used in seeking new types of subtle energy. However, if none are found, a significant milestone has been reached in demonstrating that only 9 different types of subtle energies exist.
2. Discovering additional properties, to those listed here, for each of the different subtle energies, would not only help in identifying the differences between subtle energies, but also should be beneficial in understanding and determining the theoretical aspects of subtle energies.
3. What are the Type 8 nodes, and what are their function?
4. Why should bifurcation commence from the Type 5 portal located at the entrance of a Type 8 spiral?
5. Investigate the theoretical significance of why the 4 diagonal Type 1 lines in Figure 21-8 are perpendicular to the diamond source, and why each has one geometrical vortex?
6. Similarly, why do the 4 north-south and east-west lines start at an apex of the diamond shaped source, and why do they contain 4 Type 3 vortices plus 4 Type 4 vortices? i.e. a line starting from an apex is associated with 8 vortices and 2 different types of subtle energy, but a line starting on a surface only has 1 vortex with 1 subtle energy type.
7. Why does a Type 7 subtle energy cone give the impression of being "sucked" into the source geometry, and being converted into a different subtle energy, Type 6, coming out?
8. Investigate why many subtle energy structures involve fractal geometry.
9. Research why superimposed Pythagorean triangles, with angles of sine $1/n$, produce all known types of subtle energies.

10. Similarly, why do Pythagorean triangles and polyhedral geometry not only reflect the structure of the universe, but also strongly interact with the mind and consciousness?

CHAPTER TWENTY TWO

PSI-LINES AND THEIR PROPERTIES

Introduction

Psi-lines are a well-established phenomenon. Because psi-lines are such an important part in the study of subtle energy, the mind, and the cosmos, it is inevitable that they have been mentioned several times so far in this book, under different topics. (Psi is associated with the Greek word for mind). So, what are psi-lines and how are they created?

Psi-lines are a form of linear subtle energy, often perceived to be flowing along the ground. Psi-lines have been known from ancient times, and were presumably created for direction finding and navigation. Hence, they were also known as psi-tracks, and were especially useful in the dark, in fog, or at sea. As they have great stability in both structure and time, and are easily detected, they were used as a form of "Neolithic Satellite Navigation"! Many are not only ancient and permanent, but are very straight, and, therefore, confirm they are man-made, as natural subtle energy lines (i.e. those created by the forces of nature without human intervention) meander.

Like neutrinos, they seem to pass through any obstruction in their path without being affected or deviated. They are created by the mind, sometimes to find a route from A to B, where A is the creator desiring to find a place or person located at point B. The psi-line can then subsequently be used by future people requiring the same optimum route.

Psi-lines can be placed either locally or remotely. A protocol to achieve this is by the mind's intent specifying their purpose, and visualising the locations of the two ends. They are easily created or destroyed by the mind in a few seconds, and detected noetically or by dowsing. Recent research has shown that psi-lines are also involved in animal navigation, including bird migrations.

This chapter is in three parts. The first section deals with the straight line components of psi-lines, the next section relates to their spirals and structure, whilst the last section deals with the effects of local and remote forces on the entire psi-line. The objectives of this chapter include

establishing a mathematical description of psi-lines, and the forces affecting them.

2-Dimensional Structure of Psi-lines
(as initially perceived)

General Properties

Detailed research shows that psi-lines are not just 1-dimensional, but are multi-faceted. For example, they are also associated with nodes, electric, and magnetic fields; they can also have beneficial or detrimental effects on health, and are perceived slightly differently by males and females. Local and astronomical forces, including gravity and the earth's spin, affect the properties and structure of psi-lines.

All psi-lines seem to have a similar structure, although some of their quantitative features may vary. On closer observation, psi-lines comprise 3 slightly non-symmetrically spaced component bands, as shown in Figure 22-1, where the perceived flow of the central line is in the opposite direction to the outer 2 lines. The relative "field strengths" or "intensity" of the subtle energy for each of these 3 bands is 25%: 50%: 25% ; i.e. the strengths of the outer lines exactly balance the counter-flow of the inner line, as if there was a very long loop.
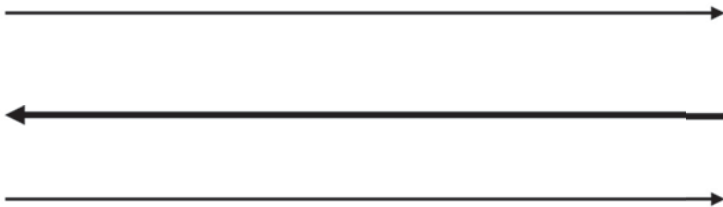
Figure 22-1 The Sub-Structure of Psi-Lines

Separation Distances between the 3 Lines

The 3 constituent lines, as illustrated in Figure 22-1, are not equidistance apart. Typically, their separation distances are in an approximate ratio of 45: 55. It is not known if this is important with regard to the theoretical aspects of psi-line production.

Fractal Geometry

In general, multiple lines of this nature are often referred to as reflections or repeating patterns, and are commonly found in the study of earth energies: So with psi-lines. Each of the above three lines comprises 3 smaller lines, each of which also comprises 3 similar components possibly ad infinitum. This is yet another example of fractal geometry in subtle energies. However, it is only possible in practice to measure down to about 5-6 levels, and then only for the widest psi-lines.

Terminating Spirals

Psi-lines are mind generated subtle energy lines that are terminated by spirals. Currently, psi-lines can only be detected noetically.

The overall shape of psi-lines, when viewed from above, not only comprises 3 straight lines, but also 2 spirals that terminate the psi-line, as shown in Figure 22-2. This footprint is the first impression perceived when encountering a psi-line.

Figure 22-2 Plan of a Psi-line Footprint

In comparison to psi-lines, at the macro level, natural subtle energy lines often comprise more than 3 component lines. For example, I have studied lines with 5, 7, and 12 constituents, on the ground, all of which travel in the same general direction, but appear to wander randomly as they go.

Experimental Protocol 1 for Measuring Linear Dimensions

Psi-lines are no different to all other subtle energies in that their measurements vary over time as a result of local and astronomic forces. The dimensions given here relate to the time of their measurement. However, ratios obtained from these measurements, at the same point in time, are consistent. The same quantified properties, as detailed here, are found along the entire length of these lines.

Prior to these experiments, checks were made that no existing subtle energy lines existed in the vicinity that could interfere with the experiments. Existing lines were either avoided or deleted by the mind's intent. Importantly, the latter also applied to deleting created psi-lines after each of the following measurements were taken.

As measurements of subtle energies and psi-lines are affected by such factors as the spinning of the earth on its axis, the earth's orbit round the sun, and planetary alignments, it is preferable to collect data over long periods of time, to statistically minimise the effects of these variations. Preferably, these findings should be plotted over at least 1 year in order to analyse the pattern of variations. For example, it readily becomes apparent if the variations are daily, monthly or annually. It also possible to determine if the cause of perturbations is due to local or cosmic factors.

It is beneficial to start with the smallest psi lines. Over a period of several months, psi-lines were created with the intent that their lengths and widths would be as short as possible. So, after creation, the width and length of the psi-line was visualised as being squeezed at both ends, to ensure minimised dimensions existed.

Length

The length of psi-lines appears to "control" other dimensions e.g. longer lines tend to be wider. The protocol adopted for measuring the length of psi-lines is to mark on the ground the vertical axes of the terminating spirals at each end of the line. In practice, these are easy to detect. Measuring the distance between the two markers is very accurate, because the axes are point like. For long psi-lines, their terminating spirals can be detected and marked on a scaled map. The length of psi-lines may range from less than a metre to many tens of thousands of kilometres.

Although of limited practical use, for research purposes, the required length of a psi-line can be specified and visualised at its creation. Subsequent on-site measurement proves that this technique is remarkably accurate to within a few percentage error. In order to research properties of the maximum length of psi-lines, several people have independently created psi-lines that travel around the circumference of the earth. At the other extreme, "laboratory" psi-lines were created with a length of less than 1 metre.

Psi-line Around the Earth

To obtain the properties of the maximum length of a psi-line on earth, the following protocol was adopted. It is possible to visualise creating a psi-line around the circumference of the earth by specifying, with markers at its ends about 3 metres apart, ensuring the psi-line is flowing away from each marker, and no psi-line is created between the markers. Simultaneously, it should be specified that the absolute minimum width is required.

To confirm that this intent has been achieved, 2 sensitive observers should stand on each end marker, but face away from all other people. An independent adjudicator silently signals when to create the psi-line line, and notes when the two observers detect the clockwise terminating spirals. Preliminary results give instantaneous reactions suggesting that the creation of psi-lines has a very fast speed of propagation. It is also necessary to confirm that

   a) there is no psi-line in the 3 metres between the 2 terminating spirals,
   b) the psi-line flows outwards from both terminating spirals.
   c) the axes of the terminal spirals are vertical and pass through the markers.

Several people have repeated this procedure many times. Although initially seeming far-fetched, it does produce consistent quantifiable results. Figure 22–3 includes data using this technique, and further examples will be presented later in this chapter, after a few more concepts have been discussed.

Overall Width of the 3 Lines

The width of the psi-line appears to be constant along its length. In theory, the width of psi-lines could be specified at inception as being from very large to very small. In practice, there is a **minimum** width, which is a function of the length of the psi-line. The overall minimum width, **W**, of psi-lines range from about 1 metre to over 10 metres, depending on the length, **l**, of the psi-line.
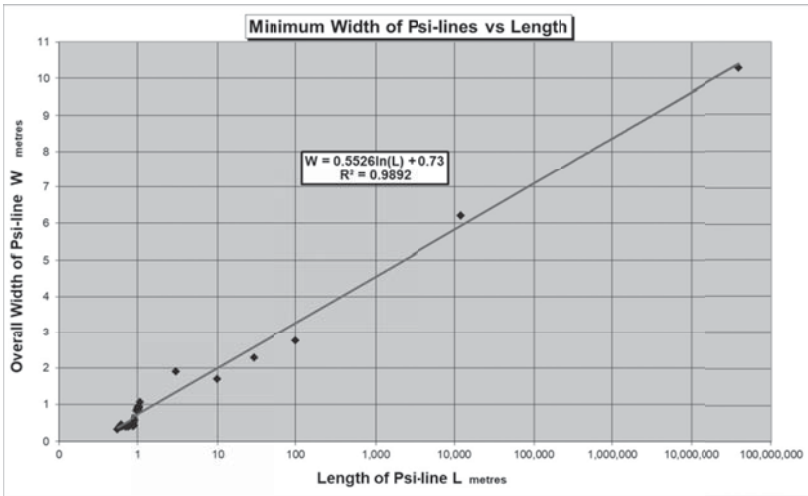
Figure 22-3 The Length to Width Relationship for any Psi Line

The very strong width to length relationship is detailed in the Figure 22-3 graph, where the data points are plotted with diamond markers. Using the Excel spreadsheet trend line gives the logarithmic equation

W = 0.55 ln(l) + 0.73
R^2 = 0.9892

This has a very high correlation coefficient. There are 42 data points, measured over 6 years, so that the perturbations caused by such variables as the earth and moon's orbits can be minimised. Chapter 25 discusses this topic in detail.

An interesting observation from Figure 22-3 is that an increase in the length of psi-lines by a factor of 10^8 only increases their width by a factor of 10. This suggests that the mind specifies and controls the psi-line's length, but a different mechanism in the structure of space-time determines the width, especially the minimum width. Therefore, the following more extensive and accurate measurements of length and width were made.

Experimental Protocol 2 for Increased Accuracy

Over a period of several months, psi-lines were mentally created using experimental protocol 1 as discussed above, with the following additional improvements to accuracy. Measurements were taken after checking that the zero of the tape measure was on the vertical axis of the spiral that started the psi-line. In addition, for maximum accuracy and minimising parallax errors, measurements involved viewing the tape measure vertically down the spirals axis, and vertically above nodes.

Psi-Lines and the Golden Ratio

Findings for Length / Width Ratio

Table 22-1 gives the dimensions of the measurements made over a period of 7 months, together with the ratio of their length over width.

Length mm	Width mm	Ratio	Date
780	435	1.793	31/12/2016
800	500	1.600	31/12/2016
696	425	1.638	01/01/2017
680	400	1.700	01/01/2017
570	400	1.425	02/01/2017
900	610	1.475	05/01/2017
898	599	1.499	05/01/2017
600	465	1.290	29/06/2017
600	410	1.463	29/06/2017
915	585	1.564	21/07/2017
910	432	2.106	21/07/2017
882	418	2.110	21/07/2017
628	422	1.488	21/07/2017
538	327	1.645	27/07/2017
880	600	1.467	28/07/2017

Table 22-1 Measurement of Length/Width Ratio

Average		
Length mm	Width mm	Ratio
752	469	1.6177
Ave Variation		0.051
% Variance		3.2%

Table 22-2 Average Readings in Table 22-1

As mentioned above, the measurements for mind created psi-lines have a variable consistency. Table 22-2 quantifies this variability and shows that the average of the readings in Table 22-1 had a variance of 3.2%. However, the important figure is the average ratio of 1.6177.

Table 22-3 sets out, for the length/width ratio, the variance from the Golden Ratio. The frequent occurrence of the Golden Ratio in subtle energy research was discussed in Chapter 5. As is apparent, the average ratio for these measurements equals the Golden Ratio within a 0.02% variance: A remarkably accurate result.

1.6180	**Golden Ratio**
0.0004	Difference from Ratio
0.02%	% Variance

Table 22-3 Comparison of Findings in Table 22-2 to Phi

Conclusions to this Section

The Golden Ratio, φ 1.61803, is often involved in subtle energy research. With this in mind, the value 0.5526 in the Figure 22-3 graph is only 0.0133 greater than $\varphi/3$ (0.53934), which is a difference of only 2.5%. This difference is well within the limits of experimental error. The relationship can therefore be postulated heuristically as

$$W = \varphi/3 * \ln(l) + 0.73 \qquad \text{(i)}$$

It cannot be a coincidence that, to a very high degree of accuracy, the ratio of the shortest to the narrowest psi-lines equals the Golden Ratio, (a fundamental universal constant of 1.6180). This result strongly suggests that, once again, the mind, consciousness, and psi-lines are intimately connected to the structure of the universe.

In order to produce a theory for psi lines, it is necessary to explain why there is a sudden cut-off in their length to about 0.75 m. A very good analogy that fits the findings is to an organ pipe, or a vibrating string with their associated harmonics and nodes. It is not possible to obtain lower notes than their natural fundamental frequency, but it is possible to obtain higher notes and frequencies. This analogy suggests that in order to explain the sudden cut-off of the plotted line at the bottom left hand corner of Figure 22–3 frequencies and wavelengths could be involved, together

with the mechanism for explaining the connection between the width and length of a psi-line, not just at its end, but along the entire line. This analogy supports the earlier suggestion that the mind specifies and controls the psi- line's length, but the structure of space-time determines the width of the psi- line, especially its minimum width.

Widths of Constituent Subtle Energy Lines

Up to now, it has been assumed that each constituent line is 1-dimensional, which is not true. Each line has width and its foot-print on the ground is 2-dimensional. As illustrated in Figure 22-4, the centre line has a width that is twice the width of the outer 2 lines. This is compatible with the earlier statement that the relative "field strengths" of the subtle energy for each of these 3 bands is 25%: 50%: 25%.
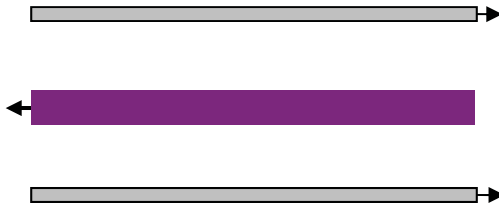
Figure 22-4 The Sub-Structure of Psi-Lines – Width

Terminating Spirals

Up to this point, it has been assumed that psi-line terminating spirals comprised only one type of subtle energy. Further research has demonstrated that psi-lines are terminated by a **double spiral**, henceforth referred to as Types A & B. This is illustrated in Figure 22-5, which also shows the relative orientations, and directions of flow. Interestingly, this is no different to other "natural" spirals, such as at Angkor Wat.
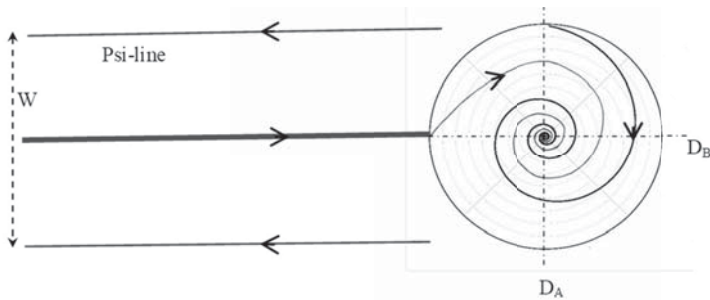
Figure 22-5 Footprint of the Double Terminating Spiral

When observing downwards from the apex of the conical helix, both spirals have 3.5 turns in a clockwise direction. This can be quickly confirmed for each type of spiral, as 8 intersections can readily be detected along diameters D_A and D_B in Figure 22-5.

Each of the twin spirals, A and B, is composed of a different type of subtle energy. Spiral A is Type 3 subtle energy, while spiral B is Type 8. As already discussed in Chapters 12 and 21, each of these subtle energies have differing physical properties; examples being, the bifurcation portals at the spiral's entry, the mathematical type of spiral, and the orientation of the entry point.

Experimental Protocol 3 for Measuring Spirals

In addition to adopting experimental protocols 1 and 2 discussed earlier in this chapter, an additional protocol is also necessary, as there are two different types of spirals, categorised as A and B, being measured. Separate measurements were, therefore, taken from the centre of each type of spiral to check that the 2 spirals were indeed coaxial. These protocols are for use, prior to and after, performing some of the experiments for the spirals discussed here, in order to check their integrity.

- Create an approximate E-W psi-line with normal intent, and confirm that on projecting it on the ground it has the following 2-dimensionsal image:-
- There are 3 sub-lines.
- Confirm the Type A spiral and flow exists as measured on its footprint.
- Similarly, confirm the Type B spiral and flow has been detected.

- Confirm that the above properties are the same at both ends for both Type A and Type B spirals.

In other words, the observer is checking that for each end of the psi line, Figure 22-5 is accurately reproduced.

Type (3) A Helices

In addition to the properties of this Type 3 helix, already discussed in Chapter 12, such as a green Mager colour, these terminating spirals have their entry point due north from the central vertical axis of their conical helix, as illustrated by the north-south line, D_A, in Figure 22-5.

To a first order approximation, the data seems to fit closely to an Archimedes spiral. The above properties are similar to numerous examples in this book of "naturally" occurring spirals. In other words, these are further examples of the mind interacting with the cosmos, in its widest sense.

Type (8) B Helices

Type B spirals terminating psi-lines are much smaller than the Type A spirals. The Mager colour for the Type B spirals is yellow, and this spiral contains the same Type 9 subtle energy as found at the psi-line's nodes, and at the centres of the 6 psi-line tubes

As illustrated by the east-west line, D_B, in Figure 22-5, the entry point for the Type B spiral is from the centre of the psi-line, along its axis, and facing the other terminating spiral.

Factors Involved in the Creation of Psi Lines

Psi-lines - Local Earth Factors

In spite of the universality of the length/width ratio for the minimized psi-line, it is well known that dowsing in general, and psi-lines in particular, are affected by the earth's gravity, magnetism, and spin. The following are examples that support this statement.

As it is very difficult to create a psi-line with a non-vertical axis, it would seem that **gravity** (and not spin or magnetism) is involved in producing conical helices.

As the entry points of the Type A spirals point north, it would seem that **magnetism** (not spin or gravity) is involved in the orientation of the spirals.

The following experiments help to isolate what features of psi-lines are created by the earth, and what aspects are created by the structure of the cosmos.

Psi-lines Visualised at the North or South Pole

When creating psi-lines whilst intent is visualising the North Pole, the psi-lines comprise the standard 3 component sub lines, but there are **no** Type A spirals, only the Type B. As spin has less of an influence at the poles than at the equator, the inference is that the Type A subtle energy in the terminating spirals is caused by the earth's spin. As the Type B subtle energy is present at the poles, it is not created or affected by spin.

As shown in Figure 22-5, the entry point for this Type B spiral is from the centre of the psi-line. The 3 sub lines stop abruptly at the edge of the spiral, without any apparent connection. This is also illustrated in Figure 22-5. In the Type B spiral, there are no subtle energy types that also exist in the straight lines. The connection between spirals and lines, therefore, requires further research.

The central axis of the conical helix can, by intent, be tilted from the vertical, but only away from the psi-line in a vertical plane. This suggests that the reduced influence of the earth's spin at the poles also reduces the effect of gravity on the axis of the Type B conical helix.

The length (l) to width (W) ratio experiments should be repeated weekly over an 18 month period to find if l or W, or both, vary, and if so, is the variation period, daily, lunar monthly, or annual.

3-Dimensional Structure of Psi-lines

Up to now, it has been assumed that psi lines were just horizontal and 2-dimensional. As we will now see, psi-lines are, in fact, complex 3-dimensional subtle energy fields. The lines are really stacked oval coaxial cylindrical tubes, with a conical helix terminating each end.

Experimental Protocol 4 for 3- Dimensional Measurements

In addition to the three sets of protocols set out earlier in this chapter, complimentary techniques can now be used to cross-check and measure the three-dimensional structure of psi-lines.

The protocol for measuring width can be by visualising and projecting the 3-dimensional psi-line onto the ground, and marking the outer extremities with a pointer.

The height of psi-lines above the ground can easily be measured by placing a vertical rod into the ground, the height of which is greater than that of the psi-line, and positioned at the centre of the psi-line. The top and bottom of the psi-line can then be marked on the rod with a pencil, and the height measured.

However, psi-lines have an elliptical cross-section, which can be confirmed by placing a vertical board or sheet of paper so that the psi-line passes through it. As stated earlier, this does not affect nor distort the psi-line. It is then possible to dowse with a pencil, and mark out on the vertical surface, the cross-section of the structure of the psi-line.

Another technique is to visualise a cross-section of the psi-line, or an elliptical cylindrical tube, which has been transposed through 90°, so it is perceived as being flat on the ground, where it can be marked out and measured accurately.

Findings for Fractal Cylinders

In more detail, the 3 component sub lines detected when walking across psi-lines are really 6 horizontal "cylinders", stacked vertically 3 + 3, as in Figure 22-6. Each cylinder has an oval cross-section comprising 2 concentric tubes. There is a void in their centres giving an impression of cylindrical torroids. There are alternate directions of flow, as well as alternate associations with magnetic and electric fields. (The latter concept requires further research to comprehend why there is the electromagnetic influence).
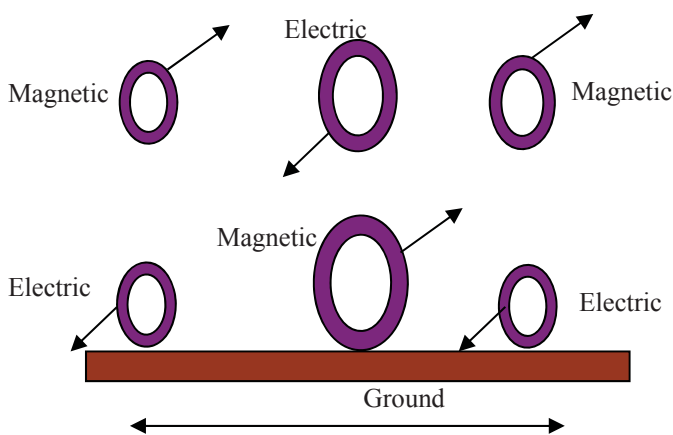
Figure 22-6 Vertical Cross-section through a Psi Line

The bottom row tubes touch the ground. For a psi-line with a length of about 30 metres, the height of the top line above the ground is about 1 metre. As an indication of orders of magnitude, the size of the central ground level oval is about 17x10 cms, whilst the size of the middle upper oval is about 10x9 cms.

Because of the fractal nature of psi lines, this structure, in Figure 22-6, is repeated smaller and smaller ad infinitum. Therefore, the measurements in the above paragraph are representative and only apply to the outer envelope.

Figure 22-7 is a more detailed cross section through one of the tubes in Figure 22-6. The 2 darker ellipses are Type 8 subtle energy, whilst the inner 2 areas are Type 9. For a short psi-line of length 1.5 metres, the overall height is about 16 cms, with an overall width of about 11 cms. The outer tube has a thickness of about 1.5 cms, whilst the inner tube has a thickness of about 3 mms.

Figure 22-7 Vertical Cross-section through an Oval Tube

Findings for Cylinder Diameter against Length

Psi-lines do not seem to extend below ground, but appear to be secured to the ground. This is important, as it explains their permanency; floating subtle energy lines drift.

Longer lines have a greater diameter as shown in Figure 22-8, where the data points are shown as diamond markers. As is apparent, the average diameter or height, **D**, of central lower psi-lines ranges from about 12 to 46 cms measured from the ground. The trend line is plotted with the best-fit Excel equation being

$$D = 1.8583Ln(l) + 13.017 \qquad\qquad (iii)$$
with $R^2 = 0.9922$.

This is a very high correlation coefficient, even though there are only 5 points of data, and these only applied to one day.
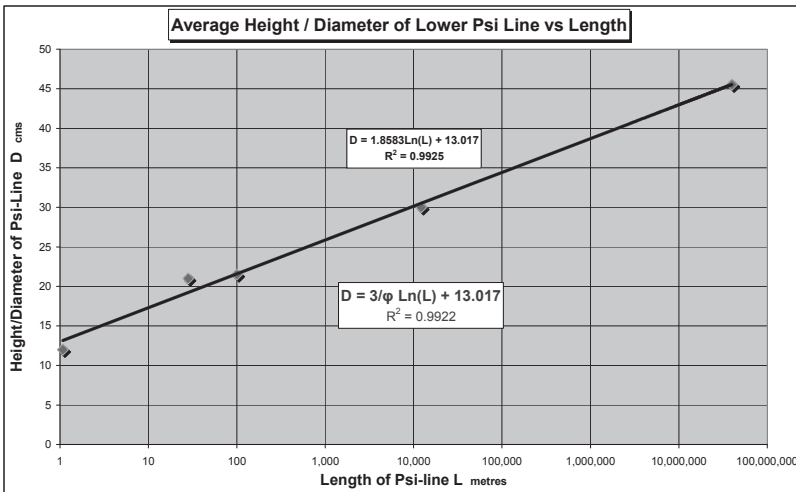
Figure 22-8 Relationship between Diameter and Length

1.8583 is only 0.0042 greater than $3/\varphi$ (1.8541), which is an error of 0.23%. The relationship can therefore be postulated heuristically as

$$D = 3/\varphi * Ln(l) + 13 \qquad\qquad (iv)$$

This equation has a similar structure as equation (i), but with different constants.

Findings for Apex Half-Angles for Conical Helixes

As already discovered, what was initially perceived on the ground as a 2 dimensional spiral is, in fact, a three-dimensional conical helix. In addition, these helices comprise 2 or more coaxial cones. Moreover, the half-angle of the cones usually form part of a trigonometric series of sine $1/n$.

For example, resulting from the series of measurements for Type 3 helixes, the half angle of the helix's apex is 19.471° to an accuracy of about 2.6%. Once again, this angle of 19.471° is the same as sine 1/3.

Resulting from measurement of the vertical dimensions of a Type 8 conical helix, the tangent of the half-angle of the apex is the reciprocal of the golden ratio (φ) to an accuracy of 0.1%. This discovery demonstrates that once again the mind is interacting with the structure of space-time in creating psi-lines and their terminating spirals. A coincidence to this level of accuracy is very unlikely.

Nodes

Psi-lines greater than a certain length possess nodes. As nodes have a different subtle energy (Type 9) than the rest of the psi-line, they are readily detectable by an experienced researcher, even though there appears to be about a 1cm gap in the Type 8 subtle energy lines at the nodes. Akin to, say, harmonics in a vibrating violin string, nodes appear along the length of the psi-line.

Experimental Protocol 5 for Nodes

In addition to the 4 protocols discussed earlier in this chapter, psi-lines were created with the following five objectives for the experiments to measure the:

1. minimum length of a psi-line without any nodes.
2. minimum length of a psi-line with just one node.
3. ratio of the above two psi-line lengths.
4. ratio of the minimum psi-line length to the minimum node length.
5. generalisation of the above findings for psi-lines of any length.

Findings for Nodes along any Psi-Line

Along all psi-lines are regularly spaced nodes that can be detected noetically, and accurately measured. The resulting data is shown graphically in Figure 22-9, where the average nodal separation, N_s is plotted against the length of the psi-line, **l**. The data points are indicated as diamond markers, and using the plotted Excel spreadsheet trend line, the equation is given as

$$N_s = 0.40Ln(l) + 0.72$$
$$\text{with } R^2 = 0.99$$

This is a very high correlation coefficient bearing in mind there are only 7 data points.

0.4013 is only 0.0032 less than $\varphi/4$ (0.4045), which is a difference of only 0.79%. This difference is well within the limits of experimental error. The relationship can, therefore, be postulated heuristically as a logarithmic equation of the form

$$\mathbf{N_s = \varphi/4 * Ln(l) + 0.72} \qquad \mathbf{(v)}$$

This is a similar format to previous Psi-line equations.
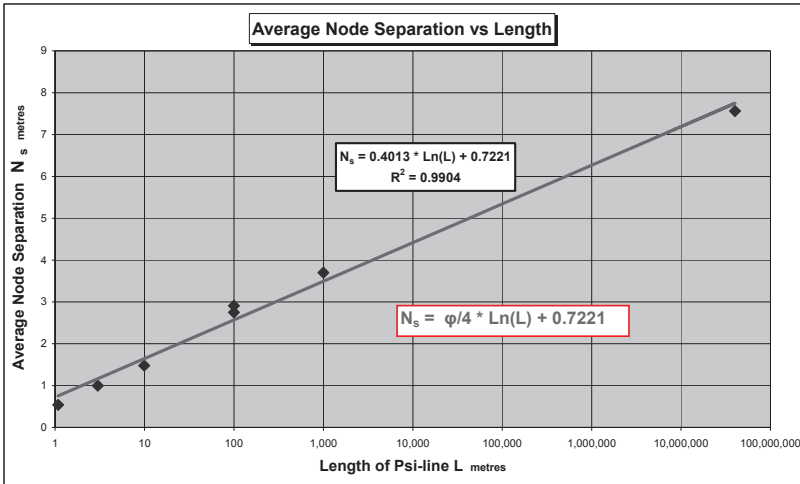
Figure 22-9 Average Node Separation Against Length

Once again, this equation needs confirmation and backed up by detailed theory. As is apparent from the smallest to the largest psi-lines, the separation distances between nodal points range from about 1-8 metres. An interesting observation from Figure 22-9 is that, once again, an increase in the length of psi-lines by a factor of 10^8 only increases their separation distance by less than a factor of 10. This finding is similar to Figures 22-3 and 22-8. The mind has already specified and determined the psi-line's length, suggesting that cosmic forces could be determining the node separation distance.

Figure 22-10 is a graph of the number of nodes in psi-lines of differing length. For the shortest psi-lines, the actual number of nodes were counted, whilst the number of nodes for the longest lines was estimated from a sample of the local nodal separations, which were accurately measured. The Excel trend line, which fits the data, gives a power relationship of the form:

$$N = 0.7547 * l^{0.9113} \qquad \qquad \text{(vi)}$$

where N = the number of nodes along a psi-line of length L. This equation has a very high correlation coefficient of $R^2 = 0.9967$. Interestingly, the multiplier, 0.7547, approximates to the minimum length of a psi-line without nodes. This could assist in determining the theoretical explanation for equation (i), but to balance the units so they are the same on both sides of the equation, this value of 0.7547 must be in units of inverse length.
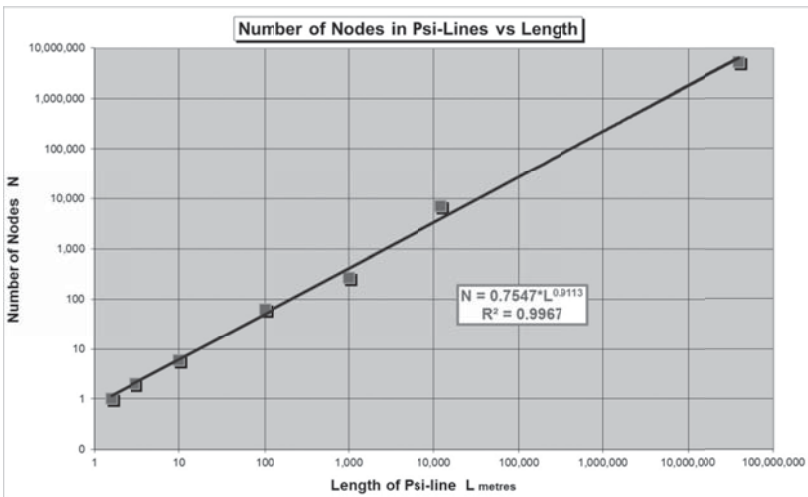
Figure 22-10 The Number of Nodes for Different Psi-line Lengths

Psi-Lines, Nodes, and their Minimum Length

Findings

For these experiments, intent was that the psi-line length was just long enough, so that only one node was created. Table 22-4 gives the position of the node with regard to the psi-line's length. Similarly, Table 22-5 shows that the readings in Table 22-4 had a variance of 4.33%.

Type 3 Start	Type 9 Node	Type 3 End	Middle	Ratio	Date
mm	mm	mm	mm	Node/End	
0	875	1,672	836	0.52	02/01/2017
0	882	1,700	850	0.52	02/01/2017
0	868	1,670	835	0.52	21/07/2017
0	950	1,930	965	0.49	27/07/2017
0	854	1,530	765	0.56	27/07/2017
0	838	1,425	713	0.59	27/07/2017
0	712	1,446	723	0.49	28/07/2017
0	753	1,546	773	0.49	08/08/2017
0	756	1,567	784	0.48	08/08/2017
0	745	1,567	784	0.48	08/08/2017
0	744	1,567	784	0.47	08/08/2017
0	786	1,572	786	0.50	18/08/2017
0	771	1,579	790	0.49	18/08/2017
0	780	1,580	790	0.49	18/08/2017
0	778	1,574	787	0.49	18/08/2017
0	756	1,496	748	0.51	15/09/2017
0	747	1,549	775	0.48	15/09/2017
0	746	1,550	775	0.48	15/09/2017
0	754	1,506	753	0.50	15/09/2017

Table 22-4 The Measurements of the Shortest Created Psi-Lines with their Nodes

Average				
Node	End	Middle	Ratio	
mm	mm	mm	Node/End	
794.47	1580.32	790.16	0.50	Dimensions
52.65	68.50	34.25	0.02	Ave Deviation
6.63%	4.33%	4.33%	4.08%	% Variance

Table 22- 5 The Averages and Statistics for the Data in Table 22-4

The most important figures from Table 22–5 are that:

1. The average distance of a node is 0.794 metres from the start of the shortest psi-line.
2. The average length of the shortest psi-line with nodes is 1.58 metres.

3. Within experimental error, the node is at the middle of a shortest psi-line.

Interestingly, one of the people creating the above data has the ability to see subtle energy and psi-lines. When attempting to create a psi-line smaller than 752 mm (Table 22-2) with no nodes, or smaller than 1,580 mm with nodes, the psi-lines quickly increased to these values.

In summary, nodes exist along all psi-lines greater than the minimum length of 1.58 metres. Depending on the length of the psi-line, node separation distances range from about 0.5 metres, for the smallest psi-line, to about 8 metres, for the very longest. Nodes, therefore, are a fundamental structure of psi lines.

Psi-lines must be greater than a minimum length of 1.58 metres before they possess nodes. At this minimum length, the distance of the node, measured from the start of the psi-line, equals 0.79 metres i.e. at its centre. Psi-lines without nodes also have a minimum length, but this is slightly less at 0.74 m. This is approximately half the minimum length of psi-lines with a node, and hence cannot be a coincidence. The findings reinforce the organ pipe analogy to explain (a) minimum width (b) nodes.

Vector Properties

Transverse Measurements

As described in Chapter 24, when a yardstick probe is moved along a psi-line, the value of its length, **L,** changes significantly. However, in each position, **L** has the same value when measured sideways to the left, right, or vertically. The data for the above measurements, relating to psi-lines of only one node, are presented graphically in Figure 22-11. It is apparent that the yardstick measurements become zero at the nodes and are at a maximum at the anti-nodes, where the length, in this case, is about 195 millimetres.
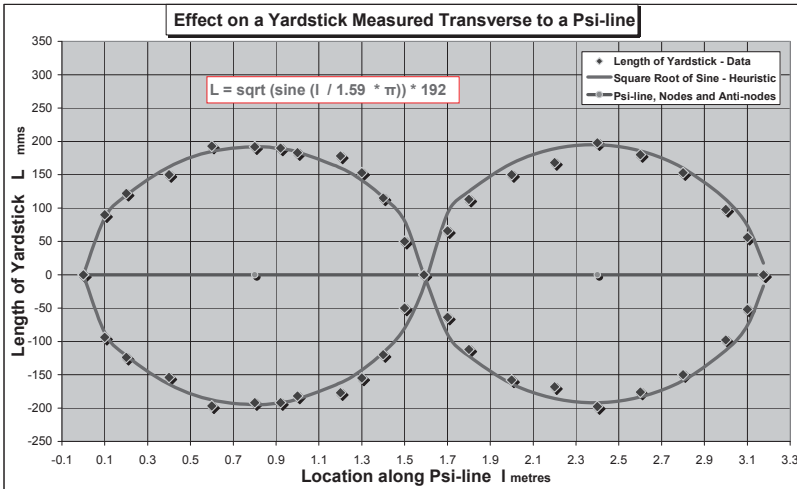
Figure 22-11 The Values of L along a Psi-line with 1 Node

When away from the psi-line, the comparable initial control yardstick measurement **L** was 286 mm, which is about 1.5 times greater than the maximum length of the yardstick, when it is on the psi-line. i.e. the psi-line always reduces the perceived length of a standard yardstick, or the radius of any object's aura.

As is apparent from Figure 22-11, as the yardstick moves along the psi- line, its perceived length forms a type of sine wave. However, this is not a standard sine wave, or even an equation for a standing wave, as its formula, found heuristically, involves a square root and has the following format:

$$L = A * \sqrt{\sin (l * \pi/d)} \qquad \text{(vii)}$$

Where:

   A = the average yardstick length at the anti-nodes, in millimetres
   d = the distance between adjacent nodes, in metres
   L = the length of the standard yardstick, in millimetres
   l = the position of the yardstick along the Psi-line.

As also apparent from Figure 22-11, the data, which is represented by the diamond shaped markers, is a very good fit to the figure-of-eight curve, which is a plot of equation (vii). This figure of 8 graph is

reminiscent of the amplitude of the standing waves in an organ pipe, or violin string.

Lateral measurements

L varies in length when measurements are taken along the direction of the psi-line's flow. This effect is depicted in Figure 22-12, where the top line in the graph shows the length of the yardstick when measured with the flow of the psi-line, i.e. the measurement of length is taken "downstream" of the yardstick. Typically, the yardstick significantly increases from its control length of 286 mm to about 600 mm. This is an increase of +110%.
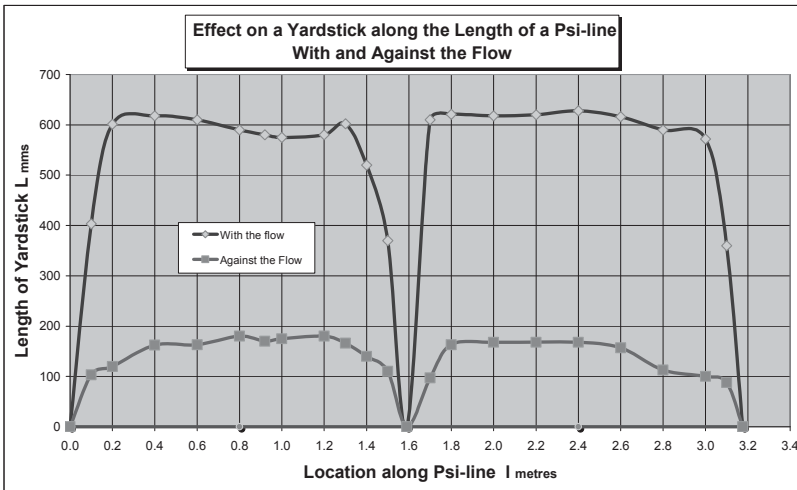
Figure 22-12 The Effect of Flow on Psi-line Measurements

In comparison, the lower line in the graph in Figure 22-12 plots the perceived length of the yardstick, when measurements are made "upstream" of the yardstick, against the flow of the psi-line. Typically, the yardstick decreases from its control length of 286 mm, to about 170 mm. This is a decrease of about -40%.

It is apparent that the values of both these 2 curves are nearly constant along the length of the psi-line, except near the three nodes, where all measurements decrease to zero. The influence of the nodes, on this latter effect, extends about 0.2-0.3m either side of the nodes. i.e. similar to the radii of the terminating spirals. There does not appear to be any similar effect at the anti-nodes. It would, therefore, seem that the anti-nodes, and

the mechanism that creates them, only affect transverse measurements. These findings could be relevant when determining the theory of psi lines and their nodes.

Conclusions to Nodal Vectors

Three distinct effects have been discovered as a result of measurements made along psi-lines.

1. Nodes reduce all measurements to zero. There is also a link between nodes and terminal spirals. This confirms that intuitively found nodes actually exist.
2. Lateral measurements confirm that the flow detected by intuition is real.
3. Transverse measurements confirm a sine-like pattern along the psi-line, suggesting that measurements are affected by the amplitude of a standing wave. This effect does not apply to longitudinal measurements.

Kinked or Zigzag Psi-Lines

As discussed earlier, the mind can create almost any visualised 3-dimensional shape. It is, therefore, possible to produce kinked or zigzag psi-lines, either by mentally joining independent adjacent lines, or by initially creating a complex random zigzag psi-line. Interestingly, in the former case, when mentally joining two separate psi lines, the touching terminating spirals disappear at the join where the line kinks and a node is formed. This suggests that there is a connection between spirals and nodes. In both cases, there are nodes at the joints, as well as the usual nodes along each straight line.
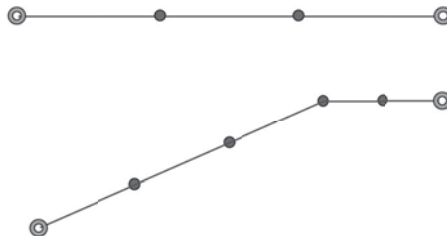
Figure 22-13 The Effect of Zigzag Psi-lines on the Number of Nodes

Figure 22-13 illustrates the difference between a straight 3-metre psi-line and a 3-metre psi-line with a kink. The nodes are illustrated with dots and the circles representing the terminating spirals. The straight psi-line has 2 nodes, but a kinked psi-line also of 3 metres has 4 nodes. What seems to be happening is that each straight part of a psi-line conforms to the formula and graph in Figure 22-10.

Using the wave analogy, these nodes could be associated with standing waves, wavelength, harmonics, and octaves. Interestingly, a 5 year old girl, who is sensitive to subtle energies without the use of devices, when walking through nodal points said she "had a sensation of rocking backwards and forwards". As she had no prior knowledge of psi-lines or nodes, this is a very good description of waves and a nodal point by a 5 year old. Further research is required to determine the nature of these waves.

Effects of Astronomical Alignments
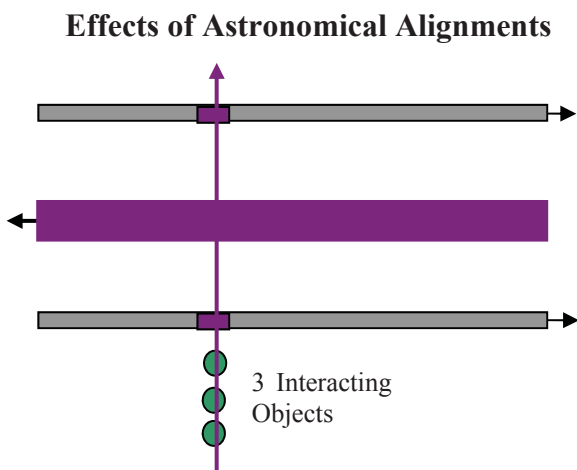
Figure 22-14 Psi-Line Interacting with a 3-Body Alignment Beam

As previously discussed, the subtle energy beam generated by 3-body alignment significantly affects psi-lines, and seems to take over their properties. As illustrated in Figure 22-14, at the local points of intersection between the psi-line and the alignment beam, the 3 oval tubes in the psi-lines become Type 8 and ultra-violet on the Mager disc.

The mauve energy lines have the same characteristics as found when dowsing geometrical shapes, in particular, during astronomical alignments with the earth, such as at new or full moon, eclipses, and conjunctions of

planets. In this case, the entire length of the psi-line changes to Type 8\9 combination with an ultra violet Mager colour, as illustrated in Figure 22-15. If appropriate, the centre line changes from detrimental to "good". When the alignment beam is removed, the psi-lines revert to their normal long-term characteristics.
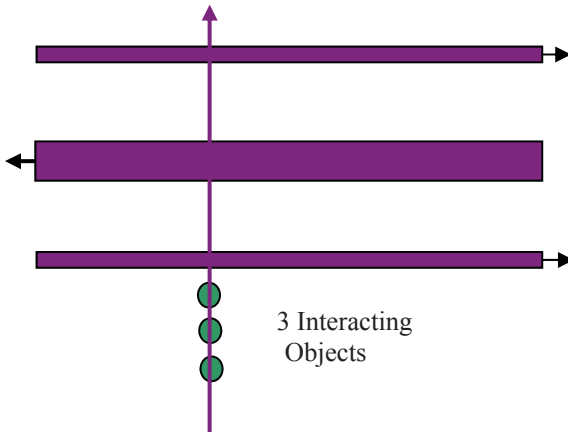
Figure 22-15 Psi-Lines at Astronomical Alignments

Health

It is often found in relation to health that both outer lines are perceived as "beneficial" energy, but the middle line is "detrimental" energy. Other times the reverse is true. Interestingly, the previously mentioned 5-year-old girl, who is sensitive to earth energies and other subtle energies without the use of devises, and unaware of what was the cause, complained of "a headache" when walking through 2 outer lines, but the middle line "made her happy". This is an unbiased, independent confirmation that subtle energies can affect health, either beneficially or detrimentally.

Summary

Psi-lines are easily created, detected, and destroyed by the mind. They are a form of linear subtle energy, and if not modified by intent, can remain stable in space-time over hundreds of years. Not only can they be detected by their creator, but, more importantly, they can be readily

detected by others. Hence, their use for tracking, and in ancient times they were presumably created as part of daily life, to assist in navigation.

Psi-lines are not 1-dimensional lines, but complex 3-dimensional cylindrical fields with nodes, and terminated by conical vortices.

Local and astronomical forces, such as gravity and the earth's spin, affect psi-lines. Psi-lines are also affected by 3-body alignments, including astronomical alignments.

Experimental data has produced formulae such as **W = φ/3 * ln(l) + 0.73,** which is the relationship between the length and width of psi-lines, where **φ** is the golden ratio 1.61803. As this and other formulae in this chapter probably involve a universal constant, this is further evidence that the mind can interact with the structure of the universe and the laws of physics.

The terminating spirals comprise Type A and Type B subtle energy, which have different properties. They are shown to be 3-dimensional helical coaxial bicones with one apex angle involving the Golden Ratio (φ), and the other involving sine 1/3. Type A spirals could, to a first approximation, be Archimedean. Type B spirals do not seem to fit a simple spiral equation.

Each type of spiral has a different orientated entry point. Type A entrance faces north. Type B spirals have an entry point facing its other terminating spiral, and along the psi-line's central axis, which passes through the centres of the two terminating spirals. Gravity, spin, or magnetism does not seem to affect Type B spirals.

Nodes form an important part of the structure of psi lines. Their number and separation distance is strongly dependent on the length of the psi line. For psi lines with kinks, the number of nodes and their separation distance is a function of each straight length of a psi-line. The "field strength" of a psi-line reduces near their nodes.

Suggested Future Research

As always in scientific research, the findings produce more questions than answers. The findings suggest the following possible avenues for future research.

1. A theoretical explanation for the minimum size psi-line of 0.74 m.
2. An explanation why psi-lines greater than 1.58 m require nodes.
3. What are the functions and structure of nodes?
4. What are the theoretical aspects of psi-lines that lead to equations (i), (ii), (iii), (iv), (v) and (vi)?

5. What is the exact nature of psi-lines?
6. More data is required to confirm the equations for the length of psi-line vs their width, diameters, size of terminating spirals, and nodal separation.
7. Experiments extending over one year duration are necessary to find the factors affecting the L/W ratio. How does the mind determine the length of a psi-line, and prove if cosmic factors determine its width? This should also lead to clues about perturbations affecting the results on Phi.
8. Why are psi-lines so easy to create, destroy, and detect by the mind?
9. Sensitive brain activity scanning equipment is required to resolve what part(s) of the brain is involved.
10. What does the magnetic and electric association represent, and how do they relate to their creation by the brain?
11. What is the perceived "flow"?
12. What is the velocity of "flow" and propagation of psi-lines?
13. What are the nodes?
14. How are the terminating spirals connected to the 3 sub lines of a psi-line?
15. Why do all cylinders give the impression of magnetic and electric fields with alternate directions of flow?
16. Are the nodal separation distances associated with quantised wavelengths or frequencies?
17. Is there a carrier wave, and what types of information can the modulation wave transmit?
18. What do the white and ultra-violet Mager colours represent?
19. Why are some lines beneficial whilst others are detrimental to health?
20. Why do astronomical alignments affect existing subtle energy lines and spirals?
21. What keeps the integrity, structure and properties of psi-lines the same over several kilometres? Is it because they are self-organised, or are psi-lines linked to the structure of space-time?
22. How do psi lines become secured to the ground?
23. How does a psi-line know how long it is and hence the number of nodes (or its width etc.) that should be created?
24. Similarly, how does a psi-line know when there is a kink in it, and change its properties along the entire straight lengths?
25. Do psi-lines involve energy in the accepted scientific understanding, such as increasing temperature or performing work?
26. Does the creation and destruction of psi-lines by the mind adhere to the conservation of energy law?

27. More data is required to determine the mathematics of the Type A, and Type B spirals.
28. In measuring the conical apex angles, more data is required, preferably using the radius from the spiral's centre to its entry point - this being the largest radius of the cone's asymmetrical base.
29. Some of the experiments in this book should be repeated in the southern hemisphere to confirm that the Type A spiral's entry point is still to the north of its centre, and so proving conclusively that magnetic north is involved.
30. What joins the psi-lines to their terminating spirals?
31. Are these experiments on psi-lines, which have been created by intent, at the earth's poles or in intergalactic space:-
    a) actually performed by the mind at the poles or in space, and the findings obtained by remote viewing? or are they
    b) actually performed physically and locally ?

If alternative (b) above, how does the mind shut out the local earth's spin when visualising experiments at the earth's poles? How does the mind eliminate the effects of gravity, electromagnetism, and spin when visualising the experiment in space?

If alternative (a) is correct, how does the effect of local magnets become transported to the poles? Are these phenomena another example of the comprehensive entanglement as discussed above?

Chapter Twenty Three

The Structure of Columnar Vortices of Subtle Energies

Introduction

This chapter is devoted to subtle energies that do not diverge significantly, but have a parallel, cylindrical, or columnar structure.

Usually subtle energies are very long lines that meander; or short conical helixes with heights measured in a few metres; or conical fields which may diverge over long distances. None of these are relevant to this chapter. The following example may clarify what are **not** subjects of this chapter. Figure 23-1 illustrates a slightly diverging conical field perceived to be emanating from the centre of a cross, an example of which can usually be experienced in any church. This subtle energy was discussed in Chapter 12, and was categorised as Type 5, having a diverging beam, comprising 9 coaxial cones, with its field strength decreasing as it leaves its source. These beams only have a simple internal structure, diminishing field strength, diverge, and are not columnar.
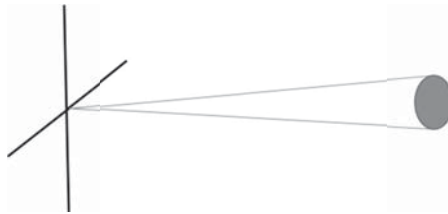
Figure 23-1 Isometric Illustration of a Conical Beam Generated by a Cross

I hope that starting with this initially negative sounding explanation, should help context and comprehension of the rest of this chapter.

Objectives

Having first examined in previous chapters different categories of subtle energies, vortices, and psi-lines in general, it is now possible to determine what constitutes a columnar vortex, and if there are different structures of columnar vortices emanating from diverse physical, mental, and abstract sources. Of particular interest is to discover how columnar vortices retain their stability, structure, and shape over long periods of time, and vast distances. Where possible, quantitative measurements were made of both vertical and horizontal columnar vortices. These findings could help to determine what parts of these vortices are affected by gravity, the earth's spin, and other earth bound factors.

Method

When measuring the structure of these vortices, their cross-section was detected noetically, and by placing a sheet of paper perpendicular to the vortex its structure was drawn on the paper using a very sharp pencil. After many years of practice, I can measure subtle energy to about 1mm accuracy. To improve clarity, this section details the internal structure of columnar vortices by using idealised symmetrical artwork.

An independent person, using a different protocol to the one I used, and who had the rare ability to actually see the detailed structure of subtle energies, confirmed the number of rings, lines per ring, and the structure of the vortex cores described in this chapter.

Summary of the Structures Discovered

The external appearance of a columnar vortex is illustrated in Figure 23-2. It is perceived as a cylindrical tube comprising 7 or 9 parallel lines of either Type 4 or Type 8 subtle energies, or a combination of both. This envelope pattern is identically repeated in 2, 3 or 4 coaxial cylinders as explained below, together with a core of subtle energy along the central axis. These "lines" comprise even smaller diameter lines, which repeat the overall columnar vortex pattern, ad infinitum. Yet another example of fractal geometry.

Node

Perceived flow
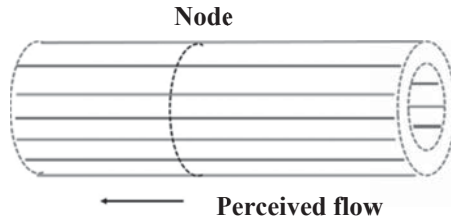
Figure 23-2 The External Appearance of a Section of a Columnar Vortex

Columnar vortices seem to possess a flow of subtle energies, with the direction of flow away from the source generating the vortex. The lengths of columnar vortices can vary from about 1 m up to tens of kilometres, or even across the solar system. They always terminate in a conical vortex of Type 3 or Types 3 and 8 combinations of subtle energy.

Some columnar vortices possess nodes, which typically are about 3 mm long. If present, they are usually equally spaced apart and, as explained in the previous chapter on psi-lines, the number of nodes is an exponential function of the length of the psi-line. The nodes comprise a mixture of Type 8 and Type 9 subtle energy, but their function requires future research.

An important discovery is that all columnar vortices contain a web like structure that provides the necessary "cross bracing", as illustrated in all the following Figures. This web is Type 9 subtle energy. It is quark-like, in that it does not appear in isolation, but only embedded deep in nodes or vortices.

Examples of Columnar Vortices

The vortices studied were generated by a range of physical objects, such as amethyst geodes, Silbury Hill, Jupiter's red spot, pyramids, cones, a stack of CDs interspersed with paper, sun spots, as well as mind generated psi-lines. The following sequence is in order of complexity of structure and subtle energy types.

Amethyst Geode, Cone, Pyramid

An amethyst geode, similar to Figure 23-3, was one source used in these experiments. It had the normal 7 ellipsoidal shells which extended 7.6m: a powerful aura for a relatively small object. In comparison, the columnar vortex that the geode produced extended over 100m.

Figure 23-3 Amethyst Geode

Figure 23-4 is a cross-section of a horizontal columnar vortex produced by the geode. It comprises 2 rings with 9 Type 4 lines, with the usual Type 9 web, and a solid Type 4 core. This is one of the simplest columnar vortex structures.

2 Rings, 9 Lines, Type 4

When drilling down deeper into the underlying structure of columnar vortices, Figure 23-4 is a cross-section through the simplest example. It comprises, along its length, 2 concentric cylindrical envelopes each comprising 9 x Type 4 subtle energy lines, totalling 18 lines. As well as an amethyst geode producing a horizontal beam, other examples of this type of columnar vortex include the vertical beam created by the apex of a pyramid with a square base, or both vertical and horizontal columnar vortices emanating from a cone with an apex half-angle of 35°.

2 x Rings
9 x Type 4 lines   ●
0 x Type 8 lines   ●
Type 9 Web   .....
Type 4 Core Cylinder
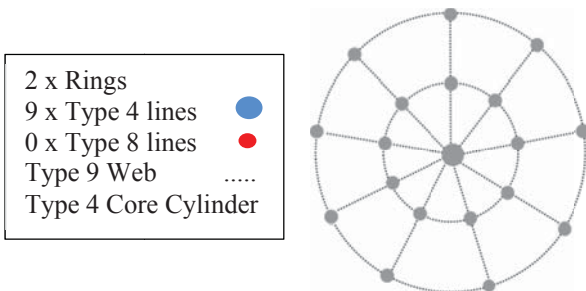
Figure 23-4 A Cross Section of a Vertical Vortex Created by a Pyramid

Pyramid – Horizontal Beam

3 Rings, 9 Lines, Type 4

Interestingly, turning the above pyramid source of the subtle energy through 90°, so the vortex is horizontal, produces an extra ring as illustrated in Figure 23-4. Presumably, this is an effect of gravity, and the discovery of *how and why* gravity achieves this would make an exciting project.

3 x Rings
9 x Type 4 lines
0 x Type 8 lines
Type 9 Web   …...
Type 4 Core Cylinder
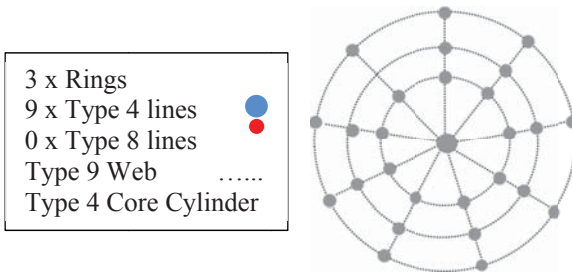
Figure 23-5 A Cross Section of a Horizontal Vortex Created by a Pyramid

Silbury Hill

3 Rings, 7 Lines, Type 4

In the previous 2 examples, the vortex core is a "solid" cylinder of Type 4 subtle energy. Figure 23-6 has similar geometry as Figure 23-5, but has 7-fold geometry (not 9-fold) and the solid core is replaced by a thin linear Type 8 axis surrounded by a thin walled cylinder of Type 4 subtle energy. An example of this type of columnar vortex is the one produced by Silbury Hill in the UK.

3 x Rings
7 x Type 4 lines
0 x Type 8 lines
Type 9 Web   …...
Type 4 Core Cylinder
Type 8 Axis
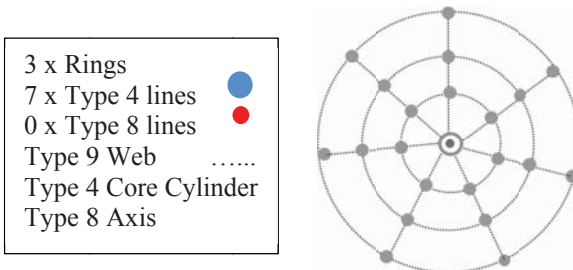
Figure 23-6 Cross Section of the Vertical Vortex Produced by Silbury Hill

Figure 23-7 is a photograph of Silbury Hill. Dowsing this photograph produces the usual 3 dimensional 7 shell aura surrounding the Hill, comprising Type 1 subtle energy. This is not shown, but interestingly, both the thickness of the aura, and the height of the inner shell above the top of Silbury Hill equals the height of Silbury Hill above the ground. Although not immediately relevant to this chapter, it could be a factor in analysing the findings.
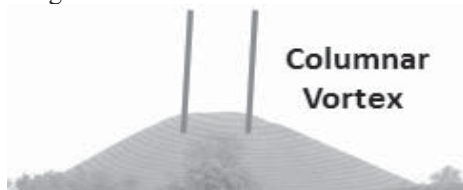
Figure 23-7 Silbury Hill

The major inclusion of Figure 23-7 is the vortex beam above the top of the hill. Its height is about 1.5 times greater than the height of the hill. This is a common ratio found in subtle energy research. The vortex also comprises 7 equally spaced Type 8 nodes.

Sun Spots, and Horizontal Psi-Lines

3 Rings, 9 Lines, Type 8, Fractal Core

Figure 23-8 is a photograph of a sunspot that produced a columnar vortex. The structure of this vortex is shown in Figure 23-9, which produces the next level of complexity. There are 3 concentric cylinders, each comprising 0 x Type 4, and 9 x Type 8 subtle energy lines, making 27 lines in total, together with a core. All of these are held together with a Type 9 web. Its length crosses the solar system, but the beam does not possess any nodes.

As a check on the consistency and logic of the protocol, the experiment was repeated with the source photograph arranged vertically and then horizontally to produce both horizontal and vertical beams. The results were identical and helped to reassure that the methodology was sound and consistent.
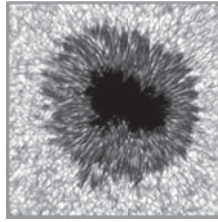
Figure 23-8 Photograph of the Sun Spot

Other than sunspots, examples of this pattern include both horizontal and vertical mind created psi-lines. The findings in this section explain many of the properties discussed in Chapter 22 on psi-lines.

Another discovery is that Figure 23-9 is an example of fractal geometry; its core repeats the entire pattern of the columnar vortex, but with a diameter about 10% smaller.
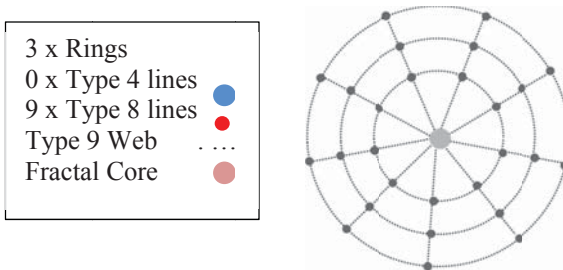
Figure 23-9 A Cross Section of One of The Peripheral Type 8 Lines of a Psi-line and the Sun Spot

A Stack of CD's

3 Rings, 9 Lines, Type 8, Type 4 Core with Type 8 Axis

Figure 23-10 is the same as Figure 23-9 except that the fractal core is replaced by a Type 4 cylindrical core with its Type 8 axis. An example of this pattern is produced by horizontal vortices from 5 CD's stacked vertically. This configuration was chosen to study the effect of a simple electrical condenser.
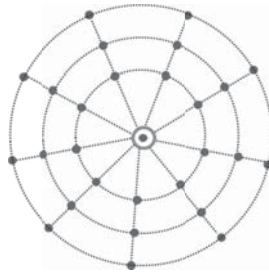
Figure 23-10 A Cross Section of a Horizontal Vortex From a Stack of 5 CD's

Vertical Cone

2 Rings, 7 Lines, Types 8+4, Type 4 Core with Type 8 Axis

The above examples contained either a Type 4 or Type 8 subtle energy. The next level of complexity is a mixture of both types of subtle energy. The example in Figure 23-11 is a vertical vortex produced by a cone having a 10° half-angle apex. It comprises 2 rings, each of which contains 7 x Type 4 lines, plus 7 x Type 8 lines. As usually found, the Type 4 lines have a much larger diameter than the Type 8 lines.

Figure 23-11 A Cross Section through a Vertical Vortex Produced by a Cone

Jupiter Red Spot

The columnar vortex emanating from Jupiter's red spot extends across the solar system. It was noetically plotted on 2 separate dates to ensure consistent results, and that the effects of variations in perception during a lunar month were as predicted. The subtle energy associated with the red spot, in the Figure 23-12 photograph, possesses **3** rings with each ring

comprising 7 x Type 4 lines interspersed with 7 x Type 8 lines. A Type 4 cylinder with a Type 8 axis completes the centre of the cross-section. Figure 23-13 is the same structure obtained independently on 2 different occasions, and demonstrates the reliability of the protocol adopted.
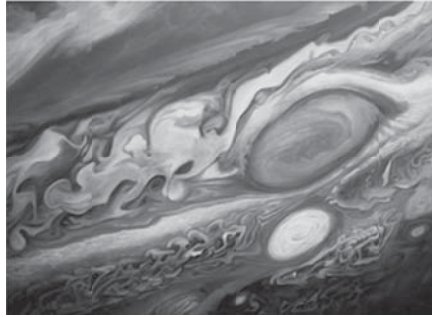
Figure 23-12 Photograph of Jupiter's Red Spot

2 Rings, 7 Lines, Type 4+8, Type 4 Core with Type 8 Axis

Figure 22-13 is a columnar vortex produced by a photograph of Jupiter's red spot. As is apparent, it is the same geometry as Figure 22-8, but with an additional ring comprising 7 x Type 4 lines interspersed with 7 x Type 8 lines.

3 x Rings
7 x Type 4 lines
7 x Type 8 lines
Type 9 Web   …....
Type 4 Core Cylinder
Type 8 Axis
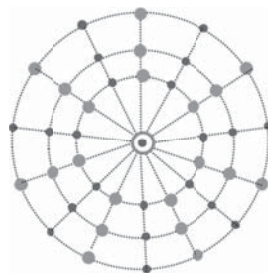
Figure 23-13 Columnar Vortex Produced by a Photo of Jupiter's Red Spot

Horizontal Cone

3 Rings, 9 Lines, Types 4+8, Type 4 Solid Core

Figure 22-14 depicts the next level of complexity and is similar to Figure 22-13 but with each of the 3 rings containing 9 Type 4 lines interspersed with 9 Type 8 lines, and a solid Type 4 cylindrical core with no Type 8 central axis. An example of this pattern is produced by a horizontal vortex created by a cone with a 10° half-angle apex.


```
3 x Rings
9 x Type 4 lines
9 x Type 8 lines
Type 9 Web        ....
Type 4 Solid Core
0 x Type 8 Axis
```
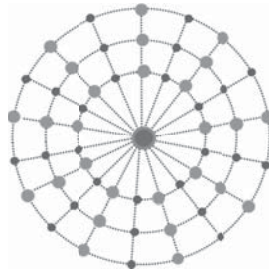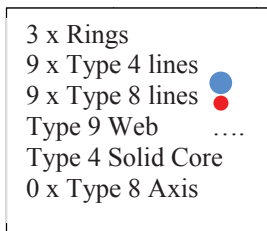
Figure 23-14 A Cross Section of a Vertical Vortex from a Stack of CD's

Vertical Psi-lines

So far, physical objects create the examples of columnar vortices in this chapter. Are there any differences to mind created columnar vortices?
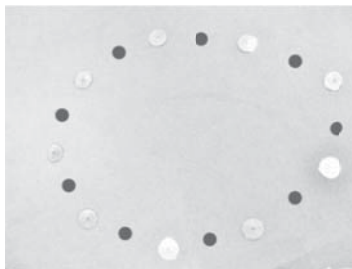
Figure 23-15 Photograph of the Structure of the Outer Cylinder
of a Vertical Psi-line

3 Rings, 9 Lines, Types 4+8, Type 4 Core with Type 8 Axis

To improve accuracy of measurements and the comprehension of structure, a wide vertical psi-line was created, which passed through a horizontal plate of glass (which did not affect its properties). Figure 23-15 is a photograph of circular markers placed on the sheet of glass on the outer cylinder of the vertical psi-line.

Over the detected 9 x Type 8 lines were placed silver coloured markers. In between these, with the darker markers, are 9 x Type 4 lines. The elliptical perimeter of the psi-line, therefore, comprises 18 subtle energy lines.

There are 3 shells (or cylinders/tubes) that complete this layer of fractal geometry. Each of these shells has the same structure as the perimeter illustrated in Figure 23-15. For each shell, there are 18 lines of subtle energy flowing along the entire height of the psi-line, arranged as alternative 9 x Type 8 lines interspersed with 9 x Type 4 lines. Therefore, the entire psi-line comprises:

> 3 x 9 = 27 x Type 4 sub-lines
> 3 x 9 = 27 x Type 8 sub-lines

This results in a total of 55 lines, including the central vertical axis line. The entire structure, therefore, appears as fractal geometry; but only at this level of observation!

The next level of measuring fractal structure could now be commenced. To demonstrate this, a cylindrical Type 4 vortex, in the bottom right-hand corner of Figure 23-15, was arbitrarily chosen for deeper analysis. Drilling down into the cross-section structure of this vertical linear cylinder continues the fractal geometry pattern of the above Type 4 vortex. 3 shells were detected, each containing 55 (smaller diameter) Types 4 and 8 lines. This is illustrated in Figure 23-16. The central vertical axis is a mixture of Types 4 and 8 subtle energies. This result demonstrates the fractal nature of the outer few levels of this psi-line.

Figure 23-16 is the same as Figure 23-14 but the core is different and comprises a Type 4 circle with a Type 8 central axis. A challenging question is why does this change in the core differentiate between a psi-line and a stack of CD's?

3 x Rings
9 x Type 4 lines
9 x Type 8 lines
Type 9 Web   ....
Type 4 Core Cylinder
1 x Type 8 Axis
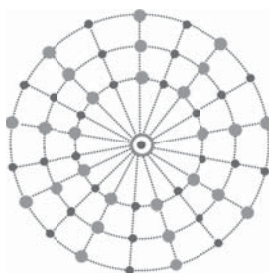
Figure 23-16 A Cross Section of One of the Peripheral Type 4 Lines of a Psi-line

Amethyst Geode, Lying on its Back

4 Rings, 9 Lines, Types 4+8, Type 4 Core with Type 8 Axis

The most complex example of columnar vortices is illustrated in Figure 23-17, which comprises 4 rings, each ring having 9 Type 4 lines plus 9 Type 8 lines, thus making 72 subtle energy lines in total. It has a solid cylindrical fractal core. This vortex is made by an amethyst geode, lying on its back, producing a vertical columnar vortex.

Compare this to Figure 23-3, which is a horizontal columnar vortex produced by the same geode placed vertically. As is apparent, by turning the vortex through 90° and making the vortex vertical, added 2 extra rings. Each of these rings added 9 x Type 8 lines. In addition, the solid Type 4 core was replaced with a fractal core. This vertical vortex is one of the most complex structures discovered. The elliptical shape of the geode's "cave" is reflected in the shape of the vortex produced.

4 x Rings
9 x Type 4 lines
9 x Type 8 lines.
Type 9 Web   ......
Fractal Core
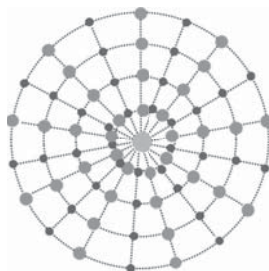
Figure 23-17 A Cross Section of a Vertical Vortex Produced by an Amethyst Geode

Chapter Summary and Conclusions

Usually subtle energy lines diverge, or meander over the earth's surface. As a contrast to the subject in this chapter, it is instructive to return to common dowsable fields, such as illustrated in Figure 23-1. An abstract geometrical cross, drawn on paper, or a physical cross, produces a beam of Type 1 subtle energy. It makes no difference if the cross is in a horizontal or vertical plane. This beam is a divergent cone with an elliptical cross-section, has a Mager colour of white, has no Types 4 or 8 subtle energy, has no nodes, no core, and no complex fractal structure. Although this is an extreme example, all these properties are opposite to those for columnar vortices.

Table 23-1 summarises the findings in this chapter. The main conclusions are that all columnar vortices have a structure that is built up of fractal geometry, each element possessing a flow of subtle energy, and contain a web like structure of Type 9 subtle energy (perceived with a Mager colour of yellow). What could be an important discovery is that the Type 9 subtle energy provides the necessary "cross bracing and scaffolding" enabling a columnar vortex to remain very stable, straight, and parallel over long distances and time. This discovery could also be the best absolute definition of columnar vortices, as the other discovered factors in this paper do not apply to all columnar vortices.

Apart from all columnar vortices having circular or elliptical cross-sections, they involve Types 4 and 8 subtle energies. It is immediately apparent that most (13 out of 17) examples of columnar vortices contain Type 4 subtle energy lines. Type 4 subtle energy is also found in multi-body interactions.

Type 8 lines appear in 11 out of 17 examples of the columnar vortices studied. Type 8 energy lines have a significantly smaller diameter than the Type 4 lines; approximately half of a Type 4 line. This is compatible with several findings for concentric conical vortices. All the Type 4 lines indicated blue on a Mager disc, whilst the Type 8 lines indicated ultra-violet.

Columnar vortices are arranged in either 2, 3 or 4 rings. The most common structure (11 out of 17) comprises 3 rings, whilst 2 rings occur in 5 out of 17 instances, and 4 rings only appear once. There are no columnar vortices with only 1 ring. Are a minimum of 2 rings required for stability?

Each ring (or, in 3-dimensions, a cylindrical envelope) comprises lines along the entire length of the vortex with either 9-fold or 7-fold geometry. 9-fold geometry occurs in 14 out of the 17 vortices studied, but 7-fold only occurs in 3 instances.

Source of Vortex	Type 4 lines Blue	Type 8 lines U-V	Type 9 web	Rings 4	Rings 3	Rings 2	9-fold	7-fold	Type 4 Solid Core	Type 4 Cylinder + Type 8 Axis	Fractal Core	Nodes & Separation Distance	Width mm	Beam Length
Pyramids														
25°, 32° Vertical	✓	-	✓	-	-	✓	✓	-	✓	-	-	√ : 2.9m	3	13.5m
25°, 32° Horizontal	✓	-	✓	-	✓	-	✓	-	✓	-	-			17.9m
Cones														
10° Vertical	✓	✓	✓	-	-	✓	-	✓	-	✓	-	√ : 2m	3	10.8m
10° Horizontal	✓	✓	✓	-	✓	-	✓	-	✓	-	-	-		> 12m
35° Vertical	✓	-	✓	-	-	✓	✓	-	✓	-	-	√ : 2.5m	3	13.5m
35° Horizontal	✓	-	✓	-	-	✓	✓	-	✓	-	-	-		> 12m
Silbury Hill	✓	-	✓	-	✓	-	-	✓	-	✓	-	√ : x 7		?
Jupiter Red Spot	✓	✓	✓	-	✓	-	-	✓	-	✓	-	√ : ?		Very Long
Stacked CD's														
Vertical	✓	✓	✓	-	✓	-	✓	-	-	✓	-	-		> 12m
Horizontal	-	✓	✓	-	✓	-	✓	-	-	✓	-	-		> 12m
Amethyst Geode														
Vertical	✓	✓	✓	✓	-	-	✓	-	-	-	✓	-		> 12m
Horizontal	✓	-	✓	-	-	✓	✓	-	✓	-	-	-		> 100m
Sun Spots	-	✓	✓	-	✓	-	✓	-	-	-	✓	-		Very Long
Psi-lines														
Vertical T4	✓	✓	✓	-	✓	-	✓	-	-	✓	-	√ : formula	3	Variable ~1m - 10's km
Vertical T8	-	✓	✓	-	✓	-	✓	-	-	-	✓	√ : formula	3	Variable ~1m - 10's km
Horizontal T4	✓	✓	✓	-	✓	-	✓	-	-	✓	-	√ : formula	3	Variable ~1m - 10's km
Horizontal T8	-	✓	✓	-	✓	-	✓	-	-	-	✓	√ : formula	3	Variable ~1m - 10's km
17	13	11	17	1	11	5	14	3	6	7	4	9		
Cross														
Vertical	-	-	-	-	-	-	-	-	-	-	-	-		Long
Horizontal	-	-	-	-	-	-	-	-	-	-	-	-		Long

Table 23-1   Summary of Properties of Different Vortices

7-fold geometry is very common in dowsing physical objects. For example, auras have 7 "shells", individual spirals comprise 2 sets of 3.5 turns making 7 turns in total, and spirals appear in vertical groups of 7. However, 9-fold geometry is very common for subtle energies produced from abstract sources. In addition, the number of the subtle energies discovered totals 9. This suggests that the odd integers 7 and 9 are fundamental to the mind interacting in space-time.

There are 3 types of vortex core in columnar vortices. A Type 4 solid core occurs in 6 out of 17 vortexes studied. Typically, these cores have twice the diameter of the constituent Type 4 lines. The other common core (7/17) is a central axis comprising a cylinder of Type 4 subtle energy, with a Type 8 central axis. The third core type (4/17) is a repeat of the overall vortex structure, but an order of magnitude smaller. This is another example of fractal geometry.

Apart from the central core, fractal geometry also exists in the sub structure of entire columnar vortices. The structure of the vortex repeats itself, but on a much smaller scale. Some columnar vortices have very short finite lengths, while others seem to have indeterminate long lengths, such as those emanating from the sun or Jupiter. Columnar vortices terminate in a Type 3 spiral.

About half of the columnar vortices seem to contain nodes. These are perceived as a gap of about 3 mm in length, containing Types 8 and 9 subtle energies. Further investigation is required to determine their structure and function.

Another interesting discovery is that most columnar vortices have different structures if they are vertical or horizontal, even if they are produced by the same source. The geometrical orientation can change the presence of subtle energies involved (Type 4 and/or Type 8); the ring geometry (2, 3, or 4 fold); the vortex core pattern structure (solid, Type 4 cylinder with a Type 8 axis, or fractal); as well as the presence of nodes.

The implication is that the changed structures are produced with the involvement of gravity, and / or the earth's rotation and orbit.

There is no obvious correlation between the presence of nodes and the structure of a columnar vortex. Neither is it obvious why sometimes the horizontal beam is more complex than the vertical beam from the same source, whilst for other sources the reverse is true.

As is apparent from Table 23-1, the main variables for columnar vortices are 2, 3, or 4 rings; 3 types of vortex core; and 2 types of subtle energy. This should give 18 variations of columnar vortex structures. As there are only 10 different structures discovered in this study, are the 8

missing structures invalid, or do they exist in other columnar vortices yet to be identified?

We can now answer the question posed at the beginning of this chapter. This was "are there different structures of columnar vortices emanating from diverse physical, mental, and abstract sources?" In general, there does not seem to be a significant difference between mind and physically created columnar vortices.

Suggested Future Research

As always in research, there are more questions raised than answers. The following are some unresolved issues that could form the basis for future research work into columnar vortices.

1. The fact that there is no difference between columnar vortices created by the mind, and those generated by physical objects, should be fundamental evidence to assist producing a theory for subtle energies and consciousness.
2. Other independent researchers need to reproduce the experiments and confirm the findings in this chapter.
3. This chapter's findings only cover static structures. Vortices imply spin, but there is no evidence here of this, as the sunspots and Jupiter's red spot are sources that involve dynamics. Therefore, there is need to enhance skills, protocols, and techniques to enable dynamic rotating structures to be plotted.
4. Investigate if columnar vortices contain torsion waves, and if so, what torsion wave equation does the data fit?
5. Do the perceived patterns for columnar vortices equate to a cross-section through a torsion field, or more probably a combination of many such fields combining the "empty" structure of the cosmos with local gravity, spin, and consciousness?
6. Using the Crick and Watson analogy of using crystallography patterns to obtain the structure of DNA, can the patterns produced in this chapter be used to produce a 3 dimensional dynamical pattern of columnar vortices?
7. Investigate whether the 8 missing columnar vortex structures are invalid or are yet to be discovered.
8. Investigate whether columnar vortices exist with only 1 ring? If not, why not?
9. Why does the cone apex angle significantly affect the structure of produced columnar vortices?

10. Do pyramids produce identical columnar vortices to cones with the same apex angle?
11. For the apex angle of cones and pyramids, what is the crossover angle for the production of different structures, and is it sudden?
12. A challenging question is why does a change in the core differentiate between a psi-line and a stack of CD's?
13. What creates nodes only in some columnar vortices?
14. The nodes comprise a mixture of Type 8 and Type 9 subtle energy, but their function requires future research.
15. Investigate why only the horizontal vortex, produced by a cone with a large apex angle, has nodes, but only a vertical vortex produced by a cone with a small apex angle has nodes.
16. Why and how does gravity only affect some vortices?
17. Changing a source of subtle energy from horizontal to vertical alters the structure of the vortex. Presumably, this is an effect of gravity, and discovering how gravity achieves this would make an interesting project.
18. Why are the odd integers 7 and 9 fundamental to all subtle energies, but to columnar vortices in particular?
19. A fundamental theory is required to explain the findings in this chapter, and, in particular, the details in Table23-1.

CHAPTER TWENTY FOUR

YARDSTICK PROBE, L

Introduction

Up to now, quantification of subtle energies has involved either measuring the external dimensions of subtle energy fields, or simply counting aura boundaries. However, these tools and techniques are very simplistic, and are only useful as a beginning. They require further development to enable other properties to be scientifically measured.

As we have seen, the inverse square law does not apply to subtle energies, and unexpectedly, this assists achieving accuracy of measurements. Fortuitously for subtle energies, the inverse square law is replaced by precise boundaries delineating the limits of subtle energy fields. This facilitates accurate measurements. Additionally, the application of geometry is a powerful tool in studying subtle energies. All these characteristics should be retained in a universal yardstick, and, ideally, further enhanced. The idealised objective is to produce a universal yardstick that enables us to make more powerful scientific research measurements and subsequent discoveries, such as recording variations over different periods of time, the effects of vector properties, and measuring astronomical phenomena.

Choice of Source

After much experimentation investigating

a) different subtle energy sources;
b) the benefits of physical or pure geometry; and
c) studying various geometrical patterns,

I discovered that subtle energies change their dimensions over time. Theoretically, any source could, therefore, be employed as a yardstick to measure subtle energies. Further experimentation demonstrated that it is beneficial to take geometry down to its extreme limits. A technique I

consequently developed, involving a singularity, is explained in this chapter for noetically studying subtle fields and abstract geometry.

I have found that the most practical and accurate protocol for scientific measurement is to use the simplest geometry – a dot. Although scientists often avoid a singularity, I am happy to research a dot for the following reasons.

Technique and Protocol

As depicted in Figure 24-1, the act of viewing a dot produces a tubular subtle energy beam, with an outward flow towards the observer. This beam ends in a clockwise spiral, which, in reality, is a 3-dimensional conical vortex with a vertical central axis. The beam has a perceived Mager colour of white. This is also beneficial for research work. The length of this beam I have defined as L. This length can be very accurately measured from the source dot to the precise central vertical axis of the spiral. In practice, L has values between 0-10 m. (The width of the beam could be up to 10 cm diameter, but as this width is not used, it is irrelevant to this protocol).

L

(0 – 10 m)

Figure 24-1 Dowsing a Dot

This subtle energy beam should not be confused with auras, which radiate out in all directions in an ellipsoid form from physical bodies or geometric shapes. The size of these ellipsoidal auras depends on many factors, which include the shape, size and composition of the source object. These complications are avoided by using a dot as the source.

My preferred technique is to draw a dot, in pencil, on a small sheet of white paper fixed (with blue-tack) vertically to a wall at floor level. The act of observing the dot is key to producing the generated tubular subtle energy beam that originates from the dot, and whose direction is aimed at the observer: this is analogous to observing quantum mechanics experiments. The orientation of the paper, or the observer, to their environment is irrelevant. It is the non-dimensional dot, not the 2 dimensional wall or paper that is important.

A tape measure is placed on the floor between the observer and the dot. The noetic observer moves towards the dot using any method of dowsing

until the central axis of the spiral is detected. To obtain the most accurate reading of L, attempting to use traditional pendulums or angle rods is probably not good enough.

Device-less dowsing (obtained after many years of practice) is required by using a pointer no thicker than 1 mm. The researcher initially walks towards the dot, to detect the approximate position of the spiral. He/she can then kneel at floor level moving the pointer along the tape-measure until the spiral's vertical axis is accurately detected. This procedure also has the benefit of removing any parallax errors in measurements between the observer's eyes and the tape-measure.

There are 3 reasons why this is a powerful technique for scientific research

1. L can be measured very accurately to within 2 mm.
2. L is very sensitive to an extensive range of both local and astronomical forces such as gravity, spin, magnetism, tides, light / electromagnetic fields, and (importantly) geometric alignments.
3. L is also affected by other subtle fields under investigation, such as their flow, colour, ability to pass through solids, or any vector properties. The latter is important because some subtle fields affect measurements, depending on the direction of measurement. This especially applies for practical fieldwork, such as the study of "earth energy" lines or psi-lines.

Validation of the Technique

No doubt, some readers will be sceptical about these claims, and require a degree of proof. In March 2008, I introduced 13 cynical UK Dowsing Research Group members to this technique. Without any practice, they individually dowsed the dot and easily measured L. This procedure was repeated on 6 occasions over 2 days. A summary of the results of the personal variations and group statistics appears in Table 24-1, and indicates a 13% variance.

	8/3/08 12:30:00 metres	8/3/08 16:00:00 metres	8/3/08 21:00:00 metres	9/3/08 09:30:00 metres	9/3/08 13:00:00 metres	9/3/08 15:00:00 metres	
DRG Member a	3.95	4.37	3.10	3.95	3.65	3.55	
DRG Member b	3.75		2.11	3.80	3.16	4.30	
DRG Member c	3.10	2.60	2.32	3.80	3.05	3.90	
DRG Member d	3.98		2.35	3.87	3.73		
DRG Member e	2.50	3.60	3.40	3.83	3.45	3.40	
DRG Member f	4.60	4.95	4.75	4.55	4.50	4.72	
DRG Member g	3.80	3.67	3.30	2.90		3.00	
DRG Member h	3.87	3.40	3.50	3.86	3.88		
DRG Member i	3.86	3.93	3.49	3.87	3.61	3.76	
DRG Member j	3.50	3.80	4.30		3.85	4.40	
DRG Member k	3.80	3.90			3.80	3.60	
DRG Member l	2.60	2.60	2.50	2.90	2.65	2.60	
DRG Member m		4.10	3.70	4.40		4.30	
Average	3.61	3.72	3.24	3.79	3.58	3.78	**3.62**
Stnd Deviation	0.46	0.50	0.63	0.32	0.36	0.50	**0.46**
%	12.64%	13.34%	19.55%	8.56%	10.12%	13.22%	**12.76%**
Maximum Value	4.60	4.95	4.75	4.55	4.50	4.72	4.68
Minimum Value	2.50	2.60	2.11	2.90	2.65	2.60	2.56
Max:Min Ratio	1.84	1.90	2.25	1.57	1.70	1.82	1.85

Table 24-1. DRG Initial Variation in the Measurement of L

Repeating the group experiment 3 months' later produced an interesting improvement in the group's performance. As shown in Table 24-2, the standard deviation had improved from a group variance of 13% to 7%. Practice makes perfect! It took me about 3 years to attain an accuracy to 2 mm. These results give confidence in the protocol when using this technique.

	14/6/08 11:30:00 metres	14/6/08 16:00:00 metres	14/6/08 22:30:00 metres	15/6/08 09:30:00 metres	15/6/08 12:30:00 metres	
Average	5.46	5.38	5.49	5.48	5.21	**5.40**
Stnd Deviation	0.43	0.42	0.36	0.40	0.37	**0.39**
%	7.86%	7.79%	6.58%	7.22%	7.01%	**7.29%**
Maximum Value	5.98	6.16	6.32	6.01	6.00	6.09
Minimum Value	3.90	4.05	4.70	4.20	4.30	4.23
Max:Min Ratio	1.53	1.52	1.34	1.43	1.40	1.45

Table 24-2. DRG Subsequent Variation in the Measurement of L

The Reasons for Measurement Variations

As previously discussed in Chapters 10 and 11, when detecting subtle energies, a physical entity is not perceived, but a model is created in the dowser's mind. A good analogy is with sight. Sight is a model in the brain – not just an image on the retina, but a perception in brain cells built up via the eyes' retina, colour separation, rods and cones, stereo vision, and information transmissions along optic nerves to the brain. These separate components are combined in the brain, and very young children learn to associate the 3-dimensional sight model in the brain with physical reality, using touch.

Dowsers "perceive" the same phenomenon, but in slightly different places in the brain. The brain attempts to superimpose its *dowsing* model onto its *sight* model. The two are not always synchronised, especially if the dowser can neither see nor touch the subtle energy being investigated. Therefore, there are differences as to how each person's brain superimposes its dowsing model onto its sight model. Each individual's measurements are not absolute, but consistent. This explains the variances in Tables 24-1 and 24-2.

It will be noticed from Tables 24-1 and 24-2 that L changes during the course of the day. Figure 24-2 is a plot of the data in Table 24-1, and is typical when measuring L in any environment. A sinusoidal curve is obtained with maxima at sunset and minima at sunrise, even if measurements are made in a darkened room on a cloudy day.

This sinusoidal curve motivated me into researching the causes of these changes, and the next few chapters briefly discuss my findings of five significant measurements of L that challenge science.
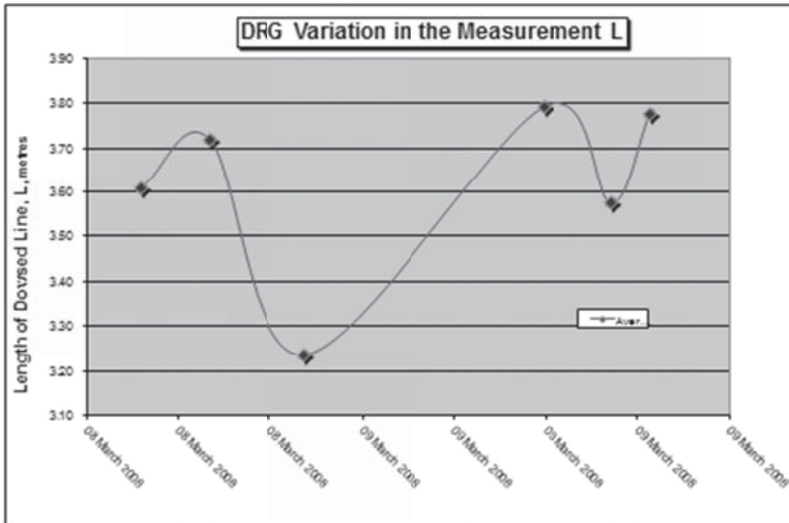
Figure 24-2 A Graphical Representation of Daily Variations in L

Summary and Conclusions

Based on the feedback I have received from my introductory lectures on this subject, this chapter has intentionally been kept short to avoid any unnecessary complexity, misunderstandings, and confusion that have arisen when researchers initially use this simple technique.

The following chapters utilise this technique to research many applications, which has produced some ground-breaking and fundamental findings. These have included accurate measurements of length and their variation over time, vector forces, changing Mager colour, and a simple non-invasive probe to analyse other subtle energy fields. Eventually, the use of **L** has led to the demonstration of instant communication across the solar system.

CHAPTER TWENTY FIVE

THE BENEFITS OF SUBTLE ENERGY MEASUREMENTS NEVER BEING THE SAME

Introduction

One of the reasons, erroneously, that dowsing has traditionally been shunned by the scientific community, is that measurements vary over time. Being a contrarian, I have taken this to be a positive rather than a negative factor. Following on from the previous chapter, I have spent many years discovering why measurements vary over time. There are fundamental reasons to account for this variability, and each of these reasons has led to a new discovery about subtle energies, consciousness, and cosmology.

Personal Factors

Towards the end of the previous chapter, a brief introduction was given into the use of the yardstick probe to quantify personal variations in scientific measurements of subtle energies. Table 20–1 summarised experiments showing that humans were one factor for variation. As we have just seen, initially experiments measuring L produced a 13% variance. However, 3 months later the group's performance improved to 7% variance.

As also explained in Chapters 10 and 11, the brain's model of sight does not necessarily use the same cells in the brain to build its noetic model. At the end of Chapter 20, it was explained that the main reason for the personal variations in measuring L was the inherent difficulty of superimposing the noetic perception of L on to a physical tape measure.

This challenge turns out to be beneficial, for 3 reasons:

1. the mind's ability to detect subtle energy improves significantly with practice,

2. group variance in measurements are rare, because subtle energy research is often done by individuals, and individuals have consistency of measurements,
3. we are about to discover in the following sections that there are at least 6 other causes of variations, which are much more significant than the personal factors.

Earth Spinning on its Axis

Daily Variations

Figure 21-1 is a graph of **L** over an arbitrary 30-hour period. Initially, it looks like a graph of the stock market! The main factors are local sunrise and sunset, indicating peaks at sunset at 8:00 pm, and a trough at sunrise at 6:18 am on the date of measurement. There is a 25% variation in L from peak to trough, but explaining this graph is not straightforward.
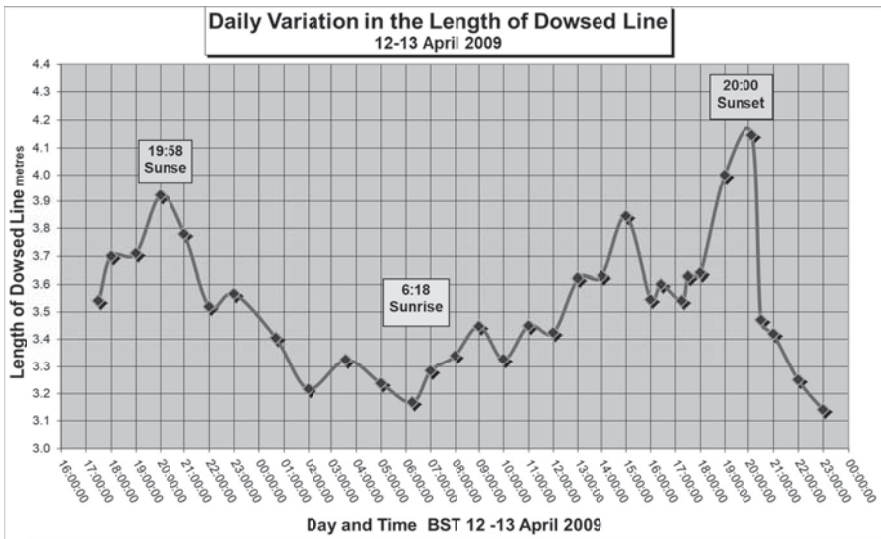
Figure 25-1 Typical Daily Variations in L
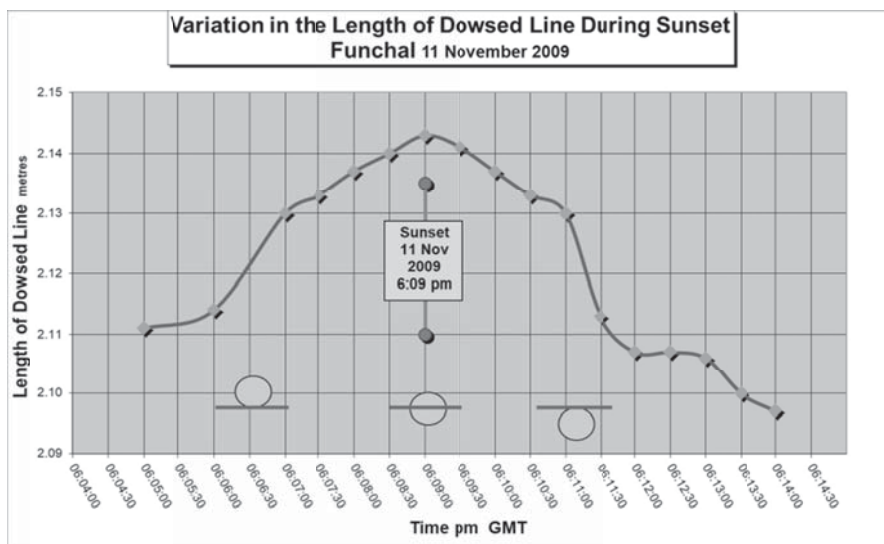
Figure 25-2 Measurements of L Taken During a Sunset at Funchal

What does actually happen at the sunset peak? The data for the graph in Figure 25-2 was measured during a sunset at Funchal in Madeira. The observing location had optimum viewing conditions, on a cliff top facing southwest, with a clear sky; the sunset was over the sea, with a clear view of the setting sun on the horizon. Measurements were taken every 30 seconds.

As is apparent, the peak starts as the sun touches the horizon. The maximum length of **L** is when half of the sun is below the horizon. The peak ends just when the sun has fully set. The effect lasted about 5 minutes.

What is the cause? It is not the obvious answer. These findings are not as a result of daylight. The same result is obtained if measurements are made in a windowless basement on a cloudy rainy day. It seemed that L was affected by a subtle energy that could pass through solids. It has taken 7 years, after the data was collected, (until I had discovered the Type 9 subtle energy), to find a partial suggestion, which is depicted in Figure 25-3.

Figure 25-3 A Cross Section of the Subtle Energy Beam L

On analysing the dot's beam during the day, 2 components are found, each with a different subtle energy:

1. a rod shape with a bluish colour
2. a yellow cylinder inside the rod

At night, the yellow subtle energy cylinder disappears and **L** shrinks. This suggests that the yellow cylinder is produced by the sun, and this subtle energy is absorbed and accumulated during the day, and released gradually during the night.

Using my categorisation of different types of subtle energies, the initial properties of the blue subtle energy is Type 5, whilst the yellow is Type 9.

More details can be found in paper number 26 at
http://www.jeffreykeen.co.uk/Papers.htm .

The Moon Orbiting the Earth

Lunar Month Variations

Figure 25-4 is a plot of **L** over a Lunar Month. The main variations are due to the interaction of the earth's and moon's gravity.
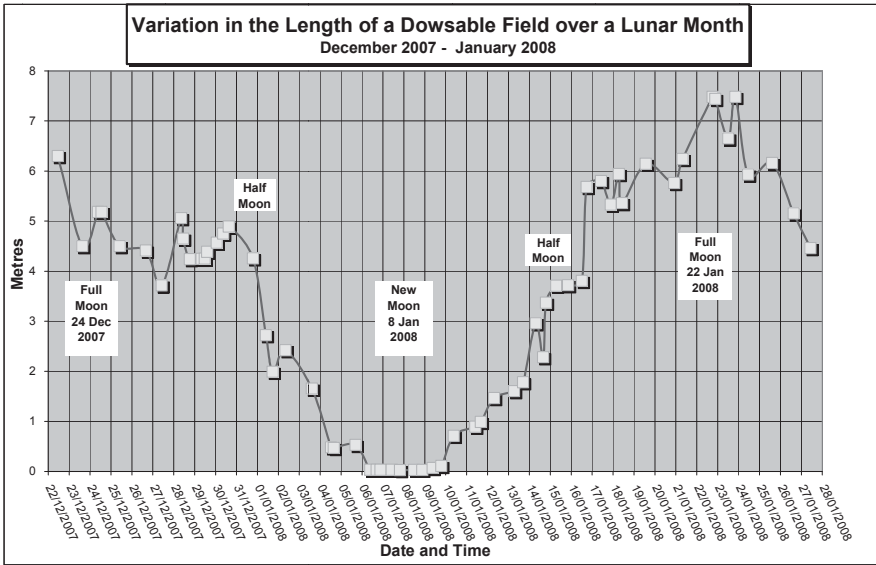
Figure 25-4 The Moon's Effect on L

As depicted in Figure 25-5, a new moon produces a higher gravitational force to an observer on earth, when the sun and moon's gravity are pulling in the same direction.
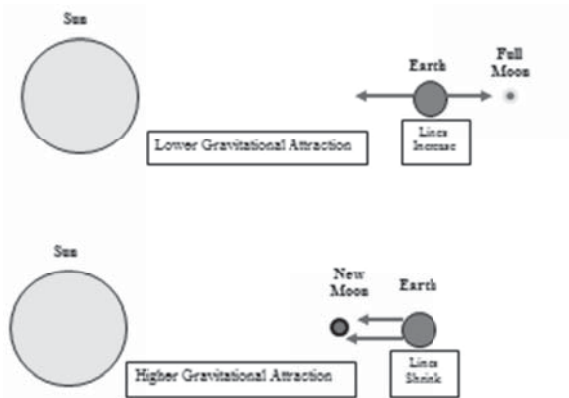
Figure 25-5 The Effect of the Moon's Gravity

Counterintuitively, L forms a trough and shrinks to 0 metres near a new moon. On the other hand, a full moon produces a lower gravitational force on earth, as the sun and moon's gravity are pulling in opposite directions. However, L increases near full moon, and in this instance, L climbs to a peak of over 7 meters.

This is not the same as the cause of tides. Tides are daily. Full and new moons are every 2 weeks. The effect on L is opposite to higher gravity causing higher tides. In general, higher gravity results in shorter lines. Lower gravity results in longer lines. The reasons for this are discussed later.

Over thousands of years, there has been anecdotal evidence of new moon and full moon affecting both plants and animal life. If the cosmos affects our dowsing and minds, what else does it affect: possibilities include health, mood swings, menstrual cycle, turtles hatching, and even lunacy?

The Earth Orbiting the Sun

Gravity in General

This section explores gravity in general across the solar system. Many years ago, I discovered that the dimensions of auras and subtle energies increased when climbing up low hills or mountains. The effect is even greater when flying at 32,000 feet: my experiments caused much consternation amongst the cabin crew on an Atlantic flight!

These observations, together with those just discussed in relation to the moon, caused a gravity paradox, as they presented 3 problems:

1. Lower gravity producing longer lines did not seem logical. (It is opposite to tides)
2. The decrease in Newtonian gravity at the top of a hill, or even at 32,000 feet, is insignificant compared to the significant increase in **L**
3. Why should the increased length of **L** be many orders of magnitude greater than the inverse of the change in the Newtonian force of gravity?

To solve this paradox, I measured L over an 18-month period, as the earth's elliptical orbit provided a varying gravitational force between the sun and earth. The protocol was refined numerous times, to eliminate all non-gravitational variations. For example, measurements were made at the

same time every day to overcome daily variance. In addition, dates were chosen to compensate for spin and rotation of the moon. The findings are presented graphically in Figure 25-6.
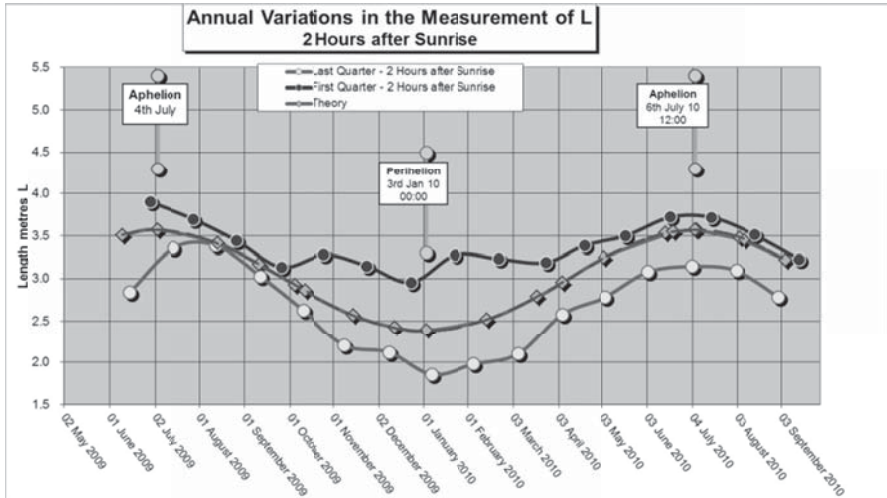
Figure 25-6 The Measurement of L over an 18-Month Period

Measurements on the top line were made when the moon's orbit was in the same direction as the earth orbiting the sun. The bottom line plots measurements taken when the moon's orbit was in the opposite direction to the earth going round the sun. The middle line is an average of these two lines, in order to eliminate the effects of spin from gravity. The main features are:

- Perihelion (when the earth is closest to the sun) produces a higher gravity: but a trough in L
- Aphelion (when the earth is furthest from the sun) produces lower gravity: but a peak in L

It is very reassuring that after this 18 month experiment, these findings, which relate to the sun, are compatible with Figure 25-4, which related to the moon, and the earlier findings detailing measurements at higher altitudes.

The Earth's Geometric Alignments

Chapter 16 explained alignment beams. These also apply to 3 objects in the solar system, as is depicted in Figure 25-7. The beams are Types 8 and 9 subtle energy, and appear to go on endlessly. They are also perceived as having a Mager violet or mauve colour.

Type 3 mauve
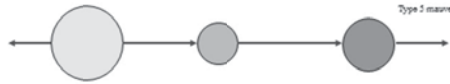
Figure 25-7 A Representation of a 3-Body Alignment Beam

Variations at New Moon

The data for the graphs in Figures 25-4 and 25-6 were collected over long time-frames – weeks, months, and years. This section details how the length of L changes at new and full moon with measurements made over short periods of time measured in seconds and minutes. There is a sudden drop in length at new moon. This same phenomenon has been confirmed for several new moons.

Variation in the Length of Dowsed Line During New Moon
20 August 2009

New Moon
20 Aug 2009
10:02

Length of Dowsed Line metres

Day and Time
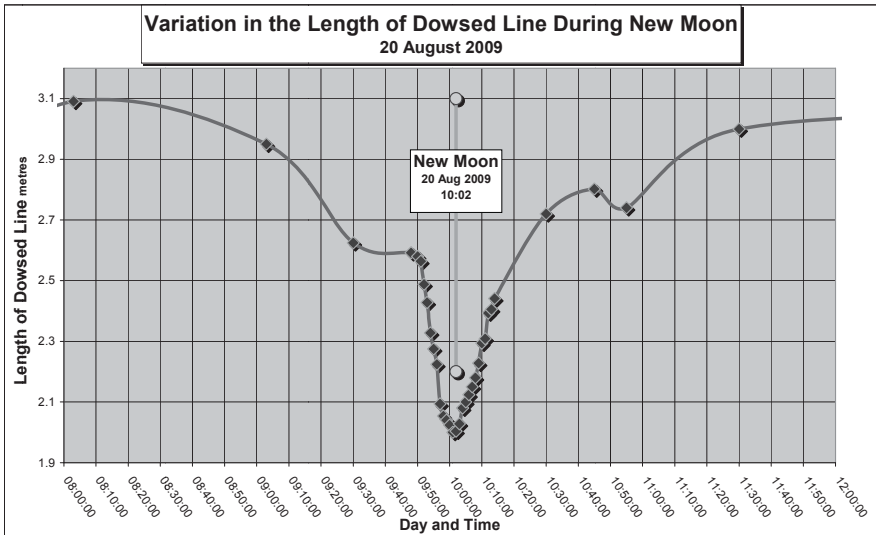
Figure 25-8 The Measurement of L at a New Moon (1)

Figure 25-8 shows the variation of L at the predicted time of the new moon which occurred on 20th August 2009 at 10:02 am. As is apparent, there was a significant drop in length about 1 hour either side of actual new moon, from about 2.9 metres down to 2.0 metres; a dip of about 31%.

Figure 25-9 shows the same experiment on the new moon of 26th March 2009 at 4:06 pm. This also produced a significant drop in yardstick length - the sharp trough occurred at the predicted time of new moon, and extended, as before, about 1 hour either side of actual new moon. On this occasion, the line reduced from about 2.3 metres down to 0.7 metres; a dip of about 70%.
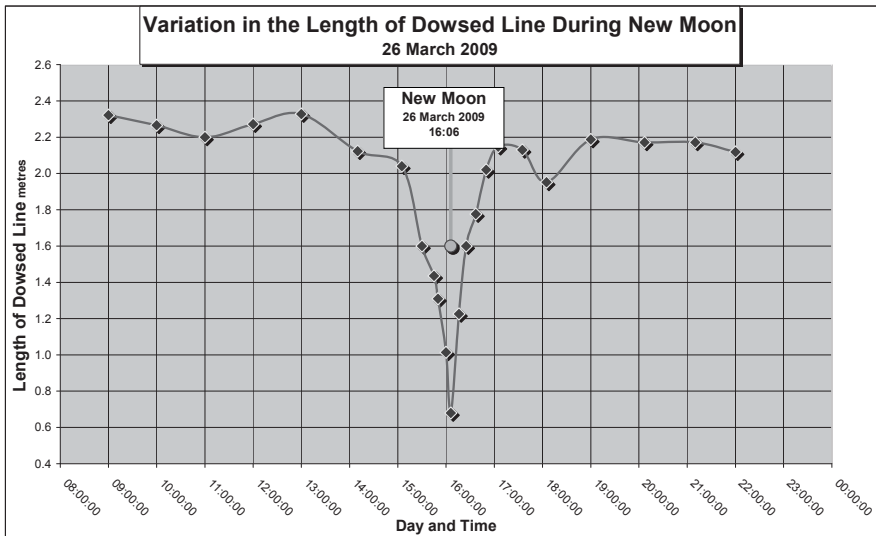
Figure 25-9 The Measurement of L at New Moon (2)

Variations at Full Moon

If significant dips occur at new moon, what happens at full moon? Figure 25-10 shows the variation over the course of an 18 hour period during the full moon on 11th March 2009, which was at 2:38 am GMT, when there was a significant peak in length, about 6 hours either side of actual full moon. The measured length increased from 4.2 metres to 6.4 metres; a peak of plus 52%.
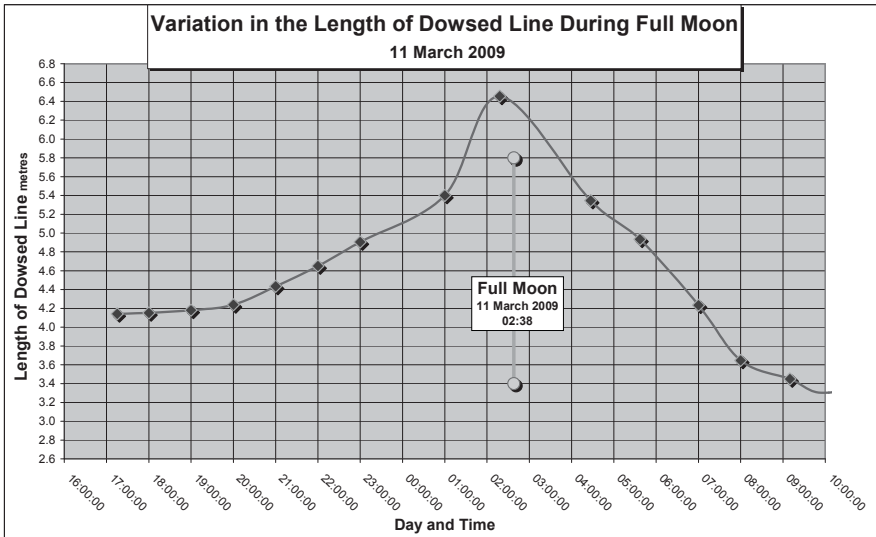
Figure 25-10 The Measurement of L at a Full Moon (1)

Figure 25-10 shows a similar variation over the course of a 12 hour period during full moon on 7th June 2009, which was at 18:12 GMT when there was the same sharp peak in length, about 6 hours either side of actual full moon. The measured length increased from 5.0 metres to 9.3 metres; a peak of plus 86%.
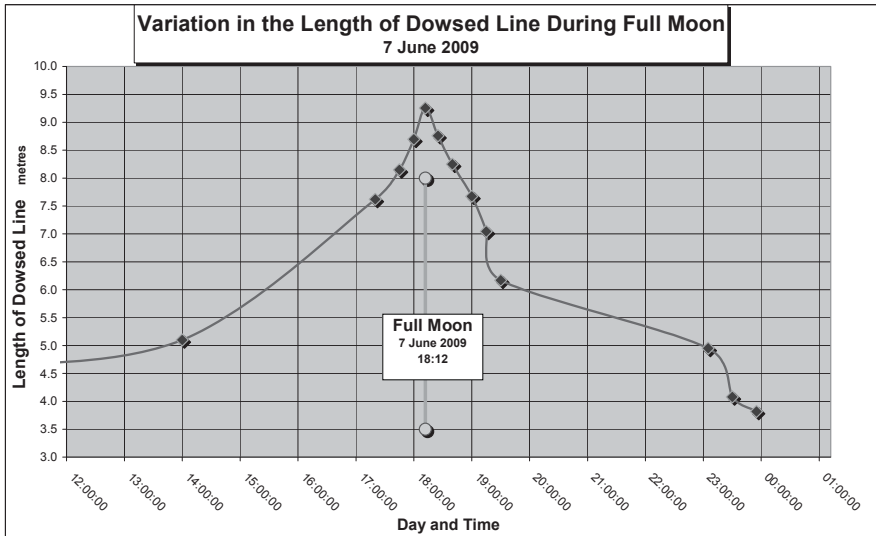
Figure 25-11 The Measurement of L at a Full Moon (2)

What causes the sudden peaks and troughs at full and new moons, and why is the effect 6 times' longer at full moon compared to new moon?

Gravity, Resonance, or an Alignment Beam

On initial inspection, the above results would appear to be consistent with Figure 25-5. It was there shown that lower gravity at full moon produces a line of maximum length, whilst higher gravity at new moon results in a shorter line of minimum length. But are the above peaks and troughs also due to gravity, or are they resonance from a different cause, or are they due to an astronomical alignment beam?

Gravitational changes associated with the orbits of the earth and the moon occur slowly over a period of time. For example, in relation to the moon's gravity in Figure 25-4, the maxima extend over 10 days and the minima over 4 days, while in relation to the sun's gravity in Figure 25-6, the minima extends over weeks rather than days or hours. Gravity, therefore, makes slow changes over weeks.

In contrast, on the new and full moon graphs in Figures 25-8 to 25-11, the peaks are sensitive over seconds and minutes. This suggests a different effect than gravity. The 6:1 ratio between the duration of the effects at new and full moon is also not explained by gravity.

A partial alignment beam, as explained in Figure 16–4, only causes the new and full moon graphs in Figures 25-8 to 25-11. It is instructive to examine a lunar eclipse, which is a practical example of a full 3-body alignment. This eclipse was not even visible in the UK, where the measurements were made. The 3-body alignment subtle energy beam, which passed through the earth, caused a peak in **L.** The data for this experiment is represented graphically in Figure 25-12. Note that the dot's white subtle energy beam, **L,** has been affected by the alignment beam's mauve colour, as plotted below the peak in Figure 21–12. This shows that the alignment beam extends over the 2-hour duration of the peak, and is the cause of this peak.
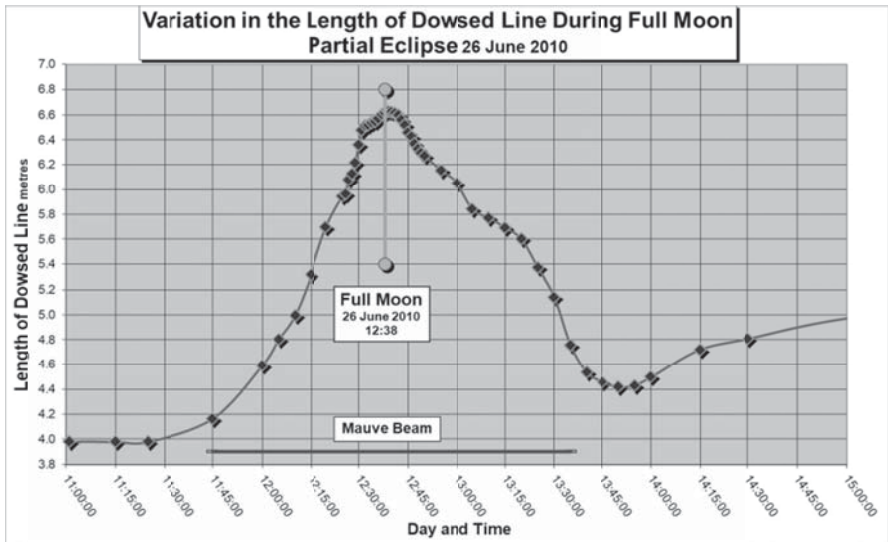
Figure 25-12 A 3-Body Alignment Beam Produced by an Eclipse of the Moon

CHAPTER TWENTY SIX

SUBTLE ENERGY AND VECTOR FLOW

Introduction

The concept of "flow" has been mentioned on several occasions in this book. Although the nature of subtle energy flow is currently not understood, this chapter makes a start in discussing the vector effects of flow, and how this can significantly alter measurements relating to some subtle energies.

In addition to the examples in the previous chapter of the use of the yardstick probe, this chapter not only details other examples of applications of **L**, but is also an opportunity to further verify findings stated in earlier chapters.

Natural subtle energy lines, or mind created psi-lines, are a useful starting point to illustrate flow, and how measurements are significantly affected by it. Measurements may be stretched or compressed depending if made with or against the direction of flow of the subtle energy. In general, it is, therefore, necessary to consider orientation when taking scientific measurements of subtle energy fields. In contrast, apart from having to compensate for wind and tides, orientation considerations are not usually a problem when measuring dimensions of physical bodies.

Practical examples

Set out below are specific examples of this interesting vector phenomenon. Four different subtle energies were analysed using the yardstick probe, L, as explained in Chapter 24. The subtle energies were:

a) a naturally occurring earth energy line,
b) a mind created psi line,
c) a 2-body interaction, and
d) a 3-body alignment beam.

These measurements were taken on arbitrary days and times, and are, therefore, only representative. However, the comparison between these differing measurements vividly illustrates the effects of the vector phenomenon.

(a) Mary Line at Glastonbury

The Mary line, together with the Michael line, are a well-known pair of subtle energies, that travel diagonally across the UK. Initially, control measurements of L were made just outside the line, where it passes through Glastonbury. When placing the yardstick on this line, its measured length in the direction of flow increased by 114% compared to its length just outside the line. However, when measured against the flow, its length decreased by 27%. This is summarised in Table 26-1.

Location	L	± %
Outside the Mary Line	0.915 metres	
With the flow	1.955 metres	+114%
Against the flow	0.670 metres	-27%

Table 26-1 Example of Vector Effects of a Natural Earth Energy Line

(b) Psi Line

As a control, the value of the length of **L** was initially measured just outside an arbitrary, indoor, mind created psi-line. When moved to the middle of the psi-line, and measured with the flow, the value of **L** increased in length by 78.2%. However, **L** decreased by 78.3% when measured against the flow. In this particular example, it is unusual for the percentage increase and decrease of values to be the same. Table 26-2 summarises these findings.

Location	L	± %
No Psi line	2.332 metres	
With the psi-line flow	4.155 metres	+78.2%
Against the psi flow	0.507 metres	-78.3%

Table 26-2 Example of Vector Effects of a Mind Generated Psi-Line

(c) 2-Body Comparison

Table 26-3 compares the properties of a naturally occurring earth energy line (different to above), 2 interacting stones, and 2 interacting abstract circles. On inspection, it is apparent that all the yardstick lengths increase when measured with the subtle energy flow, but decrease when measured against the flow. Also illustrated is an example of **L** taking on the properties of the subtle energy field under investigation. In this case, it is the Mager colour, and confirms that for these examples, it is usually white.

The unexpected conclusions from Table 26-3 are that two interacting bodies have similar properties to earth energy and psi lines. Even more surprising is that 2 stones are equivalent to 2 circles. This once again confirms statements made in previous chapters and in consciousness studies; pure geometry is equivalent to matter without mass.

	Natural Earth Energy Line	2 Stones	2 Circles
Length of Yardstick in the Subtle Energy Beam			
% change when measured with flow	56%	21%	33%
% change when measured against flow	-34%	-35%	-50%
Invariant to direction of measurement	X	X	X
Mager Colour			
Beam Mager colour	None	White	White
Yardstick Mager colour	White	White	White
Yardstick in beam	White	White	White
Yardstick takes on beam colour	?	√	√

Table 26-3 Using the Yardstick Probe to Compare 2-Body Interactions

(d) 3-Body Alignment Beam

	Central Stone	Central Circle	Actual Full Moon
Length of Yardstick in the Subtle Energy Beam			
% change when measured with flow	114%	123%	144%
% change when measured against flow	103%	133%	144%
Invariant to direction of measurement	√	√	√
Mager Colour			
Beam Mager colour	Mauve	Mauve	Mauve
Yardstick Mager colour	White	White	White
Yardstick in beam	Mauve	Mauve	Mauve
Yardstick takes on beam colour	√	√	√

Table 26-4 Using the Yardstick Probe to Compare the Middle of 3-Body Interactions

This objective was to investigate comparisons between different 3-body alignment beams, as well as at different locations within an alignment beam. These alignment beams were generated by 3 stones, 3 circles drawn on paper, and 3 astronomical bodies. The findings are summarised in Tables 26-4 and 26-5, and this sub-set of data was incorporated in Chapter 16.

Remote Location

It is logical to start measuring the properties of the yardstick at a remote location, both outside and within a 3-body alignment beam. The beam chosen for this experiment was generated by the sun, earth, and moon, at either new or full moon. The extreme remote location was on the earth during an actual full moon.

As with all alignment beams, the flow originates from the largest of the 3 bodies. In this case, the alignment beam's flow is perceived to emanate from the sun. In this experiment, the value of L **increased** by 144%, compared to the control value before full moon. Similar results were obtained from 3 stones, or 3 circles. These findings are summarised in Table 26–4

Unexpectedly, there was no difference in the values of L, if measurements were made with or against the flow.

	Outer Stone	Outer Circle	Actual New Moon
Length of Yardstick in the Subtle Energy Beam			
% change when measured with flow	-29%	-39%	-86%
% change when measured against flow	-29%	-31%	-86%
Invariant to direction of measurement	√	√	√
Mager Colour			
Beam Mager colour	Mauve	Mauve	Mauve
Yardstick Mager colour	White	White	White
Yardstick in beam	Mauve	Mauve	Mauve
Yardstick takes on beam colour	√	√	√

Table 26-5 Using the Yardstick Probe to Compare the Outer of 3-Body Interactions

Near the Middle Object

What happens if we take measurements of L near the middle of the 3 objects? This is equivalent to values of L being taken near the centre of 3 interacting stones, or 3 interacting circles, or is equivalent to an observer on the earth in the full moon configuration. As is apparent from Table 26–4, in all the above cases, lengths are always **increased.** Length is, therefore, **invariant** to the direction of measurement.

Near Outer Object

Let us now examine the properties of the yardstick near the outer object of a 3-body interaction. This is equivalent to the earth in the new moon configuration. The findings are summarised in Table 26-5, which includes 3 solid bodies, 3 drawn circles, as well as several actual new moons. These are the same 3 bodies as in Table 26-4, but with opposite vector results.

In all cases, lengths are always **decreased.** This is the only difference to the central object in Table 26-4. Length is again invariant to the direction of measurement. All other properties are the same.

Currently, as there does not seem to be an explanation for any of these 3 body interaction findings, it could make a significant and rewarding research project.

Comparison between 2 and 3-Body Interactions

The techniques discussed in this chapter contributed to the findings in Chapters 15 and 16 on 2 body and 3 body interactions, and, in particular, as summarised in Table 16–1. The subtle energy beam produced by 2 interacting objects has very different properties to the subtle energy beam produced by 3 aligned objects. All the properties measured at actual new and full moons are identical to the 3-objects column in Table 16-1. This proves that a 3-body alignment beam is produced by the sun, earth, and moon, at new and full moons.

Summary and Conclusions

The findings can be summarised as follows:

a) Whatever part of a 3-body alignment beam is used for measurements, **L** is invariant to the direction of measurement. The findings are identical, whatever the nature of the objects, their composition, size, or whether they are physical or abstract.
b) The subtle energy beam from any 3 aligned objects (such as circles drawn on paper, or physical bodies) more than doubles a measurement of length made near the centre object, compared to the same measurement made outside of the beam. This is the full moon simulation.
c) The subtle energy beam from the same 3 aligned objects, reduces a measurement of length by about 30% when made near the outer circle. This is the new moon simulation.
d) The Mager colour of the yardstick line changes from white to mauve when the 3 objects are in alignment.

The above findings suggest that the inexplicable subtle energy "flow" is a vector that affects noetic perception of subtle energies, and this general phenomenon is consistent with most earth energy and psi-lines that I have investigated. This invites the obvious question: what is "flow"?

On the surface, to a person unfamiliar with the physics of subtle energies, the findings in this chapter are yet another example of the apparent unreliability of the scientific measurements of subtle energies. A major factor in causing variability of measurements is due to the vector properties discussed in this chapter. Therefore, having identified and researched these vector properties, these findings should not be treated as negative, but positively to encourage research as to why these unusual results occur.

The Way Forward and Suggested Future Research

1. Investigate what is flow.
2. With most subtle energies, when measuring with their flow, measurements increase, whilst measuring against their flow measurements decrease. However, for 3-body alignment beams, there is no difference in the values of **L**, if measurements were made with or against the flow. Why?

CHAPTER TWENTY SEVEN

THE MIND AND VORTICITY
IN THE ECLIPTIC PLANE

Introduction

In previous chapters, vorticity applied to experiments on earth involving examples of rotating electric fans and swirling water. We are now taking the mind into the solar system, and the ecliptic plane in particular. This chapter details the effects on measurements of **L**, (the yardstick probe of Chapter 24) over a period of one year, due to the combined changes in spin vectors caused by both the spin of the earth on its tilted axis, and the earth's elliptical orbit around the sun. Figures 27-1 and 27-2 illustrate the concepts.

Protocol

Using the diagram in Figure 27-1 as a guide, the protocol for the mind was that the solar system is being visualised as if looking down on the ecliptic plane. The earth is spinning on its tilted axis, with the top of its axis gradually tilting towards and away from the sun, together with the plane of the earth's spin crossing the ecliptic plane.

The radial spin vector in the plane of the earth's spin was then visualised, leading to the component of this vector in the ecliptic plane. Simultaneously visualised was the path of the static observer located at a point on earth being affected by a vector combination of the earth's daily spin, plus the annual orbit of the earth around the sun.
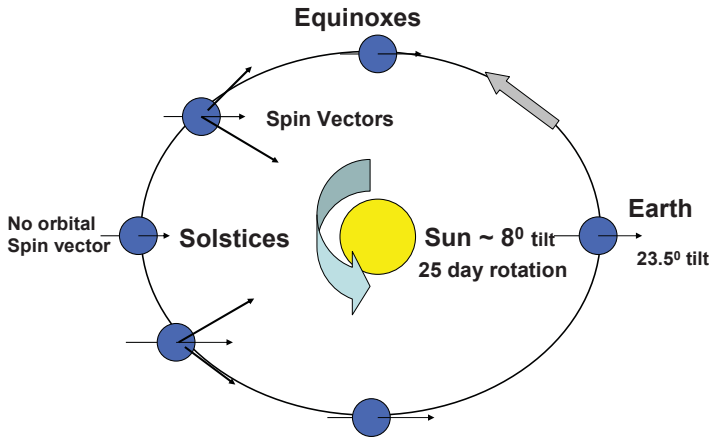
Figure 27-1 The Earth's Orbit around the Sun

L was measured when intent was focussed solely on the combined radial orbit and spin vector in the ecliptic plane.

As part of the intent, it is important to positively ignore all the other known causes that affect **L**. These include the daily, monthly and annual variations due to astronomical and gravitational changes, the sun and moon's gravity, tides, and hours of day light.

The above protocol was then repeated for the tangential vector.
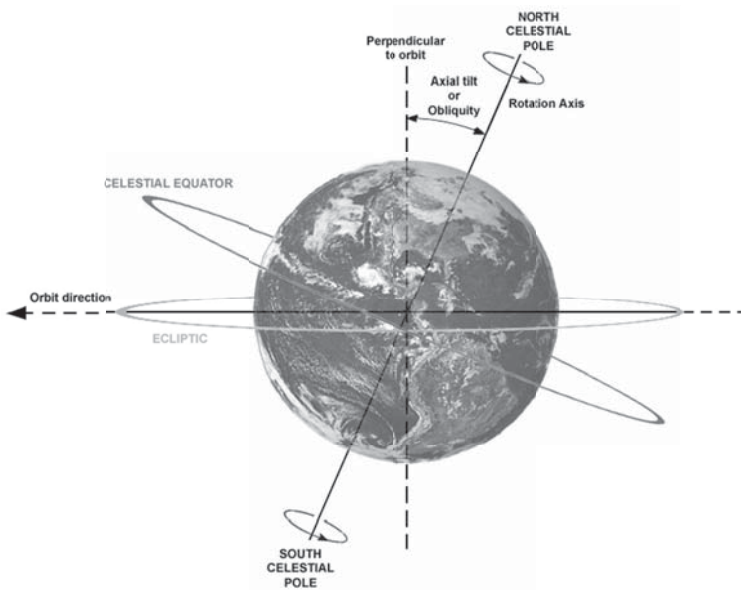
Figure 27-2 The Earth Spinning on its Axis in relation to the Ecliptic Plane

Findings

The graphs in Figure 27-3 summarise the findings, with the x-axis giving dates, and the y-axis representing the length of the yardstick line in mms. The curve with the circular marker data points are the lengths associated with the radial vector pointing towards the sun. The curve with the triangular data points are the lengths resulting from the tangential vector in the direction of the earth's orbit around the sun. Each of these curves is discussed below.

Radial Vector Pointing at Sun

There are 2 well defined turning points on the radial vector curve (circular markers) that coincide with the March (2010 and 2011) and September 2010 equinoxes. At equinoxes the plane of the earth's spin is crossing through the ecliptic plane. The curve suggests that the noetic measurements are obeying an approximation to a cosine vorticity rule, plus positive and negative vectors.

However, the effects of vorticity at the September equinox should be the same as at the March equinox. Why, therefore, are there higher values at the September equinox and lower values at the March equinox?
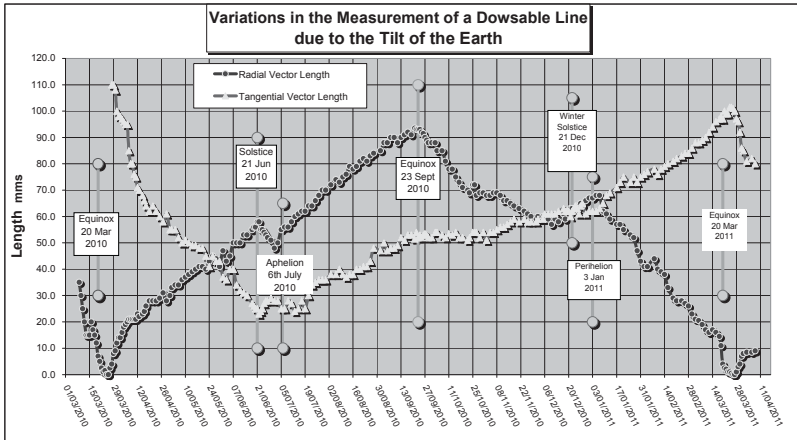
Figure 27-3 Variations in L during a Year Due to the Tilt of The Earth

It looks as if universal consciousness has been very clever and got around representing a negative length and direction of vectors by moving the x-axis down from about $L = 50$mms, so that the minimum value of the radial vector length equals 0. If so, universal consciousness and the mind must have known well in advance the results found on the 26th March, based on the initial intent on the 8th March!

These counter intuitive findings require independent confirmation – by researchers with over one year to spare!

The higher values between the summer and winter solstices are due to the representation of positive vectors, with the culmination of maximum vorticity at the September equinox. Similarly, the negative vectors are represented by the lower values between the winter and summer solstice, culminating in the minima in March 2010 and 2011.

Confidence in this vorticity technique is increased because this experiment was continued by the author whilst in the Canary Islands during a week in October, and in the Middle-East in December. In both cases, the measured lengths became greater, due to increased vorticity, nearer the equator.

However, there are several apparent anomalies. Why is the equinox minimum on 26th March 2010 and 27th March 2011 but not on 20th

March, which is the predicted date of equinox? What caused the kink in the curve just after the June solstice and before aphelion? There was the same effect at the end of December 2010 between solstice and perihelion.

Tangential Vector Pointing in the Direction of the Earth's Orbit

The tangential vector curve (triangular markers) has a minimum during June and July. This is expected as the earth is furthest from the sun at aphelion, and, hence, at minimum velocity and vorticity.

The tangential vector curve has maxima at the March equinoxes. However, there are further anomalies as the maximum vorticity should be at perihelion not at equinox? Similarly, why are the maxima on 26th March and not on 20th March, and why does the curve collapse so quickly after the March equinoxes? It is also not obvious why there is a triple dip between the June solstice and 13 days after aphelion?

From Figure 27-3, the lengths due to vorticity varied between 0 mms and 90 mms. As a comparison to the effects on dowsing by changes in gravity, the length of the same yardstick line varied by about 2 metres. The spin effect of the earth on dowsing is, therefore, an order of magnitude smaller than gravity.

Analysis and Theory

The objective here is to calculate the vorticity of a fixed observer on earth due to the combined

1. rotation of the earth on its tilted axis (i.e. 360° in 24 hours) and
2. the earth orbiting the sun (i.e. 360° in 1 year).

The following are order of magnitude calculations for the above angular velocities – the starting point for vorticity.

Angular speed of the Earth's rotation on its axis

24 hours = 24*60*60 = 86,400 seconds
2π radians/86,400 seconds = **7.27 × 10⁻⁵ rad/s**

Average Angular Speed of the Earth around the Sun

1 year = 365.25*24*60*60 seconds
2π radians / (365.25 * 24 * 60 * 60) = 1.99 x 10-7 rad/s

As is apparent, the angular speed of the earth's orbit around the sun is two orders of magnitude less than the earth's rotational speed on its axis, so it may have been thought that the former could be ignored. However, we know that auras increase as a function of both angular velocity and distance from the axis of spin.

Vorticity in the Earth's Equatorial Plane

The objective of this section is to obtain order of magnitude calculations in an attempt to explain the above findings, and to ascertain if the mind's initial intent for the experiment was realised. The simplest but arbitrary definition of Vorticity is that **V** is a linear function of radians per second (ω) multiplied by radius (**r**). i.e. **V = r . ω**. As commented below, this is different from other definitions of vorticity. A further simplification is to ignore all perturbations, including the effects of the sun's rotation and tilt, any effects of the moon, tides, planets, or oscillations of the earth's axis, etc.

The vorticity of the location of the experiment, due to the spin of the earth on its axis, is calculated as follows. The mean radius of the earth is 6,371 km. The latitude of Bournemouth, United Kingdom, where the measurements were taken, is **50° 43' 0" N.** The cosine of this angle (0.633156) multiplied by the earth's mean radius = 4,033.8 kms, or **4.034 x 10^6 m**. This is the distance of the experiments from the earth's axis.

Therefore, the (simplified) vorticity of the rotating earth at Bournemouth is

$$7.27 \times 10^{-5} \text{ rad/s} * 4.034 \times 10^6 \text{ m} = \textbf{2.9} \times \textbf{10}^\textbf{2} \textbf{ m.rad/s}$$

The vorticity of the location of the experiment due to the earth's orbit of the sun is calculated as follows. The mean radius of the earth's orbit around the sun is 150 million kilometers, or 1.5×10^{11} m. The vorticity of the earth's orbit is therefore

$$1.99 \times 10^{-7} \text{ rad/s} * 1.5 \times 10^{11} = \textbf{3} \times \textbf{10}^\textbf{4} \textbf{ m.rad/s}$$

Using the above definition of vorticity, the orbital vorticity is 2 orders of magnitude greater than the earth's spin on its axis. So when the distance between the sun and earth is taken into account, the vorticity of the earth's rotation on its axis is insignificant. This difference is 4 orders of magnitude greater if the usual definition of vorticity is adopted, i.e. **V = ½ . r^2 . ω**. It is, therefore, difficult to understand how the mind's

measurements, as depicted in Figure 27-3, was able to detect and separate out the equinox effects from the greater orbital effects.

Vorticity in the Ecliptic Plane

The experimental requirement was that the general vorticity of the rotating earth (as calculated above) needs to be resolved into a vector in the ecliptic plane. i.e. a radial vector pointing at the sun. The diagrams in Figures 27-1 and 27-2 illustrate the requirement. The tilt of the earth's equatorial plane of spin, relative to the ecliptic plane, is zero at both equinoxes, and **23.5°** at both solstices. The vorticity in the ecliptic plane is, therefore, a maximum at the equinoxes and a minimum at the solstices.

Date	Degrees	Radians	Sine	x 90
01/03/2010	9	0.1571	0.1564	14.0791
20/03/2010	0	0	0	0
08/04/2010	9	0.1571	0.1564	14.0791
27/04/2010	18	0.3142	0.309	27.8115
16/05/2010	27	0.4712	0.454	40.8591
04/06/2010	36	0.6283	0.5878	52.9007
23/06/2010	45	0.7854	0.7071	63.6396
12/07/2010	54	0.9425	0.809	72.8115
31/07/2010	63	1.0996	0.891	80.1906
19/08/2010	72	1.2566	0.9511	85.5951
07/09/2010	81	1.4137	0.9877	88.892
23/09/2010	90	1.5708	1	90
15/10/2010	99	1.7279	0.9877	88.892
03/11/2010	108	1.885	0.9511	85.5951
22/11/2010	117	2.042	0.891	80.1906
11/12/2010	126	2.1991	0.809	72.8115
30/12/2010	135	2.3562	0.7071	63.6396
18/01/2011	144	2.5133	0.5878	52.9007
06/02/2011	153	2.6704	0.454	40.8591
25/02/2011	162	2.8274	0.309	27.8115
20/03/2011	171	2.9845	0.1564	14.0791
04/04/2011	180	3.1416	0	0
20/04/2011	171	2.9845	0.1564	14.0791
12/05/2011	162	2.8274	0.309	27.8115

Table 27-1 Transforming the Data to a Sine Wave

Cos 23.5° = 0.91706. So the assumed vorticity of the earth's spin at Bournemouth in the ecliptic plane varies between **2.9 × 10², ** and 0.91706 *

$2.9 \times 10^2 = \textbf{2.7 x 10}^{\textbf{2}}$. As a first approximation, and assuming the velocity of the earth around the sun is constant, this range of values can be spread over 1 year, with 0.29 at equinox and 0.27 at solstice. Assuming a sine wave distribution, equinox can be taken as 0° and solstice as 90°. Table 27-1 illustrates the values used to produce a sine wave, with maximum amplitude of 90 mms. This sine wave is superimposed on the findings for the radial vector length, as the dotted curve in Figure 27-4.
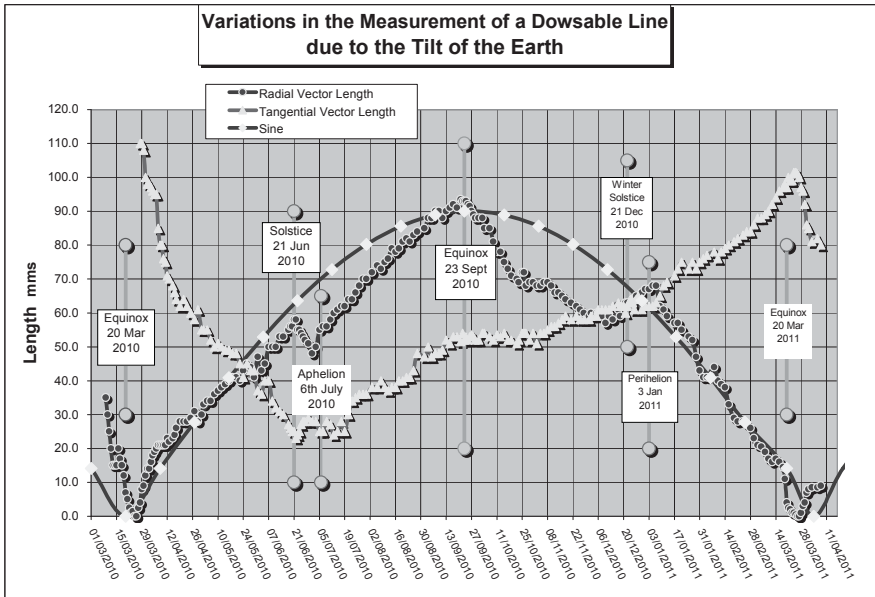
Figure 27-4 Comparison of Actual Data to Theoretical Predictions

From inspection, this sine wave with its known over simplifications is a close fit to the findings. The main perturbations are between the June solstice and the September equinox, and the September equinox and the winter solstice. Further analysis is required to explain this anomaly, together with the associated effects of aphelion and perihelion. As previously discussed, the orbit of the earth around the sun produces the latter, and their effects are at least 2 orders of magnitude greater than the curve being represented!

Author's Comments

I have not used the usual $V = \frac{1}{2} . r^2 . \omega$ version of vorticity for several reasons. From the work published 5 years ago, it was not obvious that Length squared/Time applies to vorticity of subtle energies. Similarly, it was demonstrated that the Cosine rule did not apply to dowsed spin vectors. My intention was to keep this chapter as simple as possible to try and understand the principles involved. I also wanted to try explaining the 2 factors of sun orbit and earth axis spin differing by many orders of magnitude, but appearing on the same data curve. Moreover, my arbitrary definition of vorticity does not affect the results, or the sine wave fit in Figure 27-4. The latter is a pure sine wave from 0 to 1 with a normalisation constant of 90 mms, (which I believe is the cosmic consciousness cleaver representation of +45 to -45 noetic vectors).

It is not obvious why, with the above over simplifications, no physics or vorticity explanation was required to produce a good fit to the data in Figure 27-4! Similarly, my approach highlighted the perturbations in the top half of the graph (between solstice and equinox), and may give us clue to the link between summer solstice and aphelion, and winter solstice and perihelion. It seems that after about 4 billion years of interaction, the sun and earth are in some sort of phase.

Summary of Conclusions

A major achievement of this chapter is that experimental results, when dowsing the earth's spin have, for the first time, been measured, analysed and documented. The findings here have not only been shown to be repeatable, but have demonstrated a strong link between consciousness and the solar system.

Via the use of the standard yardstick, **L**, significant turning points in curves, representing measurements of length, occur at equinoxes and solstices. Vector lengths affected by the radial spin vector pointing towards the sun have maxima and minima at equinoxes. This coincides with maximum vorticity in the radial vector as the earth's plane of spin passes through the ecliptic plane. Lengths affected by the tangential spin vector in the direction of the earth's orbit have a minimum during June and July. This is expected as the earth is furthest from the sun at aphelion, and, hence, at minimum vorticity. Solstices produce perturbations to the main curves.

These new findings demonstrate quantitatively, the effects of aphelion and perihelion on the mind and subtle energies by equinoxes and solstices

via the radial spin vector in the equatorial plane due to the earth's spinning on its tilted axis.

The Way Forward and Suggestions for Future Research

As always, discoveries in research generate more questions than answers. Interesting questions and suggested topics for future research include the following:

1. There are several apparent anomalies. Why is the equinox effect minimum on 26th March 2010 and 27th March 2011 but not on 20th March which is the predicted date of equinox?
2. What caused the kink in the curve just after the June solstice and before aphelion? There was the same effect at the end of December 2010 between solstice and perihelion.
3. What is the theoretical explanation for the sine curve of tangential vector lengths over the course of a year?
4. Why does the tangential vector length curve have maxima at the March equinoxes, but is not affected by the September equinox?
5. Similarly, in Figure 27-4, why do the 3 curves intersect at perihelion, but not at aphelion?
6. There are further anomalies as the maximum vorticity for a consistent explanation should be at perihelion, not at equinox?
7. Similarly, for the tangential curve, why are the maxima on 26th March and not on 20th March, and why does the curve collapse so quickly after the March equinoxes?
8. It is also not obvious why is there a triple dip between the June solstice and 13 days after aphelion?
9. Why does the tangential vector length curve contain the above two phenomena of equinox and solstice, when their effects are at least 2 orders of magnitude apart?
10. If the two main components of ecliptic plane spin are at least 2 orders of magnitude apart, how does the mind deal with this?
11. The simplest formula for vorticity, $\mathbf{V} = \mathbf{r} \cdot \boldsymbol{\omega}$, was used in the above analysis. What is the exact formula for $\mathbf{V} = \mathbf{Fn}\ (\mathbf{r},\ \boldsymbol{\omega})$ that explains Vorticity and the mind?

CHAPTER TWENTY EIGHT

THE WEIRD EFFECT OF THE MIND AND GRAVITY

Introduction

This chapter demonstrates that the mind can quantitatively track the earth's annual elliptical orbit around the sun, and measure the change in the earth-sun gravitational attraction.

Qualitative findings when dowsing gravity have been known for several years. Taking measurements at sea level and then repeating these measurements in an aircraft or up mountains suggest that these very small reductions in gravity produce a relatively large increase in dowsed lengths. The experiments described here attempt to determine a mathematical connection between gravity (over both terrestrial and astronomical distances) and the mind's perception, after eliminating other causes for the observed effect.

As some readers may feel it is instructive, I have set out how this research into the mind and gravity evolved over a 9-year period. Therefore, the text in this chapter is divided into 5 phases.

Phase 1 - Original Experiments (L v Random Dates)

During the period from May 2009 to September 2010, by using the yardstick probe L (as described in Chapter 24), the length of L was measured as the earth circled the sun in its elliptical orbit, causing a varying gravitational force, which significantly affected the value of L. The findings are summarised in an earlier, more random version of Figure 28-1.
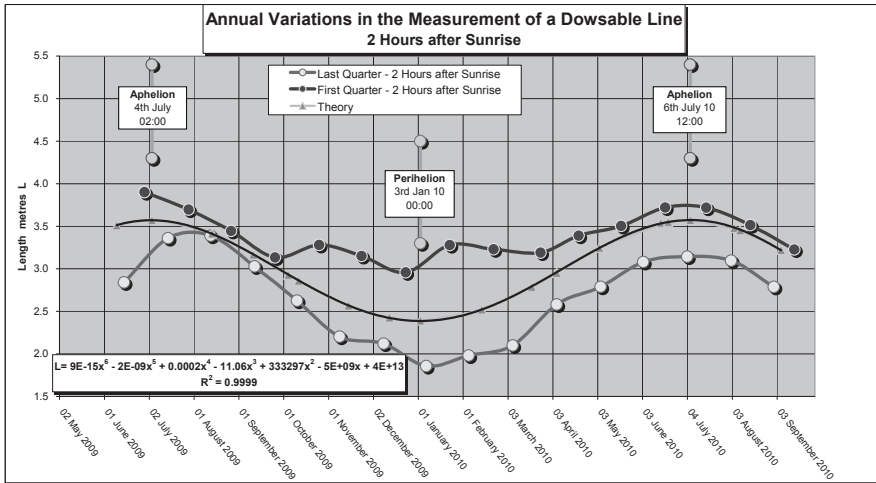
Figure 28-1 The Variation in the Value of L over a Year

As expected from the initial qualitative earth bound experiments described above, **L** is at a maximum at aphelion when gravitational force is at a minimum, because the earth is furthest from the sun. Similarly, L is at a minimum at perihelion when the earth is closest to the sun, producing the maximum gravitational attraction.

Possible Experimental Errors

As is apparent from the Figure 28-1 graph, the curve for the first quarter measurements (the top line) is significantly above the last quarter curve (the bottom line), and is much flatter. The change in gravitational force in the 2 weeks between readings for each lunar month would not cause this duality. This suggests that an additional factor(s) to gravity has inadvertently been dowsed, most likely caused by the orbit of the moon around the earth.

For the first quarter, the moon's orbit is in the same direction as the earth's orbit, but in the last quarter the orbits are in opposition. The assumption has been made that taking an average of these two curves eliminates the non-gravitational effects of the moon, and gives the optimum correlation with the desired gravitational effect. The effects due to spin have been eliminated by cancelling out the positive and negative spin vectors.

There is a second order sine wave perturbation on the two curves with a 3 and 2-month periodicity. The cause may be tidal. However, the effects of the moon's orbit on spin and tides, the weakest of the perturbations could not be eliminated, as adjusting the times for taking these measurements would have corrupted the results for the major factors. This tidal perturbation seems very small, and does not significantly affect the results.

Revised Experimental Protocol

Using the benefits of the conclusions of Chapter 25, as well as the above analysis of possible errors, an optimised protocol was adopted to avoid known daily and lunar month perturbations, as well as the special effects at new and full moon; these being the major sources of error.

Therefore, measurements were taken at the same time of the day (2 hours after sunrise), on 2 specific days during a lunar month, at the moon's last quarter and first quarter in successive lunar months.

Phase 2- the 1st Revision (L v Optimised Dates)

Phase 1 experiment was then repeated over another year to produce more accurate curves in Figure 28-1. The top curve relates to measurements taken 2 hours after sunrise during the moon's first quarter, and the bottom curve relates to measurements taken 2 hours after sunrise during the moon's last quarter.

The heuristic analysis of the average yardstick lengths on specific dates, shown as the middle theoretical curve, suggested a good visual fit. The Excel trend line suggested a complex polynomial relationship, involving the power of 6, gave a very good correlation coefficient.   (i)

However, this resulting graph was unsatisfactory, as it only connected **L** to dates and not to an absolute relevant gravitational force.

The experimental results seem to prove pretty strongly that gravity is the correct cause and effect in producing the results shown in Figure 28-1, having eliminated such possible alternative correlations as increased temperatures, or the hours of sunlight in summer. However, on closer inspection two anomalies require an explanation. Despite the apparent accuracy of these findings, these results did not resolve my double paradox:

1. Why was L affected by gravity? and
2. Why did weaker gravity produce longer lines?

Phase 3- the 2nd Revision (L v F$_g$$^{-6}$)

This section now presents a later but more accurate analysis of the above data, not as originally published, where length was a function of months in a year, but as the perceived measured length, L, as a function of the actual Newtonian gravitational force between the sun and earth at the time of the measurement.

The data in Figure 28-1 was re-analysed, about 1 year later, to find the actual distance between the sun and earth, on each date and time when the measurements of **L** were taken. This new data is combined and shown in the right hand columns of Table 28-1

	Date	L1	L2	L metres	d A.U.	d metres	d^2 metres^2	Gravitational Force F m^{1}kg^{1}s^{-2}
	06 September 2010	2.700	3.300	3.000	1.00794	1.50786E+11	2.27363E+22	3.49E+22
	05 August 2010	3.090	3.600	3.345	1.01450	1.51767E+11	2.30332E+22	3.44E+22
	09 August 2010	3.050	3.580	3.315	1.01380	1.51662E+11	2.30015E+22	3.45E+22
Aphelion	06 July 2010	3.740	3.144	3.442	1.01667	1.52091E+11	2.31317E+22	3.43E+22
	16 June 2010	3.710	3.130	3.420	1.01590	1.51976E+11	2.30968E+22	3.43E+22
Solstice	21 June 2010	3.720	3.130	3.425	1.01620	1.52021E+11	2.31105E+22	3.43E+22
	05 May 2010	2.785	3.440	3.113	1.00860	1.50884E+11	2.27661E+22	3.48E+22
	06 April 2010	2.580	3.260	2.920	1.00066	1.49696E+11	2.2409E+22	3.54E+22
Equinox	20 March 2010	2.300	3.190	2.745	0.99588	1.48981E+11	2.21955E+22	3.57E+22
	14 February 2010	2.000	3.260	2.630	0.98756	1.47737E+11	2.18262E+22	3.63E+22
Perihelion	03 January 2010	1.900	3.100	2.500	0.98328	1.47096E+11	2.16374E+22	3.67E+22
	13 December 2009	3.000	2.100	2.550	0.98446	1.47273E+11	2.16894E+22	3.66E+22
	15 November 2009	3.200	2.180	2.690	0.98910	1.47967E+11	2.18943E+22	3.62E+22
	12 October 2009	3.200	2.626	2.913	0.99799	1.49297E+11	2.22896E+22	3.56E+22
	11 September 2009	3.028	3.250	3.139	1.00655	1.50578E+11	2.26737E+22	3.50E+22
Aphelion	04 July 2009	3.200	3.850	3.525	1.01665	1.52089E+11	2.3131E+22	3.43E+22
Solstice	10 June 2009	3.980	2.800	3.390	1.01522	1.51875E+11	2.30659E+22	3.44E+22

Table 28-1 Summary of the of the Original and Enhanced Data

The well-established Stellarium astronomical software program was used retrospectively to obtain the distance, **d**, in Astronomical Units (AU), between the sun and earth on specific dates during the duration of the experiment. The standard astronomical unit of 1 A.U. = 1.49598E+11 metres was used.

Physical tables were adopted for the actual masses of the sun and earth, as well as the gravitational constant G. These figures are shown in Table 28-2.

Mass of the Earth m	5.97E+24	kilograms
Mass of the Sun M	1.99E+30	kilograms
Gravitational constant G	6.67E-11	$m^3kg^{-1}s^{-2}$

Table 28-2 Parameters Used for Calculating Newtonian Force of Gravity

The gravitational force, $\mathbf{F_g}$, between the sun and earth on relevant experimental dates, was then calculated using Newton's famous inverse square law.

$$F_g = G.M.m/d^2 \qquad\qquad \text{(ii)}$$

The results are shown in the right hand column in Table 28-1

As the objective of this exercise was to identify the relationship between L and gravitational force, it is first necessary to re-calculate L to provide the average of the top and bottom curves in Figure 28-1, on the specific dates in the left hand column of Table 28-1.

This produces the formula $\mathbf{F_g} = 7.93E+44/d^2$ $m^1kg^1s^{-2}$. After obtaining inspiration from equation (i), and in order to explain the findings, this gravitational force was increased heuristically to the power of 6, and then the reciprocal taken, as set out in Table 28-1. This theoretical mathematical conclusion produces a very good **visual** confirmation by superimposing it as a third curve, which seems to fit very well between the middle of the top and bottom curves.

To avoid confusion, this interim step is not shown, as it was not a precise mathematical fit to the average of the two raw data curves at the first and last quarters of the moon i.e. the top and bottom curves in Figure 28-1.

However, the general result was again consistent with previous qualitative findings on gravity, such as dowsing on the ground and then in aircrafts or up mountains. A very small reduction in gravity produces a large increase in noetic lengths.

The heuristic equation obtained visually produced by the average of the two curves in Figure 28-1 was $L = 6E+135 * F_g^{-6}$ (iii)

However, this did not have a satisfactory fit to the data.

Phase 4 - the 3r^d Revision (L v F$_g^{-4.6698}$)

The result of the next phase of my research is shown in Figure 28-2, which is a more accurate graph of the value of **L** plotted against the actual gravitational force between the earth and the sun at the time of data measurements.

This led to my discovery of an enhanced Newtonian gravity equation which is exponential, with a high correlation coefficient.

The Excel trend line in Figure 28-2 produces an equation

$$L = 6E+105 * F_g^{-4.6698} \qquad\qquad (iv)$$

Figure 28-2 The Results of Plotting the Final Data in Table 28-1

Phase 5 - the 4th Revision (L v F$_g^{-\delta}$)

So, my previous heuristic equation (iii), which produced a power index of -6, was less accurate than the latest figure of -4.6698. The correlation coefficient for this equation (iv) is 0.9745, indicating that the data fits the equation to an exceptionally high accuracy, so giving confidence in the experimental results. This accuracy suggested that I should postulate that the power index in equation (iv) should really be Feigenbaum's constant (4.6692),

Power Index from Equation	4.6698
Feigenbaum's Constant	4.6692
Difference	-0.0006
% Difference	-0.0129%

Table 28-3 Gravity, chaos, and the mind

As apparent from Table 28-3, the power index in equation (v) equals Feigenbaum's constant, δ, to an accuracy of 0.0129% error compared to the accepted accurate value of Feigenbaum's constant, as depicted in Table 28-3. This is to a remarkable accuracy, as these results were obtained many years after the measurements were made, and ruled out accusations of premeditated values, or coincidence.

Thus, the above arguments lead to the final equation of the form:

$L = 6E+105 \, F_g^{-\delta}$ (v)
$R^2 = 0.97$

For the non-mathematical reader, the essence of this formula is "The length **L**, of the subtle energy beam emanating from the yardstick, for observations on earth as it orbits the sun, is determined by the Newtonian force of gravity F_g raised to the inverse power of Feigenbaum's universal constant"..

Data that produces universal constants is the gold standard for producing recognised scientific discoveries.

Encouragingly, just from inspecting the graph in Figure 28-2, and without any knowledge of mathematics or graphs, this equation is compatible with all the previous findings:

L increases as gravity decreases towards the left
L decreases as gravity increases to the right.

Feigenbaum's constant is usually associated with bifurcation, fractals, turbulent flow, and chaos theory. I was obviously not only astounded by this unexpected relationship, but also with its very high accuracy. However, this still leaves 2 challenges.

1. How and why does gravity change L? A possible answer is that L is a subtle energy beam created by geometry in space-time. Using the language of general relativity, higher gravity causes a higher distortion (or greater curvature) in the local geometry of space-

time. I postulate that this diminishes L in a similar way that clocks run more slowly when gravity is stronger. On the other hand, low gravity produces little distortion in the geometry of space-time so L can expand unhindered.

2. Each side of the equation has totally different units: Length and Newtons (kg m s^{-2}). Normally, I would reject this result as bad data. However, as this equation has a very high accuracy, involving a universal constant (also to a very high accuracy), I feel this result should be taken seriously!

Conclusions

The equation $L = 6E+105 * F_g^{-\delta}$ was found with a high correlation coefficient $R^2 = 0.9745$. The power index is Feigenbaum's constant within 0.013% error. This is another example of the mind's ability to interact with gravity and produce a universal constant, suggesting that consciousness is intimately connected to the fabric of the universe and chaos theory.

The Way Forward

As usual, scientific research provides more questions than answers. Some obvious questions are:

1. How is it possible to enhance equation (v), so it is mathematically sound with the units on either side of the equation being the same?
2. How does the mind easily detect changes in the (very weak) gravitational force?
3. Are both gravity and consciousness associated with chaos theory?
4. What is the role of Feigenbaum's constant, δ, in gravity and in the mechanism of consciousness?
5. When extrapolating Figure 28-2, (which only has data relating to a relatively small range of gravitational force), what happens to **L** as gravity tends towards zero in intergalactic space, or at the other extreme, as gravity tends towards a black hole?

It is hoped that this chapter will motivate researchers to confirm these experimental findings and to develop the theoretical aspects of the interaction between gravity and consciousness.

CHAPTER TWENTY NINE

FASTER THAN LIGHT: INSTANTANEOUS COMMUNICATION ACROSS THE SOLAR SYSTEM

Introduction

All astronomy is history, as it assumes that the light being observed has left its source sometime in the past. The published predictions for the exact times of astronomical events and alignments are based on observations made on earth. Excitingly, 3-body alignment beams can be used to measure the velocity of a subtle energy beam, and hence, the speed of the mind's perception of communicating information can also be measured.

New and Full Moons

As in all dowsing or noetics, the mind's intent is important. I repeated the new and full moon experiments in Chapter 25, but this time before starting, I concentrated on 3-body interaction, with the relevant solar bodies. I have repeated minute by minute, accurate measurements of **L** on numerous full moons. Figure 29-1 is two of many examples showing the difference between the predicted time of full moon and the peak of L. In all cases, the detected peak was 5 - 10 minutes earlier than the published time of the full moon, which is depicted as the vertical lines in Figure 29-1. The 5 - 10 minute time difference is the same order of magnitude as the time sunlight takes to reach earth from the sun. This suggests faster than light communication of information by the mind.

Figure 29-1 Initial Examples of Faster Than Light Experiments

Experimental Protocols

In all the following alignment experiments, weeks after the experiment, and days after plotting the graphs, the actual distance between the earth and the planet under investigation, on the day of the experiment, was ascertained from a well-used, software program Stellarium, as well as using the US Navy astronomical tables. Similarly, prediction times were obtained by running Stellarium backwards, together with information from the International Occultation Timing Association.

Having established very accurate distance and times, and using accurate values for the velocity of light in a vacuum, the predicted time of conjunction could be calculated, and the discrepancy compared against the actual noetic peak value that had been measured, and plotted graphically.

Jupiter Alignment

What happens when accuracy is increased by using longer distances, and hence times, in the solar system? The following figures plot the experimental values of **L** for Jupiter, Saturn, and Neptune conjunctions. In all cases, the violet alignment beam (the horizontal line plotted above the peak in Figure 29–2) lasts for the duration of the peak, and changes **L** from white to violet on the Mager scale.

Figure 29-2 Instantaneous Communication Across the Solar System to Jupiter

As shown in Figure 29-2, the Jupiter peak was 45 minutes before the predicted time of conjunction, which is identical to the time light took to reach Earth from Jupiter.

Saturn Alignment

Using the speed of light in a vacuum, the time (reflected sun) light from Saturn took to reach an observer on Earth (on the day of the experiment) was 1 hour 18 minutes. Again, as shown in Figure 29-3, this time is in remarkable agreement with the 1 hour 19 minutes obtained from the noetic data plotted weeks earlier.

Figure 29-3 Instantaneous Communication Across the Solar System to Saturn

Neptune Alignment

I wanted to discover if the extended mind could receive information much faster than light from the furthest planet. There was a good opportunity in September 2016 when there was approximately a 50% transit of Neptune by the Moon. As is apparent from Figure 29-4, the graph shows all the same features as the previous alignments. The peak's maximum, as detected by the mind at 16:37:30, was 3 hours 51.43 minutes before the predicted time of the conjunction at 20:28:56, as given by the published tables listed earlier in this chapter. Light took 4.016 hours to reach Earth from Neptune at the time of transit. This demonstrates again instantaneous communication within a 3.95% experimental error.

Although the same methodology was used for all the above planetary alignments, a summary of these calculations for Neptune are set out in Tables 29-1 to 29-4, which also give an indication of the data's source. Table 29-4 confirms the conclusions of the previous tables to prove that the mind can communicate instantaneously to Neptune, with a better than 4% experimental error.

Figure 29-4 Instant Communication Across the Solar System to Neptune

Stellarium/ IOTA		
End of Transit	Start of Transit	Duration
20:52:43	20:05:10	00:47:33

Table 29-1 Start and end times of conjunction

	h:m:s
Predicted Time at Peak Conjunction	20:28:56
Time at Mind Measured Peak Conjunction	16:37:30
Difference	**03:51:26**

Table 29-2   Astronomical tables and mind detected peaks

US Navy			
Earth - Neptune distance at Conjunction	28.970749	AU	Speed of Light
1 AU =	149.597871	MioKm	metres per sec
Earth - Neptune distance at Conjunction	4333.96236	MioKm	299,792,458

Table 29-3 The Earth - Neptune distance at conjunction

	mins
Time Light takes to reach Earth from Neptune at Conjunction	240.942372
Time Difference between Predicted and Mind Measured Conjunction	231.430000
Difference	**9.512372**
% Difference	**3.95%**

**Table 29-4   Calculation of the time light takes to reach the Earth
from Neptune at conjunction**

It is also of interest to note that for Neptune in Figure 29-4, the peak of
L is 2.61% above the initial baseline; this is a similar order of magnitude
for Jupiter and Saturn. This would suggest that a 3-body alignment beam
has a constant "field strength". However, none of the above 3 conjunctions
had the centres of their 3 bodies in perfect alignment.

If rarer perfect alignments at conjunction were selected, it is possible
that the peaks of **L** would be higher, have a greater symmetry, and their
percentage increase would be more consistent. Even so, it is with some
confidence to postulate that a subtle energy 3-body alignment beam does
not diverge on its path across the solar system, and in this respect, it is
similar to terrestrial psi-lines.

Experimental error

After hundreds of years of astronomical measurements, most of the
reputable published mathematical tables used in this experiment are very
accurate. The sources are set out above, and include the velocity of light in
a vacuum, the distance between Neptune and the Earth at the time of the
experiment, and the predicted time of conjunction. The main sources of
experimental error are in the measurements of **L** and the time of
measurement.

As explained earlier in Chapter 24, **L** can be measured to ± 2 mm.
Although the radio clock used was accurate to better than 0.1 seconds, the
main problem was in synchronising the measurement of **L** with the clock.
Therefore, a conservative figure is that time could be measured to an
accuracy of ± 10 seconds. As is apparent from all the above graphs,
superimposing this experimental error has little effect on the findings and
conclusions.

Conclusions for Chapter

a. The extended mind can reach past Neptune,
b. Information detected by the mind can be transmitted not only faster than light, but instantaneously across the solar system.
c. As a consequence of this instantaneous communication of information and universal consciousness, *Inflation Theory* after the Big Bang may not be necessary to explain the current universe.
d. It would seem that the structure of the universe enables 2 or more bodies to "know" where they are in space-time. Similarly, 3-interacting bodies must also "know" when they are in alignment. They all have instantaneous communication.

The Way Forward

1. Investigate if it is possible to design and build an alignment beam detector.
2. Similarly, investigate if it is possible to modulate the alignment beam to superimpose the communication of additional physical or chemical information across the solar system.
3. A long-term objective could be to research if this technique can be extended galactically. The obvious challenge is that it would take over 4 years to assess results with a conjunction of the nearest star. However, this could be overcome by applying the technique to exoplanets with short orbiting times. The time difference between orbits should be similar to mind detected conjunctions, and those observed by astronomers, even if the measurements are 4 years apart.

CHAPTER THIRTY

THE MIND IN INTERGALACTIC SPACE

Introduction

Having proved in Chapter 29 that the mind can identify activity in the outer reaches of the solar system, I had to accept the implied challenge that "could the mind extend from the earth into intergalactic space?"

As illustrated on many occasions in this book, the results of quantitative study of subtle energies on earth are significantly affected by local forces and cosmic factors. These include the date and time of the measurement, the influence of moon, gravity and tides, electromagnetism, orientation, spin (including the earth's spin on its tilted axis and the earth's orbit of the sun), eclipses and conjunctions, energy lines, etc.

Based on the experiences of utilising as much scientific quantification as possible for researching forces locally and in the solar system, the following technique has been developed to imagine similar and relevant experiments taking place outside the solar system and our galaxy. With the correct intent, it is possible to visualise an experiment involving subtle energies associated with geometrical shapes in intergalactic space. The objective is to identify, for each experiment, which of the above listed forces is affecting earth-based findings, and hence, truly involve cosmic consciousness, and reflect the structure of the universe.

After reviewing the experiments highlighted so far in this book, several clues emerged that the mind could indeed extend outside the solar system. So, what quantifiable experiments, involving pure geometry, could be performed to demonstrate this objective, as scientifically, as possible?

The result of this preliminary work is the following possible list:

1. A dot
2. 1 line
3. One circle and perturbations in its aura
4. The 2-body separation issue
5. The 3-body interaction problem

6. Unravelling the factors causing perturbations in the measurements of psi-lines.
7. Investigating whether gravity, spin, or magnetism is involved in creating psi lines.

Experimental Protocols Adopted for the Mind's Intent

This chapter explains a useful technique whereby the effects of the Earth's environment are eliminated by visualising the experiment in intergalactic space, away from the Earth's environment.

The dowsing protocol adopted was to visualise the mind leaving the earth, going past the moon, and then towards the outer planets starting with Mars, and on towards the other planets. When mentally at Neptune, remind the mind that, as in Chapter 29, it has been there before. It is now possible to visualise reaching past the Kuyper belt, and looking down on the solar system and the ecliptic plane, whilst still moving out through our arm of the Milky Way, and eventually passing through our galaxy.

It is then possible to take the mind out of our galaxy towards and pass the Andromeda galaxy, so further galaxies are in the far distance. Finally, the mind is in intergalactic space where there is (possibly) no spin, electromagnetic forces, gravity, or orientation.

Whilst in that mental state, it is then possible to commence the following experiments.

Protocol for Actual Experimental Measurements

When undertaking physical measurements between a source geometry, its aura, or generated subtle energies, it is easier to mark dowsed boundaries on the paper on which the geometry is drawn. When taking measurements, a pencil or pointer should be moved towards the source with a second measurement made whilst moving away from the source. The boundaries being measured could have a thickness of about 1 millimetre, and a middle value can then be averaged. Initially, this technique is hard to learn, and it is also difficult for the mind to stay focussed in intergalactic space. With a few weeks' practice however, measurements become easier and consistent.

Attempting to take measurements from the centre of a circular object may not be very easy. In practice, it is easier, more accurate, and relevant, to measure from the circumference, and then add the size of the radius. One advantage is this avoids corrupting the geometric integrity of perfect

circles with rulers or tape measures, and avoids confusing noetic intent and visualisation of the pure geometric shape.

A Dot

Chapter 24 discussed the aura of a dot, and how this can be used as a measurement yardstick, L. Unfortunately, in intergalactic space, a dot remains as a dot with no additional lines or vortex. Being positive, this suggests that **L** only results from local forces. The dot is, therefore, irrelevant for quantitative experimentation into consciousness in outer space! However, this observation suggests that in intergalactic space, a different geometrical transformation between a physical object and the mind's perception is involved. So varying techniques have been adopted for quantitative mind research involving dowsing geometry.

1 Line

Chapter 3 discussed how on earth, a dowsed line is transformed into 2 groups, each group comprising 7 or 9 parallel lines either side of the source line, depending if the line was physical or abstract geometry. These 7 or 9 parallel lines are affected by, and probably created by, the local forces such as varying gravity and spin, which also affect their separation distances.

In intergalactic space, a source line of length **l** (not to be confused with the yardstick **L**) is transformed into one parallel line either side of the source line, and of equal length, **l**. Using the observations set out in Table 30-1, the diamond data points in Figure 30-1 plot the separation distance, **d**, between the perceived noetic line and the source line, against the length of the source line **l**.

Figure 30-1 Lines in Intergalactic Space

The graph demonstrates a very good fit between this data obtained experimentally noetically, and the heuristic power equation superimposed.

$$d = 0.5 * l \wedge \varphi / 2 \qquad (i)$$

Equation (i) only involves the two length variables and the universal constant Phi (**φ**). As equation (i) was only discovered many days after the data in Table 30-1 was collected, the accusation that the observer was dowsing what he was expecting is eliminated.

Length of Line	Separation Distance	
L	d	d/L
cms	cms	
0.5	0.2	2.5
1.3	0.55	2.36
4.2	1.2	3.5
5	1.8	2.78
12	3.7	3.24
20	5.7	3.51
29	7.5	3.87
40	10.2	4.59
50	11.5	4.35
65	14.23	4.57
80	17.43	4.59
91.8	20	4.59
100	20.2	4.95

Table 30-1 The Separation of Noetic Lines from their Source

One Circle and its Aura

As discussed in Chapter 8, normal earth bound dowsing of an abstract or physical circle of radius **r** results in a core aura whose boundary is a concentric circle with a radius **a**; where **a** > **r** . The problem is that the value of **a** varies in time depending on local forces, with the data changing during each day, week, month or year. The relationship is approximately linear of the form

$$a = c * r + b$$

where c is a variable constant that depends on the local forces. Another problem is that b $\neq$ 0, which is an error, as observations show that as **r** → 0, **a** → 0.

An important additional relevant factor is that an abstract circle (such as drawn on paper) has 9 concentric components to its aura, whilst a physical circle has 7 components. The core aura discussed above is the innermost perceived aura. It could be significant that the quantum mind perceives identical auras for both abstract and physical sources. Does this tell us anything significant about consciousness and the structure of the universe?

In intergalactic space, a circle has only 2 concentric auras, and these correspond with the inner 2 auras of the 9 components as detected on earth. Table 30-2 is the data for the inner core aura, which is plotted as the

dots in Figure 30-2. This shows the relationship between the radius of the noetic circular aura **a** and the radius of the source circle **r**. Superimposed is the lower line which is a simple linear plot of

$$a = 2r \qquad\qquad (ii)$$

which illustrates a good fit. This demonstrates that the mechanism that generates a core aura produces a linear relationship, whereby the perceived radius is twice that of the source radius. Ratios of 2:1 are common in this research.

Table 30-3 summarises the noetic measurements for the outer aura, and is also plotted in Figure 30-2 as the square data points. This demonstrates a very good fit to the heuristic power law equation (iii) plotted as the upper line.

$$a = \varphi * r \,\char`\^\, \sqrt{\varphi} \qquad\qquad (iii)$$

which again involves the universal constant Phi, in this case both as a constant as well as a power. As above, this equation was discovered days after the measurements were dowsed, and overcomes any accusations of self-deception. Because of the great dissimilarity of equations (ii) and (iii), the assumption is that the process that creates outer auras is very different from the one creating core auras, even though they both have a cosmic cause.

Diameter of Circle	Radius of Circle	Radius of **Core Aura** measured from Circumference of Circle								Average of Core Aura measured from Circumference of Circle	Average Deviation	% Deviation	Radius of Core Aura measured from Centre of Circle	a/r	
		1	2	3	4	5	6	7	8						
D cms	r cms	cms	cms	cms	cms	cms	cms	cms	cms	cms			a cms		
0.52	0.26	0.26	0.30	0.28	0.25	0.25	0.27	0.25	0.25	0.26	0.01	5.57%	0.52	2.014	
2.27	1.14	0.70	0.90	0.90	0.90					0.85	0.08	8.82%	1.99	1.749	
3.30	1.65	1.20	1.30	1.20	1.30					1.25	0.05	4.00%	2.90	1.758	
5.75	2.88	2.30	2.30	2.40	2.40	2.00				2.28	0.11	4.91%	5.16	1.793	
8.20	4.10	4.00	3.90	4.00	4.10	4.00	4.20	4.10	3.90	4.03	0.08	2.02%	8.13	1.982	
10.04	5.02	5.20	5.50	5.40	5.30					5.35	0.10	1.87%	10.37	2.066	
12.03	6.02	6.00	6.10	6.20	5.90	5.80	6.20	5.70	6.00	5.99	0.14	2.35%	12.00	1.995	
13.80	6.90	6.70	7.30	7.80	7.10	7.30	6.90	7.10	6.90	7.14	0.25	3.46%	14.04	2.034	
16.20	8.10	7.60	7.10	6.50	6.60	7.50	6.00	7.60	7.50	7.05	0.51	7.27%	15.15	1.870	
17.80	8.90	7.00	7.10	7.90	6.50	6.90	6.90	7.00	7.00	7.04	0.23	3.29%	15.94	1.791	
20.04	10.02	10.20	12.10	11.60	10.90					11.20	0.65	5.80%	21.22	2.118	
23.10	11.55	10.00	9.70	10.70	10.20	9.00	9.80	10.40	10.70	10.06	0.44	4.35%	21.61	1.871	Ave
26.00	13.00	14.80	14.70	14.40						14.63	0.16	1.06%	27.63	2.126	1.938
42.00	21.00	20.00	19.50	21.00	20.00	20.50	20.70	19.50	20.40	20.20	0.45	2.23%	41.20	1.962	

Table 30-2 The Separation of Core Auras from their Source Geometry on Earth

Figure 30-2 Auras of Circles in Intergalactic Space

Diameter of Circle	Radius of Circle	Radius of **Outer Aura** measured from Circumference of Circle								Average of Outer Aura measured from Circumference of Circle	Average Deviation	% Deviation	Radius of Outer Aura measured from Centre of Circle	a/r
		1	2	3	4	5	6	7	8					
D cms	r cms	cms	cms	cms	cms	cms	cms	cms	cms	cms			a cms	
0.52	**0.26**	0.67	0.65	0.66	0.60	0.64	0.67	0.65	0.61	0.64	0.02	3.16%	**0.90**	3.476
2.27	**1.14**	1.90	2.00	2.20	2.10	1.90	2.00	2.00	2.00	2.01	0.07	3.42%	**3.15**	2.773
3.30	**1.65**	1.90	1.70	1.80	1.80	1.22	1.60	1.90	1.70	1.70	0.15	8.66%	**3.35**	2.032
5.75	**2.88**	3.10	3.20	3.20	3.30	3.80	3.20	3.15	3.80	3.34	0.23	6.82%	**6.22**	2.163
8.20	**4.10**	5.00	5.60	5.00	5.20	5.20	5.20	5.30	5.50	5.25	0.16	3.10%	**9.35**	2.280
10.04	**5.02**	7.50	7.00	7.50	6.50	8.05	8.05	8.05	8.05	7.59	0.46	6.10%	**12.61**	2.511
12.03	**6.02**	9.50	9.70	9.90	9.80	9.80	9.60	9.50	10.00	9.73	0.15	1.54%	**15.74**	2.617
13.80	**6.90**	14.60	14.00	14.80	14.60	14.20	14.40	13.90	13.70	14.28	0.33	2.28%	**21.18**	3.069
16.20	**8.10**	16.50	16.30	16.50	15.00	17.30	14.40	17.30	17.00	16.29	0.79	4.87%	**24.39**	3.011
17.80	**8.90**	15.10	16.60	16.50	14.50	15.60	17.70	17.00	16.90	16.24	0.88	5.41%	**25.14**	2.824
18.25	**9.13**	18.40	18.40	18.45	18.35	19.00	18.30	18.50	18.30	18.46	0.14	0.78%	**27.59**	3.023
20.04	**10.02**	18.80	19.00	19.30	18.60	20.50	20.40	20.80	21.00	19.80	0.88	4.42%	**29.82**	2.976
23.10	**11.55**	25.00	26.00	24.50	24.60	24.00	25.10	24.70	24.80	24.84	0.40	1.60%	**36.39**	3.150
26.00	**13.00**	29.40	28.30	29.10	32.00	30.70	30.50	30.70	30.00	30.09	0.89	2.95%	**43.09**	3.314
42.00	**21.00**	60.10	59.30	59.80	60.00	60.80	60.70	59.80	61.00	60.19	0.48	0.80%	**81.19**	3.866

Ave 2.872

Table 30-3 The Separation of Outer Auras from their Source Geometry in Intergalactic Space

In normal earthbound dowsing, the shape of the aura of a circle, unexpectedly, is not an exact concentric circle. An accurate value of **a** can only be obtained after taking an average of about 20 points around the circumference. This is demonstrated in Figure 30-3

As is apparent, the size and shape of the aura depends on the orientation and direction of the measurement. Aura maxima occur at 0°, 135°, and 270°. i.e. north, south-east, and west. This suggests that the earth's magnetic field extends auras towards the north pole; the earth's rotation on its axis from west to east extends auras to the west; whilst a Coriolis effect could be the vector force causing the south-east maxima.

In comparison, Figure 30-4 shows the aura for the same sized source circle in intergalactic space. This is a near perfect concentric circle with none of the above variations, proving once again that the earth's local forces affect observations and perception.

Figure 30-3 Core Aura of a Circle on Earth

Figure 30-4 Core Aura of the Same Circle in Intergalactic Space

2 Interacting Circles

Chapter 15 demonstrates that 2-bodies in close proximity interact to produce a complex dowsable pattern. It comprises a combination of lines, subtle energy beams, vortices, Cornu spirals, null points, resonance effects, and bifurcation.

When considering reasons for the perturbations between the theoretical equation and the actual experiment results for 2-body interaction, the reasons were put down to local effects caused by the earth's environment such as magnetism, the earth's spin, and the earth's gravity. In addition, it was only possible to obtain heuristic equations, which did not totally rely on universal constants.

Exceeding the maximum separation distance, S_{max} causes all these subtle energies to disappear. However, how does one find an equation to determine the value of S_{ma} only involving universal constants?

Attempting to discover this with normal earth bound observations is very difficult, because of inconsistent and unrepeatable results producing formulae containing arbitrary constants, which change in time, and a curve that does not go through the origin, which is illogical.

In comparison, Figure 30-5 illustrates the results of repeating the identical 2-circle experiment with the mind's intent in intergalactic space,

thereby eliminating all local forces that were causing perturbations. It is a graph of the relationship between the maximum separation distance S_{max} between 2 interacting circles, and their radii, **r**. This demonstrates a very good fit between the circular data points, as set out in Table 30-4, and the heuristic power law equation (iv) plotted as the lower line.

$$S_{max} = 2 \cdot r^{\varphi} \qquad \text{(iv)}$$

Figure 30-5 The Formula for Maximum Separation of 2 Circles

Diameter of Source Circle	r Radius of Source	Smax (Circumf to Circumf)	Smax (measured from Centre to Centre)
cms	cms	cms	cms
26	13	124.5	150.5
23	11.5	102.1	125.1
20.04	10.02	82.6	102.64
18	9	63.2	81.2
16.3	8.15	67	83.3
14.15	7.08	52.3	66.45
12.04	6.02	41.3	53.34
10.05	5.03	26	36.53
8.2	4.1	18	26.13
5.75	2.88	24	29.75
2.3	1.15	2.5	4.83

Table 30-4 The Maximum Separation between 2 Interacting Circles

The measurements for equation (iv) were taken from circumference to circumference. If measurements are taken from centre to centre, the separation formula becomes

$$S_{max} = 2(r + r^{\varphi}) \qquad \text{(v)}$$

Equations (iv) and (v) only involve the universal constant Phi (φ) as an exponent, and do not involve any arbitrary constants. These equations are, therefore, both absolute and universal. It is surprising that only the dimension of length appears in all these equations (i) – (v); these being the radii of the source circles and their separation.

No other forces, factors, or dimensions are implied. Does this suggest that only the geometric structure of space-time is involved in producing the basic findings for 2-body interaction?

3 Interacting Circles

As detailed in Chapter 16, three aligned objects produce a subtle energy beam, where it was also explained that unlike 2-bodies, that need to be in close proximity to interact, 3-bodies only interact if they are sufficiently separated. However, as before, it is difficult to establish a mathematical formula because of earth bound perturbations producing

seemingly inconsistent results. Experimental results from about 10 year's ago suggested that auras are involved.

In summary, 3-bodies interact when:

1. their centres are in a straight line, and
2. adjacent circles are separated by a distance greater than S_{min}.

So how does one find S_{min}?

Diameter of Source Circle	r Radius of Source	S_{min} (Circumf to Circumf) between each pair of adjacent Circles			Distance between outer Circumfs		S_{min} (measured from Centre to Centre) of Outer 2 Circles	Comments
		1	2	Total	Theory	Actual		
cms	cms	cms	cms	cms	cms	cms	cms	
16.30	8.15	67.0	67.0	134.0	182.90	183.50	150.30	Type 4 Mauve
12.04	6.02	40.8	41.5	82.3	118.42	118.00	94.34	3 CD's, Type 4, Mauve, Same as Paper
8.20	4.10	19.0	18.8	37.8	62.40	62.50	46.00	Type 4 Mauve
2.20	1.10	2.4	2.4	4.8	11.40	11.50	7.00	3 £1coins, Type 4, Mauve, Same as Paper

Table 30-5 The Minimum Separation between 3 Interacting Circles

In intergalactic space, the answer is readily found. Table 30-5 summarises experimental measurements of the shortest distance between 3 linearly aligned bodies in order to produce the 3-body alignment beam. The 3 objects used in repeated experiments included coins, CD's, and duplicate circles drawn on paper. As usual, there is no difference in results.

Figure 30-6 Minimum Separation Distances for 3 Bodies to Interact

If the 3 objects are closer, no beam is produced. This data is plotted as the circles in Figure 30-6. Superimposed is the curve which is a plot of the heuristic power law equation

$$S_{min} = 4(r + r \wedge \varphi) \qquad (vi)$$
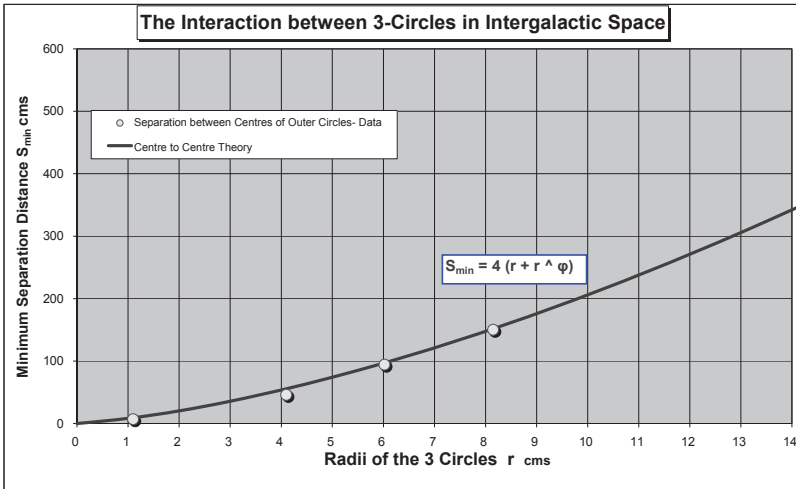
This is a very good fit, and is exactly twice the value of equation (v), which related to the maximum separation of 2 interacting circles. This complimentary result proves that the 3-bodies only interact when their separation is greater than the sum of their outer aura plus their radii, so there is no 2-circle interaction as described above.

As is apparent, these initial results are for objects up to a radius of 8 cm. Further research, and developed protocols, is obviously required for larger objects to prove if equation (vi) still applies.

Psi-lines Visualised in Intergalactic Space

Chapter 22 gave extensive and comprehensive details of psi-lines on earth. It was also shown that visualising the creation of a psi-line at the north or south poles significantly simplified the structure of the psi-line. Figure 30–7 illustrates one end of this simplified psi-line that comprises a spiral and 3 lines.
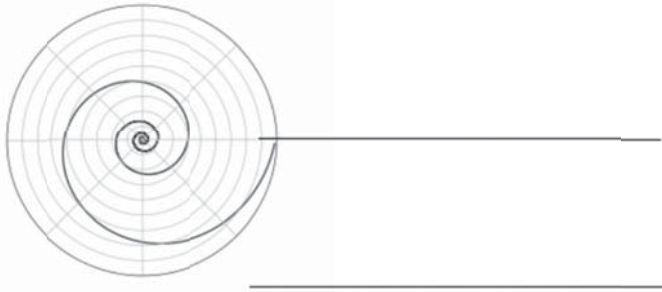
Figure 30-7 A Psi-Line at the Earth's Poles

There is no Type A spiral, only Type B. The entry point for the Type B conical helix is, as usual, from the centre of the psi-line, along its axis, facing the other terminating spiral. The axis of the conical helix can be made at any angle, not just vertical. This confirms that gravity affects the orientation of the conical helix's axis. The above properties of the Type B spirals are the same at both ends of the psi-lines.

The findings suggest that on earth, gravity, spin (the earth spinning on its axis plus the earth's revolution around the sun), and electromagnetic forces are involved in part of the structure of psi-line creation. The remaining parts are as a result of the mind interfacing with the structure of the cosmos. However, once again theoretical considerations were hampered by local forces causing complex perturbations.

Using the protocol described at the beginning of this chapter, it is possible to create a psi-line whilst visualising that it is being created in intergalactic space, where there is no gravity, spin, or electromagnetism. The central of the 3 component lines that appear on earth is not present in intergalactic space. Figure 30-8 illustrates this psi-line comprising only 2 sub lines. This suggests that the central line is caused by gravity and/or magnetism, and not spin, because the central line was present at the pole where the effect of spin is minimal.
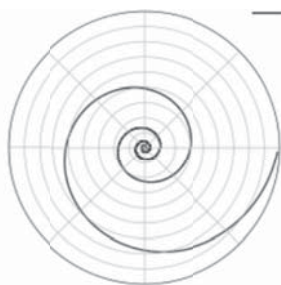
Figure 30-8 A Psi-Line Visualised in Intergalactic Space

Whilst the mind is in intergalactic space, it is also possible to perform further experiments by isolating the effects of magnetism. Place three strong magnets around the centre of one spiral, to create an artificial north pole in an otherwise empty space.

It is found that the psi-line and its terminating spirals are unaffected. There are still only 2x sub-lines; the entry point to the Type B spirals is still along the psi-line's axis through the two spirals centres, and is unaffected by magnetism. There are no Type A spirals created. Magnetism, therefore, has no perceived effect on psi-lines in intergalactic space, and this is consistent with earlier findings that the earth's spin creates Type A spirals. A similar inference is that on earth, the central of the 3x constituent sub-lines is not produced by magnetism but by gravity. Spin was eliminated by the experiments at the earth's poles, but the central line was still created.

Chapter Summary

Although counter-intuitive, many published papers have proved that scientific experiments are affected by the act of observation, as well as the mind being affected by local astronomical forces and factors, such as gravity, electromagnetism, spin, and orientation. This chapter details the ability of the mind to filter out all of these local factors, and visualise experiments as if they were being undertaken in intergalactic space.

Every experiment demonstrates quantitative results that are simple equations obeying power laws that involve the universal constant phi (φ) and no arbitrary constants. Examples are $d = 0.5 * l \char`\^ \varphi /2$, $S_{max} = 2 . r \char`\^ \varphi$, and $a = \varphi * r \char`\^ \sqrt{\varphi}$.

These formulae cannot be random results. The implications are (1) that phi forms part of the structure of space-time, (2) the important quantified

discovery that the mind can interface with the fundamentals of space-time and the cosmos. The latter concept supports ancient Eastern philosophy, although it is alien to traditional Western science.

Conclusions

The above experimental results lead to the following conclusions:

1. The mind is connected to the cosmos. This is compatible with ancient Eastern philosophy.
2. As long suspected, Phi (φ) is part of the structure of the cosmos. Several simple formulae have been discovered that involve the mind linked to the universal constant phi (φ), no arbitrary constants, and a 2:1 ratio. These are summarised below:-

    - $d = 0.5 * l \verb|^| \varphi / 2$ (i)

    The length of a source line, and the separation distance of the subtle energy line generated.

    - $a = 2r$ (ii)

    The radius of a circle's core aura.

    - $a = \varphi * r \verb|^| \sqrt{\varphi}$ (iii)

    The radius of a circle's outer aura.

    - $S_{max} = 2(r + r \verb|^| \varphi)$ (v)

    The maximum distance between 2 bodies for interaction, i.e. overlapping auras.

    - $S_{min} = 4(r + r \verb|^| \varphi)$ (vi)

    The closest 3 bodies can interact, i.e. auras do not overlap.
3. The discovery of the above equations may be analogous to Einstein's famous equation $E = mc\verb|^|2$, which linked mass to energy. It is elegant, simple, has no arbitrary constants, but a universal constant **c** (the speed of light in space). The above equations link consciousness to the structure of the universe, have the same characteristics of elegance, simplicity, with no arbitrary constants, and include a universal constant φ (Phi).
4. The results confirm that the perturbations when dowsing on earth are due to astronomical forces and local factors such as gravity, electromagnetic forces, spin, and orientation.
5. Traditional dowsing is well known to be variable due to personal effects as well as the local environment. This intergalactic technique helps to eliminate these perturbations, and is a powerful research tool for finding the structure of the universe.

The Way Forward and Suggested Future Research Projects

1. Why is φ (Phi) linked to consciousness when lines and circles are involved?
2. Further research, and developed protocols, are obviously required for larger objects, which are greater than 8 cms, to prove if equation (vi) still applies.
3. Experiments should be repeated to confirm if the same results apply to all geometrical shapes.
4. Experiments should be repeated to see if the same results apply to physical bodies, as well as to abstract geometry.

CHAPTER THIRTY ONE

ENTANGLEMENT OF LARGE SIZED OBJECTS

Introduction

The term "entanglement" is usually associated with quantum physics, and restricted to fundamental particles. For example, if two electrons or photons emanate from the same atom and fly off in different directions, they remain in contact with each other when separated by vast distances. If something happens to one particle, the same thing will happen to the other, whatever the distance. This "spooky" action at a distance has been well known in the quantum world for over 100 years, but remains an unexplained phenomenon

The objective of this chapter is to reproduce quantum entanglement into the everyday macro world. We now show how it is possible for 2 large physical bodies to communicate information to each other over considerable distances, without any apparent intermediate medium. It is surprising that there are so many different ground-breaking examples of macro entanglement as outlined below.

Experimental Protocol

These experiments are designed so they can be easily reproduced noetically by a layperson, who is aware of subtle energies and auras of physical bodies. Initially, auras are being used for quantifying the effects of entanglement. Prior to the experiments, checks should be made that no existing subtle energy lines exist in the vicinity that could interfere with the experiment's findings. Existing lines should be either avoided or deleted by the mind's intent.

For the following experiments, it is necessary for several people to measure the auras of the 2 entangled objects, and demonstrate that the physical properties being remotely entangled include the transmission of pressure, the size and orientation of auras, and magnetic effects.

Common to all the entanglement findings is the involvement of a standard Type 8 **psi-line**, with Type 9 nodes. If an existing psi-line is not

available, then a **common source** is essential for 2-body macro
entanglement. This requirement is compatible with quantum entanglement.

All of the experiments produce qualitative results that are a scientific
demonstration of macro entanglement.

Short Range Entanglement

2 Body Entanglement and auras

Chapter 15 showed that short-range entanglement naturally occurs for
any 2 large bodies when their auras are in contact. In this case, a complex
pattern of subtle energies is produced, and involves the 2 bodies being
linked by a different subtle energy and properties, compared to those
subtle energies responsible for long-range entanglement.

Figure 31-1 Pictorial Representation of the Auras for Two Interacting Objects

Figure 31-1 illustrates the effect on auras by two circular objects,
which are depicted as the central circles. It is important to realise that the
two objects can be either solid, such as two coins, or abstract such as two
circles drawn on paper. For ease of explanation, only the left hand circular
bands illustrate the effects, but these effects equally apply to the right hand
object. When the two bodies are separated, so they do not interact, the first
ring on the left of Figure 31-1 illustrates the initial extent of their auras.
The other 2 outer bands are not yet created. When the two objects are
brought sufficiently close so they interact, their auras double in size, as
shown by the combination of the two inner bands illustrated in Figure 31-
1. That entanglement is taking place can be demonstrated by putting
pressure on the right hand object. The aura of the left hand object
immediately increases its size to that of the outer third ring; the exact size
being a function of the pressure applied.

Increase in left hand body's aura size when interacting, but with no pressure	Increase in right hand body's aura size when interacting with 2.9gms pressure on partner
1.97	1.52

Table 31-1 Increase in Aura Size when in Entanglement

The quantitative results of this experiment have a high accuracy, with an error rate of between 6% and 8%. Table 31-1 gives a brief summary of how the auras expand. As is apparent, compared to their isolated state, auras double in size when near their optimum interaction separation distance. When an arbitrary weight of 2.9 gms was placed on one object, the aura of the other object immediately increased its size by about 1.5 times. The aura of the left hand object would further increase, if even greater pressure is put on the right hand object.

It should be pointed out that the above examples of entanglement only apply over relatively short distances, whilst the two objects are interacting. This is obviously different from the generalised quantum case of long-range entanglement, which applies irrespective of the separation distance between the two objects.

Basic Data		mms
Diameter of £1 coin	D	23
Radius of £1 coin	R	11.5
Distance of core aura from circumference	r_a	8.3
Distance of core aura from centre of circle	r_a+R	19.8
Separation Distance between the centres of the 2 circles	S	62

Table 31-2 Parameters and Quantitative Findings for Entanglement in a specific 2- Body Interaction

	Core Aura of One Isolated Coin	Core Aura when 2 Coins are Interacting	Core Aura when 2.9 gms Placed on one Interacting Coin
	mms	mms	mms
	9	11.5	25
	8	17.5	26
	7	17.5	27
	8	17	27
	8	18	24
	9	17.5	23
	9	17	22.5
	9	16	27.5
	8	16	23
Average	8.3	16.4	25
Deviation	0.59	1.3	1.67
% Deviation	7.11%	7.88%	6.67%

Table 31-3 Data findings for a Specific 2-Body Interaction

Tables 31-2 and 31-3 illustrate the quantitative findings for the study of entanglement in two-body interaction. The same results are obtained if two £1 coins are used, or if equal size circles are drawn on paper around a £1 coin. Measurements were taken from the circumference of the circles, as they are more accurate than locating centres of the objects.

Tree of Life Entanglement - Mood/Thought Transference

As explained in Chapter 7, the Tree of Life has interesting properties, one of which is the apparent ability to transfer moods/thought between people. A simple demonstration, involving two people, is to create a Tree of Life for person A. By measuring his or her resistance to downward pressure, initially establish the normal strength of an outstretched arm of person B when away from the Tree of Life. Person B then stands on spiral 2, (Chokmah) of person A's Tree of Life. If person A has strong negative thoughts, such as a bereavement, bad health, financial stress, etc., it seems to affect adversely person B, both mentally and physically, as muscle testing now shows weakness and little resistance.

This demonstration suggests the existence of thought and mood transference when standing on a spiral of someone else's tree of life pattern. Without realising this, people must experience this many times

each day. It suggests that we all interact with each other, we are all connected by the structure of the universe, and, if possible, one should avoid negative people, so not to be affected by their negativity, even inadvertently.

Long Range Entanglement

Below are detailed several ways of obtaining long range non-quantum entanglement of large physical objects.

Natural subtle energy line with nodes

Determine noetically, or by dowsing, the positions of two suitable nodes on a natural earth energy line. Place two dissimilar quartz crystals on each of these two nodes, which must be situated at least several metres apart. Stress one crystal by applying pressure with a screw clamp. The greater the pressure on that object, the greater the size of its aura. As the pressure increases on one crystal, the size of its core aura should be measured. The exciting observation is that, as the pressure is increased on the clamped crystal, the size of the aura of the "free" crystal increases in sympathy. A good correlation between the auras of the two crystals is obtained.

2-Bodies on a Mind Generated Psi-Line

By placing 2 **dissimilar** objects on a mind created psi-line the aura of both increases as pressure is increased on any one of the objects.

The next development is to take two pebbles, selected randomly, e.g. from a beach, and separate them by an arbitrary distance of at least 12 metres. Produce a mind generated psi-line with the axes of the terminating spirals coinciding with each of the 2 pebbles. The two pebbles become linked via the mind created psi-line. Physical pressure, by means of a screw clamp, can then be applied to one pebble. As in the experiment above, the auras of the two pebbles increase together as pressure is applied to only one of them. The psi-line would seem to be transmitting information between the two pebbles.

Psi-line and Thought Pressure

The above experiment can be developed further by repeating it, but without the physical clamp. Link the two pebbles via a psi-line, created by

one dowser. Create "thought pressure" on one pebble by means of the intent of another dowser. As before, this experiment produces the same entangled results. The auras of both pebbles increase in unison: the auras being measured by a team independent of the above two dowsers who are creating the psi-line and the experiment.

It would appear that the mind, with appropriate intent, can not only create a psi-line that carries information, it can also cause an inanimate object to respond to thought, as if the latter was a physical effect. This phenomenon is usually associated with the concept of displaying consciousness. It would also seem that an inanimate object cannot tell the difference between a physical or mental stimulus. Similarly, the entangled partner is unaware if the information it receives from its twin is caused by a physical or consciousness effect.

Separating a Leaf Cut in Two

It has long been known that a live leaf torn in two, and then separated, creates its own psi-line between both of its parts. These two parts become entangled automatically without the involvement of an existing subtle energy line, or a dowser's intent. However, it is interesting to note that this psi-line created by the separated leaves has similar properties as the psi-line created by a dowser in the above experiments. Both plants and animals seem to possess a similar ability to create psi lines.

Divided Single Crystal

The above experiment can be repeated, but using a divided inanimate object instead of a torn leaf. When a crystal, such as quartz, is broken in two, and each part is separated by at least several metres, both parts automatically become entangled and create an interlinking psi-line. Automatic entanglement can be demonstrated by clamping one of the crystals, and drawing on paper the boundaries of the aura of the other crystal before and after clamping.

Entanglement of the Two Spirals Terminating Psi-Lines

Using the ability of the mind to visualise intent in both local and remote locations, the following experiments illustrate that magnetism can be used to detect entanglement.

Create locally an approximate east-west psi-line. Place 3 strong magnets around one terminating spiral, so that the artificial north-pole is to

the real south of that spiral's centre. The Type A spiral now has an entry from the south (i.e. the artificial north pole), but the Type B spiral is unaffected and its entry remains the same as before (i.e. from the psi-lines central axis). The conclusion is that Type A spirals are affected by magnetism, but Type B spirals are unaffected by magnetism.

For the other psi-line terminating spiral, which should be many metres away from the above magnets, confirm with a compass that there are negligible affects from the artificial magnetism, and that magnetic north is in its normal direction.

It is found that the Type B spiral entry remains the same (i.e. its entry is from the centre of the psi-line along its axis, facing the other terminating spiral). However, entanglement is demonstrated for the second Type A spiral (which is well away from the artificial magnets), as its entry has changed from the north of the spiral's centre, and has become the same as the other Type A spiral, which now has its entry from the south of the spiral's centre. This experiment demonstrates that psi lines can communicate magnetic effects.

The latter effect of magnetism has led to a convincing example of remote macro entanglement. Changing the local magnetic field near the centre of one of the psi-line spirals, changes the orientation of its entry point so it is "north" of the artificial magnetic field's north pole. The other terminating spiral, which can be kilometres away, and, therefore, not physically affected by the weak remote magnet, will instantly change its orientation, so it is exactly the same as its remote psi-line terminating partner.

Sheet of Paper Torn in Half

One sheet of A4 paper is all that is required to generate a 2-body entanglement psi-line with nodes. A common source can be obtained by tearing an A4 sheet of paper in half to form two A5 sheets. A standard Type 8 psi-line with Type 9 nodes, that mediates the entanglement, is automatically created only after the 2 pieces of paper, from the same source, have been separated sufficiently, so there is no short-range 2-body interaction, as discussed above.

Until this point is reached, no entanglement occurs. This is illustrated in Table 31-4, which shows, for one of these experiments, how separation increases until a psi-line with at least one node is created. In this case, it is noted only when the 2 sheets of paper are separated by a psi-line of 1.56m does the aura of each sheet of paper increase significantly (typically by about 33%) indicating that entanglement has taken place. This is much

quicker and easier than the previous method of detecting a psi-line having Type 8 subtle energy with 9 nodes.

Location of the 2 x A5 sheets	Separation Distance between the 2 Sheets	Core Aura measured from edge of narrowest side of each A5 sheet		Comments
	metres	A mm	B mm	
Superimposed	0	135	135	No psi-line created
Sides Touching	0	134	136.5	No psi-line created
Separated	1.36	133.7	129.0	No psi-line created
Separated	1.56	176	178	Psi-line created

Table 31-4 A Simple and Quick Method to Prove when Entanglement has been Reached

Two sheets of paper were labelled A and B. Sheet A had a weight placed on it, and the auras of both sheets were measured in unison. Although auras are 3-dimensional, a 1-dimensional measurement is sufficient to demonstrate expanding auras. Measurements were made from the middle of the shortest side (14.5cm) of the A5 sheets. Each measurement was repeated 4 times: twice by moving a pointer outwards from the source until the core aura boundary was detected, and twice by moving the pointer inwards towards the boundary of the core aura.

Sheets A and B were then separated sufficiently far apart so that no 2-body interaction occurred. In this experiment, not only was a sufficiently large separation of 13.8 metres chosen, but also 3 walls existed between the 2 sheets of paper. This demonstrates that even with obstacles, as well as sufficiently large distances, entanglement occurs.

As measurements of subtle energies and psi-lines are affected by many factors, including the rotation of the earth and the earth's orbit round the sun, it is essential to collect data as quickly as possible. For example, the same experiment performed again 2 hours later had auras 20 mm shorter.

Weight on Sheet A	Core Aura of Sheet A					Core Aura of Sheet B				
Grams	1st mm	2nd mm	3rd mm	4th mm	Average mm	1st mm	2nd mm	3rd mm	4th mm	Average mm
0	110	111	111	111	**110.75**	111	110	111	110	**110.50**
22	120	119	119	119	**119.25**	117	116	117	116	**116.50**
43	124	123	126	125	**124.50**	126	125	124	124	**124.75**
101	128	125	126	125	**126.00**	124	124	125	125	**124.50**
201	135	132	134	136	**134.25**	135	136	135	134	**135.00**
402	146	147	147	146	**146.50**	147	146	147	145	**146.25**
828	150	150	149	151	**150.00**	149	150	149	152	**150.00**
1928	278	277	274	277	**276.50**	278	273	274	276	**275.25**
2756	418	428	415	425	**421.50**	418	442	439	438	**434.25**
3890	680	684	669	672	**676.25**	670	672	673	674	**672.25**
4718	734	734	737	736	**735.25**	732	734	735	731	**733.00**

Table 31-5 The Expansion of the Auras of Sheets A and B as the Weight on Sheet A is Increased

Table 31-5 sets out the details of the above experiment, and shows that the range of weights used was 0 – 4,718 grams, which produced a 7-fold increase in the auras of both sheets A and B. (As these experiments were performed on different dates to those in other tables, they produced slightly different values for aura sizes).

Figure 31-2 is a graphical representation showing the increased size of auras with increased weights on one of the sheets of entangled paper. The curves plotted for both sheets A (the dot data marker) and B (the circle marker) are, within experimental error, superimposed. A remarkably accurate result that demonstrates entanglement has taken place.

At present, the auras involved in these experiments can only be detected by the mind. This suggests that a universal consciousness is involved in entanglement; a conclusion drawn in several other experiments.

Experimental Error

As it is possible to detect and measure subtle energies to within ±2 mm, the worst cases in Table 31-5 of the 4 similar readings is better than ±2%. The major source of experimental error is in noetically detecting the boundary of the core aura. Even so, the highest variance of similar figures in Table 31-5 is about 3%. As the weights were measured on an up-to-date electronic machine, their accuracy is well within this range.
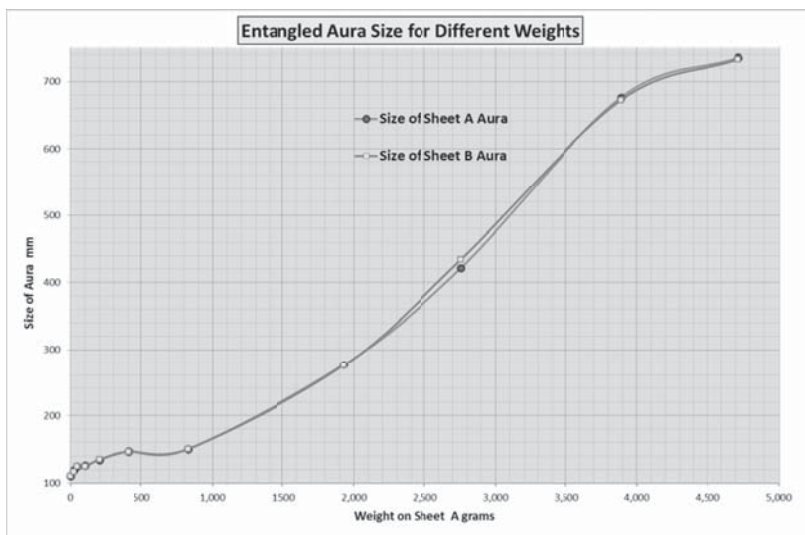
Figure 31-2 The Increase in the Size of Auras with Increased Weight on One Sheet
of Entangled Paper

Summary and Conclusions

Traditionally, entanglement has been associated with particles at the quantum level. Entanglement has now been created by linking two large objects. Naturally occurring entanglement of two objects from a common source has been demonstrated by tearing a leaf in two, or dividing a quartz crystal into two pieces.

Entanglement has also been demonstrated between two dissimilar objects, such as two pebbles or glasses of water, by placing them on subtle energy line nodes, or linking them by mind created psi-lines. Transmitted physical properties include pressures and vorticity, with their effects on auras being measured. The similarities to quantum entanglement are also noted.

Psi-lines that contain nodes are required for entanglement. Objects that come from the same source produce such a psi-line when sufficiently separated. As illustrated in Figure 31-2, it cannot be a coincidence that, to a very high degree of accuracy, the measurements for the auras of entangled objects are identical.

As proven in Chapter 29, Type 8/9 subtle energy can instantly communicate information across the solar system. As psi-lines contain

Types 8 and 9 subtle energy, entanglement information is instantaneous. This is identical to quantum entanglement.

These results strongly suggests that, once again, the mind, consciousness, and psi-lines are intimately connected to the structure of the universe. This chapter should provide relevant data for a theoretical explanation of the above experimental findings for psi-lines.

The Way Ahead

1. As a result of my 12-year experience of entanglement experiments, it is felt that these findings can be generalised, so that further experiments demonstrate that any 2 objects from a common source automatically generates a psi-line with nodes that enables entanglement to take place.
2. Psi-lines have a complex fractal structure that keeps their diameter constant, and their path, preferentially, in a straight line. Future research is required to find if quantum entanglement has the identical mechanism.
3. All of the above experiments used auras to research entanglement. Investigate whether other types of measurements can be used to demonstrate entanglement.
4. If a common source is important for entanglement, it is obviously necessary to determine, in general, what a common source is, because according to the "big-bang theory" everything has the same common source!
5. Investigate if psi lines generated by the mind are the same as psi lines occurring naturally, and also are the same as the psi lines mediating entanglement.
6. By increasing the sample size and extending the weight range in Figure 31-2, investigate if a formula can be obtained for the obtained curve.

Speculation

An obvious speculation is whether two separated fundamental particles from a common source also create a psi-line, which enables them to become automatically entangled. Another challenging question is that if we are living in a holographic universe, does this assist the formation of psi-lines in an analogous way that any part of a hologram contains the total picture. A further speculation is whether Fourier transforms are relevant to describe the standing waves and moving nodes as 2 entangled objects are separated.

To obtain the result of entanglement between the 2 remote Type A terminal spirals, information must be passing along psi-lines. This invites the question "is a similar mechanism responsible for linking any objects in the cosmos, including the classical quantum entanglement at the micro level?"

As mind created psi-lines seem to have the same properties as naturally occurring ones, a mind - matter connection seems relevant. Although the concept of "consciousness" has traditionally been associated with higher primates, the above experiments, as well as long established observations in quantum physics, suggest that some of the signs of consciousness are the same for animals, plants, and inanimate objects. It is accepted that a precise definition of "consciousness" needs to be determined.

As discussed in Chapter 33, matter and consciousness may both have been created as part of the "big bang". With this concept of the structure of the universe, an easier explanation of entanglement may be possible, in both quantum physics and in the macro world. Satisfyingly, the same mechanism would apply to both.

Universal consciousness, as discussed several times in this book, and mind generated subtle energy, could both be involved in entanglement.

CHAPTER THIRTY TWO

A 5-DIMENSIONAL UNIVERSE?

Introduction

As discussed in Chapter 2, it has long been known that geometry forms part of the structure of the universe. But, how many dimensions does this geometry contain? In everyday life, we are aware of 4-dimensions: 3 involving distance, and 1 involving time. At another extreme, string theory involves 10 dimensions, whilst extensions of string theory involve 11 dimensions.

This chapter undertakes relevant quantitative scientific experiments in order to interpret a 5-dimensional noetic response, which is found in numerous diverse situations studied in this book.

Quantum physics has long established that the mind and the act of observation can affect experimental results. Some aspects of current physics postulates information being stored as quantum phase interference fringes at the Planck level to form a 5-dimensional hologram, for example, when considering gravity and black holes. With all these concepts in mind, the raison d'être of this chapter is to discover further evidence for this 5-dimensional hologram model.

The strategy for these investigations involves the use of subtle energies. Chapter 21 categorised 9 types of subtle energies perceived by the mind, each having different properties. Whilst discussing other topics in detail, the 5th dimension was mentioned in passing, where it has been perceived by several researchers. These included:- Multi-body interactions, auras, the Kabbalah tree of life, peace grids, psi-lines, spirals in general, and a half sine wave. However, the 5th dimensional aspects have not yet been discussed in this book, but this is now remedied.

Half Sine Wave

The half sine wave, as illustrated in Figure 32-1, is possibly one of the most interesting source geometries. When dowsing a half sine wave, and specifying the mind's intent in the normal 3 and 4-dimensional space,

there is a void. Irrespective of size, the half sine wave shape appears inert to dowsing. There are no subtle energy lines either horizontally or vertically. Of all the geometrical shapes so far studied, the half sine wave is unique in this respect.

Figure 32-1 Half Sine Wave

However, an unexpected, inexplicable, and "weird" phenomenon is that dowsing a half sine wave, when the mind's intent is asking for subtle energy in 5-dimensional space, one obtains a strong pattern comprising 4 lines as illustrated in Figure 32-2. These lines are in the plane of the half sine wave, which can be fixed either horizontally or vertically – the effect and pattern seems identical. There are no lines perpendicular to the plane on which the half sine wave is drawn.
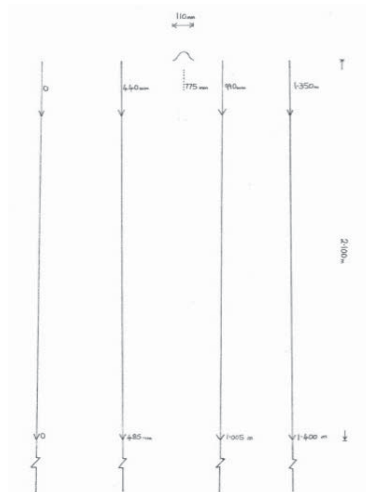
Figure 32-2 Perceived Lines in 5th Dimension

Although only measured over a distance of 100 metres, these 4 lines appear to be parallel within experimental error, have an outward flow, and seem to go to infinity. Unlike most other lines discussed in this book, they

have no termination or other spirals, no bifurcations, and no nodes. Although they do possess outward flow, these lines do not have vector properties, which can affect the measurement of length depending if measurements are made with the flow, against the flow, or across the flow.

These lines comprise Type 1 subtle energy, which in "normal" dowsing are common earth energy lines that indicate a base colour of white (augmented, depending what is being searched for). However, unlike most other subtle energy lines, they do not possess colour on a Mager disc.

Figure 32-3 is a graph illustrating the effect on the perceived pattern produced by sources having different sizes of half-wavelengths, but with consistent shape. As is apparent, the relationship is linear, with an equation of the form:

$$W = 9.\lambda + 1.2 \quad \text{(i)}$$

where W overall width of the subtle energy pattern depicted in Figure 32–2, and λ is the size of the half wavelength of the sine wave source geometry.

This is unexpected, as an exponential relationship is often obtained in these types of experiment with the exponent being a universal constant, such as Feigenbaum's constant, or the golden ratio.

As is normal in dowsing, the numerical measurements are not absolute, but vary depending on the time of day, the time of the lunar month, and the time of the year. Similarly, the amplitude of the source sine wave will affect measurements. In practice, completing experiments in less than 1 hour overcomes this fundamental limitation, and ratios seem to stay the same.

As can be deduced from Figure 32-3, for very small source objects e.g. having a half wavelength ½ λ = 0.01m, the width of the perceived pattern can be greater than 140 times the size of the source. Whilst for a large source object of say ½ λ = 1 metre, the width of the perceived "five-dimensional" pattern is only 10 times greater. Obviously, the linear relationship with its constant, results in this effect.

Although the graph in Figure 32-3 has a very high correlation coefficient of 0.993, attempting to interpret its meaning is challenging. For example, although the slope of the line and where it crosses the W axis will change in different experimental circumstances, there is a problem when the source is extrapolated towards zero wavelength; a pattern is predicted even with no source object to observe!

At present, there being no further clues to interpreting the above 5-dimensional response, what other 5-dimensional lines can be studied?
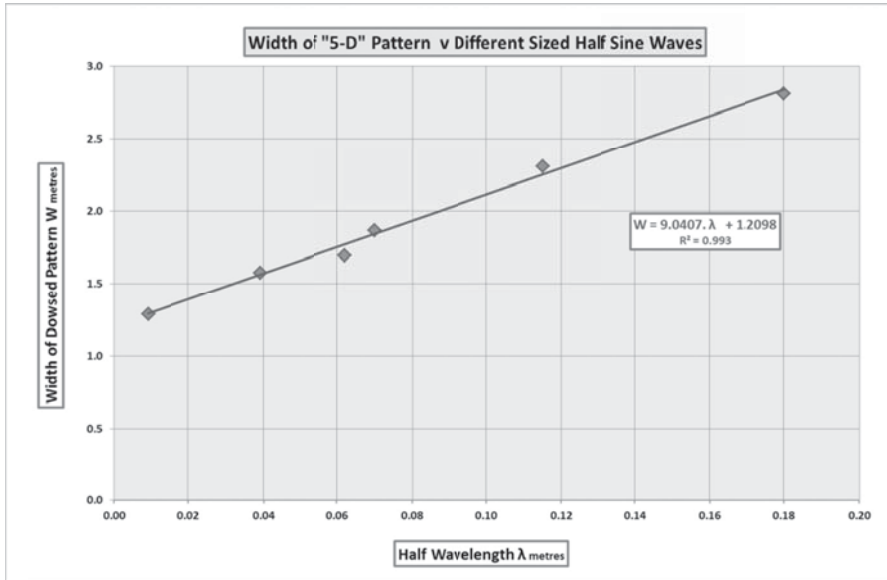
Figure 32-3 The Relationship between the Size of the Half Sine Wave Source and the Width of the Perceived Pattern

3-D Conical Helices

There are several examples where the mind perceives a 5th dimensional perception, when analysing the subtle energies produced by 3-dimensional conical helices.

Double Helix

On many occasions, spirals combine to form concentric double helices, comprising a Type 8 vortex inside a Type 3 vortex as depicted in Figure 32-4.
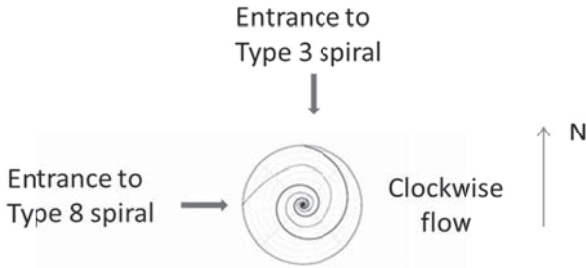
Figure 32-4 Footprint of an Isolated Double Coaxial Conical Helix

Interestingly in this configuration, the Type 8 vortex changes from its isolation preference of anticlockwise to clockwise when it is coaxial with the Type 3 spiral. (A double helix immediately brings an association with DNA!).

5-Dimensional Portals and the Entrance to Spirals

Type 3 spirals have a pair of 5 dimensional portals: one at its entrance (which is due north) and the other due west, as illustrated in Figure 32-5 by the 2 dots. These portals have no Mager colour. Interestingly, these 5 dimensional portals are on the ground vertically below the perimeter of the conical helix's base, and connected to the perimeter by a thin Type 8 thread indicating ultraviolet. This is illustrated in Figure 32-6. The vertical line suggests the influence of gravity. Another Type 8 thread runs along the ground from the Type 5 portal to the apex of the inverted cone. Further investigation is required to find how the west portal is attached to the Type 3 spiral, and if it is just the earth's spin that creates the west location.
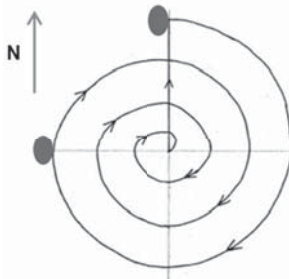
Figure 32-5 Plan view of a Type 3 Spiral and 5-Dimensional Portal
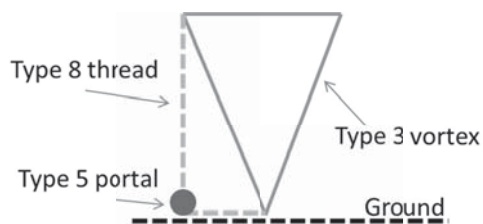
Figure 32-6 Vertical Cross-Section Illustrating the Location of its Two 5-D Portals

The western portal is smaller than its northern partner. For example, the ratio between the diameters of the two portals is about 1.5:1, a number that occurs elsewhere in this research. These Type 5 portals are ellipsoids with a circular horizontal cross-section at floor level. The vertical diameter is possibly twice the height measured from the ground because half the ellipsoid could be below the ground, as is found in many similar situations. For a spiral with a radius of 0.5m the portals have a circular horizontal diameter of about 11 cm and a vertical diameter of about 17 cm.

Bifurcation

From the 5-dimensional portals, a bifurcation process commences that is also in a northerly and westerly direction, as illustrated in Figure 32-7. The solid circles are the five-dimensional portals. The size and geometry of these portals within a typical vortex, together with the bifurcation lengths, angles, and ratios can be found on my website http://www. jeffreykeen.co.uk/Papers.htm Paper 52.
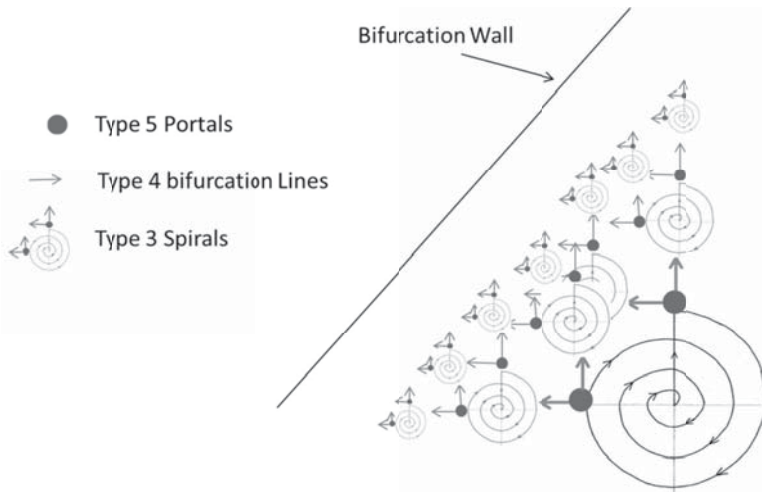
Figure 32-7 Plan View of a Type 3 Bifurcation Pattern

Bifurcation creates Type 4 lines, which, in turn, form ever-decreasing Type 3 spirals that also bifurcate. The process continues with ever decreasing lengths of bifurcation lines and size of portals. About 6 bifurcations is the practical end of this "infinite" harmonic series that eventually forms a terminating bifurcation "wall" in the 90° north-west quadrant from the centre of the spiral. This wall comprises a combination of subtle energy Types 3, 4, and 5, but there is no associated Mager colour. Typically, the distance of the bifurcation wall from the centre of the spiral is about 1.5 times greater than the spiral's diameter.

The bifurcation factor seems about 2.3, a number that occurs several times in this research, and, within experimental error, equals half of Feigenbaum's constant of 4.67 that is usually associated with bifurcation in standard chaos theory. It also invites speculation about a connection to multi-paths in quantum physics.

Single Type 3 Spirals: Maltese Cross

Figure 32-8 is a dowsable photograph of a Maltese cross taken in a public building in Malta. This generates an isolated standard Type 3 spiral several metres in diameter, the same as in Figure 32-5. It is the standard clockwise spiral with north and west orientated Type 5 bifurcation points. The bifurcations lines are Type 4 indicating blue on a Mager disc, and the distance between the 1st bifurcation from its originating Type 5 portal, on

the day of measurement, was 270 cm. The Type 5 portals on the ground indicated no colour on a Mager disc. The radius of the spiral at the spiral's entrance was about 1.1 m, while the height of the cone was about 1.9 m: a ratio of 1.68. The radius of the northerly Type 5 portal was 19 cm, whilst the height of the westerly portal was 13 mm; a ratio of 1.46. There is no Type 8 spiral produced by this source of geometry.
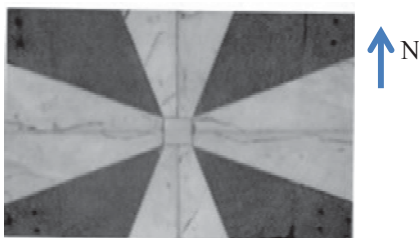
Figure 32-8 A Maltese Cross and its Spiral

Domed Buildings
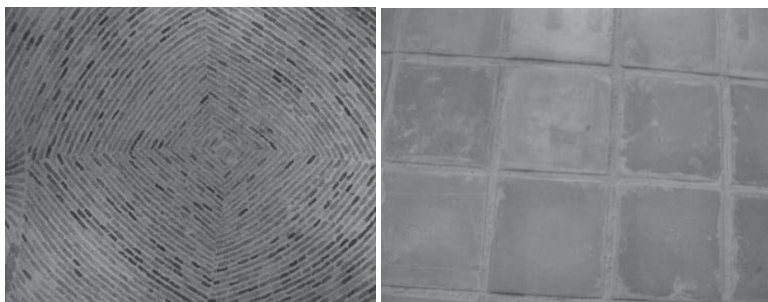
Figure 32-9 Photograph of a Domed Ceiling and Floor Producing a Vortex with a 5-D Portal

Figure 32-9 is a dowsable photograph of the original brick domed ceiling, and the floor below, in a part of the medieval castle in Lorca, Spain. A standard Type 3, Mager coloured green, clockwise spiral is produced on the floor, with the standard two Type 5 bifurcating portals having no Mager colour, and radii measured from the ground of about 12 cm.

Two Parallel Lines

As discussed previously in Chapter 2, dowsing the geometry of any 2 parallel lines (be they 2 short lines drawn on paper as in Figure 32-10, or massive banks and ditches on a Neolithic site), produces a plethora of different types of subtle energies. The main relevance to this chapter is the series of standard Type 3 spirals that are produced along the centre line, as illustrated in Figure 32-10, where the 5 dimensional portals associated with bifurcations are also shown. The Type 3 spirals indicate the usual Mager green, the bifurcating lines are Type 4 indicating blue, and the Type 5 portals indicate no colour. There are no Type 8 spirals present. Intriguingly, this perceived pattern only exists when the parallel lines are pointing North-South. If they are orientated to point East-West there is no perceived pattern obtained. This suggests that the Earth's magnetism and spin interact with the mind, to produce this perceived pattern.
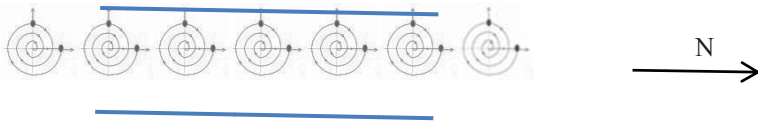
Figure 32-10 The Series of Spirals Generated by 2 Parallel Lines

5-D Portals Generated by 2-Body Interaction

As previously described in Chapter 15, an interaction between any two physical or abstract objects occurs if they are in close proximity. The observed pattern is shown in Figure 15-1. The perceived pattern comprises a complex arrangement of straight lines, dipole "lines of force", subtle energy beams, vortices, Cornu Spirals, and curlicues, which have complex dynamics and null points.

Of relevance here, are the 16 Type 3 spirals, which are also produced in this subtle energy pattern, and are associated with a fifth dimensional response. When plotting the Figure 15-1 pattern on a two dimensional floor plan, 17 spirals are perceived made up in the following 3 categories:

Terminating Beams
2 subtle energy beams, **a** & **b**, are on the axis through the centres of the 2 circles. Two shorter beams, marked **c** & **d**, are perpendicular to this axis and meet at the geometric centre of the two circles. All the beams are Type

4. When looking downwards, 4 standard Type 3 clockwise spirals, indicated in Figure 15-1 with a circle, terminate these straight beams.

Curlicues

Four sets of curlicues, marked as **g**, **h**, **i** & **j**, emanate outwards from the 2 circles. Each set comprises 3 curved lines, making 12 in total. There are 12 standard Type 3 spirals which terminate the curlicues.

Central Spiral

Between the 2 circles, where lines **e f** and **c d** meet, a clockwise spiral is formed (looking down). For some unknown reason this central spiral is not associated with Type 5 subtle energy and does not bifurcate.

In summary, 5-dimensional noetic responses are detected in 2-body interaction, which produces 16 termination spirals, each giving a Type 5 response where they bifurcate, as described above, with no additional features.

Peace Grids and Matter
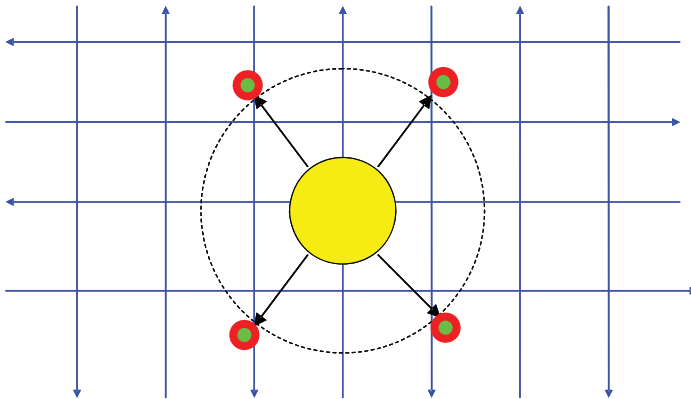
Figure 32-11 An Example of Mind and Matter Interaction

Figure 32-11 illustrates superimposing physical objects on a mind-created peace grid, when 4 diagonals are created at 45° to the grid. These diagonals, or radials, extend to the outer 7th shell of the superimposed object's aura, and end with a standard Type 3 spiral, that has the usual 5th dimension properties and bifurcation. All the grid lines and radials are Type 4. The pattern in Figure 32-11 conjures up visions of General Relativity, where matter distorts the geometry of adjacent space!

Separate Type 3 and 8 Spirals

Sometimes Type 3 spirals are combined with Type 8. There are 2 alternatives (a) they both appear together, but as separate vortices; (b) they become combined into one vortex.

Tetrahedral Geometry and Pythagorean Triangles

Chapter 20 discussed the geometry of the subtle energy produced by nested Pythagorean triangles. The geometry in Figure 24-1 contains some of the key angles found in many branches of science. These nested Pythagorean triangles produce a complex dowsable pattern illustrated in Figure 24-2, which includes arithmetically spaced Type 3 vortices, and Type 8 vortices spaced in a geometric series. These spirals possess the standard 5 dimensional portals, as discussed above.

Auras of Stones and Crystals

The auras of any solid objects were discussed in Chapter 6, and are illustrated in Figure 6-5. They consist of 7 shell ellipsoids with 6 lines and spirals radiating from the centre of the source object.

The orientation of the lines does not depend on the shape of the source object, but is determined by the environment. This can be demonstrated by rotating the source object; the lines remain in the same direction. Auras are not physically attached to their source, and this suggests they are produced by the mind and external forces. Figure 32-12 shows the preferred orientations, and suggest that the spin of the earth is involved to produce the north-south, east-west orientations. (The Type 1 lines are irrelevant in this context.)

Up to the 1st spiral, these 6 arms are subtle energy Type 4 with an outward flow, and a blue Mager colour. After the 1st spiral, this Type 4 line disappears and is replaced by an imaginary extension of this line comprising 2 different types of spirals that are consistently spaced out, as also illustrated in Figure 32-12. These series of spirals are standard Type 3 alternating with standard Type 8.
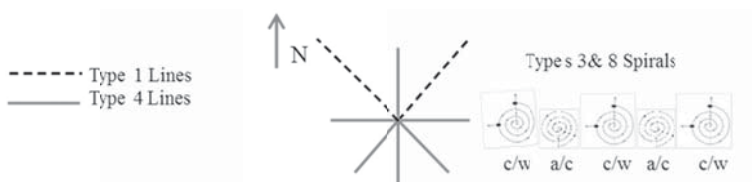
Figure 32-12 Spirals on 6 Arms of an Aura

The same pattern as shown in Figure 32-12 applies to all 6 extension lines. The spirals are referred to as standard with respect to their entrances, the location and properties of their 5 dimensional portals, their bifurcations, their Mager colour, and their spirals' direction; all of which have been discussed in Chapter 6.

When dowsing this aura with the mind's intent in just the 5th dimension, the diagram in Figure 32-13 is found. This is the same as Figure 32-12 but only showing the location of Type 3 spirals. No other types of subtle energy are found, apart from pairs of 5 dimensional portals, as indicated by the dots in Figure 32-13. This 5 dimensional response coincides with the expected location of the Type 3 spirals, confirming that only the Type 3 subtle energy shows this 5 dimensional response, and only the Type 3 spirals bifurcate. The 5-D portals have a size of about 7 cm x 8 cm x 15 cm high and have no Mager colour.
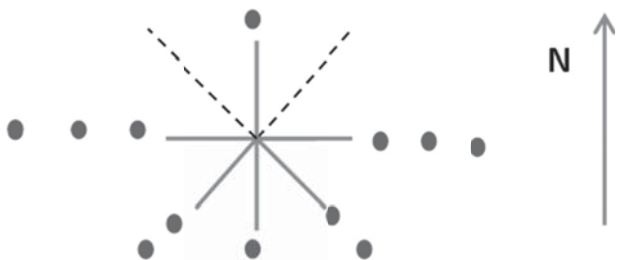
Figure 32-13 Locations of the Pairs of Type 5 Portals

Interestingly, measurements for a physical object, including the separation of the spirals, have similar values to those for abstract geometry and Pythagorean triangles. There must be an underlying cosmic structure involved in the creation of these subtle energy patterns, 5 dimensional portals, and bifurcations.

Combined Type 3 and Type 8 Spirals
Psi-lines

As discussed in Chapter 22, ground-based psi-lines are complex three-dimensional fields arranged in two rows stacked vertically. Each row comprises three horizontal coaxial tubes (i.e. totalling six sub lines in total). These lines have Type 4 cylinders with a Type 8 inner core, and indicate a Mager colour of blue.
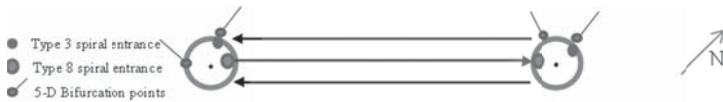
Figure 32-14 Plan of a Psi-Line Footprint, Showing the 5 Dimensional Portals

The terminating Type 3 spirals are standard as previously discussed, possessing clockwise flow, and with a green Mager colour. The Type 5 portals are in the standard position, bifurcate in the standard north and west directions, and have no Mager colour.

Of particular note is where the psi-line joins its terminating spiral. As depicted in Figure 32-15, the Type 8 spiral illustrated, has a clockwise not anticlockwise flow, and does not have its entry due west, but where it joins the centre of the Type 4 line. This is another example of the interactions between Type 3 spirals and Type 5 portals; Type 3 and 8 spirals; and Type 4 lines and Type 8 spirals.
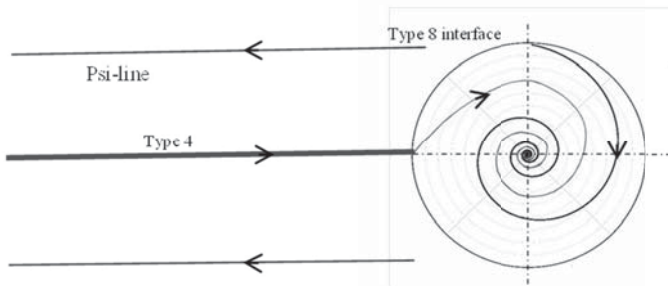
Figure 32-15 Footprint of the Double Terminating Spiral

The Tree of Life

As discussed in Chapter 7, the Tree of Life has 10 spirals comprising Type 3 and Type 8 conical double helices. The Type 3 spirals are standard:

having a green Mager colour; containing two Type 5 portals, one located at the spiral's north entrance the other due West, and bifurcating as expected. On the left of Figure 32–16 is an actual photograph of a tree of life pattern, and to the right of Figure 32-16, the spirals are depicted as the larger circles, and the 5-dimensional bifurcation points are indicated in the smaller circles.
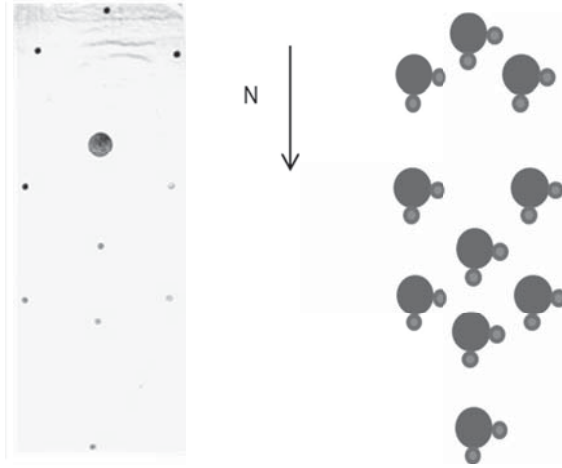
Figure 32-16 Tree of Life Pattern of Vortices Showing their 5-Dimensional Portals

The Type 5 portals indicate ultra-violet on a Mager rosette, and are connected from their position on the ground by a Type 8 thread (which has no Mager colour) to the base of their associated inverted conical helix, which is located vertically above. Both combined Type 3 and Type 8 spirals have a clockwise flow of subtle energy. The Type 8 spirals are also standard as discussed earlier, have no Mager colour, and their entrance is furthest from the source life form.

The additional features of this practical example are that lines of Type 4 subtle energy, flowing at ground level, connect these double helices. Where these Type 4 lines meet the double spirals, a vertical Type 8 thread is produced that connects the lines to the base of the Type 8 spiral. Using the numbering system discussed in Chapter 7, spiral number 10 has only 1 intersecting line and, therefore, only 1 connector, whilst spiral number 6 is intersected by 6 subtle energy lines forming 6 Type 8 connectors

Conclusions and Summary

The title of this chapter asked the question "can the mind perceive a 5-dimensional universe?" Bearing in mind that this research has not been attempted before, the evidence presented suggests that the answer is "possibly!"

Numerous examples have been given as to how the mind affects observations, thus supporting well-established quantum physics experimentation. The 5-dimensional hologram model is supported by noetic experiments that have found several unexplained examples of a 5-dimension perception in many situations. Examples include dowsing half sine waves, multi-body interaction, and bifurcation from conical helices that occur throughout the world.

On analysis of these situations, a 5-dimensional response only seems to occur with two perceived geometries - lines and spirals. These findings support the conclusion that as the mind is detecting universal laws of physics together with universal constants and bifurcations, this five-dimensional phenomenon is not just a figment of the imagination, but requires further scientific investigation.

Property	Observation
Mathematical Type of spiral	Archimedean
Number of turns	3.5
Direction of spiral looking down	Clockwise
Entry to spiral	due north
Location of 5-dimensional portal A	due north
Location of 5-dimensional portal B	due west
Start of bifurcation	due north & west
Vortex cone apex half-angle	sine 1/3 (19.5°)
Mager colour	green
Subtle energy type	Type 3
Mager colour of 5-D portals A and B	UV or No-colour
Subtle energy type of portals	Type 5
Ratio of height to portal base	1.5
Mager colour of bifurcation lines	Blue
Subtle energy type of bifurcation lines	Type 4
Bifurcation ratio	$0.5 * \delta$
Ratio of wall distance to spiral diameter	1.5

Table 32-1. Summary of Common 5-D Properties of Type 3 Conical Helices

All these different 3-dimensional "spirals" have similar properties: there being no differences between "naturally" occurring spirals and mind generated phenomena. Nor is there any significant difference between physical source objects, and abstract geometrical patterns. Tables 32-1 and 32-2 summarise these properties for Types 3 and 8 vortices,

Due to the spin of the earth, Type 3 conical helices have their entry point due north of their central vertical axis. Type 3 spirals also have two small portals at ground level, giving a 5-dimensional response that are also associated with the phenomenon of bifurcation. One of these portals is at the spiral's entrance, whilst the other portal is 90° due west. A Type 8 thread connects a portal to the periphery of its inverted conical helix's base, which is vertically above the portal, and another along the ground to the cone's apex.

Property	Observation
Mathematical type of spiral	Unknown
Number of turns	3.5
Direction of spiral looking down	Anti-clockwise
Entry to spiral	Complex alternatives
5-dimensional portals	None
Bifurcation	None
Vortex cone apex half-angle	sine 1/3 (11.5°)
Mager colour	UV or No-colour
Subtle energy type	Type 8

Table 32-2 Summary of Common 5-D Properties of Type 8 Conical Helices

Bifurcation only occurs in spirals displaying a 5-dimensional response; it does not occur in the lines giving a 5-dimensional reaction. The bifurcation wall gives a 5-dimensional response as well as Types 3 and 4.

There is a close connection between Type 5 perception and Types 4 and 8 subtle energies. Similarly, the close connection to universal angles, the numbers 1.5 and 2, chaos theory, bifurcation, and Feigenbaum's constant (δ) suggests, once again, that the mind is somehow connected to the structure of the universe and the laws of physics. These are examples of the mind interacting with the cosmos in its widest sense, encouraging further investigation into the 5-dimension noetic response. It is hoped that the findings and quantified data presented here will assist future researchers to provide a credible theoretical explanation of the subtle energies involved and, in particular, the 5 dimensional perceptions.

Future work

As always in research, the findings raise more questions than answers. The following are some unresolved issues that could form the basis for future research work.

1. Further research is obviously required to explain why a half sine wave source geometry produces a unique 5-dimensional response.
2. What is the theoretical reasons for the linear equation $W = 9.\lambda + 1.2$?
3. There is a problem with the previous equation when it is extrapolated towards zero wavelength; a pattern is predicted even with no source object to observe!
4. Further investigation is required to find how the west portal is attached to the Type 3 spiral, and if it is just the earth's spin that creates the west location.
5. Why do spirals have a 5 dimensional portal?
6. Why do 5 dimensional portals bifurcate, and what is the connection?
7. What is the reason for the north and west preference?
8. What is the theoretical basis for these findings supporting the hypothesis that the universe comprises a 5-dimensional hologram?
9. How is abstract geometry stored and accessed in this 5-dimensional model?
10. What is the connection between Type 5 perception and Types 4 and 8 subtle energies?
11. Why do all 3-dimensional conical helixes have similar properties; there being no differences between "naturally" occurring spirals and mind generated phenomena? Further, there does not appear to be any significant difference between physical source objects, and abstract geometrical patterns.

CHAPTER THIRTY THREE

SUMMARY AND CONCLUSIONS

In this book, I have tried to cover many aspects of the subject that have intrigued me over many years. As is apparent, one train of thought and line of experimentation created the next area of research. This eventually led to me to writing this book. However, as always, research work is never finished. So many areas require clarification and further development.

Having read this detailed book on subtle energies, the reader is entitled to ask, "What exactly are subtle energies and why do they not conform to conventional scientific analysis?"

Being honest, the current answer is that we do not yet know! What we can say for certain, is that subtle energies interact with the world around us in many interesting and unexpected ways. I have set out a summary of my experiments ranging over 30 years that quantify this interaction in the hope that once you are able to copy these experiments, your research can then develop them and take them forward.

Looking back, my research has led to a great many topics and unexpected findings. Some of these highlights include proving the existence of subtle energies, categorising them, analysing their complex structure, their properties and their fundamental connection to geometry.

The discovery of subtle energy alignment beams resulted in the ability to communicate information across the solar system, not only faster than light but instantaneously, thus demonstrating that Einstein's dictum that it was impossible to travel faster than light only applies to physical bodies, not to the mind and subtle energies.

It been demonstrated in this book that the mind is not just a brain in a skull. It can operate remotely, not only to anywhere on earth, but extend out to the solar system, and then into intergalactic space, where it is possible for the mind to undertake experiments that eliminate possible perturbations caused by the earth. Pleasingly, quantitative findings produce simple formulae based on the fundamentals of the structure of the universe.

Classically, entanglement could only occur at the quantum level with 2 interacting fundamental particles. It was, therefore, exciting to demonstrate

several types of entanglement of large sized physical objects that also allow communication of information. This led to the use of photographs to link the mind to the remote location where the photograph was originally taken. Current on-site subtle energies could then be detected. If the event that had been photographed had changed after the photograph was taken, this phenomenon could be extended so that with the appropriate intent, it is possible to go back in time and detect the subtle energies that were then present.

Observations suggest we could be living in a 5 dimensional holographic universe. Possibly associated with this is a weird version of Newtonian gravity that has echoes of gravitational repulsion, or quarks only attracting when they are not close together. In fact, one of the subtle energies discussed in this book has similar properties to those for dark energy.

Up to now, the study of subtle energies was mainly qualitative with minimal mathematics. Fortunately, I found a convenient yardstick with a powerful technique enabling accurate measurements to be made to demonstrate subtle energy research findings. These have included discovering associated universal constants, universal angles, and preferential numbers.

The mind's ability to create and destroy psi-lines and other subtle energies has enabled the research into the structure of subtle energies including spirals and conical helices. This has stressed the importance of the interaction between subtle energies and geometry, which has led to demonstrating that the structure of the universe encourages fractal geometry.

I hope that the experiments in this book have contributed to the knowledge within physics and cosmology, and be of relevance in our understanding of the structure of the universe, the unification of gravity and quantum physics as well as developing our knowledge of consciousness.

To sum up this book, it is apparent from the contents, that the components of a theory of (universal) consciousness and noetics includes subtle energies, the fabric and structure of the universe, waves, spin, vortices, Platonic solids, Pythagorean triangles, quantum physics, general relativity, fractal geometry, and electromagnetic radiation. In fact, included are many current research topics in physics, but these need to be melded together at both the micro and macro scale.

I hope that this book has provided sufficient information to motivate you (and your team) to expand the scope of your research into the widest aspects of physics and cosmology. A possible achievable goal would be

finding answers to some of the questions that have been raised here. This is the research challenge I would like to leave readers of this book!

Via my website, please keep me informed of substantial progress in your research that has been motivated by, and resulting from, the contents of this book.

The Long Term Vision

I also hope that this academic research will eventually lead to useful and practical benefits for mankind in such areas as health, energy, and communications. Historically, it has proved difficult to produce accurate forecasts. But, being an optimist, may I be allowed to suggest two research projects that could have significant long-term consequences?

1. The mind's weird perception of Newtonian gravity was an unexpected finding. Instinctively we have grown up expecting an increase in gravity to increase the gravitational force of attraction. Although not yet understood, the findings in this book relating to subtle energies and universal consciousness cause the opposite effect, whereby measurements decrease not increase in an increasing gravitational field. Could this be linked to dark energy, and explain the acceleration in the expansion of the universe, not the expected gravitational contraction?
2. As demonstrated in this book, when any 3 bodies, of whatever size and composition, are in alignment, they produce a subtle energy alignment beam. This beam has the useful properties of communicating information instantaneously, as well as having a structure that keeps the beam parallel indefinitely, without any attenuation. It would be a significant achievement if future research could develop this for future practical use, within the solar system and beyond!

APPENDIX 1

POSTULATIONS

Introduction

This appendix postulates on how certain aspects of the structure of the universe may create some of the phenomena discussed in this book. The level of quantified evidence presented in this chapter is not to the same depth as that of previous chapters.

A consequence of quantum physics is that space cannot be empty, hence the concept of a quantum vacuum. The following are suggestions on possible properties of such a quantum vacuum.

Tori, Spirals, and Cones

Tori, spirals, and cones could be linked to provide a basis for answers to such obvious questions as why the number 7 appears so frequently in subtle energies, and how does cosmic consciousness / the information field form conical helices?   Another puzzle is that arcsines or arctangents of 1/n seem to act as universal angles.

Let us look at each separately, but first we also need to consider a torus.

A Torus
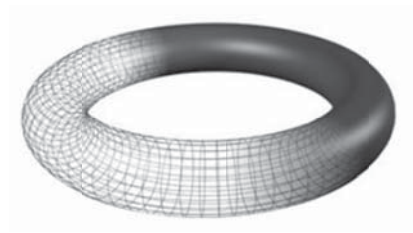
Figure A-1 A Typical Single Torus

Figure A-1 is a representation of a 3-D torus, or popularly known as a doughnut, or bagel shape. In the model about to be developed, let us assume that these infinitesimally small quantum tori are spinning like vortices to form part of cosmic consciousness / the information field, analogous to a "quantum foam".

A Torus can spin or rotate in 3 different ways:

1. If, for example, it is flexible, or a fluid, or an energy field, it can roll in and out on itself. Analogies of this could be smoke rings, vortices in a tornado, or water flowing down a plughole.
2. It can rotate about a vertical axis, so it appears to remain in the same place.
3. It can rotate about a horizontal axis like a paddle wheel.

Combining motions 1 and 2 above, and visualising a point on the surface, produces a circular spiral.

The number 7

Why does the number 7 appear so frequently in both subtle energy research as well as in the everyday physical world? A further property of a torus is that it can move in 7 different ways, or 7 degrees of freedom, which are the usual 4 space-time dimensions, plus 3 rotational movements. If this is a property of the structure of the universe, does this manifest itself in a number of different ways, not only in subtle energy but also in general physics and everyday life?

Torroids and the Cause of Sine 1/n

Torroids and conical helices occur frequently in subtle energies. Another common occurrence is a series of angles of sine 1/n. The following is a suggestion on how these are achieved by universal consciousness.

In order to illustrate how it is possible to produce a subtle energy cone, let us consider a torus where the hole in the centre has the same diameter as the thickness of the torus. Figure A-2 represents a cross-section through the horizontal centre of our special torus, where each component has a radius (a), and diameter (2a).

It is assumed that the structure of the universe at the Planck level comprises such torroids, and universal consciousness selects an increasing

number of these, depending on the mind's intent and the subtle energies produced.

1 Torroid

The simplest example is a single torus at the Planck level, having a cross-section, as shown in Figure A-2, where the diameter of the central hole equals the thickness of the torus.
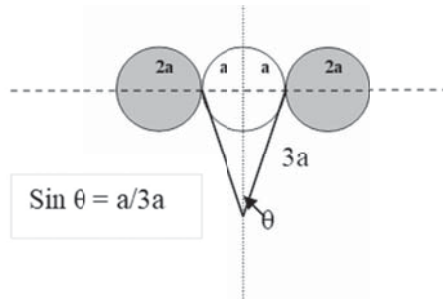
Figure A-2 A Cross-Section through a Single Torus

Consider a cone that

- has a slope length equal to the radius of the torus (3a)
- and just fits into the central hole of the torus, so it has a base radius of (a).

This cone has a half-angle whose sine is 1/3, so it represents the first spiral with a half angle apex of 19.5°.

2 Tori

Let us now add another torus of the same thickness as the previous, but fits round the first torus. This is depicted in Figure A-3. A cone that

- has a base equal to the diameter of the centre hole of the first torus (i.e. it has a radius (a) as before.)
- and a slope length equal to the radius of the combined torus (5a).

This cone has a half angle whose sine is 1/5, and represents the second spiral, having a half angle-apex of 11.5°.

$$\text{Sin } \theta = a/5a$$
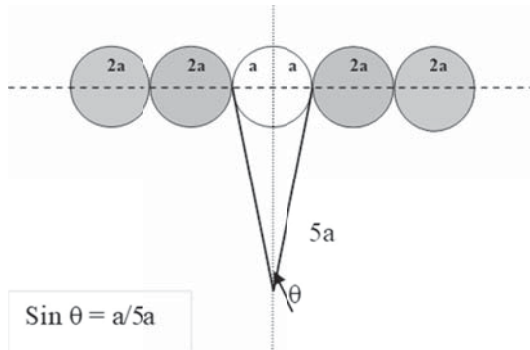
Figure A-3 A Cross-Section through 2 Concentric Tori

Interestingly, if one torus is rotating in one direction, the adjacent rotates in the opposite direction. This may explain why, in subtle energy research findings, alternate spirals are clockwise and anti-clockwise.

3 Tori

Let us introduce a third torus, that fits round the other 2, as illustrated in Figure A-4. A cone that has a base equal to the central hole of the original torus, and a slope length equal to the radius of the 3 combined tori, has a half angle whose sine is 1/7. This represents the third spiral, having an apex half angle of 8.2°.

As before, each torus is rotating in opposite directions, and as before, this could explain alternate spirals in the series being clockwise and anti-clockwise. This model of additional tori can obviously be extended to explain other cones in the series.

Although this is not a proof of the structure of the information field, it may be a good analogy or hint that the universe comprises vortices and spinning tori.

The next obvious question is why should cones at the quantum level appear 7 metres tall in our minds? The mechanism for this could be yet another example of fractal geometry, whereby phenomena at the micro and quantum level become reproduced at the macro level.
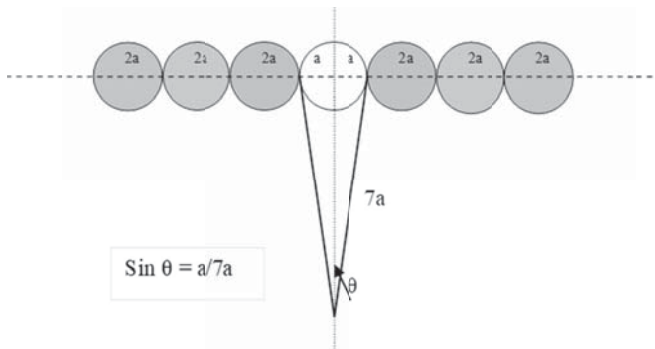
Figure A-4 A Cross-Section through 3 Concentric Tori

String Theory has long had problems in providing tangible scientific measurements, and explaining the structure of the universe. Instead of vibrating strings, it may well prove fruitful to further develop the "Spinning Bagel Theory"

Holographic Universe

Frequency, vibration, and spin would also seem to be a feature of the information field, and this leads to the concept of waves and, in particular, standing waves and nodes. Building on the above concept of waves, a useful hypothesis is that information is stored in the form of quantum phase interference patterns/fringes, which, in turn, leads to the holographic universe analogy.

Let us drill down a bit deeper into the above concepts. General research by many people in different disciplines comes to the same conclusion that we live in an information orientated holographic universe. Information could be stored similar to a hologram. The most famous property of holograms is that any part of a hologram stores the entire image. A good demonstration illustrating that noetics may be linked to holograms, is to slice off a small piece of a photograph. On dowsing the latter, one obtains exactly the same effect as the whole photograph i.e. the same subtle energy fields and measurements are obtained as on site.

The holographic universe analogy, together with fractal geometry, explains a more general concept of connectivity, whereby most information is connected, in the same way that a small piece of a larger physical hologram still contains the entire image.

A two-dimensional hologram produces a three-dimensional image i.e. the holographic recording media is one dimension less than the objects

being "hologrammed". By analogy, we perceive our world as a four-dimensional space/time continuum. Is this really only a holographic image? If so, is consciousness, in fact, a five-dimensional world, with cosmic consciousness or the information field being the fifth dimension?

A Hydrodynamics connection

There is a strong analogy with hydrodynamics; subtle energy sometimes appears to behave like flowing water or wind. Because of viscosity and friction, the flow of a gas or fluid is reduced near boundaries. Subtle energy shapes are static on the ground, but floating ones (for example those created by the mind) drift in a westerly direction with increased velocity as their height above the ground is increased. Equations with a logarithmic relationship describe this phenomenon.

Further evidence of the connection between subtle energies and hydrodynamics is that a characteristic of the latter is the change from laminar to turbulent flow, with areas of stability in between. Standard chaos theory details this phenomenon. Feigenbaum's constant, as well as null points, are frequently found in quantified results in subtle energy research.

Can this analogy be developed in producing a theoretical model for both consciousness and subtle energies?

Universal Consciousness

Throughout this book there have been numerous allusions to a universal consciousness. The following are typical examples of where a universal consciousness could apply, and the questions that need to be addressed. Do any of the above postulations assist in providing solutions?

a) How does an inanimate object, such as an electron, "know" how to behave when orbiting a nucleus; or hydrogen and oxygen atoms "know" they may combine to form water, or any 3 bodies in the solar system "know" when they are in alignment, and when to produce a subtle energy alignment beam?

b) We have seen that when a plant is threatened or "shown" water, it is aware of these situations, as it displays "comprehension" by altering the size of its aura. Is it sensible to claim that a plant is conscious because of this?

c) Taking further the above findings relating to consciousness and subtle energy, where do life forms start? If we are restricting the

discussion to consciousness, is it confined to viruses, plants, mammals, or just to humans?

Communicating with Other Lifeforms

Probably, there are numerous forms of intelligent beings in the universe. Would they want to communicate with "primitive" beings who were not au fait with universal consciousness and/or the information field? They would not wish to use electromagnetic radiation to communicate, and wait hundreds or thousands of years for a reply. They would communicate via universal consciousness and subtle energies. For example, we have demonstrated that a subtle energy alignment beam provides instantaneous communication across the solar system, and possibly across the galaxy. This would be far quicker than "old fashioned light or radio" transmissions.

APPENDIX 2

THE WAY FORWARD AND SUGGESTED FUTURE RESEARCH

Training Exercises

The following are suggested training exercises for improving personal skills in detecting, deleting, measuring, and researching subtle energies.

1. Demonstrate that the aura of pointed objects extends further than for flat surfaces, or round objects.
2. Using the mind to create and destroy psi lines at specified locations and sizes.
3. Detect and follow existing subtle energy lines, and discover if they are natural or man-made psi lines.
4. Detect spirals that terminate both ends of psi lines.
5. Detect nodes on psi lines.
6. Demonstrate that an abstract drawing on paper gives the same dowsing results as a solid object with the same geometry.
7. Detect different types of subtle energies.
8. Detect the significant peaks and troughs at new and full moon due to gravitational attraction.
9. Detect 3 body alignments, using stones or any 3 objects.
10. Detect the significant peaks and troughs at new and full moon due to an alignment beam between the Sun, Earth, and Moon.
11. Detecting the alignments of the outer planets moon and Earth.
12. Using such alignments to prove that not only is communication faster than the speed of light, but also that information can communicate across the solar system instantaneously!
13. Similarly, demonstrating, using the alignment beam from any 3 objects, that the mind is not just the brain in our skulls but, its consciousness can extend to the far reaches of the solar system.

The Way Forward

As always, discoveries in scientific research generate more questions than answers. Being positive, as a result of the findings in this book we now know what questions to ask. The following topics are suggestions for further research that may assist professors, departmental heads, or individual researchers to assign research projects and request relevant funding. To assist the reader, suggested topics and questions to be answered have been extracted from previous chapters, so that all the relevant material is in this Appendix. Where appropriate, a reference to the relevant chapter is included to assist any correlation and additional detailed information.

Introduction (Chapter 1)

1. Why, after millions of years of evolution, can only a few people see subtle energies (but usually only fuzzily), and only a few more people can feel them?
2. Why should there be less evolutionary pressures for non-physical phenomena, even though they could assist survival?

The Importance of Geometry (Chapter 2)

1. Investigate why 2-dimensional abstract geometry, such as that drawn on paper, produces the same subtle energies as a physical body having the same geometrical shape.
2. Investigate why there is a connection between geometry and consciousness, the mind, and subtle energies.
3. The interaction of 2 parallel lines drawn on paper as they are separated, not only produces very interesting subtle energy patterns, but the dynamics of the separation process and the associated mathematics, should produce insights into the correlation between geometry and subtle energies.
4. The lengths of reflected lines are about 1.5-1.6 times longer than their source. This number is tantalising close to the golden ratio (1.618). Future research is required to establish if there is an exact connection.

Subtle Energies from Geometric Shapes (Chapter 3)

1. What are the mathematical transformations from the source geometry that give the observed subtle energy patterns?

2. In particular, why is a 3-dimensional cylindrical subtle energy field perceived to be generated by a two parallel line source? How does the resonance between these 2 lines create and affect the dimensions of the observed cylinder? Why does the length of this cylinder vary from 0 – 3m
   a. As the lines are separated?
   b. Over the course of a lunar month?
3. As resonance, interference, null points, and 2 to 1 ratios have been observed, investigate if waves are involved in subtle energies.
4. If waves are involved, what is the nature of these waves? Are they
   a. Transverse, like water waves, where the variations in the amplitude is 90° to the direction of the wave. (e.g. a "stationary" cork bobbing vertically up and down in water waves).
   b. Longitudinal, like waves in an organ pipe, where the variations in amplitude are in the direction of the wave.
   c. Torsional, where the waves twist in a circular motion at right angles to the direction of the wave?
5. Investigate why there are 9 reflections of subtle energies associated with the source abstract geometry from a straight line, but only 7 reflections for a physical line?
6. Determine if the ratio of the lengths of reflected lines to their source lines equals the golden ratio (1.618). Is any discrepancy due to perturbations from the earth?
7. Further research is required to explain why a 5–dimensional result is only obtained with a half sine wave source?
8. Suggest appropriate mechanisms to explain if a half sine wave source produces a null effect because of standard wave theory, such as an interfering wave emanating from the observer mimics the geometry of the source, but is 180° out of phase. Alternatively, is a 2-body interaction effect created between the observer and the half sine wave source?
   A half sine wave produces a null effect, which is the opposite to a full sine wave, which produces a plethora of subtle energy patterns: This raises the following queries.
   a. Why is a half sine wave out of phase, but a full sine wave is not?
   b. Why do no other geometric shapes investigated in this chapter give a null effect?

Common Perceived Geometric Shapes (Chapter 4)

1. Why on closer investigation, does a single subtle energy line comprise multiple parallel lines, such as in groups of 3, 5, 7, or 12?
2. Investigate a theoretical explanation as to why spirals have 3½ turns, and why any line drawn through the spiral's centre intersects the spiral at 7 dowsable points.
3. A theory is required that explains why auras comprise either 7 or 9 concentric ellipsoids. An extension of this theory is required to explain why mind generated subtle energy has 9 components, whilst physical sources are associated with only 7.

Mathematics and Universal Constants (Chapter 5)

1. An interesting challenge for future researchers is to determine what the connection is between conic sections, and the production of subtle energies?
2. A part of future research strategy should be to investigate the connection between the angles 19.471° and 35.264° to subtle energies.
3. A rewarding project would be researching the mathematics of the transformation between source geometry and the geometry associated with its subtle energies.
4. Examine why Pi (π), the exponential or natural logarithmic constant (e), the speed of light (c), and the fine structure constant (α) are rarely found in quantified research results of subtle energies?
5. Is it relevant for subtle energy research, that all universal constants are also an irrational number?

Auras of Animate Objects (Chapter 6)

1. What are auras?
2. What do colours represent?
3. Why 7 rings?
4. Why 6 arms?
5. What determines the orientation, geometry, and angles between these arms?
6. If the source is rotated, why is there no impact on the geometry or orientation of the object's aura?
7. Is there a theoretical reason why the spirals on the arms start between the 3rd and 7th boundary of the aura's ellipsoids?

8. What is physically happening between electromagnetic light radiation/photons and atoms or molecules of the source object, that affect subtle energies?
9. After the 7 ovoids of an aura have decayed to nothing, why do all the properties of the remaining spirals appear to stay the same?
10. If 2 objects are separated, at certain separation distances the pattern of spirals cancel out, and the entire spiders web pattern disappears. Even if the source has been kept in a lightproof container, so that all the 7 ellipsoids in their auras have decayed, why does the outer spiral structure still remain
11. Although auras pass through air or walls without significant attenuation, metals can attenuate and shrink all 7-aura fields. Why?
12. What is happening at the molecular or atomic nucleus level, when the pressure (P) increases the aura size (r) in a log **P** log **r**, curvilinear relationship?
13. How does an arrow, irrespective of how it is produced, and the medium used, affect the size of any aura, depending on which way it is pointing?

Auras of Plants and Humans (Chapter 7)

1. How does a plant "know" that a sealed bottle of water is nearby, or the intentions of a human? Is there some form of telepathy?
2. More research is required into the connection between auras and consciousness in plants, animals, and humans.
3. What is the lowest form of life with a conscious aura?

The Auras of Circles and Other Abstract Geometry (Chapter 8)

1. What causes geometrical patterns such as a circle to have an aura? Is this a manifestation of consciousness? What is the theoretical link between a geometrical shape and the size of its aura?
2. Why are abstract auras similar to those observed for solids?
3. Using pure geometry sources, experiments should be repeated to isolate the factors and their effects on the constant in the equation relating source size to its subtle energy size.
4. The diameter of a core aura is approximately 1.6 times the diameter of the source circle. With more accurate experiments, and allowing for known perturbations, is this the universal constant, the golden ratio, 1.618?

5. Similar experiments should be repeated with a positive intent to see if the mind can separate the perceived perturbation effects of spin from gravity.
6. The findings in this chapter, only relate to circles up to 21 cms diameter. Further experiments are required for larger circles.
7. Discover if there is common mathematics that transforms the geometry of the source to the generated pattern of subtle energy that is perceived. For example, we know that dowsing an abstract 2-dimensional circle produces an aura
   a. that is a linear function of the radius of the circle being dowsed
   b. which contains a 3-dimensional perpendicular vortex having a small divergence angle, and
   c. with each of the above involving 9 components,
8. What is the mathematical transformation that converts a 2-dimensional circle $x2+y2 = r2$ into the above observed model? This may be used as a starting point to apply to other geometries.
9. Further research is required to understand the physics of the experiments involving the effects on auras of orientation, vorticity, magnetism, and reversed polarity.
10. Create a research project on why electromagnetic radiation should have different effects on crystals, compared to pure geometry, and metal sources.
11. Further experiments are required to see if there are exceptions to the equivalence between abstract geometry, and a physical object with identical geometry and dimensions.
12. Research why the aura of crystals expands in sunlight, but the auras produced by metals and pure geometry shrink in sunlight. Demonstrate if this phenomenon is because of the crystal lattice structure, with the lattice angles being the same as the preferred angles in the structure of the universe.

The Brain and Subtle Energies (Chapter 9)

The obvious next step is to arrange brain scans to find the exact location(s) where the brain interfaces with subtle energies. The appropriate medical equipment must be non-intrusive and avoid any magnetism that would invalidate this experiment. These scans need to be undertaken using subjects who are expert dowsers, and can see, or strongly feel subtle energies. While the scans are in progress, the subjects should be:

1. Undertaking the 4 methods of dowsing discussed in this chapter.

2. Investigating if there is any difference between local and remote activities.
3. Detecting if the 9 different types of subtle energies discussed in this book affect different parts of the brain.

As part of this research, discover what is occurring in the brain, to explain why children under the age of about 11 years old are better than adults at seeing and feeling subtle energies. Similarly, establish why elderly people, over about 70 year's old lose their sensitivity in detecting subtle energies.

A Model of Consciousness (Chapter 10)

1. The mathematics for the cosmic acceleration should be re-worked, but with a structured zero point field involving torroids and vortices, as discussed in this book. Hopefully, this may produce results that are 120 orders of magnitude **less** than the current interpretations of the zero point field and quantum physics, and, therefore, tie up with observations.
2. After having absorbed the concepts presented in this book, can a robust definition of consciousness be produced?
3. Research into subtle energies and consciousness could be directed in two parallel streams. Top down, by contributing to the development of the "theory of everything, and bottom up by performing simple experiments such as those touched upon in this book.

How Noetics and Dowsing Work (Chapter 11)

In order to improve comprehension of noetics and dowsing, further research is required into interrelated topics which include a possible 5-dimension, holographic, quantum universe that is based on information, geometry, fractals, ratios including harmonics, irrational numbers such as phi (φ), chaos theory, and yin-yang properties (e.g. male/female, positive/negative, dipoles, abstract/physical, matter/anti-matter, etc.)

Categorising Different Types of Subtle Energies - Part 1 (Chapter 12)

1. There are probably more than 9 different types of subtle energies. It is, therefore, important to find if there are new subtle energies. To assist in this quest, and based on the findings in this book, researching

different source geometrical patterns is a powerful tool that could be used in seeking new types of subtle energy. However, if none are found, a significant milestone has been reached in demonstrating that only 9 different types of subtle energies exist.

2. Discovering other properties for each of the different subtle energies, would not only help in identifying the differences between subtle energies, but also should be helpful in understanding and determining the theoretical aspects of subtle energies.

Photographing Subtle Energies (Chapter 13)

1. Why does placing an inverted photograph of a subtle energy pattern, on the actual subtle energy that has been photographed, cancel out all trace of the original subtle energy line?
2. Determine the lowest possible bit density of a photograph, that provides sufficient information to enable entanglement to take place between the mind and the actual location, where the photograph was taken.
3. Why does using a photograph assist the observer to access historic Akashic records?
4. Where and how is the historic information stored?
5. How does the mind access this information?
6. Explaining why time only goes forward has defied science for centuries. To this, must now be added how is it possible to go back in time?

Two-Body Interaction (Chapter 15)

1. What is the mathematical transformation that enables 2 circles (whose simple equations are in the form $x^2 + y^2 = r^2$) when in close proximity, to produce a complex mathematically described pattern such as in Figure 15-1? This mathematics has to explain the, complex arrangement of straight lines, dipole lines of force, vortices, Cornu spirals, curlicues, bifurcations, together with the complex dynamics of 2-body separation and null points.
2. Why do 2 abstract circles produce 9 Cornu spirals whilst solids produce 7? This is similar to abstract circles producing 9 aura rings, but solid discs only produce 7 rings
3. What is the mechanism that produces 6 null points for abstract geometry, but 4 for solids?

4. What do the null points tell us about the creation and destruction of Cornu spirals?
5. Why do the null points destroy all spirals, Cornu spirals, and curlicues, but not the straight lines?
6. Why do null points only extend over a few mms of separation of the two objects?
7. What is the connection between the null points and the perturbations caused by magnetism?
8. Does abstract thought of a geometrical shape, require more or less information than physical objects with identical shape?
9. Could the null points be caused by the outer auras of each of the 2 interacting circles cancelling out the associated information?
10. An interesting future research project would be a study of how the subtle energy pattern depicted in Figure 15-1 changes as the separation distance between the 2 bodies decreases to zero, and then as they touch. Similarly, what happens as the 2-bodies stop interacting because their separation is too great?
11. Some of the characteristics of 2-body separation can be explained by information communicated by waves, whose wavelength determines their maximum separation distance of the 2 bodies. What is the theory of this?
12. What is it in these waves that enable the 2 bodies to be aware of each other's separation and size? "Hoping" to find an interacting partner, each body must either
    a) be radiating standing waves with wavelengths that are a function of their radius/size and separation distance, or
    b) only after the auras of the 2 bodies overlap can the relevant information be communicated.
    The latter option seems more probable. How else would 2 bodies "know" where each other is, their radii and when within interaction range?
13. Experiments are required to find the factors involved leading to a formula for L_{max} the maximum length of a 2-body subtle energy beam.
14. There is only 1 optimum separation distance between 2 objects that produces a resonance peak. If this is 30cms as in the example in Figure 15-2, the half-wavelength that causes the resonance is also 30 cms. These are relatively large wavelengths and imply a macro cause, not a mechanism at the quantum level.
15. It would seem that the observer needs to look at the source geometry to be able to perceive the intricate patterns. Does consciousness create the dowsable pattern, or is it there all the time, but intent is required to

perceive it? However, if intent is present, but the dowser is not looking at the source objects the dowsable pattern is not always detected.

Three-Body Interaction (Chapter 16)

1. Any 2 interacting objects, be they solid bodies or pure geometric shapes, produce identical effects. The same applies to 3 aligned circles drawn on paper or 3 solid bodies. There seems to be an equivalence between pure geometry, and matter without the effects of mass. *Why?*
2. Irrespective of size or material, how do any 3-bodies know when they are aligned? Is this a consequence of the structure of the universe?
3. Why does alignment produce a subtle energy beam?
4. To produce a subtle energy alignment beam, why has the alignment to be better than arcsine 1/5 for full moon simulation, but arcsine 1/4 for a new moon simulation?
5. 4 examples were given of 3 objects not meeting all the criteria for the production of a subtle energy alignment beam. However, each of these incorrect geometries of the 3 bodies, produce different subtle energy beams, with different Mager colours, and different divergence angles. Discovering the logic for these findings could help in understanding the theory of subtle energies.
6. The subtle energy beam produced by 2 interacting objects has very different properties to the subtle energy beam produced by 3 aligned objects. *Why?*
7. Unlike earth energies, or the subtle energy produced by 2 interacting bodies, yardstick measurements made in the 3-body subtle energy beam are invariant to the direction of flow. *Why?*
8. In 3-body alignment, measurements are decreased if made near the outside of the 3 objects, or increased if measured near the middle of the 3 bodies. This effect is identical to dowsing at new moon or at full moon, or an eclipse of the sun. The reason is possibly the shape of the subtle energy beam. *Why?*
9. How does the moon know it is about to align with the sun and earth, and is touching the subtle energy beam, if this beam has not yet been created!
10. To produce an alignment beam, why must the 3 objects not be in 2-body interaction, (i.e. their auras not overlapping)?
11. Why must the angles of alignment be less than arcsines 1/4 and 1/5?
12. How and why do 3 aligned geometric objects "switch on" a subtle energy beam?

Mind Created Subtle Energies (Chapter 17)

1. Investigate the reasons for information loss for both local and remotely generated subtle energies.
2. Confirm if mind created psi-lines are the mechanism for transmitting, or viewing, subtle energy information - either locally or remotely.
3. Why is it impossible to create psi lines less than about 1 m.?
4. Why does mind created subtle energy have 9 reflections, each separated in a geometric series?
5. Investigate why mind created subtle energies, that have been specified as resting on the ground, remain "locked" to the ground, but subtle energies specified to float in space, do not remain constant but drift to the west?
6. As the speed of a floating subtle energy increases asymptotically with height, as illustrated in Figure 17–4, explain why floating subtle energies behave like a flowing fluid near the ground, analogous to friction or viscosity slowing the fluid's flow rate. This phenomenon is not compatible with subtle energies passing through physical barriers without any attenuation.
7. Why is this effect asymptotic, and relatively short ranged?
8. However, why does the geometry of a floating subtle energy field remain constant, when its height is flowing at different speeds? This suggests that a floating pattern of subtle energy is not affected by its flow rate. However, this contradicts Figure 17–4.

Spirals and Conical Helices (Chapter 18)

1. Why are there 3½ turns in a conical helix, and what is the connection to musical octaves comprising (2 x 3½) 7 notes?
2. Conical helices of subtle energy always seem to appear as inverted pairs, like reflections that appear as touching apexes. Why?
3. Moreover, these pairs of conical helices are stacked vertically above each other as 7 pairs. Why?
4. What causes conical helices to appear the same, if they originate from differing sources?
5. Why is there a mirror image between pairs of conical helices? This seems to apply to both vertical and horizontal "reflections".
6. Most conical helices involve bifurcations. However, some spirals, such as the central spiral between 2 interacting bodies, do not bifurcate. Why?

Vorticity, Prayers, and Dipoles (Chapter 19)

1. Why do auras and their component fields appear static when their source is rotating, and, therefore, suggest auras are only loosely coupled to their rotating source? Why is this opposite to auras of physical objects, where their size is mainly a function of the source's mass?

2. Is there an aura producing mechanism, with a mathematical transformation of axes, which has the property of being invariant to rotation?

3. What is the theoretical reason for a fluid's aura size having an asymptotic relationship to the number of turns of the associated vortex? Why is this a relationship involving a 3rd order polynomial with a high correlation coefficient?

4. Why does a fluid's aura, expanded by a vortex, retain its expansion after the spinning stops? Why is this opposite to an aura associated with a spinning solid object?

5. Investigate why rotational generated fields have the same Type 4 subtle energy as mind created fields.

6. Investigate why rotational fields comprise 9 Type 4 field boundaries, and not 7 as with static objects. Why do the distances between the 9 boundaries form an approximate geometric series?

7. Investigate why physical bodies are associated with Type 1 fields with a preference for arithmetic series, whilst mind and vortex generated subtle energies are associated with Type 4 fields in a preferential geometric series.

8. Unlike auras associated with solids, which are 3 dimensional, why are auras associated with rotation mainly 2-dimensional?

9. Investigate why rotational auras are not very symmetrical, and ascertain what perturbations cause this asymmetry.

10. What perturbations cause the discrepancy in the cosine relationship and the angle of spin? Is the fourth power relationship in Figure 19-3 the same as would be expected from a field radiated by a dipole antenna?

11. What effect, if any, does the earth's rotation have on the above experimental results?

12. What is the connection between Tibetan spinning prayer wheels, Type 4 fields, vorticity, and cosmic consciousness? Is there any measurable difference between spinning the wheel clockwise, as opposed to the preferred traditional anti-clockwise motion?

13. The 3-dimensional polar diagram of a rotational Type 4 subtle energy is similar to the radiation pattern associated with a dipole antenna.

Investigate whether this analogy is useful in finding a theoretical explanation for the perceived rotational generated fields observed in this book.

Polyhedral Geometry and the Mind's Perception
(Chapter 20)

1. Why does source geometry which comprises Pythagorean triangles containing tetrahedral angles, produce a complex pattern involving most types of subtle energy?
2. Why does an east-west magnetic field create a symmetry that is absent from a north-south magnetic field?
3. Why does the earth's north-south magnetic field make solid geometry respond differently from abstract geometry, but not when there is an east-west field?
4. Why are all the vortices, both geometric and arithmetic, appear to be attached to straight subtle energy lines?
5. Why should a converging subtle energy cone give the impression of being sucked into the easterly apex of the abstract source geometry, and being converted into a different form of subtle energy cone that exits the source geometry?
6. Why should the physical version of the same source geometry produce a chirality effect that only affects the 2 subtle energy cones, changing their entry and exit directions from left to right?
7. How does the mind / cosmic consciousness combination interact with spin, gravity, and magnetism?
8. By just turning a sheet of paper through 90° and loosing 36 vortices and Orgone energy, what does this tell us about consciousness, the mind and how geometry is transformed by the cosmos?
9. Is the optimum alignment of the tetrahedral source geometry to magnetic or true north?
10. Is the 22.5° cut-off angle the same as the earth's tilt? Alternatively, is it ½ of 45°?
11. What is the mathematical transformation that enables simple, but very common angles, to produce a complex mathematically described pattern such as in Figures 20-2 and 20-3?
12. It would seem that the observer needs to look at the source geometry to be able to perceive the intricate subtle energy patterns. Does consciousness create the dowsable pattern, or is it there all the time, but intent is required to perceive it? However, if intent is present, but

the dowser is not looking at the source objects, the dowsable pattern is not always detected.

Categorisation of Subtle Energies – Part 2 (Chapter 21)

1. There are probably more than 9 different types of subtle energies. It is, therefore, important to find if there are more new subtle energies. To assist in this quest, and based on the findings in this book, researching different source geometrical patterns is a powerful tool that could be used in seeking new types of subtle energy. However, if none are found, a significant milestone has been reached in demonstrating that only 9 different types of subtle energies exist.
2. Discovering additional properties, to those listed here, for each of the different subtle energies, would not only help in identifying the differences between subtle energies, but also should be beneficial in understanding and determining the theoretical aspects of subtle energies.
3. What are the Type 8 nodes, and what are their function?
4. Why should bifurcation commence from the Type 5 portal located at the entrance of a Type 8 spiral?
5. Investigate the theoretical significance of why the 4 diagonal Type 1 lines in Figure 21-8 are perpendicular to the diamond source, and why each has one geometrical vortex?
6. Similarly, why do the 4 north-south and east-west lines start at an apex of the diamond shaped source, and why do they contain 4 Type 3 vortices plus 4 Type 4 vortices? i.e. a line starting from an apex is associated with 8 vortices and 2 different types of subtle energy, but a line starting on a surface only has 1 vortex with 1 subtle energy type.
7. Why does a Type 7 subtle energy cone give the impression of being "sucked" into the source geometry, and being converted into a different subtle energy, Type 6, coming out?
8. Investigate why many subtle energy structures involve fractal geometry.
9. Research why superimposed Pythagorean triangles, with angles of sine 1/n, produce all known types of subtle energies.
10. Similarly, why do Pythagorean triangles and polyhedral geometry not only reflect the structure of the universe, but also strongly interact with the mind and consciousness?

Psi-Lines and their Properties (Chapter 22)

1. A theoretical explanation is required for the minimum size psi-line of 0.74 m.
2. An explanation why psi-lines greater than 1.58 m require nodes.
3. What are the functions and structure of nodes?
4. What are the theoretical aspects of psi-lines that lead to equations (i), (ii), (iii), (iv), (v) and (vi)?
5. What is the exact nature of psi-lines?
6. More data is required to confirm the equations for the length of psi-line vs their width, diameters, size of terminating spirals, and nodal separation.
7. Experiments extending over one year duration are necessary to find the factors affecting the L/W ratio. How does the mind determine the length of a psi-line, and prove if cosmic factors determine its width? This should also lead to clues about perturbations affecting the results on Phi.
8. Why are psi-lines so easy to create, destroy, and detect by the mind?
9. Sensitive brain activity scanning equipment is required to resolve what part(s) of the brain is involved.
10. What does the magnetic and electric association represent, and how do they relate to their creation by the brain?
11. What is the perceived "flow"?
12. What is the velocity of "flow" and propagation of psi-lines?
13. What are the nodes?
14. How are the terminating spirals connected to the 3 sub lines of a psi-line?
15. Why do all cylinders give the impression of magnetic and electric fields with alternate directions of flow?
16. Are the nodal separation distances associated with quantised wavelengths or frequencies?
17. Is there a carrier wave, and what types of information can the modulation wave transmit?
18. What do the white and ultra-violet Mager colours represent?
19. Why are some lines beneficial whilst others are detrimental to health?
20. Why do astronomical alignments affect existing subtle energy lines and spirals?
21. What keeps the integrity, structure and properties of psi-lines the same over several kilometres? Is it because they are self-organised, or are psi-lines linked to the structure of space-time?
22. How do psi lines become secured to the ground?

23. How does a psi-line know how long it is and hence the number of nodes (or its width etc.) that should be created?
24. Similarly, how does a psi-line know when there is a kink in it, and change its properties along the entire straight lengths?
25. Do psi-lines involve energy in the accepted scientific understanding, such as increasing temperature or performing work?
26. Does the creation and destruction of psi-lines by the mind adhere to the conservation of energy law?
27. More data is required to determine the mathematics of the Type A, and Type B spirals.
28. In measuring the conical apex angles, more data is required, preferably using the radius from the spiral's centre to its entry point - this being the largest radius of the cone's asymmetrical base.
29. Some of the experiments in this book should be repeated in the southern hemisphere to confirm that the Type A spiral's entry point is still to the north of its centre, and so proving conclusively that magnetic north is involved.
30. What joins the psi-lines to their terminating spirals?
31. Are these experiments on psi-lines, which have been created by intent, at the earth's poles or in intergalactic space:-
    a) actually performed by the mind at the poles or in space, and the findings obtained by remote viewing? or are they
    b) actually performed physically and locally ?
    If alternative (b) above, how does the mind shut out the local earth's spin when visualising experiments at the earth's poles? How does the mind eliminate the effects of gravity, electromagnetism, and spin when visualising the experiment in space?
    If alternative (a) is correct, how does the effect of local magnets become transported to the poles? Are these phenomena another example of the comprehensive entanglement as discussed above?

The Structure of Columnar Vortices (Chapter 23)

1. The fact that there is no difference between columnar vortices created by the mind, and those generated by physical objects, should be fundamental evidence to assist producing a theory for subtle energies and consciousness.
2. Other independent researchers need to reproduce the experiments and confirm the findings in this chapter.
3. This chapter's findings only cover static structures. Vortices imply spin, but there is no evidence here of this, as the sunspots and

Jupiter's red spot are sources that involve dynamics. Therefore, there is need to enhance skills, protocols, and techniques to enable dynamic rotating structures to be plotted.

4. Investigate if columnar vortices contain torsion waves, and if so, what torsion wave equation does the data fit?
5. Do the perceived patterns for columnar vortices equate to a cross-section through a torsion field, or more probably a combination of many such fields combining the "empty" structure of the cosmos with local gravity, spin, and consciousness?
6. Using the Crick and Watson analogy of using crystallography patterns to obtain the structure of DNA, can the patterns produced in this chapter be used to produce a 3 dimensional dynamical pattern of columnar vortices?
7. Investigate whether the 8 missing columnar vortex structures are invalid or are yet to be discovered.
8. Investigate whether columnar vortices exist with only 1 ring? If not, why not?
9. Why does the cone apex angle significantly affect the structure of produced columnar vortices?
10. Do pyramids produce identical columnar vortices to cones with the same apex angle?
11. For the apex angle of cones and pyramids, what is the crossover angle for the production of different structures, and is it sudden?
12. What creates nodes only in some columnar vortices?
13. The nodes comprise a mixture of Type 8 and Type 9 subtle energy, but their function requires future research.
14. Investigate why only the horizontal vortex, produced by a cone with a large apex angle, has nodes, but only a vertical vortex produced by a cone with a small apex angle has nodes.
15. Why and how does gravity only affect some vortices?
16. Changing a source of subtle energy from horizontal to vertical alters the structure of the vortex. Presumably, this is an effect of gravity, and discovering how gravity achieves this would make an interesting project.
17. Why are the odd integers 7 and 9 fundamental to all subtle energies, but to columnar vortices in particular?
18. A fundamental theory is required to explain the findings in this chapter, and, in particular, the details in Table 23-1.

Subtle Energy & Vector Flow (Chapter 26)

1. Investigate what is flow.
2. With most subtle energies, when measuring with their flow, measurements increase, whilst measuring against their flow measurements decrease. However, for 3-body alignment beams, there is no difference in the values of **L**, if measurements were made with or against the flow. Why?

The Mind and Vorticity in the Ecliptic Plane (Chapter 27)

1. There are several apparent anomalies. Why is the equinox effect minimum on 26th March 2010 and 27th March 2011 but not on 20th March, which is the predicted date of equinox?
2. What caused the kink in the curve just after the June solstice and before aphelion? There was the same effect at the end of December 2010 between solstice and perihelion.
3. What is the theoretical explanation for the sine curve of tangential vector lengths over the course of a year?
4. Why does the tangential vector length curve have maxima at the March equinoxes, but is not affected by the September equinox?
5. Similarly, in Figure 27-4, why do the 3 curves intersect at perihelion, but not at aphelion?
6. There are further anomalies as the maximum vorticity for a consistent explanation should be at perihelion, not at equinox?
7. Similarly, for the tangential curve, why are the maxima on 26th March and not on 20th March, and why does the curve collapse so quickly after the March equinoxes?
8. It is also not obvious why is there a triple dip between the June solstice and 13 days after aphelion?
9. Why does the tangential vector length curve contain the above two phenomena of equinox and solstice, when their effects are at least 2 orders of magnitude apart?
10. If the two main components of ecliptic plane spin are at least 2 orders of magnitude apart, how does the mind deal with this?
11. The simplest formula for vorticity, $V = r \cdot \omega$, was used in the above analysis. What is the exact formula for $V = Fn (r, \omega)$ that explains Vorticity and the mind?

The Weird Effect of the Mind and Gravity (Chapter 28)

1. How is it possible to enhance equation (v), so it is mathematically sound with the units on either side of the equation being the same?
2. How does the mind easily detect changes in the (very weak) gravitational force?
3. Are both gravity and consciousness associated with chaos theory?
4. What is the role of Feigenbaum's constant, δ, in gravity and in the mechanism of consciousness?
5. Why do **increases** in gravity or light, **shrink** the dimensions of subtle energies. On the other hand, other physical forces such as increasing rotation, spin, pressure, magnetism, or the presence of matter, can expand the dimensions of subtle energies. This invites yet another question; why are gravity and electromagnetic radiation different to most other natural forces?
6. Experimentation has demonstrated that the force of gravity can act on objects with no mass, such as abstract geometry! As this seems impossible classically, an explanation is required of why and how?
7. When extrapolating Figure 28-2, (which only has data relating to a relatively small range of gravitational force), what happens to **L** as gravity tends towards zero in intergalactic space, or at the other extreme, as gravity tends towards a black hole?

Instantaneous Communication (Chapter 29)

1. Investigate if it is possible to design and build an alignment beam detector.
2. Similarly, investigate if it is possible to modulate the alignment beam to superimpose the communication of additional physical or chemical information across the solar system.
3. A long-term objective could be to research if this technique can be extended galactically. The obvious challenge is that it would take over 4 years to assess results with a conjunction of the nearest star. However, this could be overcome by applying the technique to exoplanets with short orbiting times. The time difference between orbits should be similar to mind detected conjunctions, and those observed by astronomers, even if the measurements are 4 years apart.

The Mind in Intergalactic Space (Chapter 30)

1. Why is φ (Phi) linked to consciousness when lines and circles are involved?
2. Further research, and developed protocols, are obviously required for larger objects, which are greater than 8 cms, to prove if equation (vi) still applies.
3. Experiments should be repeated to confirm if the same results apply to all geometrical shapes.
4. Experiments should be repeated to see if the same results apply to physical bodies, as well as to abstract geometry.

Entanglement of Large Sized Objects (Chapter 31)

1. It is felt that these findings can be generalised, so that further experiments demonstrate that any 2 objects from a common source automatically generates a psi-line with nodes that enables entanglement to take place.
2. Psi-lines have a complex fractal structure that keeps their diameter constant, and their path, preferentially, in a straight line. Future research is required to find if quantum entanglement has the identical mechanism.
3. All of the above experiments used auras to research entanglement. Investigate whether other types of measurements can be used to demonstrate entanglement.
4. If a common source is important for entanglement, it is obviously necessary to determine, in general, what a common source is, because according to the "big-bang theory" everything has the same common source!
5. Investigate if psi lines generated by the mind are the same as psi lines occurring naturally, and also are the same as the psi lines mediating entanglement.
6. By increasing the sample size and extending the weight range in Figure 31-2, investigate if a formula can be obtained for the obtained curve.

A 5-Dimensional Universe? (Chapter 32)

1. Further research is obviously required to explain why a half sine wave source geometry produces a unique 5-dimensional response.
2. What is the theoretical reasons for the linear equation $W = 9.\lambda + 1.2$?

3. There is a problem with the previous equation when it is extrapolated towards zero wavelength; a pattern is predicted even with no source object to observe!
4. Further investigation is required to find how the west portal is attached to the Type 3 spiral, and if it is just the earth's spin that creates the west location.
5. Why do spirals have a 5 dimensional portal?
6. Why do 5 dimensional portals bifurcate, and what is the connection?
7. What is the reason for the north and west preference?
8. What is the theoretical basis for these findings supporting the hypothesis that the universe comprises a 5-dimensional hologram?
9. How is abstract geometry stored and accessed in this 5-dimensional model?
10. What is the connection between Type 5 perception and Types 4 and 8 subtle energies?
11. Why do all 3-dimensional conical helixes have similar properties; there being no differences between "naturally" occurring spirals and mind generated phenomena? Further, there does not appear to be any significant difference between physical source objects, and abstract geometrical patterns.

General challenges

1. Can consciousness and subtle energies be involved in unifying both quantum mechanics and gravitation?
2. Is there a connection between subtle energies, which currently are only detectable by the mind, and dark energy, which is a major component of the cosmos?
3. Many subtle energies seem to involve vast patterns, or an infinite number of conical helices, or many kilometres of flow, etc. Do subtle energies actually involve conventional energy, and do they conform to the conservation of energy laws?

INDEX OF FIGURES

GENERAL INDEX